NUMERICAL SIMULATION METHODS COUPLED WITH GENETIC ALGORITHM TO PREDICT COOLING ENERGY CONSUMPTION AND INFECTION TRANSMISSION IN BUILDINGS

MANOJ KUMAR SATHEESAN

PhD

The Hong Kong Polytechnic University

2023

The Hong Kong Polytechnic University

Department of Building Environment and Energy Engineering

Numerical Simulation Methods Coupled with Genetic Algorithm to Predict Cooling Energy Consumption and Infection Transmission in Buildings

Manoj Kumar Satheesan

A thesis submitted in partial fulfillment of the requirements

for the degree of Doctor of Philosophy

December 2022

CERTIFICATE OF ORIGINALITY

I hereby declare that this thesis is my own work and that, to the best of my knowledge and belief, it reproduces no material previously published or written, nor material that has been accepted for the award of any other degree or diploma, except where due acknowledgement has been made in the text.

Manoj Kumar Satheesan

Department of Building Environment and Energy Engineering

The Hong Kong Polytechnic University

Hong Kong, China

January 2023

Dedication

To,

myself,

my family,

my friends,

and

the research community of building environment and energy engineering

Abstract

The human-induced climate change is the primary cause of a rise in heat waves and other extreme weather events experienced across the globe. Buildings are one of the major contributors to greenhouse gas emissions, the primary cause of climate change. It is anticipated that climate change will reduce the global demand for heating and increase the global need for cooling. Already, the demand for space cooling has tripled since 1990. Hence, designing and constructing sustainable buildings using less energy to maintain a suitable indoor temperature is an essential strategy for reducing carbon emissions from the building sector.

Predicting the cooling energy required for a building is a complex yet vital method for creating low-energy-demand structures. This study develops a hybrid simulation methodology that combines the strengths of physical simulation (EnergyPlus™) and data-driven methodologies (artificial neural network) to estimate the cooling energy consumption of buildings. This simulation strategy is superior to its counterparts in terms of simulation time, accuracy, robustness, and flexibility to forecast the cooling energy demand. The proposed model’s goodness of fit with energy plus simulations and peer literature data was assessed to ascertain its validity, and a high degree of concordance between the results verified its capacity to be an alternative to conventional energy estimation techniques. The impact of wall and window material selection, window-to-wall ratio, shading coefficient, and indoor set-point temperature on building cooling energy consumption is evaluated. Apartments' energy consumption could be reduced by increasing thermal insulation, decreasing the window-to-wall ratio, and raising the indoor set-point temperature relative to current standards.

Despite the great benefits of the hybrid simulation approach, its development time is significant. Therefore, for its benefits to be realised, it should be applicable to a variety of structures and not just one. The generalisation potential of the model was evaluated in two distinct settings: a subdivided unit (SDU) and a general inpatient ward. Both have building parameters that exceed the simulated training range of the hybrid model. The model's goodness-of-fit test with energy plus simulation results indicated a good generalisation

capability. Using the generalised hybrid simulation model, the energy-saving measures in an SDU were analysed, and it was determined that apartment flow area, occupant per floor area, and indoor set-point temperature are crucial for energy savings.

Design exploration using standard methods is a laborious endeavour. In addition, the outcome cannot be attributed to an optimal design. Consequently, a genetic algorithm (GA) is combined with the generalised hybrid simulation model to assist the user in iteratively analysing the various design parameters and their impact on cooling energy consumption. The coupled technique would rapidly identify the optimal or sub-optimal design option from a pool of solutions, resulting in the least or highest building cooling energy consumption, respectively. A typical inpatient ward cubicle was chosen as a case study to highlight the benefits of the optimisation technique. A combination of (i) design parameters resulting in minimum envelope heat gain, (ii) greater recirculation ratio, and (iii) a reduction in lighting power density from 13 W/m^2 to 7.3 W/m^2, would be an energy-efficient strategy for a general inpatient ward, according to this study. Furthermore, infection control is comparable to or greater than the energy requirement in a general inpatient ward unit. Thus, approaches to prevent the spread of infection within a general inpatient hospital cubicle are further explored.

Infections in healthcare facilities can result in significant public health issues and financial burdens. Therefore, enhancing infection control in healthcare settings is crucial. Ventilation systems are critical in maintaining the air quality inside the building. In particular, healthcare facilities must consider infection control when designing ventilation functions. In hospitals, inpatient wards occupy a substantial amount of floor space. Yet, ventilation design guidelines for patient environments, particularly wards, remain vague. Computational fluid dynamics (CFD) was used to analyze the combined effects of air change rate and exhaust flow rate on airflow and exposure risk distributions due to droplet nuclei of size 0.167 µm (Middle east respiratory syndrome coronavirus) in an air-conditioned ward cubicle. The association between ventilation and the mechanism of infection transmission within the ward cubicle was apparent. In addition to the air change rate, the configuration of a ventilation system is identified to serve as a crucial factor in controlling pathogen exposure. The utilization of CFD yielded significant insights into the distribution of airflow and bioaerosols within an inpatient ward, with a high degree of temporal and spatial precision. However, despite the great precision and details of flow parameters provided by CFD, it is coupled with a lengthy computation time and a high cost.

Multiple factors influence the airflow and dispersion of pathogens in an inpatient unit. Developing effective ventilation strategies encompassing these factors through trial and error would necessitate numerous modifications between the initial and final designs. As a result, determining the best ventilation strategy by relying solely on CFD and the traditional method of optimization is seen as ineffective and time-consuming. Therefore, an evolutionary algorithm (GA) and an assessment mechanism (CFD) are coupled. The aim is to improve patient safety by limiting the spread of infections. The proposed method would execute fewer CFD simulations while assessing more design options iteratively. Based on the design exploration conducted with the GA-CFD approach, the location of an infected patient, the air change rate, the flow rate through a local exhaust grille, as well as the number, location, and size of supply diffusers and local exhaust grilles, that can significantly minimize the likelihood of an infection spreading from one patient to another within a ward is identified. A simple, cost-effective optimal ventilation solution that decreases infection transmission within a ward is proposed. The study also highlights the necessity for healthcare personnel to practise and implement conventional infection control guidelines, such as adequate hand cleanliness, eye protection, and always wearing a high-filtration face mask, regardless of ventilation technique.

Publications arising from the thesis

Journals

Satheesan, M. K., Mui, K. W., & Wong, L. T. (2020). A numerical study of ventilation strategies for infection risk mitigation in general inpatient wards. *Building Simulation*, Vol. 13, No. 4, pp. 887-896, Tsinghua University Press.

Mui, K. W., Wong, L. T., Satheesan, M. K., & Balachandran, A. (2021). A Hybrid Simulation Model to Predict the Cooling Energy Consumption for Residential Housing in Hong Kong. *Energies*, 14(16), 4850.

Mui, K. W., Satheesan, M. K., & Wong, L. T. (2022). Building cooling energy consumption prediction with a hybrid simulation Approach: Generalization beyond the training range. *Energy and Buildings*, 276, 112502.

Satheesan, M.K., Tsang, T.W., Wong, L.T., & Mui, K.W. (2023). Optimization of ventilation strategy in an inpatient ward through coupled simulation. (Submitted for publication, under peer review)

Tsang, T.W., Yuen, W.M., Mui, K.W., Wong, L.T. & Satheesan, M.K. (2023). Computational fluid dynamics simulation for airborne transmission of Methicillin-resistant Staphylococcus aureus (MRSA) in general inpatient ward environment. (Submitted for publication, under peer review)

Satheesan, M.K., Tsang, T.W., Wong, L.T., and Mui, K.W. (2023). The air we breathe: Numerical investigation of ventilation strategies to mitigate airborne transmission of MERS-CoV in inpatient wards. (Submitted for publication, under peer review)

Tsang, T.W., Wong, L.T., Satheesan, M.K., & Mui, K.W. (2023). Preparing for the next pandemic: Minimizing airborne transmission in general inpatient wards through management practices. (Submitted for publication, under peer review)

Conference

Satheesan, M. K., Wong, L. T., & Mui, K. W. (2020). Infection control and sustainability measures for a healthcare facility. In 16th Conference of the International Society of Indoor Air Quality and Climate: Creative and Smart Solutions for Better Built Environments, Indoor Air 2020 (pp. ABS-0391). International Society of Indoor Air Quality and Climate.

Satheesan, M. K., Mui, K. W. & Wong, L. T. (2022). Role of occupancy and indoor temperature on energy efficiency of tiny housing. In 17th Conference of the International Society of Indoor Air Quality and Climate: Healthy People in Healthy Indoor Environments, Indoor Air 2022 (pp. ABS-1668). International Society of Indoor Air Quality and Climate.

Acknowledgements

First and foremost, I am indebted to my PhD advisors, Professor Mui Kwok-wai and Dr. Wong Ling-tim, for their excellent guidance, unwavering support, and extraordinary patience during my doctoral studies. Their passion, commitment, and extensive experience have been a source of inspiration for me throughout the entirety of my academic work as well as my day-to-day life. This work embodies my profound gratitude and appreciation for my advisors; without them, completing this work would not have been feasible.

I am truly grateful to Dr. Tham Kwok Wai, Prof. LAI Chi Keung Alvin and Prof. Shengwei Wang for their time and effort in reviewing my work and providing me with constructive criticism. The valuable comments and suggestions helped me in improving my thesis, making it more robust and comprehensive.

In addition, I would like to express my sincere gratitude to my friends for being a pillar of support in this extraordinary journey. Thank you for making this more manageable and enjoyable.

I would like to express my heartfelt appreciation to my parents for providing me with the foundation to pursue this opportunity. My brother's unwavering support and encouragement have been invaluable, and I am grateful for my in-laws' acceptance and support during the times I needed it most. It goes without saying that this page is insufficient to express the admiration and affection I feel for my wife, Dr. Anjana Balachandran and my son, Byrav. You have been my greatest source of strength and happiness. I cannot thank you enough for the countless hugs, hilarious conversations, and encouraging words that have brightened even the darkest of days. It would have been impossible to create this work without your tremendous understanding, unconditional love, and encouragement over the last few years. Thank you for always believing in me.

Finally, I am grateful to PolyU for providing me with endless possibilities and opportunities during my time here. I would also like to extend my greatest thanks to the PolyU management for their tireless efforts in ensuring that my university life was nothing short of the best.

Table of contents

List of tables

List of figures

List of abbreviations

AC	Air-conditioner
ACH	Air change per hour
ACO	Ant colony optimization
AMY	Actual meteorological year
ANN	Artificial neural network
ARIMA	Autoregressive integrated moving average model
ASHRAE	American Society for Heating, Refrigerating, and Air-Conditioning Engineers
BCL	Building component library
BES	Building energy simulation
BPA	Back propagation algorithm
BPNN	Back propagation neural network
CDA	Conditional demand analysis
CDC	Center for disease control
CDD	Cooling degree days
CFD	Computational fluid dynamics
CHREM	Canadian hybrid residential end-use energy and emission model
CNN	Convolutional neural network
CO_2	Carbon dioxide
COP	Coefficient of performance
Covid-19	Coronavirus disease 2019
CPSO	Chaotic particle swarm optimization
CV	Coefficient of variation
DHW	District hot water

DNN	Deep neural network
DRW	Discrete random walk
ELM	Extreme learning machine
EMSD	Electrical and Mechanical Services Department
EP	EnergyPlus
EUI	Energy-use intensity
FLC	Fuzzy logic controller
FNN	Fuzzy neural network
GA	Genetic algorithm
GCI	Grid convergence index
GHG	Greenhouse gas
GIS	Geographical information system
GRNN	General regression neural network
GWO	Grey wolf optimization
HAI	Healthcare-associated infection
HCW	Healthcare worker
HDD	Heating degree days
HVAC	Heating, ventilation, and air-conditioning
IAQ	Indoor air quality
IEA	International energy agency
LES	Large eddy simulation
LMA	Levenberg–Marquardt algorithm
LSTM	Long short-term modelling
MAE	Mean absolute error
MAPE	Mean absolute percentage error

MERS-CoV	Middle east respiratory syndrome coronavirus
MLR	Multiple linear regression
MOGA	Multi-objective genetic algorithm
MRA	Multivariate regression analysis
MRSA	Methicillin-resistant Staphylococcus aureus
NI	Nosocomial infection
NIOSH	National Institute for Occupational Safety & Health
OPC	Overall particle concentration
OS	OpenStudio
OTTV	Overall thermal heat transfer value
PAT	Parametric analysis tool
PCA	Principal component analysis
PCM	Phase change material
POD	Proper orthogonal decomposition
PRH	Public rental housing
PSO	Particle swarm optimization
RANS	Reynolds averaged Navier-Stokes
RBF	Radial basis function
RC	Relative index of compactness
RF	Random forest
RMSE	Root mean square error
RNG	Re-Normalization Group
RNN	Recurrent neural network
SARS	Severe acute respiratory syndrome
SDU	Sub-divided Unit

SHGC	Solar heat gain coefficient
SHR	Sensible heat ratio
SVM	Support vector machine
SVR	Support vector regression
TB	Tuberculosis
TMT	Total maximum time
TMY	Typical meteorological year
WNN	Wavelet neural network
WWR	Window-to-wall ratio

List of symbols

A	Area (m^2)
A^*	Effective area (m^2)
A_{fl}	Apartment floor area (m^2)
A_{wl}	External wall area (m^2)
A_r	Area of roof (m^2)
A_{rf}	Area of roof fenestration (m^2)
A_{wd}	Window area (m^2)
a	Output from each neuron in the hidden layer
aLW	Output layer weighted value
b	Bias
C_p	Specific heat ($kJ\ kg^{-1o}C^{-1}$)
C	Contaminant concentration
C_{inlet}	Contaminant concentration at air supply inlet
C_D	Coefficient of drag
d_b	Bioaerosol diameter (µm)
DD_m	Total heating or cooling degree days in a month
E_{pd}	Equipment power density (Wm^{-2})
E_c	Annual cooling energy consumption ($GJ\ yr^{-1}$)
E	Exposure to pathogens
EA	Exhaust air
F_x	Auxiliary forces
F_D	Drag force
F_s	Safety factor

$f_{pureline}$	Linear transfer function
f_{tansig}	Tan-sigmoid function
ga	Gravitational acceleration
H	Building transmission coefficient
H_{en}	Envelope heat gain (W)
H_{in}	Internal heat gain (W)
H_{vent}	Ventilation heat gain (W)
h_{fg}	Latent heat of evaporation ($KJkg^{-1}$)
IW	Input weight matrix
k	Time in hour
K_D	Drag constant
L_{pd}	Lighting power density (Wm^{-2})
L_{sen}	Sensible load (W)
L_{lat}	Latent load (W)
l_c	Characteristic length
LW	Layer weight index
$\dot{m}$	Mass flow rate (kgs^{-1})
n_s	Number of particles exhaled by sneezing
n_w	Number of particles deposited on walls
n_c	Number of particles deposited on the ceiling
n_f	Number of particles deposited on floor
n_e	Number of particles exhausted
n	Net input vector
n_{oc}	Number of occupants
n_{out}	Net output value

N_k	Number of occupants at k^{th} hour
N_{max}	Maximum number of occupants
O_a	Occupant area ratio (psm^{-2})
p_w	Vapor pressure (Kpa)
p_{ws}	Saturated vapor pressure (KPa)
P	Input element of the input layer
PIW	Weighted input value
Q	Heat transfer
Q_h	Heat flux (Wm^{-2})
r	Refinement factor
$R_{h,o}$	Outdoor relative humidity (%)
r_w	Wall deposition ratio
r_c	Ceiling deposition ratio
r_f	Floor deposition ratio
r_e	Exhausted ratio
Re	Reynolds number
S	Source
SF	Solar factor
S_c	Shading coefficient
t	Time
t_h	Heating time in a day
T	Temperature (^oC)
T_o	Outdoor temperature (^oC)
T_a	Air temperature (^oC)
T_{base}	Base temperature (^oC)

T_{neu}	Neutral temperature (^oC)
T_{in}	Indoor set-point temperature (^oC)
TD_{eqw}	Equivalent temperature difference of wall
TD_{eqr}	Equivalent temperature difference of roof
$\overline{T}_{e,d}$	Mean external temperature of a day
u	Fluid velocity (ms^{-1})
u_p	Particle velocity (ms^{-1})
U_m	Maximum velocity for wall confluent jets (ms^{-1})
U_o	Jet supply velocity (ms^{-1})
U_{wl}	U-Value of external wall ($WK^{-1}m^{-2}$)
U_{wd}	U-Value of external window ($WK^{-1}m^{-2}$)
V	Volume (m^3)
V_{vent}	Ventilation rate
w_a	Indoor moisture content (kg kg^{-1}, dry air)
w_o	Outdoor moisture content (kg kg^{-1}, dry air)
Z	Climate index
ϕ_k	Hourly occupant load variation factor
ϕ	Heat source
ρ	Fluid density (kgm^{-3})
β	Solar altitude angle (^{o})
μ_T	Eddy viscosity
Γ	Diffusivity (m^2s^{-1})
ρ_p	Particle density (kgm^{-3})
σ_v	Vertical shadow angle (^{o})
σ_h	Horizontal shadow angle (^{o})

$\phi_{AC,k}$	Hourly air conditioner operation schedule
$\triangle T$	Temperature difference (^oC)
$\eta_{hs/cs}$	Efficiency of equipment

Chapter 1

Introduction

1.1 Background

The repercussions of human-induced climate change are unevenly spread across the globe, and its net damage costs are increasing significantly over time. An overwhelming rise in global temperature, sea level, wildfires, and tropical storms are a few factors influencing our physical environment. In contrast, the prevalence of infectious diseases, heat-related disorders, air pollution, and respiratory diseases associated with climate change adversely affects our health (Melillo, 2014, Evens et al., 2017). Rapid urbanization is also making people more vulnerable to the impacts of climate change. Around 68% of the world's population is bound to live in urban areas by 2050 (United Nations, 2018a). This estimated increase in urban population will necessitate more residential, commercial, and healthcare buildings to serve different essential purposes.

Greenhouse gas emission is the major contributor driving climate change issues impacting our climate, environment, and human health. According to International Energy Agency (IEA), climate change will be the primary driver for growth in energy demand. The human-induced warming reached approximately 1 ^{o}C above pre-industrial levels in the year 2017, with the current projected rate being 1.5 ^{o}C. Furthermore, it is projected that Asia will use half of the world's electricity by 2025 (IEA, 2023). This rapid growth in energy demand has significant implications for the building and construction sector, which accounts for 38% of global carbon emissions (Spandagos and Ng, 2017). In 2019, the CO_2 emissions from buildings were 10GT, which happened to be the highest ever recorded in history. Space cooling energy is the fastest-growing building energy end use, and its associated energy demand has tripled since the 1990s (IEA, 2022b), putting additional strain on energy resources and contributing to global warming. Moreover, the building energy demand is expected to grow by 34% in the next two decades at an average rate of 1.5% (Albadry et al., 2017). Reducing buildings' cooling energy demand is the primary means to curb the sector's impact on climate change. However, despite the continuous effort of various stakeholders, the cooling energy demand associated with buildings seems to increase relentlessly. This underscores the need for a major shift in the way we design, construct, and operate buildings to ensure that we can meet the energy demand while mitigating the impact of climate change. It is necessary to chart comprehensive research studies to develop effective strategies to assist building engineers and energy efficiency practitioners in creating new facilities or renovating existing buildings that meet sustainability goals.

Another concern that requires urgent consideration is the transmission of infections within healthcare facilities resulting in significant public health issues and severe economic burdens. Nosocomial infections (NIs) or healthcare-associated infections (HAIs) are a primary means of mortality and morbidity in hospitals worldwide (Anna Sikora & Farah Zahra, 2022). Measured incidence rates of 3.5% to 12.0% have been reported in developed countries, whereas 5.7% to 19.0% in low-income and middle-income countries are associated with nosocomial infections (Alemu et al., 2020). It is a public health issue that requires immediate attention. The severe acute respiratory syndrome (SARS) outbreak in 2003 to the outbreak of covid-19 in 2019 remains a constant reminder that infection control and prevention practices are essential and need regular updation as new knowledge surfaces. Locations within hospitals, such as general inpatient wards, are simultaneously utilized by patients, healthcare workers, and visitors; thus, the susceptibility to nosocomial infection spread is reasonably high. Hospital-acquired infections (HAIs) are a significant safety concern for healthcare providers and patients. Considering morbidity, mortality, increased length of stay, and cost, efforts should be made to make the hospitals as safe as possible by preventing such infections. In healthcare facilities, infections are explicitly considered in ventilation requirements. However, there is a paucity of research studies that address infection control mechanisms for hospital facilities such as a general inpatient wards (Beggs et al., 2008). Hence, a review of nosocomial infection control practices in presumed low-risk zones such as wards is essential. This thesis aims to highlight the significant shortcomings of existing building cooling energy studies and infection mitigation strategies and proposes innovative solutions to overcome the pitfalls with recognized limitations.

1.2 Limitations to existing cooling energy simulation models

The prediction of cooling energy consumption in buildings can be made through three approaches: the physical simulation method, the data-driven method, and the hybrid method (Robinson et al., 2017, Ahmad et al., 2018). The physical simulation method utilizes whole-building energy simulation software such as EnergyPlus (EP), TRNSYS, etc., to solve thermodynamic equilibrium equations and heat equations to predict the energy consumption associated with the building accurately. Despite its high accuracy, it needs a sizeable computational time and has limited scope for optimization (Yezioro et al., 2008). Hence, it proves to be an inefficient approach where it is required to explore the influence of diverse parameters on cooling energy consumption in a broad range of buildings.

On the other hand, a data-driven model is an excellent alternative for predicting the cooling energy consumption associated with buildings (Li et al., 2014). Data-driven methods such as artificial neural networks (ANN) and support vector machines (SVM) can easily model nonlinear multivariate interrelationships (Biswas et al., 2016). They can provide quick responses based on input parameters without significant time lag. However, the performance of these models relies heavily on the database utilized for the model development, where data inadequacy or inaccuracy could lead to massive degradation in its prediction ability (Paudel et al., 2014). New buildings with no historical data and old buildings lacking intelligent building automation systems remain an impediment to utilizing data-driven approaches. Moreover, the need for physical meaning is optional during model development, which some scholars have criticized (Ahmad et al., 2014).

Another emerging building energy consumption prediction mechanism is implementing the hybrid method. It is the coupling of physics in the physical simulation method with statistics of the data-driven approach, thereby eliminating the shortcomings posed by each method when performed individually. This coupling would result in a shorter prediction time and a physical interpretation between the input-output relationships lacking in pure data-driven approaches (Gassar and Cha, 2020). Moreover, as it is implemented by coupling the physical simulation method with a data-driven approach, it also possesses the inherent ability to model nonlinearities. In building energy prediction, a hybrid approach is a robust prediction methodology that outperforms the physical simulation and data-driven methods (Amasyali and El-Gohary, 2018). However, most of the hybrid simulation models developed are restricted to any one particular building type, and their performance in terms of generalization capability outside their training range is poor (Amasyali and El-Gohary, 2018). Firstly, several scenarios will be simulated using the physical simulation method to create the database for ANN training, leading to the development of a generalized hybrid simulation model. Despite developing a generalized hybrid simulation model, it will still be necessary to perform all combinations of parameters exhaustively to identify critical parameters that would lead to minimal cooling energy consumption in a building, which is an inefficient approach.

1.3 Limitations in strategizing infection control measures

Building ventilation system plays a vital role in maintaining thermal comfort, stable microclimate, and indoor air quality. However, it also has to take care of infection control in a healthcare environment (Yau et al., 2011). The outbreak of severe acute respiratory syndrome (SARS) in 2003 to coronavirus disease 2019 (Covid-19) in 2019 has highlighted the importance of ventilation in infection control in indoor environments. Several studies have exhibited a close association between ventilation strategies and nosocomial infection transmission (Li et al., 2007a). Although, there need to be more proper guidelines regarding ventilation design in patient settings such as wards, outpatient clinics, etc (Beggs et al., 2008). Different flow distribution patterns can arise within the indoor environment depending on the type, size, and location of the air distribution device, air change rate, room geometry, heat transfer, and internal objects such as furniture, equipment, occupants, etc (Malkawi et al., 2005). These can, in turn, influence the transport, dispersion, and deposition of contaminants within the indoor environment. Thus, a thorough evaluation of different strategies in general inpatient wards needs to be done, and with new research findings, existing guidelines need to be revised and updated. Using numerical simulation models would greatly benefit designing an effective ventilation strategy to mitigate infection transmission in an indoor environment. Advancements in computing have aided in establishing Computational Fluid Dynamics

(CFD) as an accurate and robust tool to design, analyse, and evaluate different strategies attributed to an indoor environment. However, despite the accuracy of CFD, it can be computationally expensive and time consuming to evaluate the influence of all combinations of parameters on infection transmission exhaustively.

1.4 Limitations to conduct optimization

Optimization is the process of identifying key attributes that makes something better. Optimization algorithms such as genetic algorithm (GA) (Holland, 1975) are used to obtain a sub-optimal or optimal solution that either minimizes or maximizes an objective function within a few iterations. However, it is challenging in many scenarios to write an accurate function representative of the problem. For instance, numerous parameters influence the overall cooling energy consumption and infection transmission mechanism within a building. Thus, formulating an objective function with essential parameters to perform an optimization can be cumbersome.

In numerical simulation modelling, the traditional optimization approach requires a systematic evaluation of the influence of the diverse parameters in the design space on a given problem. The conventional method would exhaustively simulate all the possible combinations of parameters to evaluate the best combination that meets the design objective. However, such an approach is deemed to be highly inefficient (Malkawi et al., 2005).

The limitations inherent within each application could be minimized by integrating the evaluation mechanism (ANN and CFD) as the objective function within the optimization algorithm to negate the individual shortcomings and bolster the strengths to create a robust and efficient prediction tool. The availability of such state-of-the-art numerical simulation models could be one of the breakthroughs in developing sustainable buildings and effective infection control strategies.

1.5 Objectives

Several parameters can exert an influence on cooling energy consumption and the mechanism of infection transmission within a facility. The evaluation of different control strategies and the identification of optimal parameter combinations that minimize cooling energy consumption and infection transmission represent a significant advancement towards attaining carbon neutrality in buildings and mitigating the occurrence of infection outbreaks. However, there is a need to look beyond the traditional design exploration approaches with traditional building simulation tools to identify optimal solutions.

The objectives of this study are:

1. To analyse and determine the primary variables that influences the cooling energy consumption and infection transmission mechanism in buildings.
2. To review and understand the limitations of existing practices for predicting building cooling energy consumption and infection transmission mechanisms in buildings.
3. To develop a generalized hybrid simulation model for predicting the cooling energy consumption in buildings.
4. To investigate ventilation strategies for infection risk mitigation in a healthcare environment.
5. To integrate numerical simulation models with an optimization algorithm to obtain sub-optimal or optimal solutions to minimize overall cooling energy consumption and infection transmission cost-effectively and time-efficiently.

1.6 Research scope

To meet the objectives listed in section 1.5, this study is divided into the following tasks:

Task 1: Understanding the progress and limitations of predicting cooling energy consumption and infection transmission in buildings

A review of existing practices for predicting cooling energy consumption and infection transmission within buildings is done to understand the progress and limitations. The role of optimization in engineering applications and the integration of optimization algorithms with building simulation models are explored. While understanding the constraints of the past methods and identifying the opportunities to improve further, this task will highlight the need to develop a robust, accurate, and time-efficient prediction model to tackle the inefficiencies of its predecessors.

Task 2: Development of a generalized hybrid simulation model

The model development will be done by undertaking the three steps shown below:

Step 2.1 Collection of input parameters for Artificial neural network

The potential building parameters that would influence the envelope heat gain will be reviewed and identified. The range of values corresponding to each parameter will be determined through an extensive data collection from open literature data, design standards, housing property websites, government housing statistics and so forth.

Step 2.2 Development of hybrid simulation model

Utilizing the parameter ranges and building layout collected in Step 2.1, a series of building energy simulations are done through EnergyPlus software to obtain the hourly envelope heat gain H_{en} (W). The building parameters collected in Step 2.1, including outdoor temperature T_o (°C), day of the year, hour of the day, and air temperature set–point T_a (°C) and their corresponding energy output (hourly envelope heat gain) are extracted from simulations to form the input-output files. These input-output files are utilized as the database for training and developing the multi-layer artificial neural network capable of predicting the envelope heat gain based on the given input.

Step 2.3 Estimation of building cooling energy consumption

The building cooling energy consumption is expressed as a sum of envelope heat gain, ventilation heat gain, and internal heat gain. The hybrid simulation model calculates the envelope heat gain, whereas physical expressions estimate the ventilation and internal heat gain. Along with the operation schedule and coefficient of performance of air-conditioners, cooling energy consumption associated with an apartment or building or buildings at the city scale can be estimated.

The proposed hybrid simulation model is tested for its generalization capability by testing it against parameters outside its training range. The proposed hybrid simulation methodology can be utilized for recommending energy-saving strategies in buildings.

<u>Task 3: Ventilation strategies in a healthcare environment</u>

An existing layout of the general inpatient ward cubicle is utilized for conducting the numerical simulations through Computational Fluid Dynamics. The airflow and particle distribution within the computational domain are validated with open literature. The influence of air change rate, local exhaust grille, and exhaust flow rate is analysed for the risk of infection transmission to ward users. The critical parameters impacting infection transmission are identified, and recommendations are provided to enhance infection control measures within the inpatient ward.

<u>Task 4: Coupling ANN and CFD with genetic algorithm</u>

The ANN and CFD are integrated with a meta-heuristic optimization algorithm, namely, a genetic algorithm, to perform design exploration to identify optimal parameter combinations resulting in the least cooling energy consumption and infection transmission within an inpatient ward cubicle in a minimal time. In the optimization algorithm, ANN and CFD will enact the role of the fitness function. GA will then iteratively evaluate diverse design solutions to obtain the sub-optimal or optimal solution for the optimization problem.

The output of ANN is used as the fitness score to evaluate different design solutions. The best solution is the input parameter set resulting in the least envelope heat gain. Similarly, particle deposition on patients extracted from CFD simulations is used as the fitness score to evaluate diverse design solutions in inpatient ward cubicles. The parameter combination resulting in the least particle deposition is chosen as the optimal solution.

1.7 Organization of thesis

This chapter presented the background and motivation behind this study. The main goal is to develop a clear framework using the state-of-the-art simulation models to assist building engineers in identifying and implementing effective strategies to minimize cooling energy consumption and infection transmission within buildings. The objectives and research scope associated with this study are also highlighted. This study's overall structure and research findings are presented in this thesis's following chapters. The organization of the thesis is given through a flowchart shown in Figure 1.1.

Chapter 2 will review factors influencing cooling energy consumption and infection transmission within buildings. It discusses the role of numerical simulation models in constructing schemes for achieving carbon neutrality and infection risk mitigation within facilities. Building simulation models' advantages, disadvantages, and limitations are reviewed and discussed. The role of optimization in engineering applications and their integration with numerical simulation models is addressed. The research gap is defined, and the necessary direction to address the shortcomings is proposed.

Chapter 3 will present the procedures undertaken to develop the hybrid simulation model. The physical expressions used to estimate the annual cooling energy consumption will be detailed. The information on building-related parameters will be collected via open literature, design standards, housing property websites, and government housing statistics. It will discuss the fundamental theory behind the artificial neural network (ANN) and give the various steps, including utilising a building energy simulation tool to create the database for training the ANN. The results of the test run against peer literature and energy simulation modelling results for checking the validity of the hybrid model will be shown. The influence of construction, building materials, and climate on cooling energy consumption will be discussed.

Chapter 4 will evaluate the generalisation ability of the hybrid model for predicting the cooling energy demand for parameters beyond its training range. To do so, two distinct premises are chosen: a sub-divided unit and a general inpatient ward. The subdivided units are further investigated using a generalised hybrid simulation model to examine the numerous strategies employed to reduce the energy associated with this unit. Additionally, to overcome the limitations related to design exploration through a traditional approach, the generalised hybrid simulation model is integrated with an evolutionary algorithm to assist the user in iteratively evaluating the influence of various design conditions on cooling energy consumption. A standard inpatient ward cubicle is used as the application case to illustrate the approach and its advantages in predicting cooling energy usage.

The implementation of ventilation strategies to mitigate infection transmission within a healthcare facility will be presented in Chapter 5. A preliminary numerical study is conducted to discuss the framework adopted in computational fluid dynamics to model the multiphase flow utilised to predict airflow and particle distribution within a six-bedded mechanically ventilated inpatient ward cubicle. To overcome the drawbacks associated with the traditional approach for ventilation optimisation, CFD is integrated with an evolutionary algorithm to evaluate various design solutions iteratively to find an optimal or sub-optimal solution with fewer simulations. The influential parameters in the infection transmission mechanism are explored, and recommendations are made to enhance infection control.

The thesis will be concluded with Chapter 6 by emphasizing the main research findings and their significance. Furthermore, future research directions will be highlighted.

Chapter 1
Introduction

Chapter 2
Literature review:

i. Exploration of factors influencing cooling energy consumption and infection transmission in buildings
ii. Existing methods for assessing and modeling cooling energy consumption and infection transmission
iii. Role of optimization in engineering applications and its integration with building simulation tools
iv. Understanding past successes and identifying research gaps

Chapter 3
Development of hybrid cooling energy simulation model:

i. Collection of building related parameters, performing building simulation, creation of database, training and development of hybrid EP-ANN model
ii. Check for validity of the hybrid model
iii. Prediction of cooling energy consumption with construction, building materials and climate.

Chapter 4
A generalized hybrid simulation model coupled with a genetic algorithm:

i. Evaluation of generalization capability of the hybrid model to predict for parameters beyond its training range.
ii. Explore strategies to reduce energy consumption in sub-divided units with generalized hybrid simulation model.
iii. Integration of an evolutionary algorithm with hybrid simulation model to overcome drawbacks associated with traditional optimization approach.
iv. A standard inpatient ward cubicle is used as the application case to illustrate the coupled simulation approach to predict the optimal parameter combination minimizing the cooling energy demand.

Chapter 5
Ventilation strategy to mitigate infection transmission in an inpatient ward:

i. Conduct a preliminary numerical study to establish the CFD framework for multiphase flow simulation in an inpatient ward cubicle.
ii. Integration of an evolutionary algorithm with CFD to overcome the drawbacks associated with the traditional approach for ventilation optimization.
iii. Explore and evaluate the design space iteratively to find optimal or sub-optimal ventilation strategies to minimize infection transmission in the inpatient ward cubicle.

Chapter 6
Conclusions

Figure 1.1 Organization of thesis

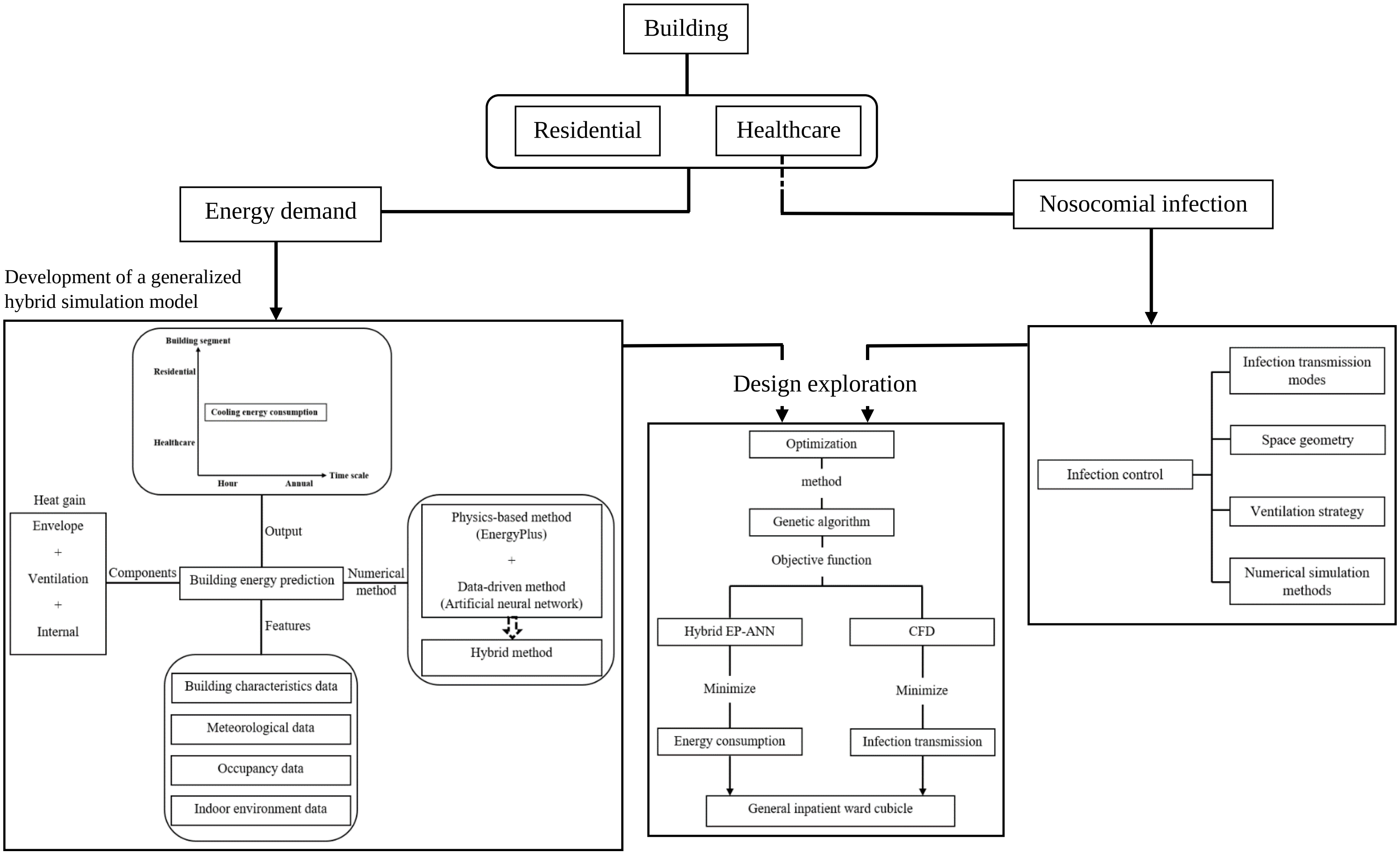

Figure 1.2 Theme of thesis

Chapter 2

Literature review

2.1 Introduction

The building sector forms a large carbon footprint in the world. It accounts for nearly one-third of the global energy and process-related carbon emissions. Climate change is driving a rise in heat waves and other extreme weather events. Record-breaking temperatures were reported mainly in Asia, the middle east, and Europe in mid-2022. It is suggested that climate change can have a dual effect: a decrease of 30% in global heating demand and an increase of 70% in global cooling demand (Isaac and Van Vuuren, 2009). The energy demand associated with space cooling has tripled since 1990 (Mui et al., 2021). The global space cooling energy demand rose to 6.5% in 2021 compared to the year before, with an increase close to 8-9% in Asia Pacific and Europe. It has been growing at an average rate of 4% per year since 2000 (IEA, 2022b). It is required that there should be a decline of 30% in final energy intensity for space cooling in 2030 compared to 2022 to meet the net zero scenarios (IEA, 2022a). Despite, the rise in global temperature, it is quintessential that space cooling needs must be met equitably. Effective envelope design is a primary way to reduce the cooling energy demand associated with buildings. Hence, the Identification of influential parameters on cooling energy consumption as well as the adoption of effective methods to evaluate each design solution is paramount.

The spread of infections within healthcare facilities, which can lead to serious public health problems and severe financial burdens, is another issue that needs to be addressed as soon as possible. The hidden carrier of infectious pathogens in hospitals can cause widespread outbreaks of diseases in the community. Thus, it is of utmost importance to enhance infection control measures within healthcare facilities. Inpatient wards occupy a significant amount of floor space in hospitals. The role of ventilation in infection transmission is an established fact (Li et al., 2007a). Hence, reviewing the ventilation techniques adopted in these facilities for infection control is essential. The design of a ventilation system, location of the patients, space geometry etc., can all influence the spread of infection in an indoor environment such as wards. Hence, a clear understanding of the adopted physical and operational configurations is necessary to recommend a clear framework for improvements. Moreover, it is vital to understand the routes of infection transmission to lay down effective infection mitigation strategies. The adoption of state-of-the-art prediction tools to evaluate each design solution is considered very important as an effective method to speed up infection mitigation efforts.

Thus, a systematic review is carried out in this chapter through a rigorous process that involves formulating research questions, identifying relevant literature, evaluating the identified works, and interpreting the resulting findings. The Web of Science tool was employed to facilitate the identification of noteworthy research endeavors in the realm of building energy and infection control. The present chapter aims to elaborate on the current advancements, extant obstacles, constraints, and gaps in the relevant domain of research. Initially, an investigation will be conducted on the correlation between building-related parameters and cooling energy demand. Additionally, the chapter will examine the diverse approaches employed to assess this correlation. Subsequently, the distinct modes of infection transmission and the corresponding approaches implemented for infection management within healthcare settings will be examined. Furthermore, this chapter will investigate the existing prediction techniques to assess the effective approaches for mitigating the transmission of infections.

2.2 Factors influencing the building cooling energy consumption

The envelope heat gain, ventilation heat gain, and internal heat gain (lighting, equipment, and occupants' loads) are three major components that affect the energy demand associated with air-conditioning (Wong et al., 2008). The envelope heat gains through exterior walls and fenestrations significantly contribute to building cooling energy demand. Envelope design is a critical aspect in the development of buildings, as it can dramatically influence a building's thermal needs, indoor environmental quality, and safety. The increase in global space cooling energy demand is partially associated with neglecting the importance of choosing the correct envelope structure and building materials (IEA, 2022a). Thus, progress in building envelope design is of utmost importance to meet the space-cooling energy demand equitably. In addition to that, the utilisation of a cooling system and its effectiveness can also have a substantial impact on the energy performance. Thus, this section would review the various factors that could influence the cooling energy requirement associated with a building.

2.2.1 Building envelope characteristics

Building materials

The building envelope plays a critical role as a separation between buildings indoor and outdoor environment. The material properties of envelope components such as wall, fenestration, roof can influence the rate of heat transfer across the envelope and eventually, impacting the thermal needs of the inhabitants. The thermal transmission through the building envelope dictates a major part of the building cooling energy demand. The U-value is a popular index for thermal transmission, and it accounts for the rate of heat transfer per unit area of wall, window or roof for every degree difference in temperature between buildings indoor and outdoor environment. It is expressed through a mathematical equation as shown in Equation 2.1, where Q is the heat transfer, A is the area, and $\triangle T$ is temperature difference.

$$U = \frac{Q}{A\Delta T} \tag{2.1}$$

The U-values of external opaque wall U_{wl} and external window U_{wd} are often used to determine the insulation characteristics provided by these envelope components against heat transfer, where a low U-value reflects good insulation. The U_{wl} and U_{wd} value would vary based on the construction materials and its available in open literature and international standards (ASHRAE Standard 90.1, 2013, ISO-10077-1, 2009, Reilly et al., 1992). A review of the thermal insulation requirement in various building enclosures across different countries can be found in (Rodríguez-Soria et al., 2014).

The transmission of heat into indoor space through window by solar radiation can happen while it is exposed to direct sunlight. Shading coefficient is an index that quantifies this thermal transmission, where it can be estimated through the Equation 2.2.

$$S_c = \frac{Solar\ heat\ gain\ coefficient\ (SHGC)}{0.87} \tag{2.2}$$

A lower value of S_c for a window glazing indicates it has good resistance to solar radiation. For instance, a tinted or low-emissivity glass with S_c equal to 0.7 would have better insulation characteristics compared to a clear glass with S_c value equal to 0.96. The S_c value of different glazing type can be accessed through open literature and international standards (ASHRAE Standard 90.1, 2013, Reilly et al., 1992).

The heat gain through building envelope is a major contributor in cooling energy demand of buildings and thus influence of envelope material properties are often analysed through numerical simulations and analytical methods. Pereira and Ghisi (2011) indicated that improving the U-value of envelope would reduce the thermal discomfort within naturally ventilated buildings. A numerical simulation of a building located in a tropical region was conducted to study the influence of external wall, external window, and ceiling on the building energy demand. External walls were identified to have major impact on the building energy demand and it was suggested that by using reverse brick veneer R20 as wall material would aid in reducing the thermal heat gain (Sadeghifam et al., 2015). A similar conclusion was obtained by Turhan et al. (2014) that U-value of wall is one of the most effective parameter that influences the energy demand associated with a building. Addition of advanced materials such phase change materials (PCM) near to wall cavity have resulted in lowering the peak cooling load (Kishore et al., 2020).

Studies have indicated a large amount of heat gain generated in indoor space is associated to the thermal transmission across windows. The U-value and shading coefficient of windows were two of the major determinants that would impact the building energy demand (Chua and Chou, 2010). According to Bojić and Yik (2007), installation of single low-e glass instead of clear glass would prove to be a cost effective strategy to reduce the heat gain. Similarly, Chua and Chou (2010) found that the shortest payback period with satisfactory cooling energy was achieved through the implementation of single low-E single glazing. However, double-layer glazing would provide large reduction in heat gain, it felt short in providing adequate daylighting compared to single low-E glazing (Huang et al., 2014). The largest cooling energy demand in residential apartments located in South Korea was reported to be caused by the use of glazing system with high solar heat gain coefficient, whereas a reduction in thermal transmittance value lead to 26% energy savings (Kim and Suh, 2021).

Impact of wall insulation thickness on building energy demand have also been subjected to study. The influence of wall insulation thickness was evaluated for four different exterior zones of an office building at four different orientations with different external wall insulation thicknesses under three different climates in china. It was observed that the increase in wall insulation resulted in significant energy savings in Beijing's climate, whereas the insulation thickness hardly had any impact on the energy conservation under Guangzhou's climate (Pan et al., 2012). Cheung et al. (2005) found that reducing the solar absorptance value of wall by 30% can result in 13% energy saving in residential buildings of Hong Kong.

Window area and shading designs

According to a study conducted by Lawrence Berkley National Laboratory, 29-34% of energy consumption in residential and commercial buildings were windows-related (Apte and Arasteh, 2006). Thus, it is estimated that about 10-40% reduction in lighting and mechanical system energy use can be achieved by well-designed fenestration (Ander, 2014). The contribution of windows in comparison to the external wall to generate heat gain can be mapped through an index named as Window-to-wall ratio (WWR), which represents the portion of window area to the overall gross external wall area. As per Lam et al. (2005), the WWR of Hong Kong housing sector ranged from 20 to 40%, where bigger flats were attributed with larger WWR. Reducing the WWR from 40% to 25% would result in 18% cooling energy savings according to Sang et al. (2014). A reduction in window area might lower the thermal heat gain, however, it may also lead to reduction in the natural light, in turn resulting an increase in internal heat gain through use of artificial lighting (Huang et al., 2014). Ghisi and Tinker (2005) conducted a study to find the optimal WWR to reduce the energy consumption arising from artificial lighting in two different regions, namely Leeds in the United Kingdom and Florianapólis in Brazil. It was found that WWR ranging from 10.8 to 44% would be suitable for Leeds, whereas WWR range from 20.6-86.2% is ideal for Florianapólis. However, in this study, the optimal WWR was recommended based only on lighting energy use.

Overhangs are one of the oldest and popular external shading devices used in buildings. Aldawoud (2013) analysed the influence of overhangs on building energy efficiency and reported that it could efficiently reduce the cooling load in summer season. The depth of overhang is an important parameter. A study conducted by Alaidroos and Krarti (2015) on residential buildings of Kingdom of Saudi Arabia suggested that_overhangs with_projections ranging from 0.1-1.0 m can aid in energy conservation. An overhang projection of 0.5m lead to generate an energy savings of 3.6% in Dhahran, whereas the same projection leads to save 5% of energy in Riyadh. In a study conducted to analyse the thermal and daylighting performance with shading device on an office building envelope located in a cooling dominated region, it was suggested that effectivity of overhang subdues if its depth is more than half of the window height (Huang et al., 2014). Additionally, they suggested that overhangs have better performance compared to interior blinds.

Bansal et al. (1994) provided means to quantify the efficiency of shading device by relating the vertical and horizontal shadow angle to relationship between length of shaded area on window or wall surfaces. This is expressed through Equation 2.3.

$$tan\sigma_v = \frac{tan\beta}{cos\sigma_h} \tag{2.3}$$

where σ_h is the solar azimuth angle and β is the solar altitude angle.

Building construction characteristics

The floor area, orientation and morphology of buildings also have significant influence on the building cooling energy consumption. The impact of floor area and external wall on the building energy demand could be explained through physical sense and heat transfer equations such as Equation 2.1. As per the International Energy Agency (IEA) report, there was increase of 60% in the building floor over the last two decades and another 20% increase is set to happen in this decade, resulting in a total floor surface area of 45 billion m^2. These increase is estimate to happen in cooling dominated regions (IEA, 2022b). The increase in floor surface area is one of the primary reasons associated with an increase in global space cooling energy demand (IEA, 2022a). Tso and Yau (2003) highlighted the significance of floor area to electricity consumption during the summer season in a sub-tropical region. It along with other parameters such as building shape and orientation are taken in to account to get more insights on building energy consumption or at times it is also used as input variable for a statistical tool for making building energy prediction (Wong et al., 2008, Chou and Bui, 2014).

The building orientation would play significant role in the resulting energy consumption due to the sun path in different climatic regions. Cheung et al. (2005) conducted simulation of cooling energy consumption of residential buildings of Hong Kong for different orientations. The apartments facing west direction had the highest cooling energy demand followed by the ones facing south-west and north-west directions. Similarly, Qin and Pan (2020) studied the influence of orientation as a building energy saving measure. It was observed that it has the highest energy use intensity while the building is facing West and East, whereas the lowest value was reported when the building is oriented towards South and North. Abanda and Byers (2016) also confirmed that the building orientation plays a very important role in the energy demand generated within a building. They utilized the building information modelling tool *Revit* and energy simulation software *green building studio* to analyse the influence of different orientation on building energy consumption. The best orientation was towards south (+180), whereas the worst orientation was towards north-east (+45).

The shape of a building would influence the building cooling energy demand, as the solar radiation received by it can increase the energy requirement for cooling by 25% (Mingfang, 2002). Compactness index and shape factor are two variables related to shape of a building that would influence its associated energy demand. The compactness index is ratio of volume to external area of a building, where a very compact building will have least amount of surface exposed to possible heat gains or loss. The relative index of compactness (RC) of a building is the ratio between its compactness index and the compactness index of a reference building (Pacheco et al., 2012). Ourghi et al. (2007) studied the impact of building shape on building energy consumption. It was found that for a building with a higher RC, there was small perimeter wall area exposed to the outside and thus, resulted in lower cooling energy load. They further studied the influence of RC on two building shapes, namely rectangular and L-shaped with WWR of 25%. A similar trend for higher RC was observed as earlier in energy requirement. Yang et al. (2008) adopted a parameter named shape coefficient, which is the ratio of total building envelope area to enclosed volume to evaluate the energy requirement of office buildings in five different climatic zones of China. The study indicated the energy requirement for heating as well as cooling would increase with an increase in shape coefficient.

2.2.2 Weather

Weather is an important parameter that would drive a significant portion of energy transfer within a building. While it is difficult to predict the actual weather condition of a location at a given time, the general climate can be described in a meaningful way. As the weather can change from one year to another, a methodology to encompass the weather variation over multiple years were developed and it is commonly referred to as Typical Meteorological Year (TMY) (Wilcox and Marion, 2008). The TMY data represents a location's annual average weather as well as the range of weather extremes. Thus, this data is generally considered to be more relevant compared to the Actual Meteorological Year (AMY) for prediction of future energy requirement (Fumo, 2014).

The American Society for Heating, Refrigerating, and Air-Conditioning Engineers (ASHRAE) classifies the climate zone of a location based on its TMY data (ANSI/ASHRAE Standard 169, 2013). ASHRAE climates zones are labelled from 0 for extremely hot to 8 for sub-arctic. Along with these zone numbers, alphabetic letters are attached to form the subtype, where A refer to Moist, B for dry and C for Marine. These zone numbers are a function of heating degree days (HDD) and cooling degree days (CDD) obtained from TMY data. The HDD is obtained by summing of difference between a base temperature and average hourly outdoor air temperature over a year, provided the hours that report an outdoor air temperature above the base temperature is discarded. The same calculation is adopted for CDD provided a different base temperature for cooling is used. The HDD and CDD is determined by the expression as shown in Equation 2.4 and 2.5 (Brackney et al., 2018).

$$HDD = \sum_{i=1}^{8760} \frac{MAX(T_{base\ heating} - T_i, 0)}{24} \tag{2.4}$$

$$CDD = \sum_{i=1}^{8760} \frac{MAX(T_i - T_{base\ cooling}, 0)}{24} \tag{2.5}$$

Other aspects such as altitude, wind speed, psychometric conditions and solar insolation are reported in weather data files. The subtype in climate zone is related to humidity and is a function of rainfall as well as outdoor temperature. The outdoor temperature is a critical factor, as its increase owing to climate change can deeply impact the cooling energy requirement today and the years ahead. An increase of outdoor temperature was predicted by Radhi (2009), where it showed that outdoor temperature would rise from 1.6-2.9 ^{o}C in 2050, whereas rise of 2.3-5.9 ^{o}C is estimated in the 2100. Owing to the impact of climate change, it is being predicted that there will be a rise in cooling demand compared to heating demand. Consequently there will be an increase in carbon emissions associated with buildings (Yau and Hasbi, 2013). One of the primary mitigation strategy is create a better envelope design and increasing the set-point temperature (Mui et al., 2021).

2.2.3 System operations

Indoor set-point temperature

The indoor set-point temperature is another critical parameter that significantly influences the building cooling energy consumption. Setting a higher indoor set-point temperature is considered an effective strategy for reducing cooling energy consumption. The indoor set-point temperature within residential buildings can vary in wide range compared to an office building having pre-set temperatures. The Indoor temperature is closely associated with occupants' cognitive ability and productivity (Tham and Willem, 2010). A temperature set–point that is neither too cold nor too warm is typically referred to as the neutral temperature T_{neu} (ºC), which the occupant judges as the optimal temperature for comfort (Mui and Wong, 2007b). It is claimed that there is a substantial correlation between T_{neu} and the outside air temperature. Rodríguez-Soria et al. (2014) conducted research comparing the operative temperature ranges for residential buildings proposed by various standards. According to Lam and Li (2000) research, the temperature ranges inside air-conditioned homes in Hong Kong range from 21 to 23.5 degrees Celsius. Since it is difficult for room air conditioners to control the set–point of relative humidity, it is typically not stated in residential buildings. Nevertheless, the dehumidification effect does have an impact on the effectiveness of the cooling system (Kosar, 2006). In the case of healthcare facilities, the typical design temperature of patient rooms and intensive care wards in the United States of America ranges from 21-24 ºC, whereas in the United Kingdom, it is 20-22 ºC (Beggs et al., 2008).

Coefficient of performance (COP)

The coefficient of performance for cooling is defined as the ratio of rate of heat removed to the rate of electrical energy input to the air-conditioning system. It is often used as an indicator of system efficiency due to its significant influence in the prediction of building energy consumption (Neto and Fiorelli, 2008). While predicting the cooling energy consumption for high residential buildings, Chua and Chou (2010) utilized COP varying from 2.5-4.5. Its value is dependent on heat rejection efficiency of machine as well as other factors including outdoor temperature, moisture content and sensible heat ratio. A drop in COP with an increase in outdoor temperature was evaluated by the Japan refrigeration and Air-conditioning Association (Shimoda et al., 2007). Kosar (2006) evaluated the relationship between COP and sensible heat ratio and associated the drop in COP to extra dehumidification demand arising in sub-tropical regions. Despite the change in sensible and latent loads with respect to time in an indoor environment, a fixed COP is often utilized in building energy simulation. Hence, the use of dynamic COP with respect to sensible heat ratio would present a more realistic estimation.

Ventilation rate

The ventilation rate supplied to an indoor space varies based on building type and occupants need. It is vital to supply adequate fresh air to ventilate an indoor space to maintain good indoor air quality by dilution of indoor contaminants. The ventilation rate can be expressed in terms of occupant outdoor air rate, area outdoor air rate and air change per hour. As per ASHRAE recommendation, an ACH of 0.35 is recommended for residential buildings, whereas a review done by Yoshino et al. (2004) suggested an ACH of 0.5. It is difficult to maintain a specific ventilation rate in residential buildings installed with a window type or split type air-conditioner compared to an office having a centralized air-conditioning system. A study done by Lin and Deng (2003) showed that ventilation rate within a residential bedroom can vary from 1.5 Ls^{-1} ps^{-1} to 4.5 Ls^{-1} ps^{-1}. It was suggested that 3.0 Ls^{-1} ps^{-1} would be optimal value.

Infiltration rate

In addition to supply of controlled outdoor air rate through air conditioning system, outdoor air can ingress into building through cracks or other openings, a phenomenon termed as Infiltration. The infiltration is often driven by the wind and stack effect as well as it is associated with age of a building, its construction as well as ventilation system (Sadineni et al., 2011). In a building thermal energy simulation, it is possible to model a completely airtight building, however it would not be representative of the reality. Hence, a small air leakage is often modelled. A study indicated that air-tightness in taller building with sophisticated design and construction is superior compared to shorter buildings (Persily et al., 2009).

2.2.4 Internal loads

The heat generated indoors by occupants, lighting, and equipment's contribute towards the internal load. In practice, the lighting and equipment load is often evaluated by using an index that is normalized by the floor area, known as lighting and equipment power density. These power density value would change based on internal load schedule, appliance and building type. On the other hand, the occupant load is related to occupancy and metabolic rate. The metabolic rate associated with each activity can be found in ASHRAE Standard 55 (2020) and the number for occupants at a given instant of time will be based on the occupancy schedule.

The occupant activities and behaviour are identified to be a significant contributor in the variation of energy consumption among different building types. It is also a cause of large uncertainty in the prediction of building energy consumption (Yan et al., 2015). In building energy use prediction, a general pattern is seen where the occupancy data is substituted with building or equipment schedules. For instance, to mimic the presence of occupants in building, Kwok et al. (2011) used the power consumption of primary air handling units as occupancy data. The practice of equating the operation of air-conditioner to occupancy schedule would not be suitable for a residential building, where the AC operation is depended on occupant behaviour. Li et al. (2007b) found that the electricity requirement for cooling in 25 households within a large residential building located in Beijing varied widely despite sharing a similar building envelope. The study found out that the discrepancy was associated with variation of operating mode of the split-type air-conditioning system. Mui and Wong (2007a) showed that there would be a variation of 1-5 % in cooling load capacity with the integration of a time varying occupant load profile in an office building located in Hong Kong.

In building performance simulation tools, the occupant profile is mimicked in a static manner (Hoes et al., 2009). However, the dynamic interaction of occupant with its indoor environment should be modelled stochastically or probabilistically. A study found that there is a high inter-individual variation in occupancy for four office buildings located in Austria (Mahdavi et al., 2008). It is also observed that time of presence and absence of occupants within the indoor environment is significant in the dynamic interaction of occupants with building. Wong and Mui (2006) conducted a survey of 720 households in Hong Kong to evaluate the occupant load variation. Based on the survey, they proposed that the number of occupants at a given time could be estimated from the multiplication of hourly occupant load variation factor and maximum number of occupants as shown in Equation 2.6. This probabilistic approach could aid in determining the variation of hourly cooling energy consumption within a residential building.

$$N_k = N_{max}\varphi_k \qquad where\ k = 0,1,2,3 \dots \dots .23\ hour \tag{2.6}$$

The air-conditioner schedule should also be subjected to variation as seen in occupancy pattern as it is dependent on an individual's behaviour, physical and socio-economic factors. Schweiker and Shukuya (2009) analysed the AC operation pattern based on occupant's choices. The study noted preference of operation and demographic factors as influencing factors amongst few others. The preference is the choice of an individual to be in an air-conditioned space, whereas demographic factors would be the income, age, gender, and others related to an individual. Further, a study also showed the influence clothing on the cooling energy consumption.

In building energy estimation simulation tools, the common practice to represent the AC operation is in terms of time or other factors such as indoor set-point temperature, occupant schedule, etc. However, it is often challenging to implement a schedule that would imbibe the occupant behavior. A regression approach considering two or three factors to determine the status of air conditioner have been used previously. One typical example is the model developed by Kempton et al. (1992) where an outdoor temperature and hour of the day was used to predict the air conditioner status. Schweiker and Shukuya (2009) also followed a similar approach, although used different factors such as mean value of outdoor temperature, occupants' preference, and some other factors to predict the status. A promising approach was proposed by Ren et al. (2014) where AC usage was determined based on conditional probability analysis. Although, the approach is flexible with respect to simulation time, it was rendered difficult to implement for large scale simulation. A simpler probabilistic approach-based AC operation scheduling method is recommended.

2.3 Existing prediction methodologies

In the section 2.2, the impact of the relationship between influencing parameters and building cooling energy consumption was presented. This section discusses the method of evaluating this relationship, which is the most important factor in confirming that the prediction is accurate. The building attributes, equipment and systems, weather, and occupants are influential factors that all play a role in the complicated relationship between energy performance and buildings (Asadi et al., 2014). In the past 30 years, numerous simulation models and energy prediction tools, each using a unique approach, have been developed to forecast the amount of energy used in buildings. A brief discussion of these approaches will be given in this section.

2.3.1 White-box models

The white box model is an engineering-based building energy prediction method in which the inner aspects of building physics are apparent. It's the only method that doesn't require past energy data. The appliance ownership and usage patterns can be utilised to forecast end–use consumption. White box models will do extensive dynamic building simulations using physical relationships like heat transfer or thermodynamics. Although, developing these equations is hard, and manual calculation is time-consuming. Thus, Engineers are developing computer simulation tools to enhance simulation time and accuracy (Crawley et al. 2008, Coakley et al. 2014). The inability to forecast behaviour and extended model building and simulation time are limitations of this simulation approach. This section will briefly overview the available models, their applications, and their advantages and disadvantages.

2.3.1.1 Analytical methods

Over the years, different approaches have been adopted to perform building energy analysis, and these approaches can be classified into steady-state and transient models (Boodi et al., 2022). These approaches use physical principles to determine the thermal dynamics and energy behaviour within buildings or sub-level components. The degree-days method is a steady-state method representing a simplified way to determine the building energy consumption (Al-Homoud, 2001). It is primarily based on the assumption that energy consumption is proportional to external and internal temperature differences. The monthly energy consumption E_m can be calculated as shown in Equation 2.7, assuming a global building transmission coefficient H (De Rosa et al., 2014).

$$E_m = \frac{H * DD_m * t_h}{\eta_{hs/cs}} \tag{2.7}$$

where t_h heating time in a day, $\eta_{hs/cs}$ represents the efficiency of the equipment, and DD_m is the total heating or cooling degree days of a month. To perform the heating and cooling calculations, the degree days can be estimated through Equations 2.8 and 2.9,

$$Heating: DD_m = \sum_{d=1}^{D_m} \left(T_{b,hs} - \overline{T}_{e,d}\right)^+ \tag{2.8}$$

$$Cooling: DD_m = \sum_{d=1}^{D_m} \left(\overline{T}_{e,d} - T_{b,cs}\right)^+ \tag{2.9}$$

where $\overline{T}_{e,d}$ stands for the mean of maximum and minimum daily external temperature of a day d, $T_{b,hs}$ represents the base temperature for heating and $T_{b,cs}$ represents the base temperature for cooling. The + sign indicates that only the positive values are considered for summation. Based on the external temperature, different approaches can be adopted to determine the degree days (Al-Homoud, 2001). An application of this method can be seen in (Büyükalaca et al., 2001).

The overall thermal heat transfer value (OTTV) used to be a popular index to determine the thermal performance of buildings (Chan and Chow, 1998, ASHRAE Standard 90-75, 1975). It was a suitable method applicable to buildings in hot climates as it accounts for average heat gain into the building through the envelope. It has three major components, namely, (a) conduction through opaque walls, (b) conduction through window glass, and (c) solar radiation through window glass (Hui, 1997). The two equations that are used to estimate the OTTV value for wall $OTTV_{wl}$, and roof $OTTV_r$ are expressed as shown in Equation 2.10 and 2.11,

$$OTTV_{wl} = \frac{\left(A_{wl} \times U_{wl} \times TD_{eqw}\right) + \left(A_{wd} \times S_c \times SF\right) \times \left(A_{wd} \times U_{wd} \times \Delta T\right)}{A_e} \tag{2.10}$$

$$OTTV_r = \frac{\left(A_r \times U_r \times TD_{eqr}\right) + \left(A_{rf} \times S_c \times 434.7\right) \times \left(A_{rf} \times U_{rf} \times \Delta T\right)}{A_r + A_f} \tag{2.11}$$

where A_{wl}, A_{wd}, A_e, A_r, and A_{rf} are the area of the opaque wall, window, external envelope, roof, and fenestration at the roof, U_{wl} and U_r are the thermal transmittances of wall and roof, TD_{eqw} and TD_{eqr} are the equivalent temperature difference of wall and roof, S_c is the shading coefficient, *SF* is the solar factor, ΔT is the difference between indoor and outdoor temperature. Yang et al. (2008) utilized the OTTV approach to study the effect of building envelopes based on different climate zones in China. The steady-state modelling techniques have found their application in determining building energy performance owing to their simple and fast calculation approach. One of the major limitations of this approach is that the inertia of the building envelope is neglected (De Rosa et al., 2014). Moreover, newer technologies such as free cooling (Brun et al., 2013, Rouault et al., 2013) and phase change materials (Zhou et al., 2012, Álvarez et al., 2013) that exploit the building inertia cannot be analyzed with a steady state approach. Furthermore, ASHRAE abandoned the usage of OTTV in 1989, where the reliability of using thermal transmittance to quantify the thermal storage effects in the envelope was criticized (Wilcox et al., 1985). Also, the emergence of building energy simulation software for building energy analysis has proven to have better efficiency and flexibility with respect to the physical index (Hui, 1997).

2.3.1.2 Simulation programs for building energy analysis

The whole building energy simulation software, such as EnergyPlus, TRNSYS, Dymola, etc., solves the thermodynamic equilibrium and heat transfer equations to model the dynamic thermal behaviour of buildings. These are developed on a multizone or nodal approach, where the whole building or one room is divided into segments, with each segment represented through a node (Pedersen, 2007, Clarke, 2007). This approach assumes that the building zone is a homogenous volume zone with uniform state variables. The energy conservation equations are applied on each node, and the whole nodal network is solved simultaneously. The nodal approach can model the behaviour of multiple zone building over a considerable time. Also, it is a well-suited approach to determine the energy consumption and time evolution of space-averaged temperature in a room (Foucquier et al., 2013). These building energy simulation tools are also known as the white box method, as the inner aspects of building physics adopted for building energy modelling are evident (Mui et al., 2021).

Over a hundred simulation software can be utilised to model the building energy, as summarised by the US Department of Energy (DOE, 2021a). Crawley et al. (2008) discussed the performance of the commonly used building energy simulation tools and confirmed their capability to do a detailed energy analysis. Li and Wen (2014) explained these programs' simulation and data flow procedures, as shown in Figure 2.1. The input parameters of building characteristics (geometry, material, and zones), system description (HVAC, operation schedules, ventilation rate, and set-point), and component description for the internal load can be estimated from existing or pre-construction phase buildings. The weather data can be extracted from the regional weather observatory. The simulation engine comprises various mathematical equations to simulate the building operation and estimate the energy consumption. The output from the engine can be extracted based on specific needs such as hourly envelope heat gain, the peak load of a zone or zones, etc.

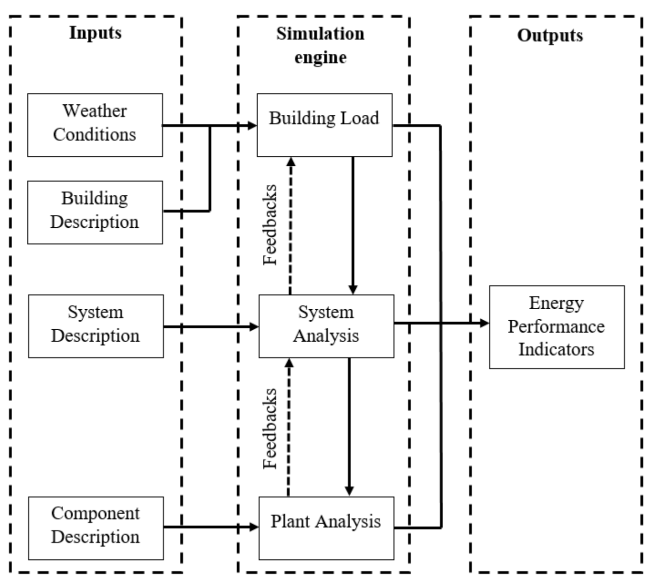

Figure 2.1 Data flow and procedure in a simulation model (Li and Wen, 2014)

A review by Nguyen et al. (2014) revealed that EnergyPlus is the most famous building energy simulation tool for building optimisation, followed by TRNSYS and DOE-2. EnergyPlus is an open-source program developed by the United State Department of Energy based on the nodal approach (DOE, 2021b). Owing to its fast simulation speed and precise energy consumption estimations, it is widely used to calculate and analyse the energy consumption of buildings and systems (Trčka and Hensen, 2010). A case study done by Westphal and Lamberts (2005) revealed the prediction capability of EnergyPlus by showing that the annual electricity consumption was only 1% lower than the actual value. Fumo et al. (2009) showcased the ability of EnergyPlus to analyse the combination of cooling, heating, and power systems. The EnergyPlus program is considered superior in terms of variable time steps and user-configurable modular system compared to its predecessor models, BLAST and DOE-2 (Crawley et al., 2001). Since these programs are based on physical principles, the input-output relationship is explainable. It can also be used in various buildings and even on an urban scale. Hence it has universality. Moreover, these simulation program doesn't necessitate the collection of historical data for energy consumption prediction. A virtual building can be simulated by collecting the required information, such as building construction and material properties (Yu et al., 2022). However, these programs are also attributed with a few drawbacks. These tools would prove inefficient in conducting energy estimation for many buildings, as it would be challenging to collect the data of all the facilities that need to be analysed (Yu et al., 2022). Further, the model construction for energy estimation would be complex, and it would restrict the usage to only personnel with high expertise (Mui et al., 2022).

2.3.2 Data-driven approaches (Black Box model)

The data-driven approaches are based purely on data or statistical methods for prediction. Regression, support vector machines (SVM), and artificial neural networks (ANN) are commonly used models. These approaches have been widely used in building energy consumption prediction, and they can do so without any knowledge of the building physics involved. Thus, these approaches are also known as black box models. A basic overview of the application of each method in building energy prediction is given in this section.

2.3.2.1 Statistical regression

The statistical regression models are primarily used to correlate energy consumption with influencing variables. The utilisation of these empirical models necessitates the generation or collection of historical data. A review done by Zhao and Magoulès (2012) classified the use of statistical models into three main areas: (a) Identification of essential parameters in energy consumption, (b) energy prediction with few simplified variables, and (c) prediction of performance with energy index.

The linear regression was introduced by Sir Francis Galton (Galton, 1886) in 1886, and its first application to predict energy consumption in buildings was seen in (Parti and Parti, 1980). Parti and Parti (1980) developed a new method with linear regression, conditional demand analysis (CDA), a linear multivariate regression technique used for building energy forecasting. Lafrance and Perron (1994) used the CDA method as a signal-processing tool to determine the evolution of residential electricity demand at a regional level. In contrast, Aydinalp-Koksal and Ugursal (2008) used it to estimate the end-use energy consumption at the national level. Mastrucci et al. (2014) developed a geographical information system (GIS)-based multiple regression model to evaluate the energy-saving potential of retrofit options such as window replacement, envelope insulation, and HVAC upgrade for building stocks at the city scale. The method was simple and could provide quick energy consumption prediction.

The technique has been used to evaluate the relationship between one or two variables, such as climatic conditions and building characteristics, with the building energy demand. Wong et al. (2008) utilised a multivariate regression model to predict the building fabric load in office buildings located in Hong Kong. A study by Amiri et al. (2015) using the multiple regression analysis concluded that out of the 17 building-related parameters, occupancy schedule and exterior wall construction strongly influence building energy consumption. Ciulla and D'Amico (2019) used a multiple linear regression (MLR) method to forecast building energy performance. An energy database was created by running 1560 simulations, and important parameters influencing the thermal balance during heating and cooling were identified based on the Pearson coefficient. Utilising the MLR method, a linear relationship between a few model input parameters and response variable was established through the fitting procedure. Simple correlations were obtained from a few well-known parameters to determine the heating and cooling energy demand.

The regression model has found its applicability in evaluating the building energy consumption based on the energy index. A multiple regression model benchmarked energy efficiency by developing a relationship between the energy-use intensities (EUIs) index and explanatory factors such as operating hours (Chung et al., 2006). A Principal component analysis (PCA) on the weather condition of a sub-tropical region was conducted in (Lam et al., 2010), and a climatic index *Z* based on dry bulb temperature, wet bulb temperature, and solar radiation was developed. The correlation between building energy use and simulated cooling load with climatic index *Z* was done using the regression model. Wu et al. (2020) utilised a linear regression model to predict the energy consumption index of multifunctional areas. The energy index from different functional sectors would evaluate the overall energy consumption within buildings.

However, the multiple regression models are associated with a few limitations, such as the inability to model non-linear problems, lack of flexibility, and difficulty managing multicollinearity within prediction results (Foucquier et al., 2013).

2.3.2.2 Support vector machines

Vapnik and his co-workers (Boser et al., 1992) developed a supervised algorithm for classification in 1992, which evolved into the Support Vector Machines (SVM) that we know today (Cristianini and Shawe-Taylor, 2000). It also finds extensive application in forecasting and regression problems besides classification. They are considered to be highly effective in modelling non-linear problems with relatively lesser training data (Zhao and Magoulès, 2012). In this approach, by utilising a kernel function, the input space containing input data is mapped into high dimensional feature space through a non-linear mapping method to perform linear regression (Li et al., 2009). One of the limitations of SVM is selecting the appropriate kernel functions, as it is mainly accomplished based on the data characteristics and user experience. The SVM method has broad applicability in building energy forecasting. Dong et al. (2005)

were the first to utilise an SVM approach for building energy consumption prediction by training the SVM model with three years of monthly electricity bills. The model exhibited good prediction performance too. Shao et al. (2020) utilised an SVM approach to predict the energy consumption of hotel buildings. Weather conditions and HVAC system operation parameters were used as the model's input variables. They provided insight into the actual energy usage and suggested potential improvements in building operations to reduce energy consumption. A comparative study was done between SVM and autoregressive integrated moving average model (ARIMA) in the estimation of the cooling load of the HVAC system. It was reported that SVM had better prediction performance than ARIMA (Hou and Lian, 2009).

2.3.2.3 Artificial neural network

An artificial neural network was conceived from generalising biological neural connections in the human brain to mathematical models. An ANN often comprises one or more hidden layers sandwiched between the input and output layers. The layers are connected through several neurons that receive signals or information from the preceding neuron and propagate this signal with a weighting factor. The weighted sum received at the hidden layer from its preceding layer would be summed as a net value to transform it into an output value using appropriate activation functions (Mui et al., 2022). There are several learning algorithms linked to a neural network, such as a back propagation neural network (BPNN), general regression neural network (GRNN), recurrent neural network (RNN), and fuzzy neural network (FNN). However, backpropagation is the most widely used learning algorithm in building energy prediction (Ekonomou, 2010).

The technology advancements in the last two decades have aided neural networks in finding applications in various fields such as aerospace, manufacturing, energy, buildings, etc. ANN is widely used in the building sector during different stages: conception, control optimisation, prediction of energy consumption, retrofitting, and performance evaluation (Ahmad et al., 2018). Numerous variables can influence the energy consumption associated with buildings, and these variables would have complex non-linear multivariate interrelationships among them. With its inherent ability to model non-linearities without any time lag, ANN is beneficial in forecasting building energy consumption. Moreover, ANN is a very robust, noise-immune system (Runge and Zmeureanu, 2019). ANN is also superior in simulation speed compared to its physical simulation counterparts for prediction (Liu et al., 2019).

ANN can predict building energy consumption for short-term or long-term loads. At the same time, it can indicate the energy consumption for an individual apartment or entire building or block of buildings or at a city scale. A study by Mena et al. (2014) for predicting short-term electricity demand suggested that outdoor temperature and solar radiation were the most important variables influencing building energy consumption. Similarly, a short-term building energy demand model was developed by Chae et al. (2016). Mihalakakou et al. (2002) developed a neural network to predict the hourly energy consumption of a dwelling in Greece. However, as dates were not used as an input variable in the study, it limited its applicability to predict annual energy demand change. Utilizing the short-term energy data, an ANN model predicted the yearly heating demand of buildings with high prediction accuracy (Olofsson and Andersson, 2001). Aydinalp et al. (2002) used the ANN model trained on data from 1993 household energy use and weather database to predict the residential cooling energy consumption at the national level. Ekonomou (2010) conducted a long-term energy consumption prediction of Greece utilizing the artificial neural network. The model was termed effective in implementing energy policies in Greece.

Based on a study conducted by Chou and Bui (2014) to predict the heating and cooling demand using data-driven approaches, it was shown that ANN and support vector regression (SVR) would have better prediction accuracy compared to other statistical techniques. Ahmad et al. (2017) employed the ANN and random forest (RF) technique to predict the hourly electricity consumption of the HVAC system. In the study, ANN provided superior performance compared to random forest. A study by Farzana et al. (2014) used six prediction models for the energy forecast of residential buildings. It was concluded that ANN had higher precision than the other five prediction models: first-order differential grey model, second-order derivative grey model, regression model, polynomial model and polynomial regression model. Aydinalp-Koksal and Ugursal (2008) utilized ANN, conditional demand analysis (CDA) and an engineering model to predict the national-level residential end-use energy consumption, in which ANN produced better prediction results than the other two. In a study by Neto and Fiorelli (2008) to predict building energy consumption under different climatic conditions, ANN and EnergyPlus exhibited similar prediction accuracy.

Despite the several advantages attached to ANN for providing an accurate prediction accuracy for building energy consumption, it also has a few limitations. The data-driven approaches such as ANN for energy consumption prediction rely heavily on data. The new buildings with no historical data and old buildings with no advanced building automation system remain challenging in the growth and development of data-driven approaches due to the insufficiency of quality data (Li et al., 2021). ANN is also associated with poor generalization capability for unseen data beyond its training range, thus limiting the trained neural network models to a specific range (Foucquier et al., 2013, Amasyali and El-Gohary, 2018). The prediction performance of neural networks is also greatly influenced by the database used for training the neural network, where data inadequacy or insufficiency can significantly degrade its implementation (Paudel et al., 2014). Moreover, one of the significant limitations of neural networks is that underlying physics is often opaque and hence the interpretability of input-output is difficult (Mui et al., 2022).

2.3.2.4 Summary of black box models

The statistical tools discussed in this section exhibit significant advantages regarding simulation time, accuracy, robustness, and flexibility for building energy consumption forecasting. Considering the various statistical tools listed in the above sections, the easiest statistical tool for prediction is the linear regression model. It can provide good prediction performance and doesn't require high expertise for its implementation. However, it is limited by its inability to model non-linear problems. However, this shortcoming can be overcome by utilizing a support vector machine or artificial neural network. The support vector machine can work efficiently with non-linear problems and provides good prediction capability with relatively fewer data. However, the choice of the kernel function in the model is purely based on the data characteristics and user experience. A wrong choice of kernel function can significantly impact the learning and generalization ability of the model. Additionally, SVMs are associated with a high computational burden compared to ANN. On the other hand, ANN can easily handle non-linear multivariate problems and can provide prediction without a significant time lag. It can also work with noisy data, as it is noise immune. ANN has been used more widely for building energy prediction than other statistical tools. ANN models don't need any starting hypothesis. However, the model lacks interpretability in the input-output relationship as it functions as a black box. Further, it relies primarily on the completeness of data, where any inadequacy or insufficiency can lead to massive degradation of its performance. ANN is also associated with a lack of generalization capability for parameters falling outside its training range, restricting its use as a design exploration tool. In short, each tool has its advantages, disadvantages and limitations and the choice of tool to be used is purely at the user's discretion and the targeted outcome to be achieved.

2.3.3 Hybrid methods (Grey box model)

As discussed in earlier sections, physical simulation and statistical tools used for building energy prediction have inherent advantages and drawbacks. The hybridisation of these tools would result in the development of an improved tool for energy prediction that would embrace the strength and expel individual shortcomings. The hybrid approach follows a two-step development process wherein a physical model is utilised to represent buildings' physical and operational characteristics and its associated system with energy consumption. After that, by identifying and quantifying the key parameters through statistical analysis, the model will be enabled to provide good energy consumption estimation.

Hygh et al. (2012) utilized Monte Carlo simulation to conduct a building design space exploration and estimated the annual energy consumption of each design instance using EnergyPlus (EP). The resulting dataset from Monte Carlo simulation is utilized to develop a multivariate linear regression model. They suggested this regression model would be an effective tool compared to the usage of a detailed energy simulation model during early design stage to predict the influence of key parameters on building energy consumption. A similar study was done by Asadi et al. (2014) to predict the energy consumption of commercial buildings. The DOE-2 building energy simulation software was utilized within the Monte Carlo framework to predict the energy consumption for each design instance. Building materials, building shape, orientation and occupant schedule was utilized as input parameters. The building energy dataset created through the Monte Carlo simulation was utilized to conduct the multi-linear regression analysis. The regression model will act as a pre-diagnostic tool to predict the energy performance within office buildings. Thus, hybrid approach provides a fast design space exploration strategy to identify the key variables combinations in a cost-effective manner.

Valovcin et al. (2014) developed a hybrid model by modelling the energy consumption from 1250 building through building energy simulation (BES). The output from BES was utilized as an input for the multiple linear regression model to post process the results of building physics based tool. Brøgger et al. (2019) noted that assessment of energy saving potential necessitate accurate estimations, usually obtained through building physics-based approaches. However, due to lack of data compels users to take normative assumptions leading to biased estimations. In order to overcome the limitations within traditional buildings physics-based approaches, a regression-based hybrid modelling approach was developed to predict the energy saving potential of Danish building stock. The statistical part of the hybrid model was based on multiple linear regression model. These are good examples of physics-based data-driven models. Another version of hybrid method includes data-driven based physical methods. One of the typical example of this approach is the Canadian hybrid residential end-use energy and emission model (CHREM) developed by Swan et al. (2013). It is a hybrid model that models the district hot water (DHW), appliance and lighting end-uses in a statistical tool and uses this an input for the building physics-based model. Although such a model would automatically model the usage profile, few parameters such as indoor temperature and air change rates remained uncertain.

The combination of statistical approaches is another hybridizing technique to forecast the building energy consumption. Zhang et al. (2020a) utilised a hybrid method composing of long short-term modelling (LSTM) and artificial neural network to predict the short-term building energy load. The operation data of a public building in Shenzhen, China and outdoor meteorological data were obtained to develop the hybrid model. Fourier transform is used to identify the intrinsic periodicity of cooling loads and based on the analysis; the maximum time lag is set as 24 hours in the study. The time lag measurements with time lags shorter than the intrinsic period is fed into the LSTM network to extract new features. These new features are then utilized to train an ANN for making the building cooling energy prediction. The results of study indicated that for one-hour-ahead cooling prediction, the hybrid model has better prediction accuracy compared to the conventional prediction methods.

With the similar intentions to improve the prediction capability, a hybrid method was developed by Yan et al. (2018), combining LSTM and convolutional neural network (CNN) to forecast the energy consumption within a single household. The CNN is added as pre-processing stage in the hybrid method to extract useful features from the original data and convert the univariate data into multidimensional convolution. These are then utilized to train the LSTM network in the hybrid method to forecast the energy consumption. The results of RMSE, MAE and MAPE indicated that the hybrid method deep learning model outperformed the standalone prediction models such as ARIMA, SVR, and LSTM.

Amasyali and El-Gohary (2022) developed a hybrid machine learning model that learns from simulated data as well as real data. It basically consisted of three machine learning models: a machine learning model to predict the hourly values of occupant-behaviour factor, another machine learning model to predict the hourly values of weather factor and lastly, an ensemble model that would predict the hourly cooling energy consumption by utilizing the prediction from other two machine learning models. The good results of root mean square error (RMSE) and coefficient of variation (CV) showed that is a promising approach for building energy prediction.

2.4 Optimization

Optimisation methods have profound use in building energy-related applications. The methodology can be utilised to conduct design exploration by evaluating different design solutions iteratively by performing fewer simulations with respect to traditional parametric studies. This would result in a significant reduction in computational time and cost compared to the conventional approach. This section will discuss the application of optimisation strategies in building energy prediction.

The simplex and non-random complex methods were applied by Bouchlaghem and Letherman (1990) to reduce the discomfort level by variation of fabric properties. Al-Homoud (1997) utilized simplex and non-linear programming methods to optimise energy consumption. The design variables to be optimised were fabric properties, shape, and orientation of buildings. In a later study, Al-Homoud (2005) utilised the Nelder-Mead method to minimise energy consumption through variations in fabric properties. Based on a dynamic thermal model in the Passive House Planning Package, Leskovar and Premrov (2011) used a brute force search method to vary the glazing area to minimise energy consumption. Despite the capability to model dynamic effects, the simulation program was limited to domestic buildings. Moreover, the brute force method is computationally expensive, which would limit the number and resolution of variables. A similar conclusion was made by Bambrook et al. (2011) while using the brute force method to determine the optimal house model based on the life cycle cost analysis.

Such issues can be addressed by the utilisation of meta-heuristic algorithms. Nguyen et al. (2014) analysed 200 papers on building energy optimization and identified the optimizer engines utilised in each. Genetic algorithm and particle swarm optimization were recognised as the most used optimization algorithm, indicating their efficiency and reliability. Similarly, Evins (2013) reviewed the computational optimization methods used in building design to find that genetic algorithm was the most used optimization algorithm. Further, it was indicated in the review that most studies were focussed on minimizing the energy use by optimizing the building envelope. A genetic algorithm was implemented by Coley and Schukat (2002) to minimise energy use. The novelty of the study was attributed to the combination of GA with human judgement. The optimal or sub-optimal solutions could be accessed visually, enabling one to make a choice based on an individual’s preference. A study was done by Tuhus-Dubrow and Krarti (2009) to compare the performance of GA, particle swarm optimisation (PSO) and sequential search in the design of residential building envelope. GA was identified as the best choice when there were more than 10 parameters to be optimised. Further, they utilised GA to optimise nine construction and two shape parameters to reduce the life cycle cost (Tuhus-Dubrow and Krarti, 2010). Similarly, Sahu et al. (2012) utilised GA and the admittance method to minimise the energy consumption associated with an air-conditioned building located in a tropical climate by variation in the selection of construction.

A single-objective optimisation study was conducted for a residential building to determine its life cycle cost by varying the envelope and HVAC system. A comparison was made between GA, PSO, and sequential search for their robustness and effectiveness. The sequential search was identified to be performing poorly with regard to computational effort. Also, while taking a holistic approach to optimising the envelope and system separately, the former proved more effective (Bichiou and Krarti, 2011). The influence of variation of shading and geometry (for a constant floor area) to minimise energy use was investigated with a GA for a degree-hour calculation by Znouda et al. (2007). A simple simulation method was employed with only one climatic condition. A similar study was conducted with a multi-objective genetic algorithm (MOGA-II) to minimise energy use by optimising the depth and angle of shading for diverse glazing options. In this study, the energy simulations were done by utilising the building simulation software ESP-r and Radiance with a Mediterranean climatic condition (Manzan, 2014). Ferrara et al. (2015) studied a classroom to reduce heating, cooling, and lighting energy use with TRNSYS. The energy demand was then optimized by using a genetic algorithm integrated with the TRNSYS software.

Holst (2003) adopted the weighted sum approach to minimise the multi-objectives (energy use and percentage of people dissatisfied) using the Hooke-Jeeves method. The window area, type and thermal properties were used as design variables, whereas the annual hourly simulation was conducted in EnergyPlus. To analyse the trade-off between energy consumption and the life cycle cost of a typical single-family house located in the United States, Fesanghary et al. (2012) combined the harmony search method with a building simulation tool (EnergyPlus) to find the optimal building envelope design that minimises the objectives. With the identification of the Pareto optimal solutions, a better understanding of the trade-off relationship between economic and environmental performance becomes possible. In a recent study, Delgarm et al. (2016) attempted to integrate EnergyPlus with the multi-objective particle swarm optimization method. Building-related parameters such as orientation, shading, window size, glazing, and wall material qualities were chosen as effective and variable parameters. It was demonstrated that by adopting a reliable and robust simulation tool, significant reduction in cooling, heating, lighting, and total energy use can be achieved. Possibly the first multi-objective optimisation study addressing the issue of glare was conducted by Gagne and Andersen (2012). The MOGA approach was utilised in their study to maximise illuminance and minimise glare.

To investigate the potentials of parametric design optimization in sustainability of residential buildings, a closed-loop framework was developed by Toutou et al. (2018) to optimize building parameters such as WWR, construction material, glass material, and shading device. The optimization framework involves a model, simulation, and the optimization evaluation that is performed automatically in a single canvas. In this framework, many software and simulation engines were involved. The parametric modelling is done in Grasshopper, whereas the ladybug and honeybee served as a platform for building performance simulation. Energy simulations is conducted in Energy plus and OpenStudio, while the daylighting simulation is performed via Radiance and DaySim. After parametric modelling and simulation, genetic algorithm can optimize solutions using via Octopus plug-in that supports multi-objective optimization. Finally, the optimum solution that provides best daylighting and energy performance is identified through the proposed framework.

ANNs in building energy prediction encounter three basic issues. First, ANNs initialise randomly, resulting in a local optima and unstable performance during training. Hence, the weights and biases must be adjusted more reasonably. Second, it's hard to choose ANN inputs, such as the amount of energy-related variables and the length of historical energy values. Third, setting hyper parameters is a time-consuming operation in deep learning. The number of layers, neurons, epochs, optimizers, and activation functions affect prediction performance. To solve these difficulties, ANNs must optimise weights and biases, input characteristics, and hyper parameters (Lu et al., 2021).

BPNN was used by Yokoyama et al. (2009) to estimate the cooling demand of a building, and they utilized a global optimization method termed the "Modal Trimming Method." This method helped them to identify the model parameters and enhance the prediction performance. Moazzami et al. (2013) developed a GA-ANN model for daily peak load forecasting in Iran in 2013. The wavelet decomposition method was used to extract the low and high frequency components from the database. In contrast to single data-driven models, this study utilized two separate data driven models to which the low and high frequency data were separately fed. The two ANN were then trained upon these data by utilizing an evolutionary algorithm namely, GA. After testing the trained ANN, each ANN would predict the low and high frequency peak loads. The wavelet reconstruction of low and high frequency would generate the final forecasted peak load. The outcomes of the study demonstrated the efficiency and benefits of the hybrid technique.

A study by Gu et al. (2018) pointed out that it is essential to take into account the influence of indoor temperature and thermal inertia of a building along with the outdoor temperature in the prediction of heat load. The prediction of heat load is carried out by utilizing four models, namely, wavelet neural network (WNN), extreme learning machine (ELM), support vector machine (SVM) and back propagation neural network optimized by a genetic algorithm (GA-BP). The study indicated that GA-BP model performed better compared to the WNN higher prediction accuracies. The weight and biases associated with the back-propagation algorithm was optimized by the GA.

Luo et al. (2020) developed an integrated artificial intelligence-based approach comprising of feature extraction, evolutionary optimization, and an adaptive DNN model to predict the week ahead energy consumption in buildings. A deep neural network (DNN) with several hidden layers is used to show the intricate relationship between multiple influencing elements and building energy usage. Patterns of daily weather data is extracted through clustering and yearly profile was grouped into multiple clusters. Consequently, each cluster's datasets with their own characteristics was utilised to train a DNN submodel. Utilizing a genetic algorithm (GA), the ideal architecture of DNN sub-models for each collection of datasets is determined by choosing the optimal number of hidden layers, number of neurons in each hidden layer, activation function, and training strategy. Therefore, the architecture of the predictive model was made inherently adaptive.

A research study developed an expert ANN trained using a backpropagation algorithm to predict the heating energy consumption of a shelter in a cold area of Iran. Honeybee, Ladybug, and Galapagos add-ons for the Rhino/Grasshopper software were used to analyse the energy use of the models. The ANN-BP was then simulated using a total of nine input shelter parameters (wall thickness, wall U-value, Wall R-value, Window U-value, Window R-value, Number of occupants, Area, Equipment load, infiltration rate). In addition, particle swarm optimization (PSO) and grey wolf optimization (GWO) techniques increased the training performance of the ANN-BP models. Furthermore, various sensitivity tests were conducted on the best ANN model using the garson algorithm. Finally, the Galapagos (based on genetic algorithms) and Silvereye (based on particle swarm optimization) plug-ins were used to optimise the energy usage of the proposed models (Keshtkarbanaeemoghadam et al., 2018).

ShangDong and Xiang (2006) created a novel ANN algorithm that incorporates Chaotic PSO (CPSO). The primary purpose of this combination is to increase load forecasting performance. In comparison to PSO-ANN and GA-ANN, the CPSO method demonstrated better searching efficiency and quality. It also proved to be superior in short term load forecasting compared to PSO-ANN and GA-ANN. Niu et al. (2010) utilized the ant colony optimization (ACO) with neural networks to forecast power load. In the study, an RBF neural network was integrated with the ACO, and it was compared with GM (1, 1), GM (1, 1, 0), and ARIMA using absolute average error. The ANN–ACO exhibited the lowest absolute average error of 1.139%, compared to GM (1,1) (2.339%), GM (1,1,0) (1.257%), and ARIMA (2.04%).

2.5 Summary

Thermal energy demand contributes significantly to building energy costs. This chapter discusses building thermal energy evaluation factors and methods, focusing on building cooling energy use. Materials, construction, climate, cooling systems, interior loads, and occupant behaviour are influential factors that affect building thermal energy use. Since building envelope heat gain is the main heat source, building materials and construction designs have a large energy impact. Outdoor climatic variables affect building cooling energy use by altering heat transfer to internal spaces. Raising the indoor temperature set–point is regarded as the most effective strategy for minimising future cooling energy usage.

The building cooling system may affect space heat rejection relative to cooling needs. Indoor temperature set–points, system COP, and infiltration and ventilation rate are essential. Adjusting the temperature set–point can affect cooling energy usage, although the desired neutral temperature varies by living environment. A set COP for a residential air conditioner may not accurately reflect system performance. A dynamic approach with COP dependent on a sensible heat ratio can override this shortcoming. Equipment, lighting, and people contribute to a building's internal heat load. The first two are expressed as power density normalised by floor area, while the third is based on occupant activity level and the design internal load schedule. Energy performance evaluation emphasises tenant behaviour, especially in residential buildings. Occupancy and air–conditioning in occupied spaces is directly connected. In building energy simulations, a fixed schedule altered by time or preferred condition (i.e., set–points) does not accurately depict occupants' AC usage. Hence, probabilistic occupancy and AC schedules are advised to mimic actual building and occupant variation.

Thermal energy prediction helps with system sizing and energy conservation. The three widely used prediction methods are physical, data-driven, and hybrid simulation. The physical method accurately predicts thermal energy within the building by solving thermal equilibrium and heat transfer equations. Despite its high accuracy, it is associated with the need for high computational cost and limited scope of optimisation. Moreover, high expertise is deemed necessary to perform dynamic building energy analysis. On the other hand, statistical analysis tools such as regression models, support vector machines and artificial neural networks can quickly respond to given inputs and easily handle non-linearities. However, these models necessitate large databases for training and development. Any inadequacy or inaccuracy would significantly reduce its prediction performance. Additionally, there is a lack of physical interpretability in the prediction output.

The hybrid method is the hybridisation of the physics in the pure physical method with statistics in the data-driven approach. This method not only requires less time to simulate when compared to the physical simulation tool, but it also makes up for the fact that the pure statistical approach does not provide a physical explanation of the connection between the input and output data. The application of this hybrid model is promising, and, recently, a trend toward employing this strategy more frequently in the simulation of building energy use is evident. It has the potential to improve the adaptability of thermal energy modelling performance. However, the development of these tools is also associated with a highly time-consuming and complex process. Thus, the development of single-building prediction models is often useless. Generating hybrid simulation models for a set of buildings would maximise its capacity, bringing huge benefits. Moreover, many case studies would justify the development expenses of hybrid simulation models. However, a generalised hybrid simulation model is lacking that could predict energy demand associated with buildings with diverse types of parametric characteristics outside its training range.

Optimisation methodology has been widely used to determine optimal solutions for building energy-related applications. Genetic algorithm has been the most popular meta-heuristic method that has been employed in building energy prediction. The use of optimisation in traditional BPS tools would enhance its applicability to explore more design solutions. However, it would still require performing computationally expensive building performance simulations for each design selection. Optimisation has also been integrated with statistical tools to improve prediction performance by identifying optimal model parameters such as the number of neurons, number of hidden layers, activation function, and training strategy. However, its application to hybrid simulation models needs to be better developed. Moreover, its applicability to conduct design exploration to identify key parameter combinations from the design space to minimise the building energy demand is unfounded.

2.6 Nosocomial infections

Healthcare-associated infections (HAIs) or Nosocomial infections (NI) are acquired by an individual while visiting or staying at a healthcare facility. It is considered one of the primary events that would affect the patient's safety. It is associated with significant mortality, morbidity and financial burden for patients and the healthcare system. HAI affects about 3.2% of hospitalised patients in the United States of America and 6.5% in the European Union, and the worldwide prevalence is estimated to be higher (Magill et al., 2018). It accounts for 4-56 % of death rates in neonates, with an incidence rate of 75% in southeast Asia and sub-Saharan Africa (Khan et al., 2017). HAI costs the US healthcare system a whopping $28-$45 billion annually, whereas, in the European Union, it is estimated to be € 7 billion (Vincent et al., 1995). At this stage, it is vital to recall Florence Nightingale's assertion that a healthcare facility's first obligation is not to harm the sick (Nightingale, 1883). These infections can occur at various healthcare facilities such as hospitals, long-term care facilities, ambulatory settings etc. A recent study has revealed an increase in the prevalence of healthcare-associated infections during the ongoing covid-19 pandemic (Lastinger et al., 2022).

Based on the epidemiologic triad, a combination of three factors: host, agent, and environment leads to the cause of disease in an individual, as shown in Figure 2.2 (CDC). The host factor for HAI relates to the patient's intrinsic characteristics, such as age, comorbidities, etc., that aggravate their risk of developing an infection. The agent factor is associated with the features of the pathogen, such as infectivity, viability to cause infection etc. The common pathogens causing nosocomial infections are bacteria, fungi and viruses. Finally, the environmental factor is the extrinsic characteristics that provide the opportunity for exposure, such as the healthcare environment, contaminated invasive procedures, inadequate infection control practices etc. Infectious pathogens such as methicillin-resistant Staphylococcus aureus (MRSA), Clostridium difficile, and norovirus can survive in hospital environments for hours to days and even months, facilitating the risk of healthcare-associated infections. Table 2.1. shows the survival period of some pathogens causing nosocomial infections. A detailed list of other pathogens and their survival time can be found in (Kramer et al., 2006).

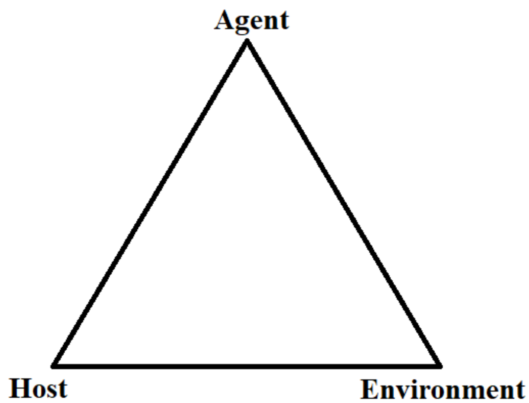

Figure 2.2 Epidemiological triad

Table 2.1. Survival time of pathogens in the environment causing nosocomial infections

Microorganisms	Environmental survival time
Gram-negative bacteria	
Escherichia coli	From 1.5 hours to 16 months
Pseudomonas aeruginosa	From 6 hours to 16 months
Klebsiella spp.	From 2 hours to 30 months
Acinetobacter spp.	From 3 days to 5 months
Gram-positive bacteria	
MRSA	From 7 days to 7 months
vancomycin-resistant enterococci	From 5 days to 4 months
Clostridium difficile	> 5 months
Fungi	
Candida albicans	From 1 to 120 days
Viruses	
Norovirus	From 8 hours to 7 days

According to the CDC, HAI is classified into four types: central line-associated bloodstream infections, catheter-associated urinary tract infections, surgical site infections, and ventilator-associated infections. A survey conducted in the United States showed that Pneumonia was the most prevalent healthcare-associated infection in an acute hospital setting (Magill et al., 2018). Pneumonia is often associated with coughing, nausea, diarrhoea, and other symptoms that can be identical to conditions arising from coronavirus infections, such as SARS-CoV-2, MERS, etc. Thus, the risk of infection to other patients from an undiagnosed infected individual who is later confirmed with an infectious disease would lead to causing an outbreak within a facility. Thus, understanding the infection transmission mechanism and laying down an effective infection control strategy is necessary.

2.6.1 Infection transmission routes in a healthcare setting

The respiratory activities of an infected individual, such as breathing, talking, singing, coughing, or sneezing, can expel many infectious pathogens that could transmit the infection to a susceptible. The three major routes of infection transmission can be classified as contact, droplet, and airborne. According to Shiu et al. (2019):

Contact transmission refers to the transfer of infectious pathogens from an infected patient to a susceptible either through direct contact (physical) or indirect contact (surfaces or objects).

Large droplet or droplet transmission refers to the transfer of infectious pathogens expelled by an infected individual, which gets deposited onto a susceptible person's mucosal surfaces (eyes, nose, mouth).

Airborne or aerosol transmission relates to the transfer of fine respiratory droplets generated by exhalation by an infected individual or through medical aerosol-generating procedure that gets inhaled by a susceptible individual.

There are confusion and debates associated with the conventional terms related to these traditional infection transmission routes (Tellier et al., 2019). The most confusing is contact transmission. The term *contact* can be associated with direct physical contact between the infected and susceptible individual, and it can refer to indirect contact via an intermediate surface or object. The latter form of transmission is also known as the fomite route of infection transmission. Further, the term intermediate refers to a surface or objects that is in between an infected and susceptible that gets contaminated by an infected person before a susceptible person touches it. Although, a surface can also get contaminated by a healthy person through surface touch network (Lei et al., 2017). Moreover, in physical sense, an aerosol transmission and a large droplet transmission can be associated with indirect contact transmission. The term *droplet transmission* would imply that all droplets are large that would deposit on the mucosal surfaces. Lastly, short range aerosol transmission is not considered, as traditionally aerosol transmission is associated only with long-range transmission. According to Li (2021), the criteria used for categorizing the traditional routes of infection transmission mechanism is unclear. Thus, a new categorization based on transfer process and media as a criterion was proposed:

Spray transmission involves transfer through spray of virus-laden drops that gets deposited on the mucosal surface of a susceptible person. Here, the transmission media is drop.

Inhalation transmission involves the transfer of virus-laden droplet from an infected person to a susceptible person through inhalation. Here, the transmission media is aerosol. The aerosol inhalation can happen within short-range and long-range.

Touch transmission refers to the transfer of virus laden drops or droplets deposited on an animate or inanimate surface to the hand of a susceptible person, and subsequent transfer to his/her mucosa by his/her contaminated hand. Here, the transmission media is surface.

It was also proposed that further classification through distance is possible. There are two transmission types based on distance: close-contact (distance within 1-2 m of an infected person) and distant (greater than 1-2 m distance from an infected individual) (Li, 2021). An illustration of transmission routes is depicted in Figure 2.3.

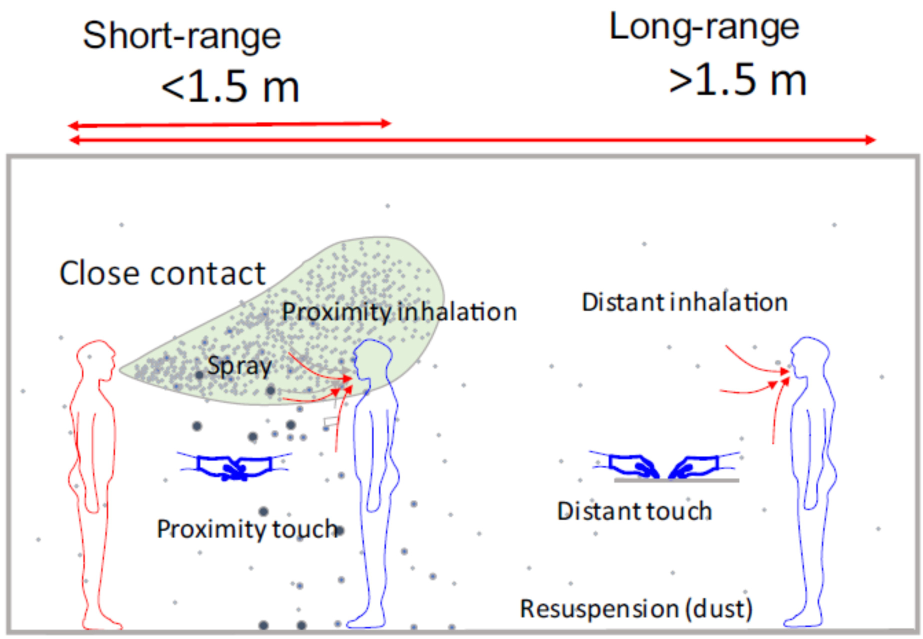

Figure 2.3 Illustration of short-distance transmission routes (spray, inhalation and touch) and long-distance transmission (inhalation and touch). The range of expired jet is shown in light green, the infected person shown in red and susceptible person in blue. The drop is represented as large black circles and aerosols as small black circles (Li, 2021).

Similarly, a transmission media with distance based approach was taken by Zhang et al. (2020b) to clarify the existing categorization of infection transmission. Three sub-routes were proposed under the close contact transmission: large-droplet, short range airborne (fine droplet) and immediate body-surface. *Large-droplet* sub-route refers to the deposition of large droplets generated as a consequence of exhalation of an infected person that gets deposited on the mucosal surfaces of a susceptible person located within a distance of 1-2 m. These droplets could also get deposited on the face of the same susceptible person, and subsequent transfer of these infectious pathogens to the mucosa of the susceptible person through his/her hand would lead to the second sub-route termed as *immediate body-surface*. The third sub-route termed as *short-range airborne* refers to the transfer of fine droplets or droplet nuclei, which is dried out residual of a droplet due to evaporation, to the same susceptible person through inhalation. The fine droplet could also go beyond the close contact range to be inhaled by a susceptible person through the *distant airborne route*. The inanimate surfaces within the space can also get contaminated by the deposition of these large droplets or airborne droplet nuclei to cause infection transmission by self-inoculation through the mechanism of *distant fomite route*. The categorization of infection routes suggested by Zhang et al. (2020b) and its relationship with traditional routes in shown in Table 2.2.

Table 2.2 Infection route categorization and its relationship with traditional route categorization are shown in bold italics: contact (direct/indirect), large droplet and airborne (Zhang et al., 2020b).

	Distance		
Transmission media	**Body contact (0 m)**	**Close contact (≤1.5 m)**	**Distant contact(>1.5 m)**
Body fluid	Direct transfer, *including direct transfer of body fluid and infectious microbes (e.g., kissing)* (***Direct contact)***	Not applicable	Not applicable
Fomites (both *large droplets* and *fine droplet nuclei*) and skin	Indirect transfer via skin/clothing-to-skin/ clothing contact, *such as handshaking, face kissing followed by hand touching of the face* ***(Direct contact)***	Immediate body surface/ clothing ***(Direct contact)***	Distant fomite (*may even extend beyond the enclosed space*) ***(Indirect contact***
Air (with *fine droplets and droplets nuclei*)	Not applicable	Short-range airborne (*face-to-face only*) ***(Airborne)***	Distant airborne (*mostly within the enclosed space*) ***(Airborne)***
Large droplets	Not applicable	Large droplets (face-to-face only) ***(Droplet)***	Not applicable

Apart from three principal routes of infection transmission, there two other routes: vehicle and vector borne (CDC, 2007). Infection transmission from sources other than individuals are those associated with environment or vehicle. The *vehicle* can be referred to as transmission of infection through sources such as food, water, medicines, or equipment's that serve to transmit infection to multiple people. This could be avoided by maintenance of standards in preparation of consumables such as food, water. The transmission of malaria is a typical example of *vector borne* diseases, where infection is spread human through vectors such as insects or parasites. However, such vector borne diseases are quite uncommon in developed nations.

2.6.2 Ventilation and infection control

Ventilation is the act of introducing fresh outside air into a building with an aim to provide healthy air for breathing by the dilution and removal of indoor contaminants. The three basic elements of building ventilation are:

Ventilation rate refers to the quantity and quality of outside air provided to a space.

Airflow direction refers to the overall direction of airflow in a building, which in an ideal scenario should be from a clean zone to dirty zone.

Airflow distribution or airflow pattern involves the strategies through which the outside air is delivered to a room to maintain adequate indoor air quality and acceptable thermal comfort.

The ventilation of a building can be done through three principal methods: natural, mechanical and hybrid ventilation.

Natural ventilation involves the flow of outside air into a building happening through a temperature gradient (buoyancy or stack driven methods) or through natural forces (wind driven methods). This primarily depends on the climate, building design and human behaviour.

Mechanical ventilation involves the use of fans to supply air into, and exhausting air out of a room. Based on the climate, there will be a variation in the type of mechanical ventilation used. For instance, in a warm, humid climatic region, a positive pressure mechanical ventilation system will be used. The room will be positively pressurized, and room air will leak through envelope leakages. In contrast, a negative pressure mechanical ventilation system will be used in cold climatic regions, where the room will be negatively pressurized, and room air will be compensated through sucking in outside air.

Hybrid ventilation refers to the coupling of natural ventilation and mechanical ventilation. The natural forces will be used to drive the design flow rate and when the natural ventilation alone cannot provide this flow rate, the mechanical ventilation would be used.

Menzies et al. (2000) studied the influence of ventilation rate and spread of TB among healthcare workers (HCW) working in a hospital. A high TB infection risk for HCWs working in non-isolation rooms with a ventilation rate less than 2 air changes per hour was indicated. A study was conducted by Jiang et al. (2003) to estimate the risk of infection for HCW working in different wards within two hospitals. It was found that the ward with window providing higher ventilation had lower infection risk. A study in patient rooms indicated that 4 ACH with supplemental heating and cooling would be good in terms of thermal comfort, and ventilation effectiveness. Further, it was also suggested that 6 ACH would be optimum. Another study in a four bed patient room suggested that there is a reduction in infection transmission through hand colonization while the ventilation rate changes from four to six ACH (King et al., 2015). There is a plethora of studies indicating that lower ventilation rates would result in an increase in infection transmission risk, however relying solely on increasing the ACH wouldn't result in mitigation of infection risk. A study conducted in a two bed hospital room indicated that an increase in ACH would cause an increase the risk of cross-infection transmission (Bolashikov et al., 2012). A similar conclusion was attainted by a study conducted in an environmental chamber (Pantelic and Tham, 2013). Based on an extensive review of literature, it was found that there is no conclusive evidence to suggest the minimum and maximum ventilation requirement in hospitals for effective infection control. English (2016) identified that the influence of ventilation requirement on infection rates is largely unclear in healthcare facilities except for operation rooms and airborne isolation rooms. Memarzadeh and Xu (2012) found that in a mechanically ventilated room, an increase in ventilation rate is not the potential factor that would lower the infection risk, whereas ventilation system design and location of susceptible from the infection source is more important. Similarly, a review done by Shajahan et al. (2019) suggested that along with ACH, it important to consider the location of susceptible from infection source, supply and return air grille as well as the air distribution pattern.

Table 2.3 Ventilation guidelines for general and intensive care ward spaces (Beggs et al., 2008)

Code	Country	Pressure	Minimum outdoor air change rate (ACH)	Minimum total air change rate (ACH)	Design air temperature (ºC)	Design relative humidity (%)
Patient rooms/general wards						
AIA	United States	Neutral	2	6	21-24	-
ASHRAE	United States	Neutral	2	6	21-24	30-60
HTM 2025	United Kingdom	Neutral	Not Specified	Not specified+	20-22	40-60
Intensive care wards						
AIA	United States	Neutral	2	6	21-24	30-60
ASHRAE	United States	Neutral	2	6	21-24	30-60
HTM 2025	United Kingdom	Neutral	Not Specified*	Not specified+	20-22	40-60

* Minimum outdoor air rate of 8 l/s per person
+ 100% outdoor air encouraged

Different ventilation strategies and air distribution mechanism are adopted to control the transmission of infectious diseases in healthcare facilities as shown in Figure 2.4. Mixing ventilation is most commonly adopted ventilation scheme (Qian and Zheng, 2018). Mixing ventilation is based on the principle that it dilutes the contaminated indoor air by mixing the indoor air with fresh supplied air to lower the contaminant concentration. Generally, an air jet at high velocity (typically > 2.0 m/s) is supplied at the upper parts of the room to provide jet circulation along the peripherals of the room. The main principle associated with displacement ventilation is to displace the contaminated indoor air with fresh outside air. In this method, normally a cold supply air at a low velocity (typically < 0.5 m/s) is delivered at or near the floor to develop an upward movement caused by warming of the air by the heat sources present in the room. Thus, its leads to generate a vertical gradient of temperature, velocity and contaminant concentration. In downward ventilation, the cooler air, which is heavier, is dispersed from the ceiling diffuser at a low velocity and the unidirectional airflow is likely to remove the indoor contaminants through an opening provided at the lower part of the wall. A review conducted by Cao et al. (2014) provides additional information regarding the state-of-the-art ventilation and air distribution systems used in buildings.

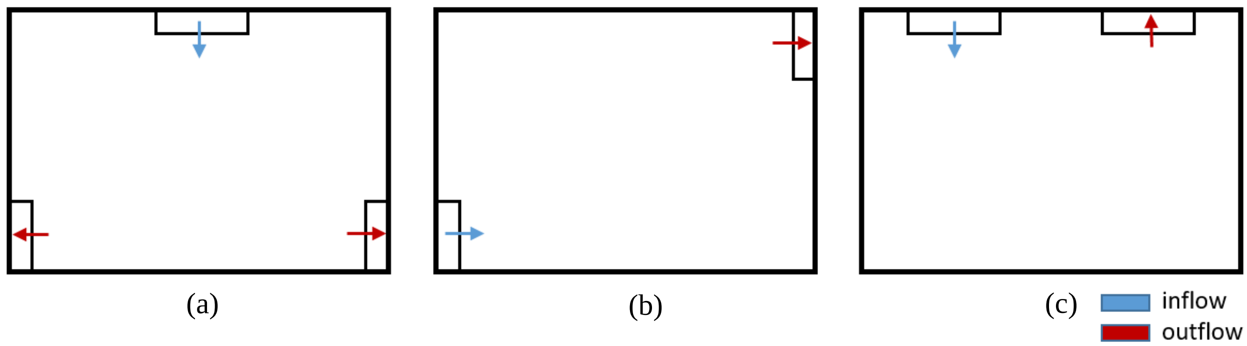

Figure 2.4 Illustration of room air distribution (a) downward ventilation; (b) displacement ventilation; (c) mixing ventilation

There exists a strong correlation between the air distribution pattern and infection transmission with in a room (Beggs et al., 2008). A study done in patient rooms with displacement ventilation was indicative that large bioaerosols would remain suspended in air for longer duration, whereas smaller particles would leave the room (Zhao et al., 2004). A study by Qian et al. (2006) in a multi bed patient room reported that the spacing of bed should be farther apart in displacement ventilation compared to the scenario under mixing ventilation. It was also reported under displacement ventilation the exhaled droplet nuclei took longer time to dissipate in comparison to mixing ventilation. Another study done in a hospital ward indicated that displacement ventilation system would result in higher contaminant concentration compared to mixing ventilation where the secondary exhaust is placed at the lower part of the wall. Although, in the same study, when the exhaust location was changed to the upper part of the wall, the displacement ventilation at 4 ACH had lower contaminant concentration compared to the mixing ventilation at 6 ACH (Yin et al., 2009). In a study conducted by Olmedo et al. (2012), the cross infection risk increased by 12 times in displacement ventilation compared to mixing ventilation. A study done in a hospital ward with ceiling mixing type ventilation system found that the dispersion of contaminants is strongly affected by the location of exhaust vent (Wan et al., 2007). It was also found that with a complete mixing ventilation system the contaminant concentration decay rate is exponential. In a study where the ventilation air flow was driven from ceiling to floor level, the infection control was deemed to be poor (Kao and Yang, 2006). However, in another study, where the air was supplied and extracted through the ceiling resulted in being an effective infection control strategy (Beggs et al., 2008). It could be seen from above discussion that along with ACH, the location of supply diffusers and exhaust grilles have great importance while laying down ventilation strategy for mitigation infection risk.

2.7 Methods to evaluate airflow and contaminant distribution

In buildings, ventilation creates a thermally comfortable environment with appropriate indoor air quality by managing indoor air parameters such as air temperature, relative humidity, air speed, and chemical species concentrations. Thus, it is necessary to possess appropriate prediction methodologies to anticipate ventilation effectiveness in buildings if one wishes to regulate indoor air characteristics successfully. Prediction tools offer information concerning the indoor air parameters in a room or building even before the structure is built. This section will provide a brief overview of the various approaches used to predict the airflow and contaminant transport within a space. These include analytical methods, empirical models, experimental models, multizone models, zonal models, and Computational Fluid Dynamics (CFD) models (Chen, 2009).

2.7.1 Analytical models

Fundamental equations of fluid dynamics and heat transfer, such as mass, momentum, energy, and chemical-species conservation equations, are used to build analytical models. The analytical models simplify geometry and thermo-fluid boundary conditions to obtain a solution. As a result, the final equations obtained for one case may not be used without modification for another. However, the methodology and approximations for different cases may be similar. Fitzgerald and Woods (2008) developed an analytical model that studied the influence of stacks on flow patterns and stratification associated with natural ventilation with two openings. With a distributed heat flux Q_h, the analytical model calculates the temperature elevation in the room △T by,

$$\Delta T = \left(\frac{Q_h^2}{\propto \rho^2 C_p^2 A^{*^2} g(H - h_b)}\right)^{1/3} \tag{2.12}$$

And the flow rate V by,

$$V = \left(\frac{\propto Q_h\, A^{*^2}\, g(H - h_b)}{\rho C_p}\right)^{1/3} \tag{2.13}$$

Where A^* denotes the effective area, H is the termination height of a vertical stack, h_b is the height of a vent from floor, α is the coefficient, ρ is the density, g is gravity and C_p is the specific heat.

Mazumdar and Chen (2009) developed another analytical model using the principle of superposition and the method of variable separation. They obtained an analytical solution of contaminant concentration C as a function of position x in an airline cabin for a contaminant source located at L_1 as,

$$C = C_{inlet} + A_{L_1} e^{m_1(L_1 - x)} + B_{L_1} e^{m_2(L_1 - x)} + a_0 e^{-\beta_0^2 t} + 2\sum_{n=1}^{\alpha} a_n \cos[\alpha_n(L_1 - x)]\, e^{-\beta_n^2 t} \tag{2.14}$$

where C_{inlet} denotes the contaminant concentration at the air supply inlet, t is the time, and the coefficients (A, B, a, α, β) can be determined using mathematical equations with several approximations.

Analytical models are probably the oldest method that is still widely used today due to their simplicity, richness in physical meaning, and low computing resource requirements, though they may not be accurate for complex scenarios and the results may be misleading.

2.7.2 Empirical models

The empirical models, like the analytical models, are derived from mass, energy, and chemical species conservation equations. In many cases, experimental measurement data or advanced computer simulations are also used to develop empirical models to obtain some coefficients that allow empirical models to work in a specific range. The analytical and empirical models differ little in theory. However, the empirical models are thought to use more approximations than the analytical models. Cho et al. (2008) developed a set of equations to determine jet behaviour in terms of velocity profiles, the spreading rate of jets on the surface, and jet decay using CFD and experimental results of wall confluent jets in a room. They calculated the maximum velocity, U_m, for wall confluent jets as,

$$\left(\frac{U_m}{U_o}\right) = 2.96 l_c^{-0.79} \tag{2.15}$$

where U_o is the jet's supply velocity and l_c is its characteristic length. It should be noted that the throw constant (2.96) was determined empirically. Most design handbooks and design guides contain empirical formulae of this format. It represents maturity in engineering practice. Cornick and Kumaran (2008) compared four popular empirical models for predicting interior relative humidity to measured data. NIOSH developed an empirical model describing the relationship between flow rate, pressure differential, and leakage area using data from 67 airborne infection isolation rooms (Hayden et al., 2007). The model was capable of accurately estimating the actual leakage area in these rooms. These empirical model applications show that the models are cost-effective tools for engineers and designers to predict ventilation performance in buildings. The empirical models' performance is comparable to that of the analytical models. However, they are also highly case sensitive.

2.7.3 Experimental methods

The experiment methods for evaluating the transport of airflow and contaminant concentration can be classified into small-scale and full-scale.

2.7.3.1 Small scale experimental models

Small-scale experimental models use measuring techniques to predict or evaluate airflow and contaminant distribution on a smaller scale of buildings or rooms. A small-scale experimental model is far more cost-effective than a full-scale building or room. If the flow in the model is similar to reality, one can obtain a realistic prediction by directly measuring thermo-fluid conditions in a small-scale model. However, important dimensionless flow parameters in a small-scale experimental model, such as Reynolds number, Grashof number, Prandtl number, etc., must remain the same as those in the actual building or room to achieve flow similarity. Yu et al. (2007) used a 1:3 scale model to investigate airflow in a ceiling slot-ventilated enclosure. They measured airflow patterns, velocity and temperature decay at the centreline, velocity and temperature profiles, airflow, and thermal boundary layers, etc. The information was used to create empirical models. Morsing et al. (2008) investigated the effects of internal airflow and floor design on gaseous emissions from animal houses using several 1:10 scale models. Small-scale experimental models are very useful and cost-effective. However, in addition to scaling issues associated with dimensionless thermo-fluid parameters, scaling complex flow geometry can be difficult. Small-scale experimental models were used primarily to validate analytical, empirical, or numerical models. The validated analytical, empirical, or numerical models were then scaled up to investigate the ventilation performance of real-world buildings.

2.7.3.2 Full-scale experiments models

The full-scale experimental models were comparable to the small-scale experimental model. Full-scale experimental models are further divided into two types: laboratory experiments and in-situ measurements. An environmental chamber is frequently used in laboratory experiments to simulate a room or a single-story building with several small rooms. If outdoor wind conditions must be considered, the chamber should be housed in a wind tunnel, which would be a very expensive facility. Zhang et al. (2009) simulated a section of a twin-aisle airliner cabin using an environmental chamber. Even a full-scale experimental model frequently approximates thermo-fluid boundary conditions and flow geometry. Zhang et al. (2009) measured the distributions of air velocity, temperature, and contaminants simulated by tracer-gas and mono-size particles using ultrasonic anemometers. The contaminants were thought to be viruses released by a passenger suffering from an infectious disease. Larsen and Heiselberg (2008) developed a new expression for calculating the airflow rate in single-sided natural ventilation using data from a full-scale wind tunnel experimental facility. Hummelgaard et al. (2007) used temperature and CO_2 concentration measurements in five mechanically, and four naturally ventilated office buildings to correlate occupant symptoms and negative perceptions with ventilation. Recent applications show that full-scale models based on laboratory experiments or in-situ measurements provided the most realistic prediction of airflow and contaminant distribution. However, they were generally costly and time-consuming. Furthermore, the experimental measurements were not error-free. The current trend is to use full-scale experimental models of laboratory experiments and in-situ measurements to obtain data for validating computer models, such as CFD models and then use the validated computer models to predict ventilation performance or design ventilation systems. In-situ measurements were more commonly used to assess the performance of existing buildings.

2.7.4 Multizone models

Multizone network models are primarily used to predict air exchange rates and airflow distributions in buildings that have or do not have mechanical ventilation systems. Axley (2007) provides a thorough background and theory of multizone models. The multizone models solve conservation equations for mass, energy, and chemical species. The models, however, assume quiescently or still air in a zone, allowing the momentum effect to be ignored. In addition, the models assume uniform air temperature and chemical-species concentration in a zone. Wang and Chen (2008) discovered that these assumptions can lead to significant errors in some cases. Hu et al. (2007) used CONTAM to calculate particle resuspension in a three-zone building's indoor environment. It was found that CONTAM provided fast convergence speed and good agreement of results with an analytical model. They also attempted to fine-tune the model by varying the airflows, flow resistances, and other parameters. COMIS is another well-known multizone program. For example, it was used to predict airflow, pressure, and contaminant distribution in a building (Khoukhi et al., 2007), to calculate the effect of wind speed velocity on stack pressure in a building (Maatouk, 2007), and to determine airflows between zones due to temperature differences (Sohn et al., 2007). It provided a similar performance compared to CONTAM. Two national laboratories in the United States of America developed both tools. However, both had a poor user-friendly interface and graphical presentation schemes limiting its use.

2.7.5 Zonal models

The multizone models' well-mixing assumption is invalid for large indoor spaces or rooms with stratified ventilation systems, such as displacement ventilation. Therefore, zonal models have been employed to solve the challenge of predicting air temperature distributions. The number of cells in a zonal model for a three-dimensional region is normally fewer than one thousand. Each cell's air temperature is calculated to determine the space's non-uniform distribution. Megri and Haghighat (2007) discussed the evolution of zonal models. Based on measured airflow patterns or mass and energy balance equations, zonal models were created. Those dependent on measured airflow patterns determined air temperature distributions based on the patterns. The availability of airflow patterns restricted their applications. Models employing mass and energy balance equations were prevalent. The mass balance and energy equation can be written as,

$$\sum_j \dot{m}_{i \to j} = 0 \qquad (2.16)$$

$$\sum_j \dot{m}_{i \to j} + \emptyset_{source} = \rho_i V_i C_p \frac{\partial T_i}{\partial t} \qquad (2.17)$$

where *i* refers to current cell, *j* refers to neighbouring cell, $\dot{m}$ is the mass flow rate, $\emptyset$ is the heat source from *i*, ρ is the density, *V* is volume, C_p is specific heat, and *T* is the temperature. In equation, the right-hand side represents the energy accumulated in cell *i*.

Integrating the zonal model with a dynamic model for heat and moisture transfer as well as airborne pollutants were developed by Song et al. (2008). They used the model in a room with displacement ventilation to determine the dynamic air temperature, relative humidity, and pollutant concentrations. A good comparison in results were obtained between zonal model and Computational Fluid Dynamics. However, in applications with strong flow momentum, the zonal model simulations would be considerably less accurate. This is due to fact that in order to reduce computational costs, zonal models based on mass and energy balance equations do not solve momentum equations. In regions strongly affected by thermal flume, necessitates special treatment that would increase the complicity of the model. These complicities would eventually increase the computational cost as well as greatly affect the stability of the zonal model equation system. Using a zonal model is more complex than one might believe, especially when dealing with special cells. Compared to simulations of fluid dynamics with a very coarse grid, zonal models do not significantly reduce computing time. In many instances, the time required to prepare input data for a zonal model can be longer than that required for a CFD simulation. As a result, CFD models would replace the zonal models as computers become even faster and the CFD interface becomes more user-friendly.

2.7.6 Computational Fluid Dynamics (CFD)

A set of partial differential equations for the conservation of mass, momentum (Navier–Stokes equations), energy, chemical-species concentrations, and turbulence is numerically computed by the CFD approach. The solution provides indoor and outdoor field distributions of air pressure, air velocity, temperature, relative humidity, contaminants, and turbulence parameters. CFD models have become more prevalent in predicting ventilation performance owing to the rapid increase in computer capacity and the development of user-friendly CFD programme interfaces. The models have broad applicability in studying indoor air quality (IAQ), thermal comfort, fire safety, HVAC performance, etc., associated with diverse types of buildings (healthcare, residential, commercial, institutional, and industrial), transportation services, underground facilities, among others. Most CFD models consist of Large Eddy Simulation (LES) and Reynolds Averaged Navier–Stokes (RANS) modelling. The LES model is superior to RANS models because it has only one or no empirical coefficient. However, it will solve transient flow, even if the flow is steady and extreme flows details are unnecessary. Moreover, LES necessitates extremely fine grid as its accuracy is depended on the grid resolution. Hence, for steady-state flows, LES always demands more computing time (at least two orders of magnitude longer) than RANS modelling.

A set of transport conservation equations for continuity, momentum, energy, and chemical-species concentrations are solved by the RANS model. For an incompressible, two-dimensional equations of continuity, momentum and energy written as, the time averaged governing equations can be written as,

$$\frac{\partial \bar{u}}{\partial x} + \frac{\partial \bar{v}}{\partial y} = 0 \tag{2.18}$$

$$\frac{\partial \bar{u}}{\partial t} + \frac{\partial \overline{u u}}{\partial x} + \frac{\partial \overline{v u}}{\partial y} = -\frac{1}{\rho}\frac{\partial \bar{p}}{\partial x} + \frac{\partial}{\partial x}\left(\vartheta \frac{\partial \bar{u}}{\partial x}\right) + \frac{\partial}{\partial y}\left(\vartheta \frac{\partial \bar{u}}{\partial y}\right) + \frac{\partial}{\partial x}\left[\vartheta \frac{\partial \bar{u}}{\partial x}\right] + \frac{\partial}{\partial y}\left[\vartheta \frac{\partial \bar{v}}{\partial x}\right] - \left[\frac{\partial(\overline{u'u'})}{\partial x} + \frac{\partial(\overline{u'v'})}{\partial y}\right] \tag{2.19}$$

$$\frac{\partial v}{\partial t} + \frac{\partial \overline{u v}}{\partial x} + \frac{\partial \overline{v v}}{\partial y} = -\frac{1}{\rho}\frac{\partial \bar{p}}{\partial y} + \frac{\partial}{\partial x}\left(\vartheta \frac{\partial \bar{v}}{\partial x}\right) + \frac{\partial}{\partial y}\left(\vartheta \frac{\partial \bar{v}}{\partial y}\right) + \frac{\partial}{\partial x}\left[\vartheta \frac{\partial \bar{u}}{\partial y}\right] + \frac{\partial}{\partial y}\left[\vartheta \frac{\partial \bar{v}}{\partial y}\right] - \left[\frac{\partial(\overline{u'v'})}{\partial x} + \frac{\partial(\overline{v'v'})}{\partial y}\right] \tag{2.20}$$

$$\frac{\partial \bar{T}}{\partial t} + \frac{\partial(\overline{uT})}{\partial x} + \frac{\partial(\overline{vT})}{\partial y} = \frac{\partial}{\partial x}\left(\frac{k}{\rho C_p}\frac{\partial \bar{T}}{\partial x}\right) + \frac{\partial}{\partial y}\left(\frac{k}{\rho C_p}\frac{\partial \bar{T}}{\partial y}\right) - \left[\frac{\partial(\overline{u'}\overline{T'})}{\partial x} + \frac{\partial(\overline{v'}\overline{T'})}{\partial y}\right] \tag{2.21}$$

where u, v, p, T are mean values of flow parameters; and u', v', p', T' are the turbulent fluctuations in the flow. The turbulence Reynolds stresses that appear in the form $\overline{a'b'}$ is solved through the Reynolds stress modelling, which links the Reynold stresses to Boussinesq eddy-viscosity approximation as shown in Equation 2.22,

$$-\rho\overline{u'u'} = 2\mu_T \frac{\partial \bar{u}}{\partial x} - \frac{2}{3}\rho k; -\rho\overline{v'v'} = 2\mu_T \frac{\partial \bar{v}}{\partial y} - \frac{2}{3}\rho k;\ -\rho\overline{u'v'} = \mu_T\left(\frac{\partial \bar{v}}{\partial x} + \frac{\partial \bar{u}}{\partial y}\right) \tag{2.22}$$

where μ_T is the eddy viscosity that need to be calculated through the eddy-viscosity modelling. Based on the number of transport equations used to determine the eddy-viscosity, the models can be classified as zero-, one-, two-, three- and four-equation models as shown in Figure 2.5.

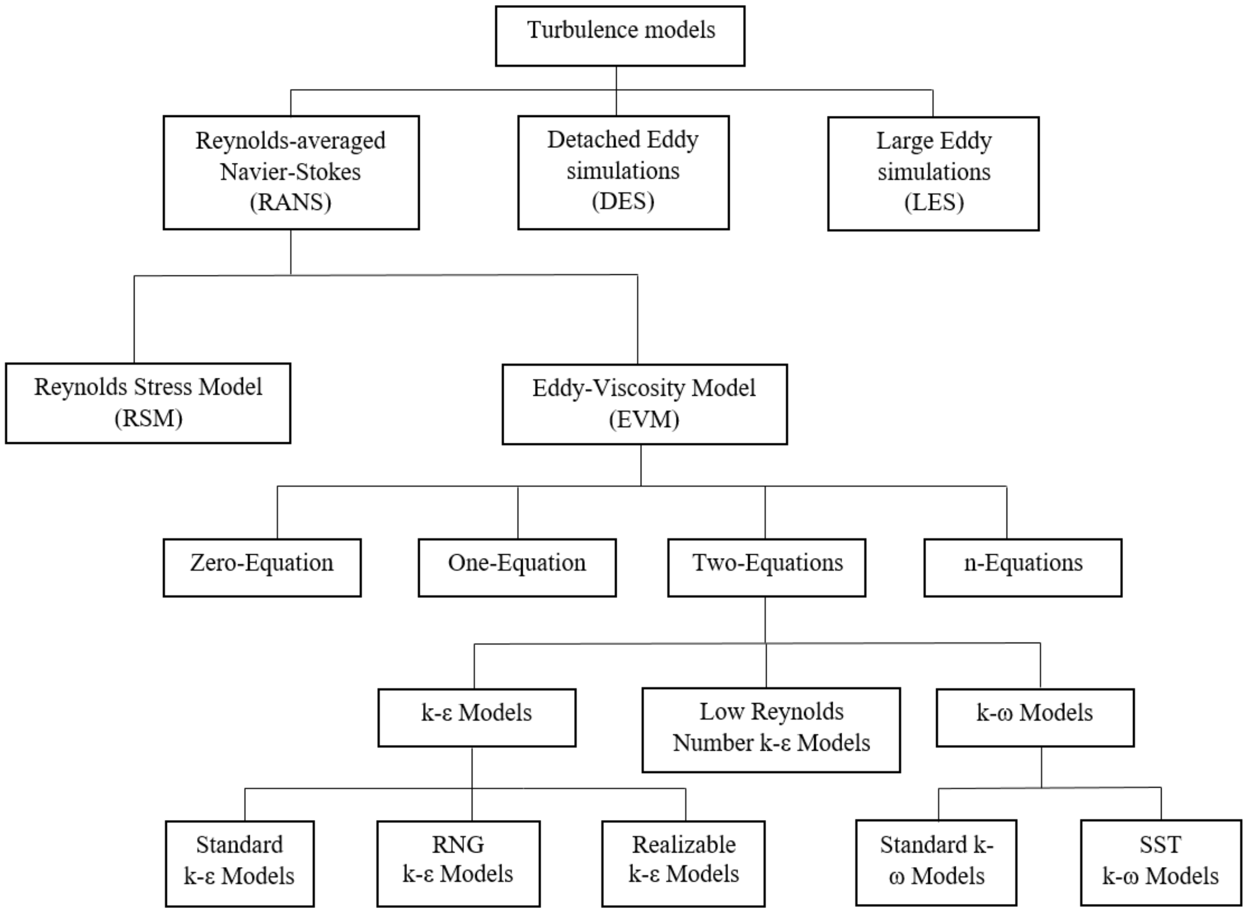

Figure 2.5 Turbulence models in computational fluid dynamics used for indoor airflow predictions

Zhai et al. (2007) conducted a study to evaluate different turbulence models used for predicting airflow and turbulence in enclosed environments. As a result, they highlighted the importance of mean air parameters over instantaneous turbulent flow parameters in the study of air distribution in enclosed environment. This was indicative of the increased interest in RANS simulations, which provide quick predictions, as opposed to LES simulations, which are more detailed but also more time-consuming. Indeed, LES was viewed as a research tool rather than a design tool. Zhang et al. (2007) validated around eight turbulence models for different convection cases within ventilated spaces. Among RANS models, they found that v2f-dav and the Re-Normalization Group (RNG) k-ε model had the best overall performance.

In addition to turbulence modelling within an indoor airflow, CFD approach is also widely used to investigate the transport, dispersion, and deposition of microorganisms. The two methods commonly applied for this purpose: Passive scalar transport and Lagrangian particle tracking.

2.7.6.1 Passive scalar transport

A passive scalar field, which can be thought of as a massless dye, is the most fundamental method of monitoring pollutant spread. In this approach, only advection and diffusion govern the movement of contaminants; particle dynamics are disregarded. The scalar transport equation can be written as,

$$\frac{\partial \rho \emptyset}{\partial t} + \nabla . (\rho U \emptyset) = \nabla . (\Gamma \nabla \emptyset) + S_{\emptyset} \tag{2.23}$$

where $\emptyset$ is the pathogen concentration, U is the velocity vector (u, v, w) of the air, Γ is the diffusivity and S is the source term. The lack of body force interaction on the scalar field may be appropriate for respiratory particles that are expelled through coughing and rapidly evaporate to a size below 1 µm (Hathway et al., 2011). As a result, the model is ideal to demonstrate the ventilation efficacy (Loomans and Lemaire, 2002), modelled in a steady-state. However, for large size distribution such as Skin squamae, it would be difficult to model it well. Despite its limitations, numerous studies have been conducted, demonstrating its ability to estimate exposure to airborne pathogenic particles (Hathway et al., 2011, Li et al., 2005). This method has the advantage of treating airborne bioaerosols smaller than 1 µm (Loomans and Lemaire, 2002, Loomans et al., 2008) as a massless dye. Consequently, this method is widely used to model the dispersion of contaminants in indoor air. However, this method has disadvantages when both buoyancy and the effects of gravity must be considered, implying that the particles would behave differently based on its diameters (Fuks, 1989), thereby invalidating the initial assumption that body forces have no effect on particles.

In the middle of the first decade of the 21st century, researchers such as Karthikeyan and Samuel (2008) and Zhang and Chen (2007c) used species transport to predict infection transmission within airliner cabins. Nielsen (2009) compared NO_2 and smoke tracers to multiphase CFD simulations in hospital double-patient rooms. So, it was concluded that the comparison was of high quality. However, tracer gases fail to represent particle sizes, evaporation rates, or deposition rates.

2.7.6.2 Lagrangian particle tracking

The Lagrangian method tracks particles individually when a secondary phase within the fluid domain has a negligible volume regardless of mass, such as particles released through expiratory activities. This method permits the discrete phase, in which mass and size play a significant role in the transport dynamics, to possess a variable space and time coordinate. It considers the particle's inertia, gravity, and drag forces while determining the trajectory of a particle. Consequently, the position and velocity of the particles form a coupled ordinary differential equation as shown in Equation 2.24. However, the lagrangian approach may prove to be a computationally expensive method for tracking *n* number of particles. A fifth order Runge-Kutta method is used to calculate the particle trajectories by considering the change in particle velocity u_p due to drag force F_D, inertia (u-u_p), gravity g_x, and other necessary forces. Only x-direction is considered in Equation 2.24, where ρ_p *and* ρ refers to the particle and fluid density.

$$\frac{\partial u_p}{\partial t} = F_D\left(u - u_p\right) + \frac{g_x(\rho_p - \rho)}{\rho_p} + F_x \tag{2.24}$$

Numerous studies of indoor particle dispersion employ RANS-Lagrangian particle modelling compared to the LES-Lagrangian particle modelling (Liu and Novoselac, 2014). Lai and Chen (2006) conducted the first comparison between small scale experimental model and numerical simulation for transport of biological organism in an environmental chamber. They predicted the deposition of 0.01 µm to 10 µm particles, with strong evidence that larger particles drop close to the source. Since that time, (Qian et al., 2008) have demonstrated that Lagrangian particle tracking accurately characterises respiratory droplets. Using this validated techniques, the effect of healthcare facilities layout on airborne particle distribution was compared (Ren et al., 2021, Satheesan et al., 2020).

2.8 Optimization

Thermal and ventilation evaluations within conditioned spaces are significantly influenced by air distribution, which is controlled by the supply flow rate, but the resulting airflow distribution is difficult to predict. This is because air distribution depends on many factors, including the type, size, and location of the air distribution device, space geometry, heat transfer across space boundaries, and internal objects. With the advent of CFD, it became possible to evaluate flows in spaces with high levels of precision, something that is impractical to do through experimentation and impossible with lower-level simulations. Parametric analyses are often used to evaluate and possibly optimize the thermal environment of a building. In parametric studies, the problem is solved multiple times with different sets of parameter variables in order to locate solutions. It is possible to examine and assess the influence of the parameter variables on the design problem. By varying key design parameters and comparing the resulting design solutions, a tradeoff can be sought.

Cross-infection can be caused by a virus carrier's sneezing, as demonstrated by Wang et al. (2021). This study provided two evaluation parameters: Total Maximum Time (TMT) and Overall Particle Concentration (OPC), which can be used to reflect particle motion and the likelihood of cross-infection. Ten air distribution systems were evaluated in the study through CFD simulations. Through numerical analysis, the authors proposed a method of bottom-in and top-out ventilation as an optimised air distribution system that effectively reduces the risk of cross-infection. Méndez et al. (2008) conducted a CFD-based numerical study to assess the ventilation efficiency of a two-bed hospital room in terms of air age and velocity fields. The analysis of the initial configuration revealed inadequate ventilation at the patient's location. Thus, three alternative configurations were evaluated, and the optimal configuration in terms of patient comfort and cost of execution was identified. In practice, the above studies simply mean that, beginning with an unsatisfactory configuration, they tried two or three alternatives before selecting the best one. Undoubtedly, this relates to optimization, albeit in a minimal sense.

One of the major drawbacks of parametric studies involving CFD simulations is that they are tedious and time-consuming. Every change in the value of a parameter necessitates the CFD user to remodel, remesh, and then recalculate the airflow, which is a laborious process. In addition, it is frequently difficult to track the complexity of relationships between a set of design parameters and the resulting design objective. Moreover, the trade-off between various design modifications remains obscure. Therefore, it is difficult to explore the design space systematically, and solutions may be overlooked. Thus, the resulting enclosing environment may not fulfil the design's intent. Thus, the optimal strategy for designing an HVAC system for a desirable enclosed environment is, to begin with, the design objective (e.g., the desired thermal comfort and indoor air quality level). Using a single series of evaluations to determine the required HVAC system, the inverse design method can achieve the desired interior environment (Liu et al., 2015).

The inverse design method can be categorised as either a backward or forward method (Chen et al., 2017). To identify contaminant sources in an enclosed environment, backward methods such as the quasi-reversibility method, pseudo-reversibility method, and regularised inverse matrix method can be utilised. In qausi-reversibility method, the irreversible governing equations are solved by a stabilization technique. This approach was utilized to find the location of the contaminant source in an aircraft cabin by performing an inverse simulation by utilizing contaminant concentration distribution provided by a forward CFD simulation as initial condition (Zhang and Chen, 2007a). However, this approach is deemed inapplicable, if the design of an enclosed environment also necessitates the inverse prediction of the flow field.

On the other hand, the pseudo-reversibility approach solves the inverse contaminant transport with reverse flow, instead of time reversing as used in quasi-reversibility. However, similar to quasi-reversibility, this approach also necessitates prior knowledge of the flow field. This method has found its application in groundwater contaminant transport as well as in inverse identification of contaminant source in an aircraft cabin (Wilson and Liu, 1994, Zhang and Chen, 2007b). The regularised inverse matrix method inverts the cause-effect governing matrix A and enhances the stability of the inverse operation through regularisation. Based on limited sensor data, Zhang et al. (2013) utilised this technique in an office to inversely predict the temporal rate profile of a gaseous pollutant source. A good agreement was obtained between the actual and predicted rate. In short, Backward methods solve reversed scalar transport equations and identify contaminant sources inversely. The major drawback is that they provide only an approximation of the solution and require prior knowledge of known flow field. Moreover, these methods cannot be used to design an indoor environment in reverse, as backward methods are incapable to inversely predict the flow field (Liu et al., 2015).

In the inverse design of airflow and heat transfer in an enclosed environment, forward methods such as the CFD-based adjoint method, CFD-based genetic algorithm method, CFD-based artificial neural network method, and proper orthogonal decomposition method show promise. The first three involves the integration of CFD with an optimization algorithm. Extensive applications are found for forward methods in comparison to backward methods. These methods convert the inverse problem to a control problem by formulating an objective function. For instance, if objective is to achieve good thermal comfort, the objective function can be constructed using predicted mean vote, which is a function of three primary parameters: air velocity, air temperature and relative humidity.

In adjoint method, derivative of an objective function over a design variable is computed to find the direction to minimize the objective function. In the case of Navier-Stokes equations, the derivative cannot be computed directly due to the strong non-linearity associated with the equations. Hence, a lagrange multiplier is introduced by the adjoint method. This can transform the unconstrained problem to constrained control problem. Since its introduction by Lions (1971), it has been widely applied in heat transfer problems, design optimization and identification of pollution source.

To determine the optimal design of indoor airflow, Liu and Chen (2015) developed a CFD-based adjoint method. The thermo-fluid boundary conditions were used as design variables, whereas flow and/or temperature fields were defined as the design objectives. Different initial inlet air conditions led to distinct optimal inlet air conditions, indicating the existence of multiple solutions. Additionally, the location of the air supply and size was included as design variables by Liu et al. (2016). The adjoint method based on CFD is precise and capable to manage large number of design parameters without causing significant increase in computing costs. However, it may find a locally optimal design that meets the design objective with constraints (Liu et al., 2015).

Holland (1975) introduced the genetic algorithm (GA) in the 1970s. In search of optimal solutions, GA is a gradient-free optimization method that simulates natural evolution. Based on the number of objective function, GA is classified into single-objective genetic algorithm or a multi-objective genetic algorithm. Malkawi et al. (2003) is identified to be first to couple CFD with GA in the design of an indoor environment. Malkawi et al. (2005) proposed a decision-support design evolution model using the genetic algorithm and computational fluid dynamics. In this approach, an iterative design evaluation is done using CFD analysis to maximize the thermal and ventilation criteria. Design changes are made, remeshed, and displayed based on evolutionary algorithms. The process continues until the designer can visualize the evolution of the final set of design alternatives and allows the user to experience the design's transformation based on its performance. A similar approach was undertaken by Kato and Lee (2004) to optimize a hybrid air-conditioning system.

The coupling of CFD and an evolutionary algorithm is also used in monitoring indoor air quality. The initial cost of a sensor is one of the most important factors in sensor selection. To reduce the number of sensors, sensor system designers must adopt techniques for optimizing sensor placement. Mousavi et al. (2018) utilized the integration of CFD and genetic algorithm to determine the optimal number of sensors and their location to effectively monitor the indoor air quality within a parking lot of a residential complex. Upon optimization, the number of sensors with their location that provide maximum coverage in a cost-effective manner would be determined.

Using CFD, Arjmandi et al. (2022) evaluated the effectiveness of five ventilation systems in controlling the spread of airborne particles within a classroom. The ventilation system with air inlets on the floor and air outlets on the ceiling resulted in the lowest exposure risk for infection transmission in a classroom with thirty students and a teacher. After a parametric study determined the best ventilation system for infection control, it was further utilised to conduct an optimisation to improve thermal comfort metrics. The process of optimisation utilised the design of experiments, response surface method and multi-objective genetic algorithm to study the influence of inlet channel width, air change per hour and inlet air temperature on thermal comfort and indoor air quality parameters (predicted mean vote, predicted percentage dissatisfied, air change effectiveness).

A global optimal design satisfying the design objective without constraints can be achieved by implementation of CFD-based genetic algorithm method compared to CFD-based adjoint method. However, the CFD-based genetic algorithm method necessitates numerous CFD simulations during population evolution and the number of design parameters can dramatically increase the computational cost.

The CFD-based artificial neural network method can be used as a surrogate model to reduce computational costs but the design results can be compromised. The Artificial neural network (ANN) is a highly sophisticated paradigm that utilises characteristics of human and animal brains to recognise patterns in data. It builds a memory capable of associating many input patterns with outputs or effects to solve problems. By training and adapting itself to diverse input–output pairs, ANN can map the relationship between input and output, making it possible to solve problems that are difficult for humans or even conventional computers (Yi and Malkawi, 2011). It can also effectively model the nonlinear relationship between the input and output. The ANN is widely used in fields such as finance, medicine and environmental science, among others.

ANN was used by Qin et al. (2012) to describe the annual dynamic process with detailed parameter data with a reasonable calculation time. It can predict dynamic energy consumption and thermal environment parameters with reasonable accuracy. Ayata et al. (2007) investigated the possible application of ANN in natural ventilation. The results indicated that the ANN method would be an effective tool for predicting the distributions of indoor air velocity. Zhang and You (2014) employed ANN to determine the indoor boundary conditions based on velocity and temperature measurements at observation points. To train ANN, the Bayesian Regularization training algorithm was used. Four sensors were configured to measure the velocity and temperature and four unique boundary conditions were investigated. A comparison between the actual boundary conditions and the ANN-obtained boundary conditions indicated that accurate predictions were made.

Zhang et al. (2020c) proposed the integration of a genetic algorithm, an artificial neural network, multivariate regression analysis, and a fuzzy logic controller to optimize the indoor environment and energy consumption based on CFD simulation. Thermal comfort (mean predicted vote) was established as the limiting design objective, whereas indoor air quality (air age) and energy consumption were designated as the optimal design objectives. Ventilation rate, inlet temperature, and angle were the design variables. GA would find the optimal solution (individual), whereas ANN and CFD determine the objective values for each individual. MRA would reduce the variable space, while FLC was employed to control the CFD process's execution routine. Compared to the other two design variables, the ventilation rate had a lesser effect on the design outcome. Integration of MRA and FLC in the design process resulted in a reduction of 50% and 35% in variable space and computational cost, respectively.

Another approach is to use the proper orthogonal decomposition method, a reduced-order method to significantly decrease the computing costs but at the expense of accuracy. Forward mapping of a thermo-fluid distribution from different boundary setting conditions can be rapidly characterised using the POD method. POD lays the groundwork for the modal decomposition of an ensemble of data, such as thermo-flow fields. The thermo-flow field derived from CFD simulations or measurements can be expressed as a combination of orthogonal spatial modes and their amplitudes or coefficients (Liu et al., 2015). This approach was first proposed by Lumley (1967) to analyse structure of inhomogeneous turbulent flows. In enclosed environments, POD is primarily utilised for the rapid prediction of indoor thermo-flow and pollutant concentration, optimization of air-supply parameters, and development of controllers for dynamic ventilation control.

Elhadidi and Khalifa (2005) used POD analysis to accurately predict the velocity and temperature distributions inside a vacant office. Sempey et al. (2009) utilized POD to predict the distribution of temperature in air-conditioned rooms. Allery et al. (2005) tracked the movement of particles in a two-dimensional ventilated cavity where a POD construction provided the airflow. Wang et al. (2018) proposed an inverse design method based on the POD of thermo-flow data from CFD simulations. Initially, the orthogonal spatial modes and coefficients of the thermo-flow fields was extracted. After that, the thermo-flow field was subsequently expressed as a linear combination of the spatial modes and their coefficients. Each spatial mode's coefficients are functions of air-supply parameters that can be interpolated. The optimal air-supply parameters were determined from design targets using a quick map of the cause–effect relationship between air-supply parameters and thermo-flow fields. The proposed method inversely determined air-supply parameters in two aircraft cabins using the percentage of dissatisfied passengers and the predicted mean vote. A full CFD simulation took 8 hours to solve a single case with snapshot fields, while the POD took less than 2 seconds. In this study, 2871 POD interpolations were constructed by employing 40 CFD simulations. The majority of the total computing time (321 hours) was spent on CFD simulations. On the other hand, Full CFD simulations would have required 23,000 hours of computing time for 2,871 simulations. Hence, the POD method proved to be very efficient.

There is reason to be optimistic about the use of forward approaches in the inverse design of enclosed spaces. The CFD-based adjoint technique may only identify the local optima of the design objective; however, the amount of computing work required is unaffected by the number of design variables. The evolutionary algorithm approach based on CFD is capable of finding the global optimal solution for the design objective; however, the amount of computational work required is quite substantial. The ANN and POD approaches have the potential to lower the amount of processing effort required, but the accuracy may suffer as a result.

2.9 Summary

Healthcare-associated infections (HAIs), also known as Nosocomial infections (NIs), cause significant death, morbidity, and financial impact on patients and the healthcare system. It is shown that healthcare-associated infections (HCAIs) may be related, at least to some extent, to the design and layout of the built environment. Nevertheless, it is still not entirely clear how these infections are spread, and there is much debate about the most effective way to treat them. At the very least, on a logical level, it is known that the transmission of infections requires at least three components. These components are namely, source of infecting pathogenic microorganisms, a susceptible host and a mode of transmission. It is of the utmost importance to understand the modes of infection transmission; however, these modes are still not well defined and even less well understood. Transmission might be influenced by the microorganism involved and made more difficult by a process involving multiple transfer routes.

It is evident that there is a close association between ventilation and infection spread mechanism in an indoor environment. Thus, assessing the danger of exposure to infectious pathogens requires knowledge of the impact of ventilation strategies and the indoor environment on the dispersion and deposition of infectious bioaerosols. The ventilation rate within isolation and operations rooms is well established, but ventilation requirements for other spaces such as wards, outpatient clinics etc., remain unclear. It is observed that there is great uncertainty about specifying the minimum and maximum ventilation rate within wards to mitigate infection transmission. Moreover, it is found that the ventilation rate alone cannot reduce the risk of infection transmission. The design of the ventilation system and the location of susceptible patients from an infected individual are potential factors that need to be considered while laying infection control strategies.

A variety of prediction methods that can be used to assess the airflow and contaminant distribution inside an indoor environment was explored. These included analytical approaches, empirical models, experimental models, multizone models, zonal models, and Computational Fluid Dynamics (CFD) models. Analytical approaches were proven to be unsatisfactory for complex problems, despite the fact that they were easy to use, included a wealth of physical meaning, and required few computational resources. The empirical models have a similar outcome connected with them. The experimental method is utilised most frequently in modern times with the primary purpose of validating analytical, empirical, or numerical models. It is generally agreed that an in-situ experimental method can provide a more accurate prediction of airflow and the dispersion of contaminants. However, in comparison to numerical methods, experimental methods might be known to be significantly more time-consuming and costly. The multizone, zonal, and CFD numerical approaches are the most prevalent ones utilised when attempting to forecast the airflow and contaminant distribution.

The multizone models don't take momentum effects into account, and they also assume that the air temperature and chemical species are uniform throughout each zone. These assumptions would be very different from what occurred, which would lead to severe inaccuracies in some circumstances. Zonal models that are based on airflow patterns have some limitations due to the lack of known airflow patterns. On the other hand, models based on mass and energy do not solve momentum equations, leading to inaccurate findings for flows with significant momentum. On the other hand, CFD has developed into a viable tool frequently used to study various aspects of buildings, including indoor air quality (IAQ), thermal comfort, fire safety, HVAC performance, and so on. The growth of computing power and the creation of more intuitive user interfaces have contributed to its growing prevalence. RANS, one of the several turbulent models that are accessible in CFD, has been proven to be suitable for predicting indoor airflow and pollutant dispersion. This model offers a good balance between the amount of computing effort required and the level of accuracy achieved. The passive scalar approach has its limitations when it comes to determining the distribution of contaminants because there is no body force interaction involved. On the other hand, the Lagrangian approach is widely used for tracking individual particle dispersion and deposition in studies concerned with indoor environments.

The conventional method of designing a heating, ventilation, and air conditioning (HVAC) system for an enclosed space entails much trial and error to achieve a particular design objective. Between the preliminary and the final design, this process could require a great deal of back-and-forth editing depending on the skills and domain knowledge of the designer. In addition, the process of design could be lengthened by several days or even weeks if an advanced simulation technology like CFD were utilised. Moreover, it is possible that the enclosing environment that is produced will not fulfil the requirements of the design objective. Therefore, the most effective strategy would be to combine a cutting-edge simulation tool, such as CFD, with a few different optimization methods. The CFD-based adjoint approach, the CFD-based genetic algorithm, the CFD-based artificial neural network, and the proper orthogonal decomposition method all have potential in this area. These techniques have been utilised in designing environments to achieve design goals such as a comfortable thermal environment. On the other hand, the use of these approaches to optimise ventilation strategies to mitigate infection transmission within an enclosed space has not been investigated to a great extent.

Chapter 3

Development of a hybrid cooling energy simulation model

3.1 Introduction

The building sector accounts for a significant portion of the world's total carbon footprint. With the increase in global temperature, population, urbanisation, and improved living standards, it is expected that the air-conditioning units and its usage in buildings is set to increase. The cooling energy demand associated with the building sector is a major contributor to greenhouse gas (GHG) emission. GHG emission drives climate change and its associated impacts on our environment are evident. Thus, it is necessary to cut down carbon emission associated with building sector by introducing effective strategies to design and operate buildings, with focus on sustainability.

The strength and limitations of different approaches utilized for prediction of energy in buildings were reviewed in Chapter 2. Despite the highly accurate building energy prediction capability of physical simulation approach, its application is limited by the computational expense and need for high domain knowledge. Moreover, it would prove highly inefficient, if it is needed to thoroughly exploit the influence of numerous variable combinations on building energy requirement. In contrast, the data-driven approach driven by statistics is superior for building energy prediction with its low computational time and inherent ability to model non-linear multivariate interrelationships. However, this approach demands a large database for model development, and results are not physically interpretable. On the other hand, the hybrid approach that couples the physics in physical simulation method with statistics in data-driven approach is a more promising approach for building energy prediction.

Cooling energy prediction in residential buildings is often complex and influenced by factors such as construction and building materials, climatic conditions, and occupant behaviors. These factors can have non-linear multivariate interrelationships with the overall cooling energy demand of a building. Thus, a hybrid simulation model to predict the cooling energy consumption that is efficient in handling non-linearities is developed in this chapter that offers an interpretable result with physical meaning. The hybrid model could evaluate the influence of building construction, materials, and indoor-outdoor temperature on the cooling energy demand. Thus, this approach would enable a user to identify key relationships between building physical characteristics and operational strategies to reduce the cooling energy demand at a minimal time compared to traditional building energy estimation methods. The proposed hybrid model would be an indispensable tool for building energy efficiency practitioners in the development of sustainable buildings.

3.2 Selection of city, climate, building type and parameters

The geographical coordinates of Hong Kong are situated at a latitude of 22° 18' N and a longitude of 114° 10' E. The climate of this region is categorized as sub-tropical. During the winter season spanning from November to February, the average temperature ranges from 15 to 18 degrees Celsius. As per the Hong Kong Observatory, it is a frequent occurrence for temperatures to descend below 10 °C in metropolitan regions, and the Observatory has documented the minimum temperature of 0 °C. However, sub-zero temperatures and frost are occasionally observed in elevated terrains and the new territories. The spring season is short with high levels of humidity, and occasional instances of dense fog. The temperature exhibits significant fluctuations daily. During the period spanning from May to September, the prevailing climatic conditions are tropical in nature, characterized by high temperatures and humidity levels, interspersed with sporadic episodes of precipitation in the form of showers or thunderstorms. During the period of June to September, it is common for the afternoon temperatures to surpass 32 °C, while the average temperature ranges from 27-29 °C. The autumn season is short, commencing in the middle of September and concluding in early November. The average yearly precipitation amounts to approximately 2225 mm, with the majority, or 80%, occurring during the months of May through September. The extended period of high temperatures and humidity in the summer results in a significant need for air-conditioning to provide comfort cooling (Cheung et al., 2005).

Hong Kong is one of the world's most densely inhabited cities, with 7.5 million inhabitants (CENSTATD, 2020). Currently, half the world's population lives in urban areas, and another 2.5 billion will by 2050 (United Nations, 2018b). Population growth necessitates the development of affordable and environmentally responsible housing to satisfy the population's future requirements. Hong Kong has made significant investments in the development of high-rise residential structures to meet the housing demands and make the high-density environment more livable for society. Currently, 53% of Hong Kong citizens' housing needs are provided by private housing, 31% by public housing, and 15% by housing authority subsidized sale units (LCS, 2016). Between 2003 and 2013, the number of private housing apartments climbed from 1,258,000 to 1,458,000, whereas the number of public housing apartments increased from 679,00 to 766,00 (Hong Kong Housing Authority, 2013).

In Hong Kong, buildings consume 90 percent of the electricity generated and are responsible for almost sixty percent of the city's carbon emissions (EB, 2017). According to Hong Kong's 2018 energy end-use data (EMSD, 2020), electricity was the primary source of energy consumption, accounting for 55% of total consumption of 159,493 TJ, with the residential sector accounting for 26% of this total electricity consumption. In addition, Hong Kong's residential sector consumes more electricity than the transportation and industrial sectors. During the period from 2008 to 2018, the residential sector's electricity consumption increased by 13.1%, with an average annual growth rate of 1.2% during the same time frame (EMSD, 2020). Along with the growth in electricity consumption, an increase in population and household size was also observed, and if immediate energy conservation measures are not implemented, it is anticipated that electricity consumption would continue to climb in the future. In 2018, residential buildings in Hong Kong consumed a total of 60,793 TJ of energy, of which 69% was consumed as electricity, of which 52% was consumed by private housing and 26% by public housing (EMSD, 2020). This indicates that private and public housing are the two largest contributors to GHG emissions from Hong Kong's residential sectors. In addition, as Hong Kong is a cooling-dominant location, it is important to highlight that 38% of the electricity usage was utilized for air conditioning the buildings. During the period between 2008 and 2018, the residential sector's electricity consumption for air conditioning increased by 34% (EMSD, 2020). Consequently, decarbonizing the building sector and increasing the cooling energy efficiency of both existing structures and new constructions are essential initiatives for Hong Kong to achieve its sustainable development objectives.

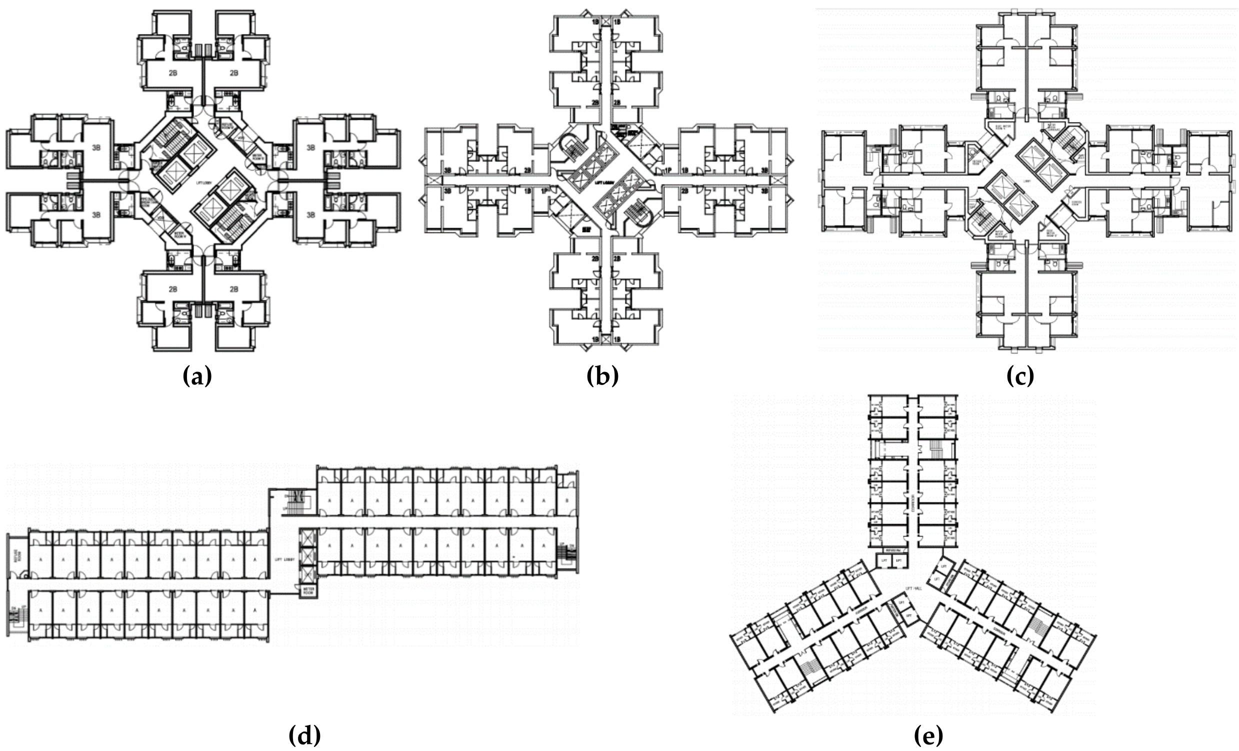

Figure 3.1 Standard public housing block layouts in Hong Kong: (a) Concord; (b) Harmony; (c) New Cruciform; (d) Slab; (e) Trident.

As was said earlier, the private and public housings sectors are also the two primary constituents of GHG emission within the residential building segment. As a result, both the public and private housing stock of Hong Kong was analyzed. This allowed us to investigate various permutations of building physical characteristics and operational strategies that have the potential to lower the amount of carbon emission associated with buildings. As can be seen in Figure 3.1, the public housing sector in Hong Kong adheres to one of five conventional block plans. These layouts are known as Concord, Harmony, New cruciform, Slab, and Trident (Hong Kong Housing Authority, 2021). The housing layouts in the private sector likewise closely reflect the designs chosen by the public housing sector; however, there is more unpredictability to be found in terms of the building design layout. In addition, as compared to public housing, the design of buildings in the private housing sector in Hong Kong is sometimes attributed to provisions for having larger apartment floor areas and a higher window-to-wall ratio.

To minimize the heat gained from the outdoor environment, an effective envelope design is necessary for residential buildings. Envelope heat gain and fenestration are the two main contributors to the cooling energy demand in buildings. The range of input parameters listed in Table 3.1 was extracted from design standards, Hong Kong residential property websites, and open literature data (Feng, 2004, Lam, 2000, ASHRAE Standard 90.1, 2010, Bojic et al., 2002, Wan and Yik, 2004).

Table 3.1 Input parameters

Input parameters	Ranges
Outdoor temperature, T_o (°C)	Weather data of Hong Kong 1989
Day of a year	[1–365]
Hour of a day	[1–24]
Air temperature, T_a (°C)	[20–30]
Window area, A_{wd} (m^2)	[2.32–58.179]
External wall area, A_{en} (m^2)	[5.659–133.631]
Apartment floor area, A_{fl} (m^2)	[12.624–150.049]
Orientation (°)	[0–360]
Window U-value, U_{wd} (W/(K·m^2))	[4.2–6.9]
Wall U-value, U_{wl} (W/(K·m^2))	[0.4–2.9]
Shading coefficient, S_c	[0.4–0.97]
Vertical shadow angle, σ_v (°)	[0.0–89.9]

3.3 Annual cooling energy consumption estimation

The three primary contributors towards the cooling energy requirement of a building are: Envelope heat gain, ventilation heat gain and internal heat gain (lighting, equipment, occupants). Equation 3.1 can be utilized to estimate the annual cooling energy consumption in a building (Mui et al., 2021, Mui et al., 2022).

$$E_c = \sum_{\mathrm{k}} \frac{\emptyset_{AC,k}(H_{en} + H_{in} + H_{vent})_k}{COP_k} \tag{3.1}$$

where $\emptyset_{AC,k}$ is the hourly air conditioner operation schedule in a year for $k = 1, 2, \ldots, 8760$ hours, H_{en} is the hourly envelope heat gain, H_{in} is the internal heat gain and H_{vent} is the ventilation heat gain (Wong et al., 2008).

H_{in} is the internal heat gained from lighting and electric equipment, it can be expressed by Equation 3.2 in terms of floor area A_{fl} and the sum of equipment power density E_{pd} and lighting power density L_{pd} (Cheung et al., 2005).

$$H_{in} = (E_{pd} + L_{pd}) \times A_{fl} \tag{3.2}$$

The ventilation heat gain H_{vent} can be expressed as the sum of sensible load L_{sen} and latent load L_{lat},

$$H_{vent} = L_{sen} + L_{lat}\ ; \begin{cases} L_{sen} = N_k \rho V_{vent} C_{pa}(T_a - T_o) \\ L_{lat} = N_k \rho V_{vent} h_{fg}(w_a - w_o) \end{cases} \tag{3.3}$$

where N_k is the number of occupants at hour k, air density $\rho = 1.2$ kg m^{-3}, latent heat of evaporation h_{fg} = 2,436 kJ kg^{-1}, heat capacity of air C_{pa} = 1.01 kJ kg^{-1}°C^{-1}, T_a (°C) is indoor temperature, T_o (°C) is outdoor temperature, and average ventilation rate V_{vent} = 3 Ls^{-1}ps^{-1} (Lin and Deng, 2003). The indoor moisture content w_a (kg kg^{-1}, dry air) can be estimated based on the psychrometric chart while the outdoor moisture content w_o (kg kg^{-1}, dry air) can be estimated using Equation 3.4, where p_w is the vapor pressure (kPa), p_{ws} is the saturated vapor pressure (kPa) and $R_{h,o}$ is the outdoor relative humidity (%),

$$w_o = \frac{p_w}{101.325 - p_w} \times 0.622\ ;\ p_w = \frac{R_{h,o}}{100} \times p_{ws} \tag{3.4}$$

Existing air conditioners are reported to have a maximum coefficient of performance (COP) of 2.9; their cooling efficiency, which will drop (Kosar, 2006), can be calculated by Equation 3.5.

$$COP_k = \frac{(SHR_k + 0.45)^{4.9}}{1.1} + 0.75 \tag{3.5}$$

The hourly occupant load N_k is estimated by Equation 3.6, where ψ_k is the hourly occupant load variation, N_{max} is the maximum number of occupants in an apartment, O_a (ps m^{-2}) is the occupant area ratio and A_{fl}

(m^2) is the apartment floor area (Wong and Mui, 2006). For a realistic prediction of cooling energy consumption, occupant behavior should be taken as an essential factor. Hence, a stochastic occupant behavior is considered (Richardson et al., 2008).

$$N_k = N_{max}\psi_k;\ N_{max} = O_a A_{fl} \tag{3.6}$$

3.3.1 Annual envelope heat gain estimation by physical simulation

The apartment models were created using SketchUp 2019, and the building energy simulation was carried out using the OpenStudio® (OS) cross-platform tool that supports EnergyPlus™ (EP). EnergyPlus™ is a whole building energy simulation programme that is superior to its predecessor programmes, BLAST and DOE-2, in terms of user-configurable modular system and variable time step simulation. OpenStudio® is an EnergyPlus/Radiance framework that allows users to easily extend the base capability of EnergyPlus™ for a variety of purposes. Additionally, the abstractions of EP that OpenStudio® provides make it easier to understand new energy models and automate a wide variety of energy analyses (Hale et al., 2012, Long et al., 2013). Utilizing advanced building energy modelling, more specifically EnergyPlus™, is a strategic component of the United States Department of Energy's mission to enhance the design and operation of buildings. The OpenStudio®-created base energy model can subsequently be put to use in the parametric analysis tool (PAT), which is part of the OpenStudio® software package and allows for the generation of alternative design configurations (Long et al., 2013). Figure 3.2 provides an illustration of the workflow for the modelling and energy simulation process that was utilized in this investigation.

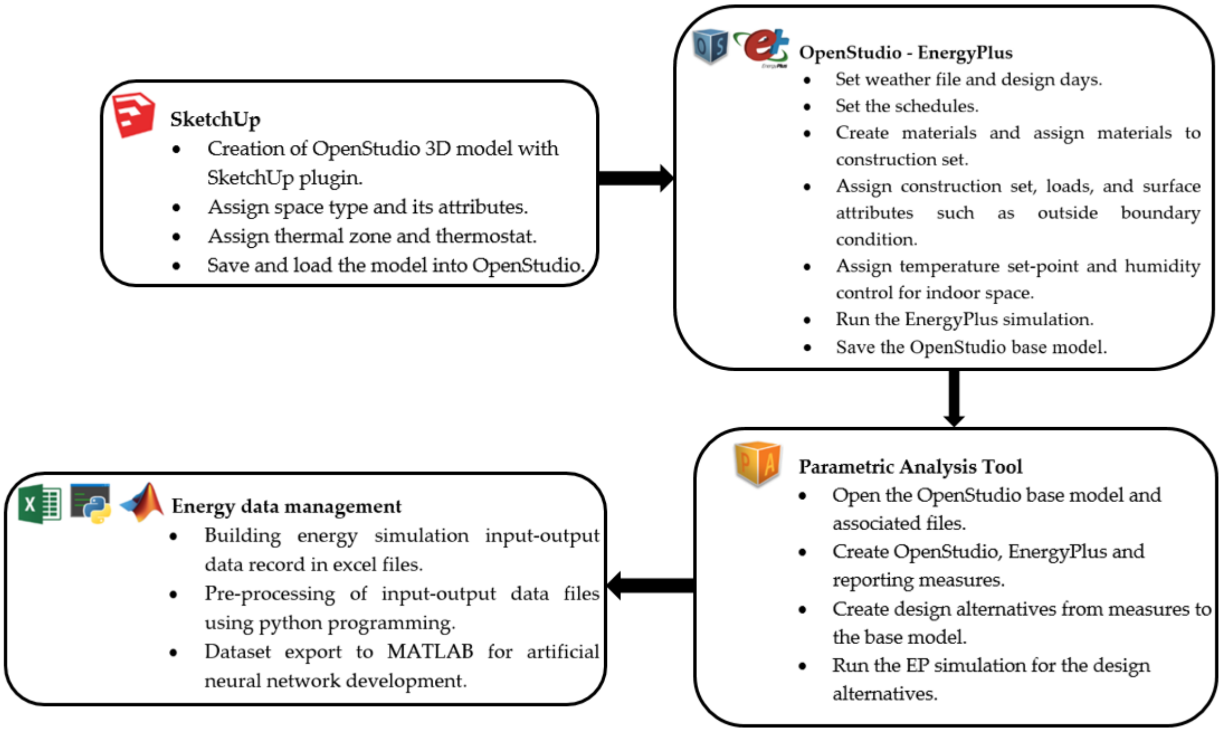

Figure 3.2 Workflow of the modeling and energy simulation process

The parametric analysis tool gives users the ability and flexibility to manually compare many design alternatives that are generated from a variety of measures and scripts within the tool. The measure is a script programme that was written in the programming language ruby. It offers the functionality to change the insulation properties of walls, modify window to wall ratios, operational settings, occupancy schedules, generate detailed reports of input–output of energy models, and so on. As an illustration, a window overhang can be easily generated on a prototype room model by utilizing a measure that is titled *Add Remove Or Replace Window Overhangs*. This is demonstrated in Figure 3.3. The script file is too long to be listed here, but it is easily accessible from the user community's building component library (BCL), which is a digital archive that stores building components and measures (Fleming et al., 2012). As a result, the PAT tool, with all its various functionalities, was utilized to carry out EP simulations for a variety of different apartment layouts, operational conditions, and material properties.

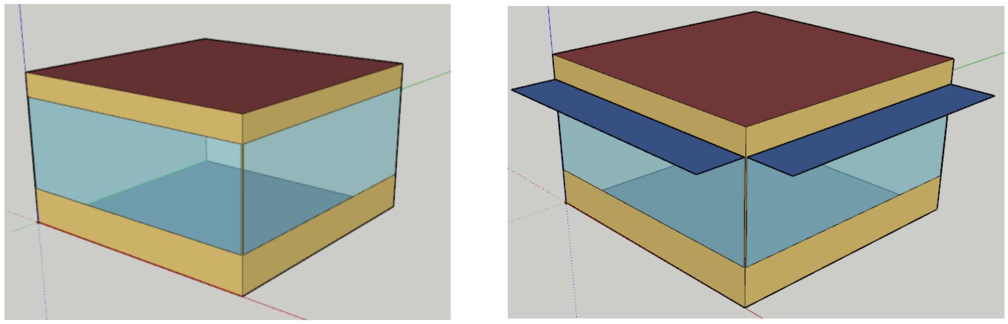

(a) **(b)**

Figure 3.3 Illustration of a simple room model: (a) Before application of overhang measure; (b) After application of overhang measure.

The physical and operational parameters, also known as the input parameters in Table 3.1, were configured in a total of 620,000 different random ways. For the purposes of the EP simulations, the data regarding the weather in Hong Kong in 1989 was obtained from the Hong Kong Observatory (Mui and Wong, 2007a). To train the ANN model, we used a database that contained the ranges of the input parameters and the hourly envelope heat gains that corresponded to those ranges that were generated by the simulations. This is illustrated in Figure 3.4.

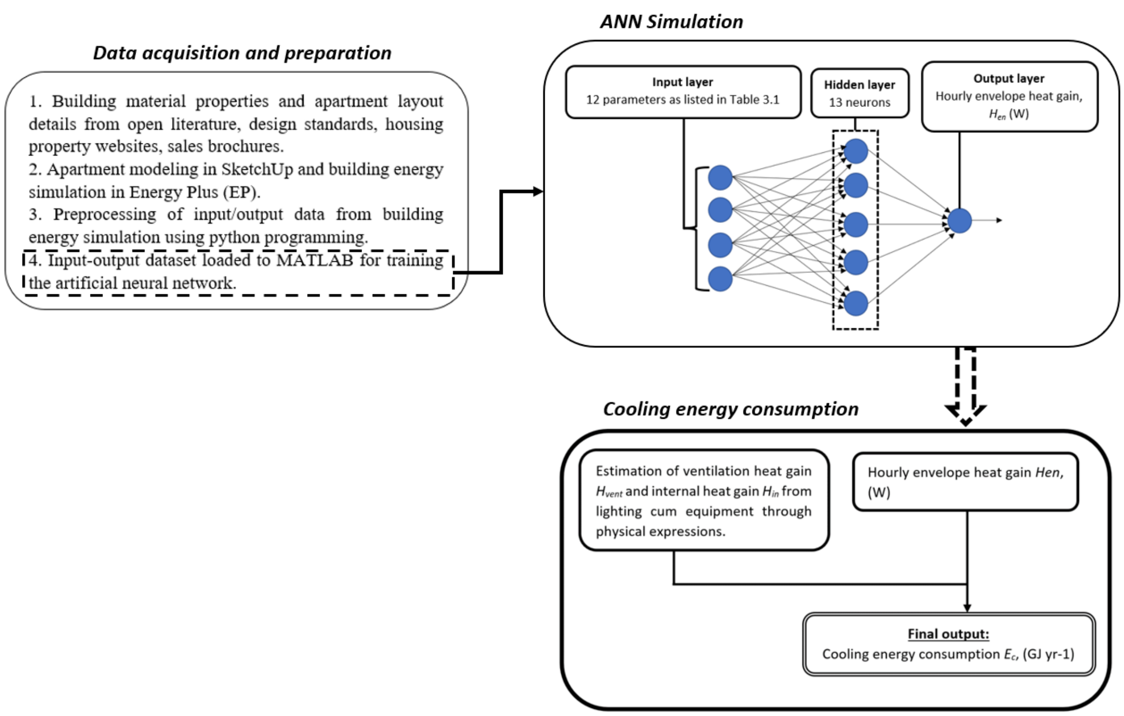

Figure 3.4 Schematic of the proposed cooling energy consumption estimation model

3.3.2 Artificial neural network

The development of an artificial neural network can be traced back to the process of generalizing the neural connections found in the human brain and translating them into a mathematical model. The development of new technologies over the course of the past 20 years has paved the way for ANN to find applications in an almost infinite number of fields. Some examples of these fields include aerospace, energy, and medical science. The building industry is not immune to the adoption of artificial neural networks, and it is applied to various stages of a building project, such as conception, control optimization, energy consumption prediction, retrofitting, and performance evaluation (Ahmad et al., 2018, Guyot et al., 2019). The exponential growth of computing capacity and processing speeds has greatly increased the applicability and reliability of ANN to predict building-related energy performance (Kumar et al., 2013). In addition, the ability of ANN to process non-linear input–output relationships with high precision have made it a popular choice for building energy efficiency practitioners over conventional theoretical and empirical methods.

When developing an ANN model for accurate predictions, the architecture of the neural network that is used and the inherent hierarchical characteristics of that architecture should be given careful consideration. The backpropagation algorithm (also known as BPA) serves as the foundation for this model. The input–output data from the EP simulations were used as the dataset to train the BPA-based neural network. The database comprising 620,000 datapoints were partitioned to 70% for training and 30% for testing the artificial neural network. An ordinary feedforward network with three layers is used. This network has an input layer that contains 12 neurons, a hidden layer that contains 13 neurons, and an output layer that contains one neuron. Training the input vectors and the target vectors that correspond to them is accomplished with the help of the Levenberg–Marquardt algorithm (LMA). As was demonstrated in earlier research studies, LMA performs better than other models such as gradient descent and conjugate gradient methods (Torrecilla et al., 2007, Hagan and Menhaj, 1994). LMA was developed to approach second-order training speed without directly computing the Hessian matrix. The Hessian matrix is a matrix of second-order partial derivatives of the error function with respect to the weights and biases of the network. The convergence rate of second-order methods is comparatively higher than that of first-order methods, such as gradient descent, due to their utilization of additional information concerning the curvature of the error surface. This phenomenon can lead to a reduction in the number of iterations required to attain the error function's minimum and expedite the convergence process. However, it is computationally expensive to directly compute the hessian matrix, especially for large neural networks. The LMA overcomes this limitation by approximating the hessian matrix by using a combination of the gradient information and damping parameter, allowing them to attain second-order training speed. The Hessian matrix, abbreviated as Hm, can be approximated as,

$$Hm = J^T J \tag{3.7}$$

$$\beta = J^T e \tag{3.8}$$

where J represents the Jacobian matrix, β represents the gradient, and e represents the vector of network errors. An update method that is similar to that of Newton allows for the approximation of the Hessian matrix to be obtained.

$$x_{n+1} = x_n - [J^T J + \mu I]^{-1} J^T e \tag{3.9}$$

where μ is a scalar variable that is referred to as the Marquardt adjustment parameter. Equation 3.9 operates similarly to Newton's method when μ equals 0 and uses the approximate Hessian matrix; however, when μ is large, the equation transforms into a gradient descent algorithm with a small step size.

A collection of test data can be applied to the trained network to validate the generalizability of the predictions made by the neural network. It is recommended to use the *trainbr* function, which is an LMA-based Bayesian regularization technique available in MATLAB R2020b (Demuth, 2010). This will help to improve the trained neural network's capacity for generalization. The objective function incorporates the conventional error function as well as the weight decay components, and Bayes' rule is applied to optimize the regularization parameters contained within the objective function. A Gaussian distribution with random variables has been applied to both the weights and the biases. The tan-sigmoid activation function, as shown in Equation 3.10, is applied to the hidden layer, while the output layer makes use of the linear transfer function $f_{pureline}$, as shown in Equation 3.12.

$$a_j = f_{tansig}(n_j) = \frac{2}{1 + \exp(-2n_j)} - 1; \tag{3.10}$$

$$n_j = \sum_{j=1}^{13} \sum_{i=1}^{12} P_i IW_{j,i} + b_j \tag{3.11}$$

where i and j represent the number of elements in the input vector and the hidden layer, respectively; a_j is the output from each neuron in the hidden layer; n_j is the net input vector; P_i is the input element of the input layer; i can range from 1 to 12; IW is the input weight matrix; $P_iIW_{j,i}$ represents the weighted input value; and b_j represents the bias.

$$H_{en} = f_{pureline}(n_{out}) = n_{out};\ n_{out} = \sum_{j=1}^{13} a_j LW_j + b_{out} \tag{3.12}$$

where H_{en} is the hourly envelope heat gain in watts, a_jLW_j is the output layer weighted value, $f_{pureline}$ is the linear transfer function, n_{out} is the net output value, and LW_j is the layer weight index.

3.3.3 Model validation

To validate the hybrid model that was developed, it was tested using a variety of various operational and design combinations. During training, the ANN was given one hidden layer, and the number of neurons in that layer ranged from 12 to 14. For the purposes of training and testing the neural network, the dataset was divided into 70:30 proportions. Because the LMA-based Bayesian regularisation technique does not fundamentally require a validation set, it allows for the utilisation of a greater quantity of data in the training process of the network. This is a significant benefit of the technique. However, validation is done with a wide range of values as indicated in Table 3.2, that were within the lower and upper range of values that were utilized for training the ANN as shown in Table 3.1. In addition, to test the generalization capability of the hybrid model, it was again tested with values of parameters that were beyond the range of values that were used for training the ANN, as indicated in Table 4.1 of Chapter 4. Figure 3.5 illustrates the degree to which the results of the EP and the ANN are a good match for the various setups detailed in Table 3.2. It was found that with 13 hidden neurons, the ANN gave a better correlation (R^2 = 0.947) and a Root Mean Squared Error (RMSE) of 0.0389, indicating a well-trained and well-equipped neural network for predicting envelope heat gains. The selection of a number of hidden neurons was carried out on a trial-and-error basis (Kumar et al., 2013).

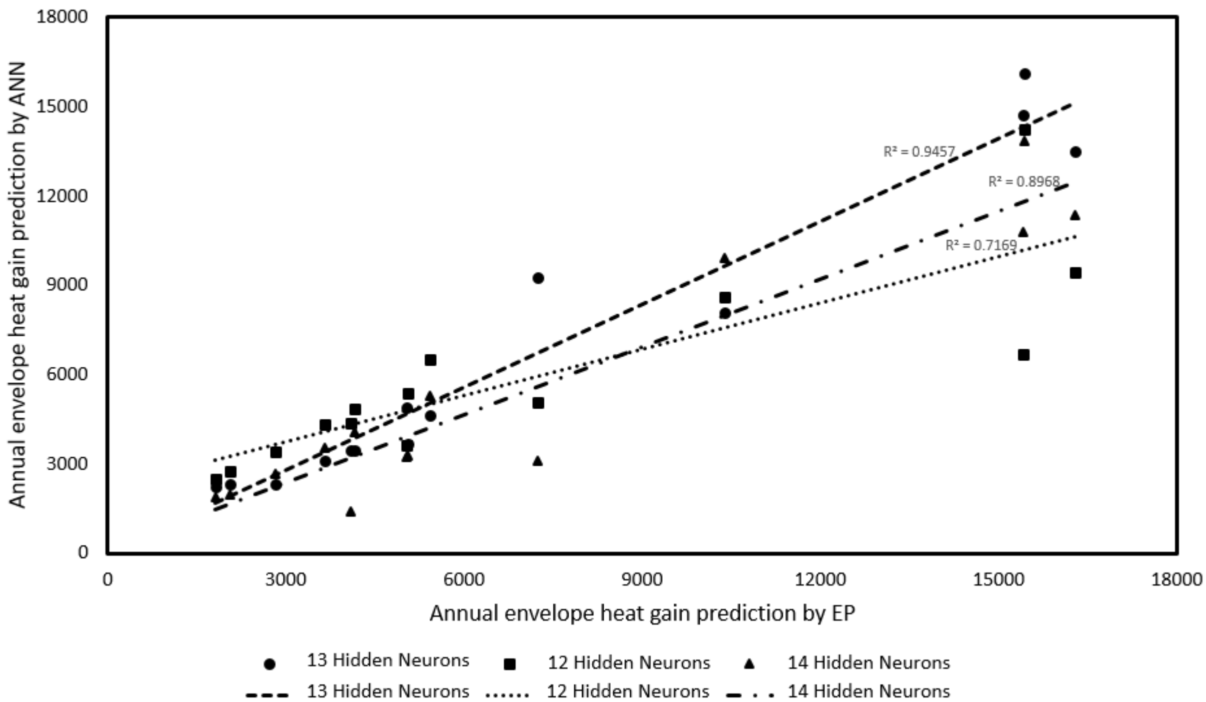

Figure 3.5 Comparison between artificial neural network (ANN) and EnergyPlus (EP) predictions of the annual envelope heat gain (KW yr^{-1})

Table 3.2 Apartment details and other parameters for model validation

Case	Floor Area (m^2)	External Wall Area (m^2)	Window Area (m^2)	Indoor Set-point Temperature (°C)	Wall U-value ($W/(K·m^2)$)	Window U-value ($W/(K·m^2)$)	Shading Coefficient	Orientation (°)	Vertical Shadow Angle (°)
1	30	22.8	12.3	22	0.5	5	0.9	180	0
2	35.8	31.9	7.6	24	2.9	6.9	0.97	45	75.3
3	65	36.1	15.5	26	1.5	5	0.9	-90	40
4	30	22.8	12.3	24	1.5	5.8	0.7	90	70
5	110	63.8	36.9	22	1.5	4.2	0.9	0	70
6	30.4	30.4	4.2	24	2.9	6.9	0.97	45	75.3
7	145	75.2	40.5	24	1.5	5	0.7	0	70
8	23.9	32.8	5.1	27	2	4.2	0.7	-45	40
9	35.9	40	9.2	24	2.9	6.9	0.97	45	75.3
10	15.1	21.1	4.6	24	2.9	6.9	0.97	45	75.3
11	120	70	35.1	28	0.5	4.2	0.5	180	0
12	135	48.3	63.2	26	0.5	5.8	0.7	0	70
13	52.1	46.4	11.5	26	0.5	5.8	0.5	-90	75.3
14	19.7	17.6	3.7	24	2.9	6.9	0.97	45	75.3

The validity of the hybrid simulation strategy was tested against a previous study that was performed by Cheung et al. (2005). They studied the influence of the passive design strategies on cooling energy consumption of a public housing apartment. The researchers used TRNSYS to do energy simulations for eight apartments situated in the middle floor of a concord type housing block. The energy simulations utilized the weather data of Hong Kong in 1989. In their study, it was considered that the apartment remained unoccupied from 07:00 in the morning until 19:00 in the late evening and occupied by 3-4 people during the remaining hours. Cheung et al. (2005) had utilized this standard occupancy pattern that was directly related to the AC operation schedule, while a stochastic occupancy pattern was utilized in the proposed hybrid simulation model of this study for cooling energy prediction (Richardson et al., 2008). The apartment of the prior study all maintained an indoor set-point temperature of 24 °C. The present study, akin to its predecessor, neglected the impact of self-shading and inter-block shading on cooling energy consumption. Moreover, an averaged lighting power density (L_{pd}) of 18 W/m^2, and an equipment power density (E_{pd}) of 26 W/m^2 from the previous study was used in this current investigation.

The material properties of the building envelope along with required physical dimensions and operational conditions from the previous study were then utilized to run the hybrid simulation model to estimate the cooling energy consumption. Figure 3.6 clearly demonstrates that there is an increase in cooling energy consumption with increase in shading coefficient and window area. The trends seen in the predicted results of annual cooling energy consumption provided by the hybrid simulation approach and by the study carried out by Cheung et al. (2005) are very similar. It's possible that the change in COP was the cause of the former results having a larger percentage (about 8.5%). In the study done by Cheung et al. (2005), a constant COP of 2.5 was employed. In contrast, a consistent and lower hourly COP_k (as low as 1.5; notably during humid summer nights with a low sensible heat ratio (SHR_k)) is utilized in the hybrid simulation approach. Importantly, the results indicate that it has a physical significance, as these variations in cooling energy consumption are anticipated when we consider the fundamental laws of heat transfer. The model is therefore physically plausible.

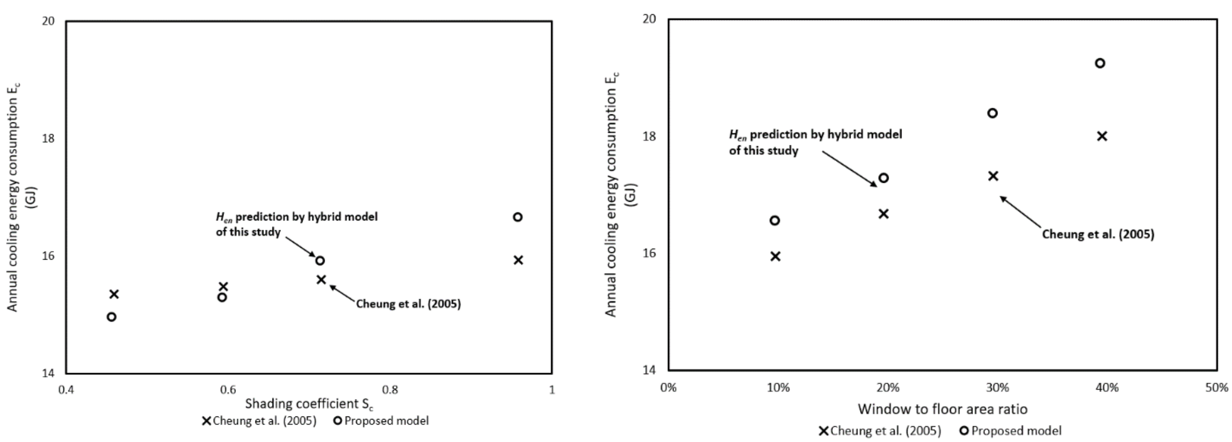

(a) (b)

Figure 3.6 Comparison of results by the proposed model and (Cheung et al., 2005) study (**a**) Annual cooling energy consumption (E_c) v/s Shading coefficient (S_c); (**b**) Annual cooling energy consumption (E_c) vs. window-to-floor area ratio.

3.4 Influence of building-related parameters on cooling energy consumption

The insulating qualities of walls and windows were determined for the purpose of this research by referring to a variety of design standards and open access databases. An apartment with a floor area of 60 m^2 and a range of window U-values varying from 4.2 to 6.5 W/(K·m^2) and a range of shading coefficients varying from 0.4 to 0.8 is used to show the influence of window insulation on the annual cooling energy consumption in Figure 3.7. It has been noticed that the amount of energy required for cooling an apartment increase with the U-value of the windows. For example, if the shading coefficient is 0.6, then the yearly cooling energy consumption values are 8.8 GJ and 9.19 GJ for windows with U-values of 4.2 W/(K·m^2) and 5.5 W/(K·m^2), respectively. This results in an increase of 3.4% in the annual cooling energy load. A similar pattern can be seen with the cooling energy requirement exhibiting an upward trend when the shading coefficient is increased while the U-value of the window remains the same. In addition, Figure 3.7 demonstrates that an annual cooling energy consumption estimate of 8.85 GJ is the lowest possible value for a U value of 4.2 W/(K·m^2) with a shading coefficient of 0.4, while an annual cooling energy consumption estimate of 9.58 GJ is the highest possible value for a U value of 6.5 W/(K·m^2) with a shading coefficient of 0.8. Windows with a low U-value (e.g., 4.2 W/(K·m^2)) and a low shading coefficient (e.g., 0.4) reduce annual cooling energy use by 8.19%.

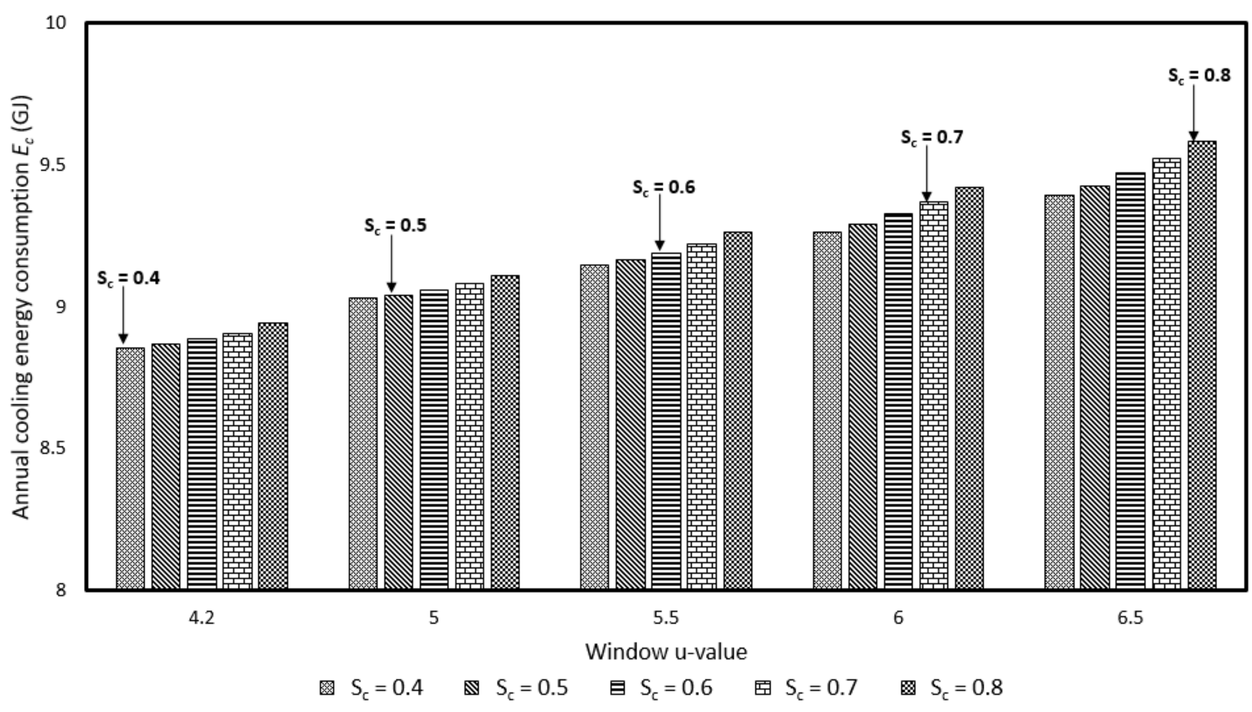

Figure 3.7 Annual cooling energy consumption with variation in window U-value (W/(K·m^2)) and shading coefficient S_c

The effect that external wall insulation has on the amount of cooling energy used annually in an apartment was another factor that was taken into consideration. Figure 3.8 depicts the amount of energy required for apartment cooling when the U-values of the external walls ranged from 0.4 to 2.5 W/(K·m^2) and the floor areas were 30, 60, and 90 m^2 respectively. The consumption of yearly cooling energy in the apartment that is 30 square meters in size and has a U-value of 2.5 is shown in the figure to be 4.28 gigajoules, while the consumption of annual cooling energy in the apartment that is 90 m^2 in size is 14.42 gigajoules. According to Figure 3.8, when the U-value is changed from 2.5 W/(K·m^2) to 0.4 W/(K·m^2), an average reduction of 7.56% may be achieved in the annual cooling energy consumption of all flats. This can be accomplished by lowering the U-value.

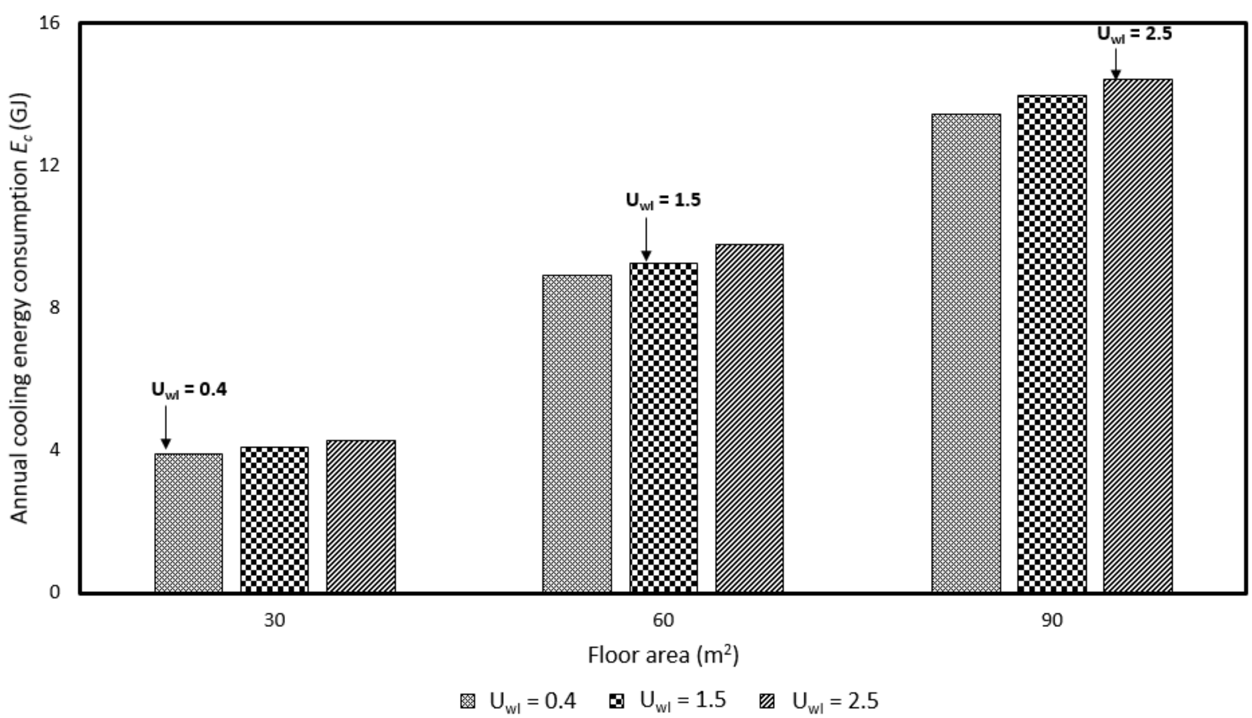

Figure 3.8 Annual cooling energy consumption with variation in external wall U-value (W/(K·m^2))

The window-to-wall ratio, commonly known as the WWR, is an essential building arrangement that not only produces a pleasing visual aesthetic but also has significant influence on the amount of heat gained through the envelope of an apartment. The estimation of the annual cooling energy consumption for a 60 m^2 apartment is shown in Figure 3.9. The WWRs range from 20% to 80%, and there is a step of 20% between each value. The values for cooling energy consumption that are 7.85 GJ when WWR is equal to 20% and 9.96 GJ when WWR is equal to 80%, respectively, are the lowest and maximum possible values. According to the findings, elevating the WWR from 20% to 80% resulted in an increase in the annual quantity of energy required for cooling. On the other hand, lowering the WWR from 80% to 40% can bring about a savings of 18% in annual cooling energy usage. This can be accomplished without compromising the needs for proper ventilation and visual aesthetics.

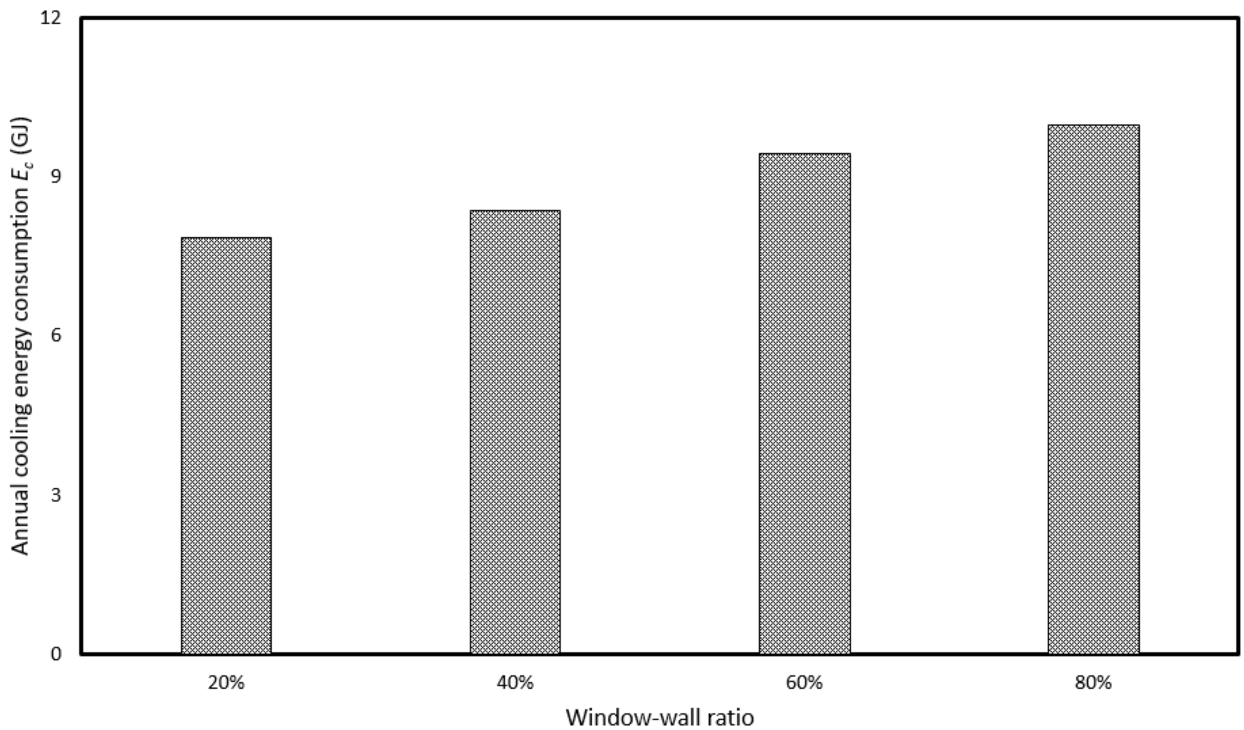

Figure 3.9 Annual cooling energy consumption with variation in window-wall ratio

3.5 Influence of indoor set-point temperature on cooling energy consumption

Figure 3.10 depicts the forecast of annual cooling energy usage for a 60 m^2 flat using the fluctuation in outdoor temperature T_o based on Hong Kong's meteorological data in 1989 and a range of indoor set-point temperatures T_{in} between 23 °C and 26 °C. The effect that global warming has on the natural temperature range was another factor that was considered. At indoor set-point temperatures of 23 °C and 26 °C, respectively, one can see the highest annual cooling energy consumption (10.35 GJ) and the lowest annual cooling energy consumption (7.63 GJ). This is because the higher temperature requires more cooling energy. If the indoor set-point temperatures are raised from 23 °C to 26 °C or 24 °C to 26 °C, annual cooling energy consumption can be reduced by 26% and 13.65% respectively. On the other hand, annual cooling energy consumption can be reduced by 21% and 13.03% if the indoor set-point temperatures are raised from 23 °C to 24.5 °C or 24 °C to 25.5 °C. If the indoor temperature is above 25 °C, then every increase of T_{in} by 0.5 °C will yield a reduction of 2.5% in annual cooling energy consumption. In the temperature range of 23–25 °C, a reduction in annual cooling energy consumption of 7.66% can be achieved by increasing T_{in} by 0.5 °C. When the outdoor temperature rises by 1 °C, it is estimated that the annual cooling energy load will rise by 4% from the existing level to keep the indoor set-point temperature at 24 °C. On the other hand, it is estimated that the annual cooling energy load will rise by 6% from the existing level to keep the indoor set-point temperature at 23 °C. This helps put global warming into perspective.

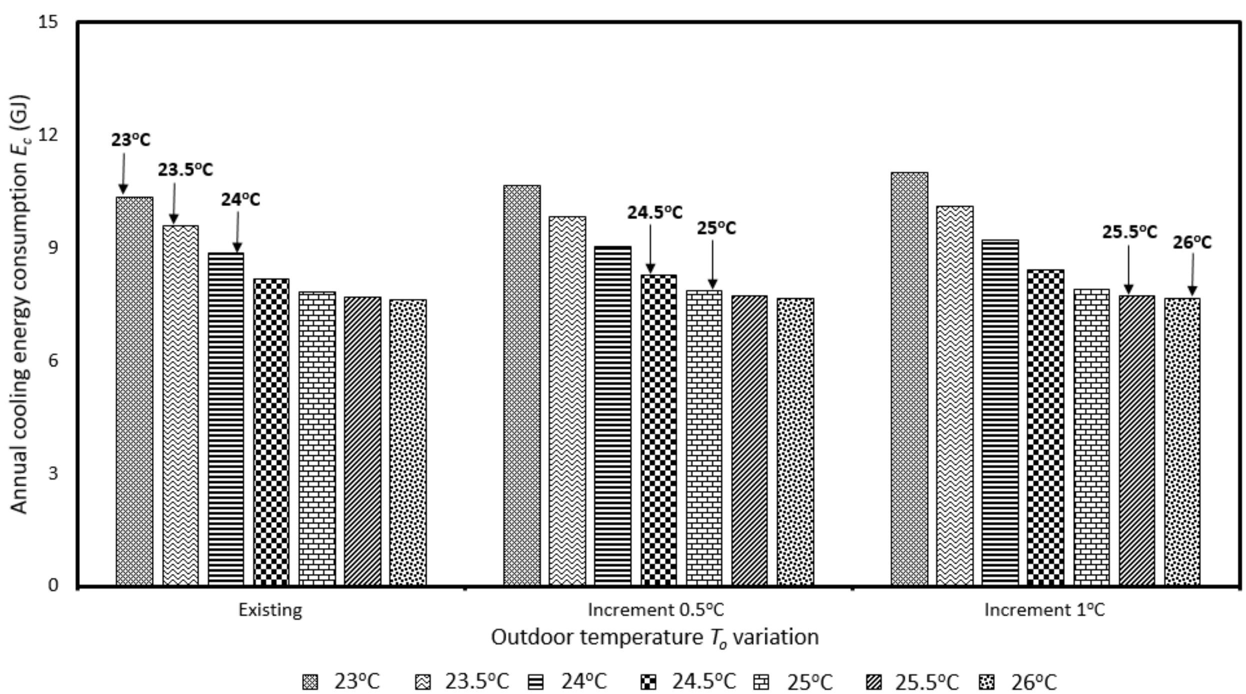

Figure 3.10 Annual cooling energy consumption forecast based on indoor set-point temperature

3.6 Discussion

The heat transfer that occurs via the building envelope is the primary factor that can have an impact on the amount of electricity required for the process of cooling an apartment so that its occupants can continue to enjoy a satisfactory level of thermal comfort. Based on the findings of this research, selecting construction materials with an appropriate U-value is essential since this factor can influence the amount of energy required for apartment cooling. When looking at the different floor areas that were taken into consideration for this study, it was found that the amount of energy needed to cool the building grew proportionally with the U-value of the external wall. It goes without saying that there is a linear relationship that exists between the amount of energy required for cooling and the U-value of the building material. As a result of the apartment's floor area being doubled while the apartment's walls maintained the same U-value, the apartment's cooling energy usage nearly doubled. Taking this scenario into consideration, it is vital to note that the cooling energy consumption of flats with large floor areas might be very high if ideal thermal insulations are not supplied on the building envelope. Buildings that rely on natural ventilation can minimize thermal discomfort by upgrading the U-value of their building envelopes. This is because U-value can be a critical element in limiting the amount of heat that is transported to the interior environment.

An index of thermal insulation related with glazing is referred to as the shading coefficient S_c. The higher the S_c, the lower the resistance to heat transfer through solar radiation; conversely, the lower the S_c, the higher the resistance to heat transfer through solar radiation. According to the findings of this study, both the window's U-value and its S_c play a significant part in the rise or fall in the amount of cooling energy that is consumed. It is important to note that the selection of tinted or low-emissivity glass with lower S_c values compared to standard clear glass is always preferable for buildings located in the sub-tropical climatic region. This is because tinted or low-emissivity glass helps reduce the amount of heat that is transferred into the building. Altering the shading coefficient of a window that has a constant U-value can help cut down on the amount of cooling energy that is needed to keep the room at a comfortable temperature. To get to the heart of the matter, it is vital to interpret from this study that a mix and match of U-value and

S_c can be obtained depending on the demand. For instance, if passive solar heating energy is sought, a window combined with a high S_c and a low U-value can be specified. It is recommended that buildings situated in subtropical climate zones make use of windows that have a lower U-value and a lower S_c value, as this can significantly minimize the amount of energy required for cooling the structure.

In order to place even more focus on the role that the building envelope plays in determining the amount of energy required for cooling, the influence of window-to-wall ratio (WWR) was also investigated. When calculating the amount of energy needed for cooling, one extremely important factor to consider is the total area of a window that is exposed to direct sunlight. When there is a greater amount of window surface area that is exposed to an environment that has a low level of thermal insulation, the amount of energy required to cool the building will increase. The findings of this investigation made it abundantly clear that there is a linear connection between WWR, and the amount of energy required for cooling. In Hong Kong, huge luxury flats typically come with larger window-to-wall ratio (WWR) than public housing buildings. Large windows may be aesthetically pleasing to the eye, but they are also a significant factor in the introduction of additional heat into an interior space. The provision for having large WWRs must be provided with suitable thermal insulations to decrease the amount of heat that is gained within the building. In the same vein, the findings of this study suggest that decreasing the WWR may be an effective method for cutting down on the amount of energy required for cooling. As a result, it is essential to create a balance between the required amount of energy consumption for cooling and the visual aesthetics of the space.

It was said before that during the past hundred years in Hong Kong, there has been a rise in the number of days and nights that are extremely hot, while there has been a fall in the number of days that are cold. This tendency is essentially same in other parts of the world, where there has been recorded a significant shift in the average daily temperature. The need for cooling energy in indoor areas is being driven by the rise in average temperature that is occurring as a direct effect of climate change. It is necessary to lower the indoor set-point temperature to bring down the amount of energy that is consumed by the cooling system. According to the findings of this study, there is great potential to cut energy consumption by adjusting the temperature set-points already in place inside buildings. As a result, it is strongly recommended that people all over the world immediately begin the practise of raising the indoor temperature set-point above the current levels to cut the amount of carbon emissions linked with the energy that is used for building cooling. Building energy efficiency practitioners can use the confluence of solutions revealed in this study as a good reference point to improve upon existing knowledge and mitigate the carbon emission related with the residential sector by using the information presented in this study.

3.7 Summary

In this chapter, it was identified that a significant contributor to greenhouse gas emissions is the utilization of electrical power for the purpose of air conditioning in residential buildings situated in climate zones classified as subtropical, such as Hong Kong. Between the years of 2008 and 2018, there was a rise of 13.1% in the total amount of power that was consumed in the residential sector. If suitable measures are not implemented to reduce the amount of energy needed for cooling, it is anticipated that Hong Kong's residential energy consumption will increase along with the city's population as well as the average size of households. Benefits that extend far and wide might result from implementing energy efficiency measures to reduce carbon emissions in the construction industry.

Thus, a hybrid simulation strategy was proposed. This strategy is a testament to the potential of integrating artificial intelligence techniques with a building energy simulation tool (EnergyPlus™) to predict the annual cooling energy consumption for buildings in Hong Kong. Its purpose will be to identify key relationships between building physical characteristics and operational strategies to reduce the cooling energy demand in a minimal amount of time in comparison to traditional methods of energy estimation. To check its validity, it was tested for goodness of fit with energy plus simulations and for an open literature data. A satisfactory energy prediction performance was achieved as result of the validation assessment, indicating its suitability to replace traditional building energy prediction methods. The generalization ability of the proposed hybrid simulation model for parameters beyond its training range will be evaluated in Chapter 4.

The hybrid simulation model can analyze building materials, construction solutions, and indoor–outdoor temperature variations on apartment cooling energy. The effect of passive design strategies on cooling energy consumption has been explored in detail, while ignoring the effect of inter-block shading and self-shading on the cooling energy demand. Therefore, all simulations in this chapter considered a scenario that generates maximum solar heat gain condition to a space. It was identified that by using low thermal conductivity building materials for windows and external walls can reduce annual cooling energy consumption by 8.19%, and decreasing the window-to-wall ratio from 80% to 40% can save 18%. Changing the indoor set-point temperature from 24 °C to 26 °C can save 13.65% in cooling energy annually. Taking global warming into perspective, when the outdoor temperature rises by 1 °C, annual cooling energy load increases by 4% and 2.5% for maintaining 24 °C and 25.5 °C indoor set-point temperatures, respectively. The expected alterations in the energy consumption for cooling, as observed in this study, can be attributed to the underlying principles of heat transfer. Therefore, it can be inferred that the outcomes anticipated by the hybrid simulation model hold significant physical significance. Consequently, the hybrid simulation model that was formulated can be deemed as being physically plausible.

Chapter 4

A generalized hybrid simulation model coupled with a genetic algorithm

4.1 Introduction

In Chapter 3, a robust hybrid simulation model was developed to predict the cooling energy consumption in residential buildings. The amount of energy used on cooling an indoor area is highly dependent on the construction of the building as well as the materials used. The simulation model proved to be an efficient prediction tool that could determine the influence of building-related parameters within its training range on the cooling energy demand. However, the ability of the model to predict the energy demand for parameters outside its training range was untested.

The construction of a hybrid simulation model to evaluate the energy performance of a building is a time-consuming and important procedure that requires multiple simulations to be carried out with dependable BPS tools. Because of this, models that are only valid for a single building are often worthless. Generating hybrid simulation models for a set of buildings would allow one to fully use its capacity, generating enormous benefits. In fact, the computational costs of creating hybrid simulation models would be justified by their application in many case studies. They would be a powerful energy-prediction tool. Hence, in this chapter, the generalization ability of the hybrid simulation model for parameters beyond its training range is evaluated.

To ensure that the model would continue to perform well outside of the training data range, two distinct types of premises were selected: 1) sub-divided units (SDUs), which are residential spaces with specific building characteristics that fall below the lower limit of the training data range; and 2) healthcare facilities, which are non-residential spaces that have specific building parameters that fall beyond the upper limit of the training data range. Further, they were selected as application cases to serve as examples of the various ways for cutting down on energy use in these facilities.

Design space exploration done through parametric study is laborious if done through the conventional approach. Moreover, the results so obtained cannot be attributed to an optimal solution to the problem. Hence, the hybrid simulation model is coupled with an evolutionary algorithm to support the user to iteratively evaluate the various design conditions and their corresponding impact on the cooling energy demand. The integration of GA with hybrid simulation model would enable the user to find the optimal or sub-optimal solution for certain building settings from a pool of solutions in a time efficient manner.

4.2 Generalization beyond the training range

Early stopping and Bayesian regularization are two well-known strategies for enhancing the predictive power of an ANN beyond the scope of its training data. Bayesian regularization has been effectively utilized for the training of neural networks by academics from a variety of disciplines and fields of study. Bayesian regularization was found to have superior generalizability when compared to early stopping, according to research conducted by Doan and Liong (2004). The seminal work that was done by Foresee and Hagan (1997) confirmed that the integration of Bayesian regularization with the Levenberg-Marquardt algorithm for training a feed-forward neural network would reduce the computational overhead as well as provide excellent generalization capabilities. The Bayesian regularization technique was applied in a study conducted by Mahapatra and Sood (2012) to increase the generalization capability of the neural network and avoid the possibility of overfitting. The Levenberg-Marquardt algorithm was improved by Suliman and Omaro (2018), who additionally included Bayesian regularization. The method demonstrated cost-effectiveness computationally while offering good classification with high sensitivity. In addition, a Bayesian regularization-based Levenberg–Marquardt neural model developed by Kayri (2016) not only possessed a superior capacity for prediction but also possessed the potential to uncover intricate connections. These studies confirm the use of Bayesian regularization in the hybrid simulation model built in Chapter 3 was significant to enhance the generalization ability of the model.

To evaluate the generalization capabilities and performance of the model, two different kinds of premises were selected: 1) sub-divided units (SDUs), which are residential spaces with specific building characteristics that fall below the lower limit of the training data range; and 2) healthcare facilities, which are non-residential spaces with specific building parameters that fall beyond the upper limit of the training data range. In Hong Kong, the area for household in an SDU can be less than 7 m^2 (Wong, 2018). This is below the range of floor area values that were used for training the ANN. On the other hand, inpatient wards were noted to have floor areas beyond the range of values used for training the ANN. Furthermore, it was noted in the literature that this facility may also possess material characteristics, such as the U-value of the exterior wall and window, that fall outside the range of values used to train the ANN. The ANN was put through its pace under a variety of operational and physical conditions, which are outlined in Table 4.1. The table contains parameters that are associated with buildings such as public housing flats, private apartments, SDUs, and hospitals. The goodness-of-fit test, which is depicted in Figure 4.1, shows that the ANN can generalize well (R^2 = 0.95). Thus, it confirms that the hybrid model is capable of efficiently predicting the annual envelope heat gains of different physical and operational configurations.

Table 4.1 Physical and operational parameters

Case	Floor Area (m^2)	External Wall Area (m^2)	Window Area (m^2)	Indoor Set-point Temperature (°C)	Wall U-value (W/(K·m^2))	Window U-value (W/(K·m^2))	Shading Coefficient	Orientation (°)	Vertical Shadow Angle (°)
1	10	3.2	4.9	24	0.5	5	0.6	180	0
2	30	22.8	12.3	22	0.5	5	0.9	180	0
3	35.8	31.9	7.6	24	2.9	6.9	0.97	45	75.3
4	65	36.1	15.5	26	1.5	5	0.9	-90	40
5	30	22.8	12.3	24	1.5	5.8	0.7	90	70
6	110	63.8	36.9	22	1.5	4.2	0.9	0	70
7	30.4	30.4	4.2	24	2.9	6.9	0.97	45	75.3
8	145	75.2	40.5	24	1.5	5	0.7	0	70
9	7	4.9	3.2	24	0.5	4.2	0.5	180	0
10	23.9	32.8	5.1	27	2	4.2	0.7	-45	40
11	35.9	40	9.2	24	2.9	6.9	0.97	45	75.3
12	120	70	35.1	28	0.5	4.2	0.5	180	0
13	135	48.3	63.2	26	0.5	5.8	0.7	0	70
14	52.1	46.4	11.5	26	0.5	5.8	0.5	-90	75.3
15	19.7	17.6	3.7	24	2.9	6.9	0.97	45	75.3
16	270	24.3	16.2	24	0.5	4.2	0.5	180	0
17	270	8.1	32.4	22	0.5	3.8	0.5	180	0

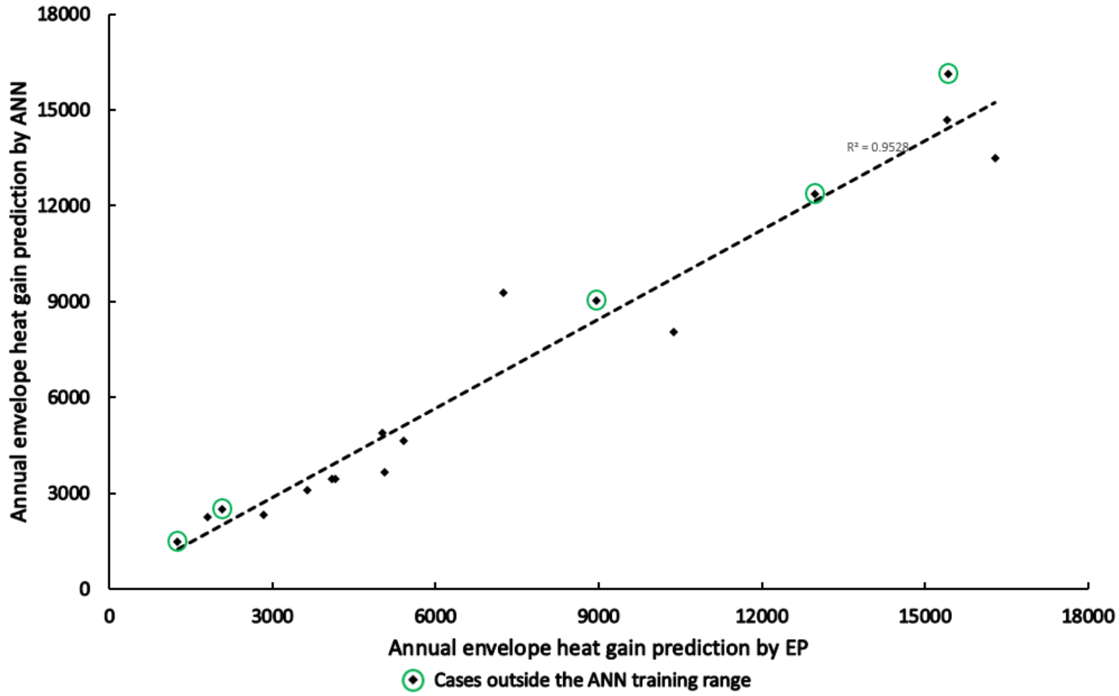

Figure 4.1 Annual envelope heat gain (kW yr^{-1}) predictions by ANN and EnergyPlus (EP)

In section 4.3, the sub-divided units are further explored with the aid of a generalized hybrid simulation model to analyze the various approaches that can be taken to reduce the amount of energy associated with this unit. Furthermore, in section 4.4, the integration of an evolutionary algorithm with the hybrid simulation model to conduct an optimization is discussed. To demonstrate the procedure and its consequent advantages in prediction of cooling energy consumption, a general inpatient ward cubicle is chosen as an application case. The impact of passive design strategies on cooling energy usage has been investigated, with little attention given to the influence of inter-block shading and self-shading on cooling energy requirements. Thus, the simulations conducted in this chapter incorporated a scenario wherein space experiences the highest possible solar heat gain.

4.3 Sub-divided units (SDU)

The housing market in Hong Kong is consistently ranked as one of the most unaffordable in the world. The high cost of private housing, the extremely long wait times for allotment of public housing (an average of

5.8 years), and the ongoing lack of available housing have contributed to the development of housing alternatives such as subdivided units (SDU). The floor plan of a residential apartment is shown in Figure 4.2 (a), and the apartment subdivided into two or more separate units, which are referred to as sub-divided units is illustrated in Figure 4.2 (b). The sub-divided units are designed to accommodate more people so that they can be rented out. The average per capita floor area in a SDU in Hong Kong in 2013 was reported to be 6.2 m^2 (Wong, 2018). However, according to latest report from the Hong Kong government, the average per capita floor area has plummeted to 5.3 m^2 (LCS, 2018). The number of SDUs in Hong Kong has increased steadily over the past few years, going from 66,900 in 2013 to 92,656 in 2016 (Wong, 2018, LCS, 2018).

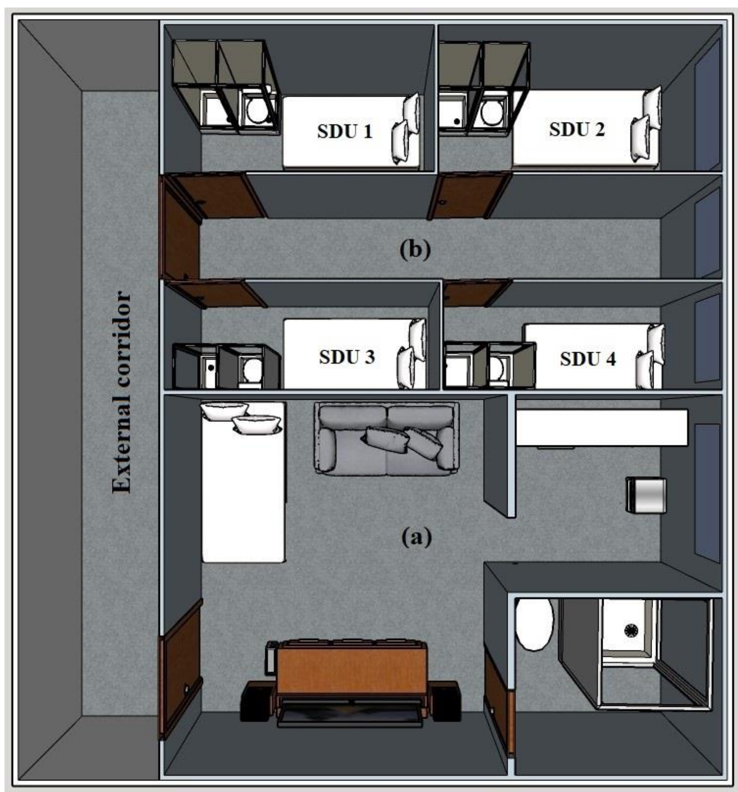

Figure 4.2 Example model of: (a) Residential apartment; (b) Residential apartment with four tiny sub-divided units (SDUs).

4.3.1 Influence of area per occupant on cooling energy consumption

It is estimated that the average area per occupant in a subdivided unit (SDU) is relatively less compared to public housing (13.4 m^2/person). Due to this fact the maximum number of occupants that reside within a SDU is relatively high when compared to an apartment in public housing. The annual cooling energy consumption in a sub-divided unit is plotted against floor area as shown in Figure 4.3, and it is observed that annual cooling energy consumption tends to increase with floor area. The average floor space per person in an SDU is used to calculate the number of residents. It is a widely acknowledged fact that the mere presence of individuals within a given space can result in an increase in heat gain attributable to the occupants. Thus, the increase in occupants could lead to variations in cooling energy consumption. Even slight fluctuations in the amount of energy used for cooling can alter the amount of electricity used, changing the amount of carbon dioxide emitted.

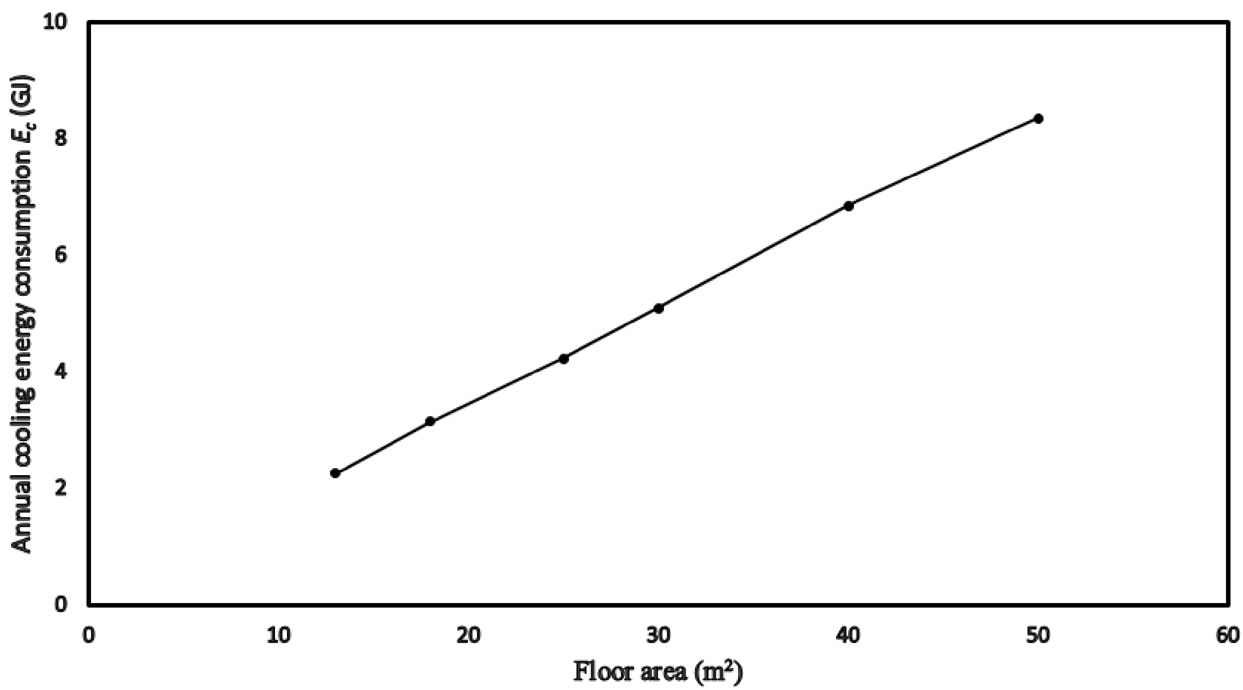

Figure 4.3 Annual cooling energy consumption variation with floor area for sub-divided housing

Figure 4.4 illustrates how the variation in annual cooling energy consumption can occur within an apartment with the same total floor area but a different number of residents. It should come as no surprise that the amount of energy used will rise proportionately to the number of occupants present within a particular floor space. For instance, when the number of occupants increases from two to five, there is a corresponding increase of twenty percent in the annual cooling energy consumption for a floor area of 30 m^2. The annual cooling energy consumption tends to be relatively high as the floor area increases; this trend can have a negative effect on the city's efforts to achieve its sustainability goals.

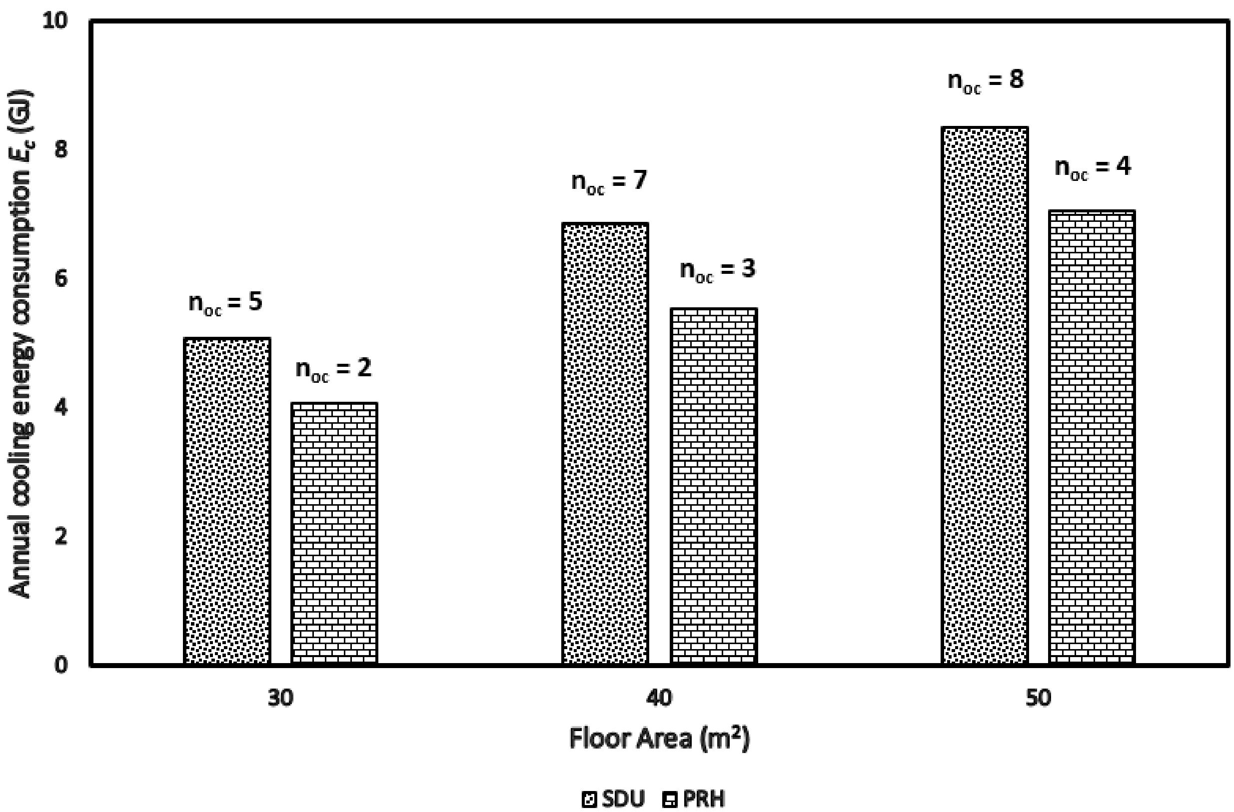

Figure 4.4 Variation of annual cooling energy consumption with number of occupants (n_{oc}) in different floor areas of sub –divided unit and public housing.

As mentioned earlier regarding the impact of the number of occupants and the apartment floor area, it has been observed that the number of occupants within a household, particularly one that consists of SDUs, can be quite energy intensive when compared to public housing that shares the same floor area. In light of this observation, the variation in annual cooling energy consumption with change in area per occupant for different floor areas in a sub-divided unit is studied, and the results are shown in Figure 4.5. It has been observed that there is a significant opportunity to cut carbon emissions by regulating the typical amount of space occupied by each person. For instance, in an apartment with a floor area of 18 m^2, increasing the area per occupant from 6.2 m^2 to 8 m^2 can result in a savings of 11.5% of the apartment's total energy consumption, whereas increasing the area per occupant from 6.2 m^2 to 12 m^2 can result in a savings of 24.6% of the apartment's total energy consumption. The area per occupant as well as the apartment floor area are both potential parameters that can influence the amount of cooling energy that is consumed within a sub-divided unit. There needs to be control measures and policy regulations in place to regulate the amount of space that is set aside as a subdivided unit for households of varying sizes.

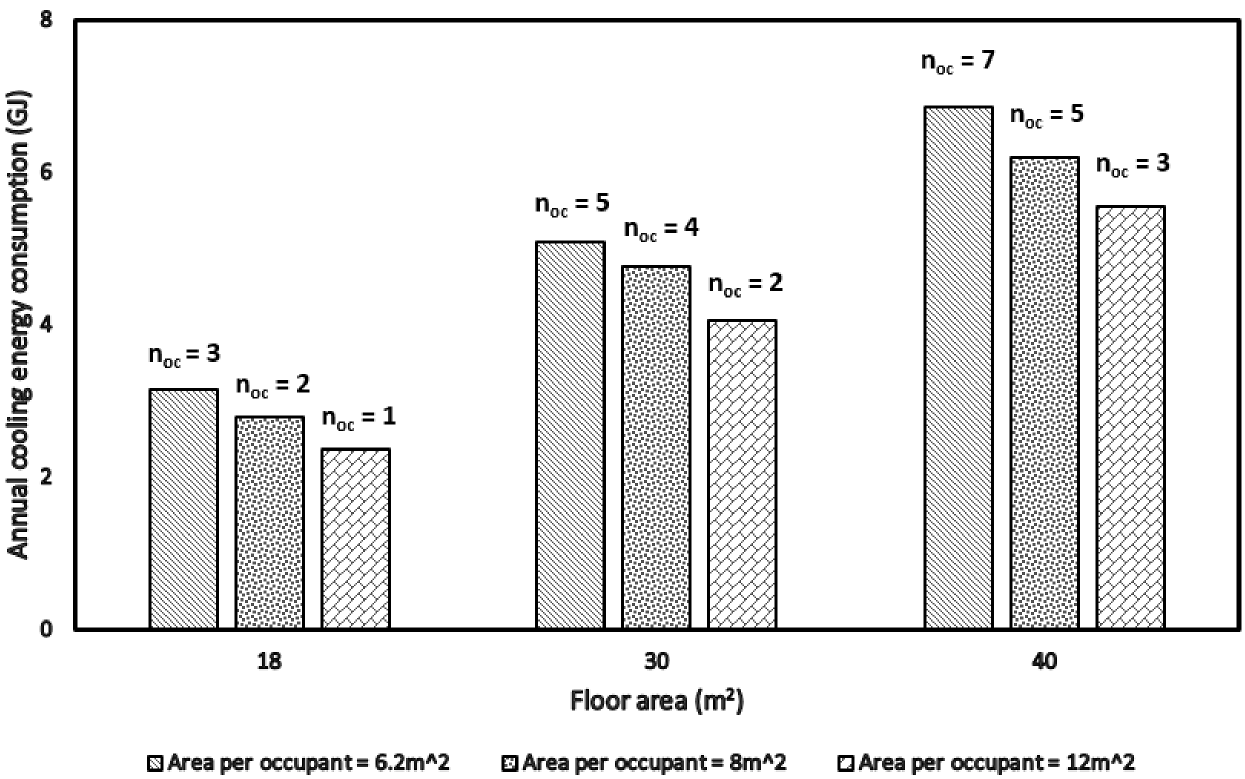

Figure 4.5 Variation of annual cooling energy consumption for floor areas (18m^2, 30m^2, 40m^2) with variation in area per occupant.

4.3.2 Influence of indoor-set point temperature

When we work toward lowering the carbon emissions that are associated with apartments, the temperature that we decide to maintain inside the unit at all times can be an important determining factor. Figure 4.6 depicts the effect of indoor set-point temperature on annual cooling energy usage for subdivided units with varying space per occupant. In order to evaluate the influence of indoor set-point temperature on cooling energy consumption for a space with a floor area of 18 m^2, the indoor set-point temperature is varied from 23 ^oC to 26 ^oC. At the same time, the influence of variation of the average area per person on cooling energy requirement is analyzed. Thus, three average area per occupant scenarios are considered, namely, 6.2 m^2, 8 m^2, and 12 m^2, resulting in a maximum of 3, 2, and 1 inhabitant per unit with a floor space of 18 m^2, respectively. With regards to an average area per occupant of 6.2 m^2 in an SDU, the maximum yearly cooling energy consumption is 3.6 GJ when the indoor set-point temperature is 23 ^oC, and the lowest is 2.69 GJ when the indoor set-point temperature is 26 ^oC. It has been observed that a reduction in energy consumption of 26.42% can be attained by raising the indoor set-point temperature from 23 ^oC to 26 ^oC, whereas a reduction of 14.16% can be attained by raising the indoor set-point temperature from 24 ^oC to 26 ^oC. Similarly, as the average area per occupant increases from 6.2 m^2 to 8 m^2, the cooling energy consumption decreases by 11% while the indoor set-point temperature is maintained at 24 ^oC. Furthermore, as the indoor set-point temperature is increased from 24 ^oC to 26 ^oC for an average occupant area of 8 m^2, the annual cooling energy consumption decreases by up to 16.14%. Changing the average area per occupant for SDU from 6.2 m^2 to 12 m^2 results in a 24.6% reduction in annual cooling energy consumption when the indoor set-point temperature is maintained at 24 ^oC. Changing the indoor set-point temperature from 24 ^oC to 26 ^oC for an average occupant area of 12 m^2 results in an additional 18.94% reduction in annual cooling energy consumption.

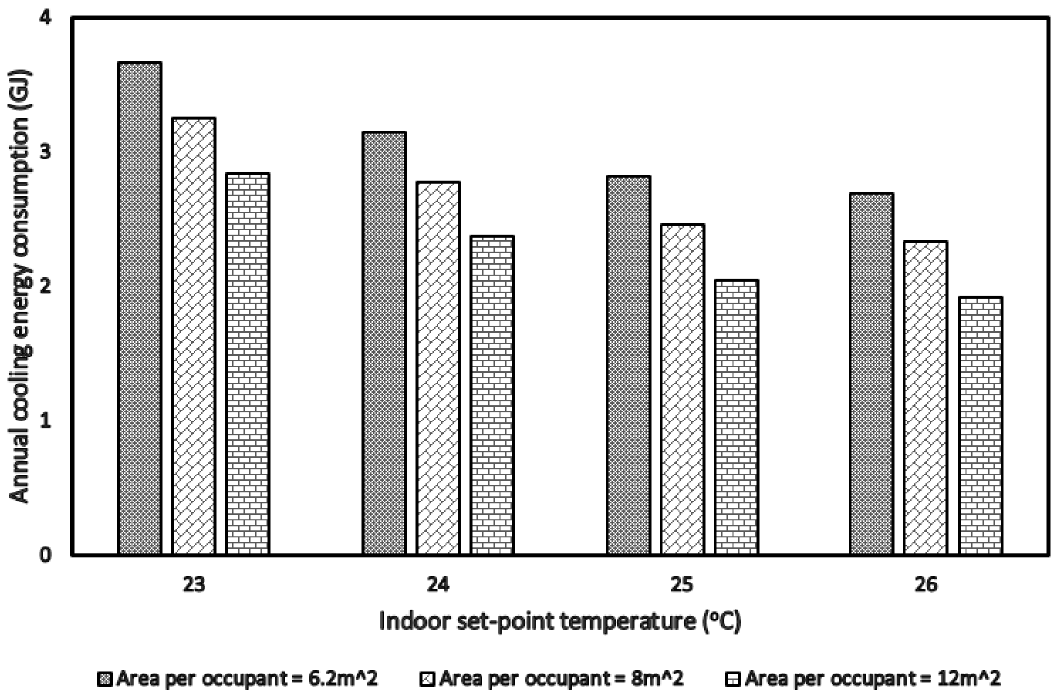

Figure 4.6 Annual cooling energy consumption based on indoor set-point temperature with variation in area per occupant for an apartment.

4.3.3 Discussion

It is generally believed that the reduced space associated with tiny houses will ease the load on the environment and make housing more affordable. However, in certain situations, such as when there is a lack of buildable land, affordable housing, and minimum standards of living space per person in cities like Hong Kong, many people are frequently crammed into spaces, which results in increased levels of discomfort and increased levels of energy consumption. By utilizing the generalized hybrid simulation model, the influence of apartment floor size, occupant per floor area, and indoor set-point temperature on annual cooling energy usage was evaluated. It was revealed that a living space with the same square footage in public housing and a subdivided unit, the latter utilized more energy. It was also observed that when apartment floor space increased, so did the energy usage of subdivided apartments. The average square footage per occupant in SDUs was a major factor in the rising demand for energy. It was observed that raising the average area per occupant in an 18 m^2 flat from 6.2 m^2 to 8 m^2 reduced cooling energy consumption by 11.5%, whilst increasing the average area per occupant from 6.2 m^2 to 12 m^2 reduced cooling energy consumption by 24.6%. In addition to the area per person, the indoor set-point temperature has been identified as a significant factor in reducing energy use. Changing the indoor set-point temperature from 24 ^{o}C to 26 ^{o}C for an apartment unit with an average occupant area of 8 m^2 and 12 m^2 results in a 16.14% and 18.94% reduction in annual cooling energy usage, respectively. While environmental factors are considered, subdivided units in Hong Kong frequently experience problems with thermal discomfort and inadequate ventilation. In such units, it is thus essential to strike a balance between the occupants' comfort and health while examining the possibility of adjusting the indoor set-point temperature for energy savings. Therefore, an investigation that strikes a balance between energy consumption and thermal comfort for occupants in tiny housing units is recommended.

4.4 Coupling of ANN with a genetic algorithm

The selection of the physical parameters of the building and the operational conditions plays a significant impact in either minimizing or maximizing the required amount of energy. A hybrid simulation model developed in Chapter 3 was combined with a genetic algorithm to pick diverse operational and physical configurations that would either minimize or maximize the envelope's potential heat gain. One of the population-based meta-heuristic algorithms that is frequently utilized for gradient-free optimization is the genetic algorithm (Holland, 1975). It is a class of evolutionary algorithms that were inspired by Charles Darwin's idea of natural selection. These algorithms develop solutions to optimize a given problem through the processes of selection, mutation, and crossover to get optimal results. The evolutionary algorithm is well-suited for the resolution of nonlinearity problems, which are typically challenging to resolve using more traditional approaches. Additionally, rather than converge to the local minima, it has a tendency to converge to the global minima (Reynolds et al., 2017). The genetic algorithm (GA) generates a population of probable solutions by utilizing a fitness function that is based on a generalized pre-trained neural network. Each solution in this population is represented as a chromosome, and each chromosome has a string of values that are referred to as genes. Here, the genes serve as the input parameters to the neural network, and the two chromosomes that were determined to have the highest overall fitness values using the roulette wheel selection method are the parents.

Elitist, crossover, and mutation are the three primary forms of genetic operators that are utilised in the process of reproduction. Using the elitist selection strategy ensures that only the chromosome that possesses the highest level of fitness will be passed on to the following generation. Through a process known as crossover, the genes on one chromosome are swapped with the corresponding genes on another chromosome to produce children with improved fitness values in comparison to their parents. This is accomplished by performing random mating in the mating pool. The process of mutation involves a change to the genes that are included within the chromosome, which assists in the process of escaping from local minima. New generations will be produced until a particular stopping criterion, such as the maximum number of generations, is fulfilled. Until then, new generations will be produced. When the stopping requirement is satisfied, the GA delivers the optimal chromosome or solution with either the smallest or largest envelope heat gain. The optimal set of input parameters will be fed back into the ANN to produce the annual envelope heat gain. The global optimization toolbox found in MATLAB R2022a was utilized for optimization process (MATLAB, 2022). Figure 4.7 depicts the coupling of the artificial neural network (ANN) with the genetic algorithm (GA) in MATLAB to optimize the input parameters.

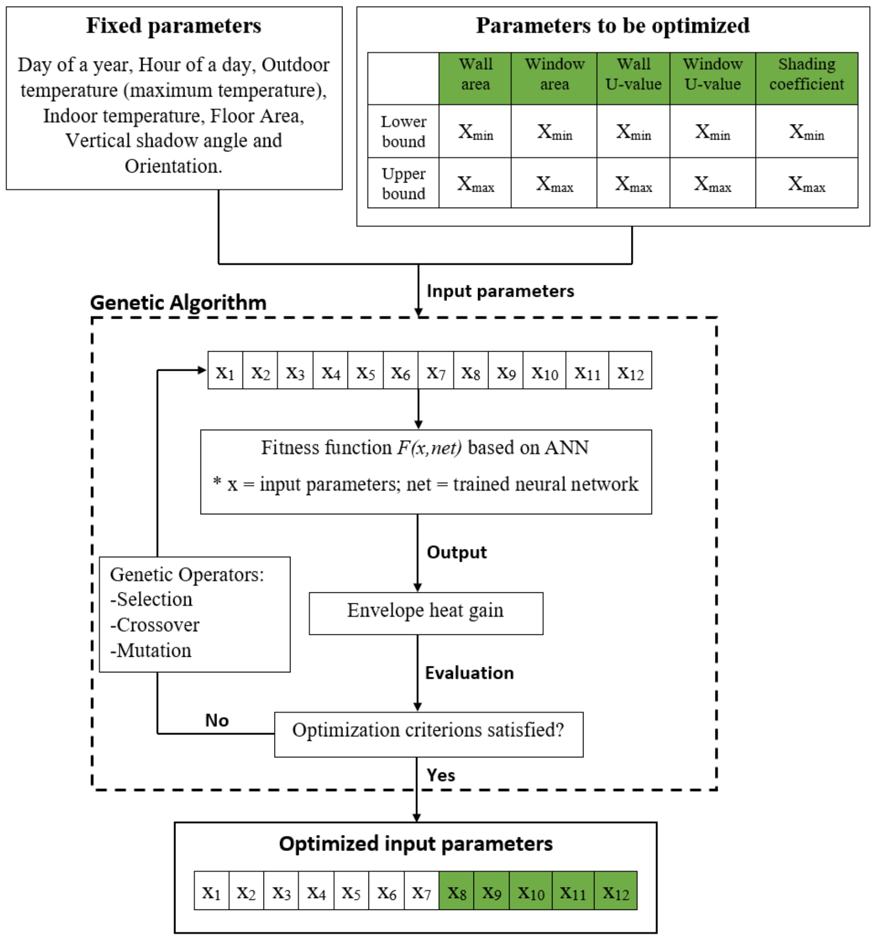

Figure 4.7 Coupling of ANN with genetic algorithm in MATLAB for parameter optimization

4.5 General inpatient ward

It is of the utmost importance to take into consideration building spaces falling under the healthcare category. There are not many studies that have been done on healthcare buildings and the demand for energy. It is possible that reducing costs and lowering carbon emissions in healthcare facilities will be impossible without significant improvements in energy efficiency. An air change rate in a ward can range anywhere from four to six with a design temperature of 24 ^{o}C, as outlined in the guidelines. According to the findings of a number of studies, there is a significant relationship between the ventilation strategy and the distribution of contaminants in indoor environments (Li et al., 2007a). According to research carried out by Yu et al. (2017) in a general hospital ward, an air change rate of 9 h^{-1} was found to effectively cut down on the amount of time that particles spent floating around and depositing in the ward. Considering this development, it is critical to revise and update the existing guidelines in a timely manner based on new evidence in order to reduce the likelihood of an infection outbreak in the future. Nevertheless, hospitals continue to face a significant challenge when attempting to reduce their energy consumption without compromising infection control.

The amount of overall floor space that is taken up by inpatient wards is typically quite significant in hospitals (Morgenstern et al., 2016). The image depicted in Figure 4.8 serves as a representative example of the standard configuration of a general ward in Hong Kong (Li et al., 2005). The ward featured a nursing station, a storeroom, and four individual patient cubicles. The ward had centralized air conditioning, and each of the four semi-enclosed cubicles was separated from the others by a corridor. The fan coil unit brought in fresh air from outside the building and combined it with the air that had been previously circulated inside the building. The resulting supply air was then distributed to the ward via a four-way air supply diffuser that was installed in the false ceiling. The exhaust grille directed the air back into the fan coil unit so that it could be reused. It is a typical operational configuration of general inpatient ward in Hong Kong.

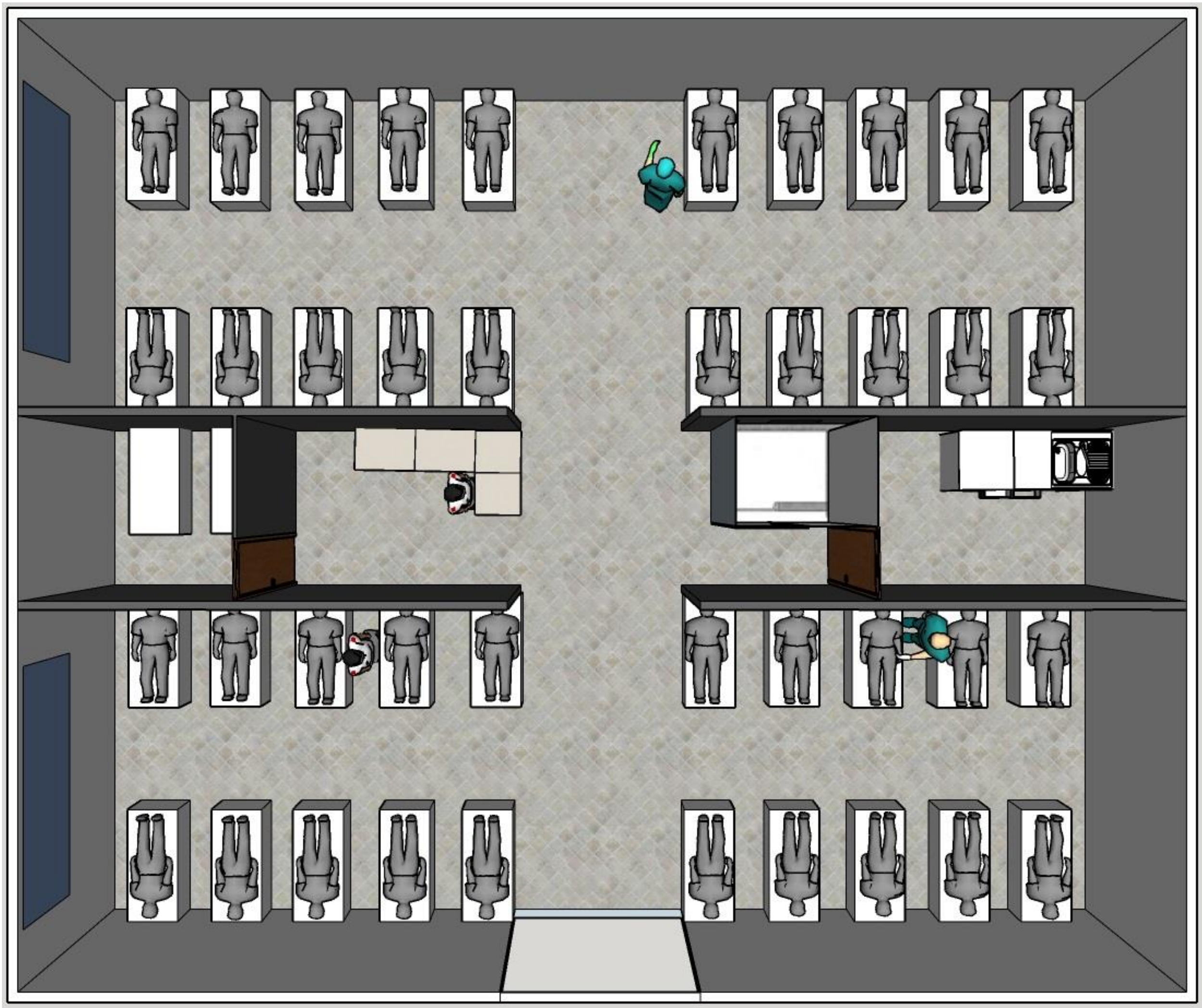

Figure 4.8 Representative image of a general inpatient ward with four cubicles

An energy consumption analysis was performed using a semi-enclosed mechanically ventilated general inpatient ward cubicle that measured 7.5 m x 6.0 m x 2.7 m (Yu et al., 2017, Satheesan et al., 2020). The same six-bed ward cubicle will be utilized in Chapter 5 to perform a computational fluid dynamics (CFD) analysis to determine the risk of infection in a semi-enclosed space under a variety of ventilation strategies. In the current investigation, it was presumed that the cubicle was completely occupied, and the pressure in its corridor was kept at a positive level to reduce the risk of cross-contamination. The supply air (with air change rates of 3 h^{-1}, 6 h^{-1}, 9 h^{-1}, and 13 h^{-1}, respectively) was distributed throughout the ward cubicle by means of four diffusers that were mounted on the ceiling. It was determined that the ventilation system, the lighting, and the plug loads were operating properly and effectively 24x7x365 (that is, 24 hours per day, 7 days per week, and 365 days per year). This research made use of the envelope parameters that are outlined in Table 3.1 in Chapter 3. The material properties of the design parameters of the building envelope associated with hospitals, such as the external wall and the external window, which are essential for carrying out the energy consumption analysis, were taken from the open literature and design standards (Ascione et al., 2013, Buonomano et al., 2014, Papantoniou et al., 2015, Ruggiero et al., 2022, Radwan et al., 2016). The values of these material properties were all considered to fall within the range that was presented in Table 3.1. It should also be noted that a value of 3.2 W/m^2K was reported for the U-value of an external window, and 4.1 W/m^2K was reported for the U-value of an external wall in the literature (Ascione et al., 2013, Buonomano et al., 2014). These values fell outside of the training range of the prediction model. While carrying out the process of optimization depicted in Figure 4.7, these two values were taken into consideration for the lower and upper bounds of their respective parameters. In addition, the window-to-wall ratio of the cubicles used in this study ranged anywhere from 20 to 80 percent. In each of the cases that were scrutinized, the optimal parameter combination that resulted in the lowest or highest envelope heat gain was selected.

As mentioned earlier, the hybrid simulation model is combined with the GA to find the combination of operational and physical characteristics that would either result in the smallest or largest amount of envelope heat gain. In this regard, the maximum annual temperature acquired from the Hong Kong Weather Data 1989 was held constant, along with the indoor temperature (24 ^{o}C), floor size (45 m^2), vertical shadow angle (0^o), and orientation (180^o). However, the shading coefficient, the external wall and window areas, and the U-values of the external wall and window were all assigned lower and upper bound values for optimization purposes. As a result, a genetic algorithm (GA) that used an artificial neural network (ANN) as its fitness function was given a chromosome that contained 12 input parameters as genes. The size of the population was chosen to be 200, and the maximum number of generations was limited to 100. The likelihood of a crossover was 0.85 while the probability of a mutation was only 0.1. Figure 4.9 is a graph that depicts the progression of generations.

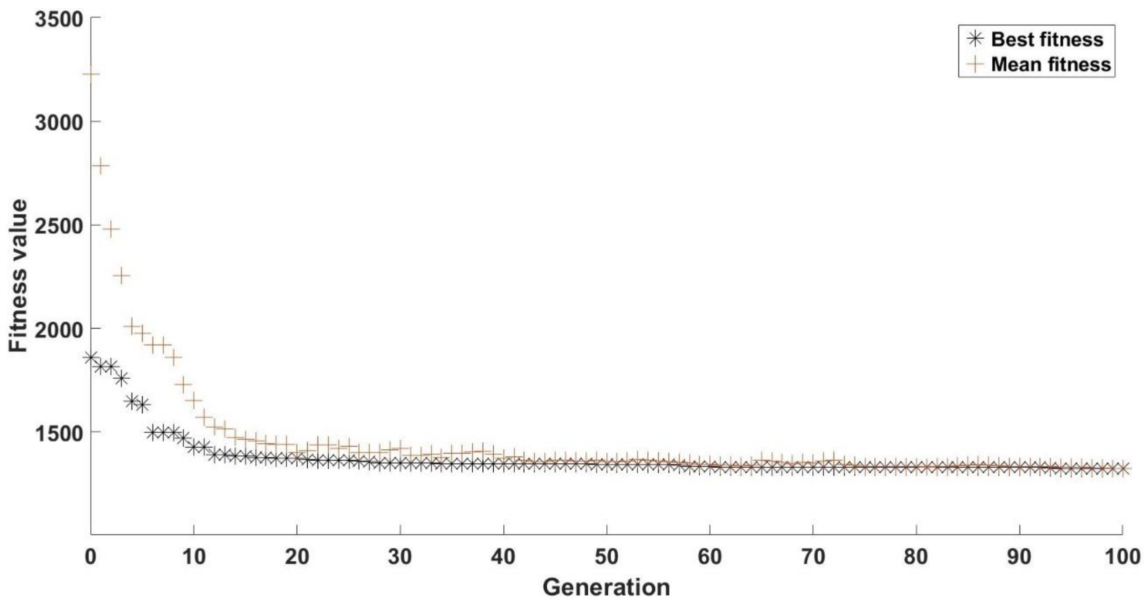

Figure 4.9 Evolution of generations for parameter optimization

4.5.1 Influence of building envelope

The amount of a building's energy consumption can have a substantial association to the building envelope design parameters that were used. These factors include the external wall U-value, the external window U-value, the shading coefficient, and the window to wall ratio. Therefore, determining the impact of design parameter combinations on the heat gain of building envelopes is of the utmost importance, and that is achieved with the assistance of a hybrid simulation model linked with a genetic algorithm. The coupled methodology, which is explained in section 4.4, has the potential to determine the critical parameter combination that would either limit or enhance the envelope's heat gain.

It is noted that by adopting an external window area of 20 % along with selection of low U-value for external window (U-value = 3.2 W/m^{2}K) as well as external wall (U-value = 0.4 W/m^{2}K) and low value of shading coefficient (S_c = 0.4) can lead to a reduction of 69.4 % in annual envelope heat gain when compared to the case with an external window area of 80 % with a high U-value of external window (U-value = 6.9 W/m^{2}K) as well as external wall (U-value = 4.1 W/ m^{2}K) and high value of shading coefficient (S_c = 0.9).

This finding provides more evidence that the choice of envelope parameters has a significant impact on the amount of heat gained by the envelope, which in turn has a bearing on the amount of energy used by the building. In the next section, annual cooling energy consumption will be calculated by employing either the minimum or maximum building envelope heat gain condition in conjunction with various recirculation ratios and lighting power densities. In addition, we will explore the physical settings, as well as the operational parameters, that have the potential to either lower or increase the amount of energy required for cooling.

4.5.2 Influence of recirculation ratio

The design of a ventilation system for a healthcare facility is often complex and must meet several standard-specific operating characteristics to reduce nosocomial infections and provide acceptable thermal comfort. Numerous studies suggest that a high ventilation rate will help dilute pathogenic microorganisms, but a low ventilation rate will increase the risk of infection (Atkinson, 2009, Qian and Zheng, 2018). However, lower ventilation rates are frequently maintained in hospital emergency wards and clinical settings (Morawska et al., 2020). Therefore, ventilation strategies must be able to strike a balance between infection risk and energy usage. In the early days, hospitals were thought to require 100% exhaust or 100% outdoor air. Although Chaddock (1983) foundational work determined that recirculation of the majority of hospital air is acceptable, there are exceptions. A study by Satheesan et al. (2020) that investigated the effects of positioning an exhaust grille adjacent to a patient in a general inpatient ward revealed that a high exhaust flow rate (50%) can significantly prevent the spread of infection among ward residents. In addition, the path between the contamination source (the patient) and the exhaust can be a determining factor in effective infection management. Without recirculation, cooling energy use is significantly higher, as seen in Figure 4.10. As depicted in Figure 4.10, increasing the recirculation ratio will result in a decrease in cooling energy usage. In the case of minimum envelope heat gain and a recirculation ratio of 50%, for instance, energy savings of 30.5%, 37.9%, 41.23%, and 43.58% can be achieved at 3 h^{-1}, 6 h^{-1}, 9 h^{-1}, and 13 h^{-1}, respectively, when compared to the scenario with no recirculation. Using the highest envelope heat gain condition and a recirculation ratio of 50%, energy savings of 25.67%, 33.92%, 37.99%, and 41.02% can be achieved at 3 h^{-1}, 6 h^{-1}, 9 h^{-1}, and 13 h^{-1}, respectively. Clearly, one can obtain more energy savings by selecting a method that results in a lower envelope heat gain and a larger recirculation ratio.

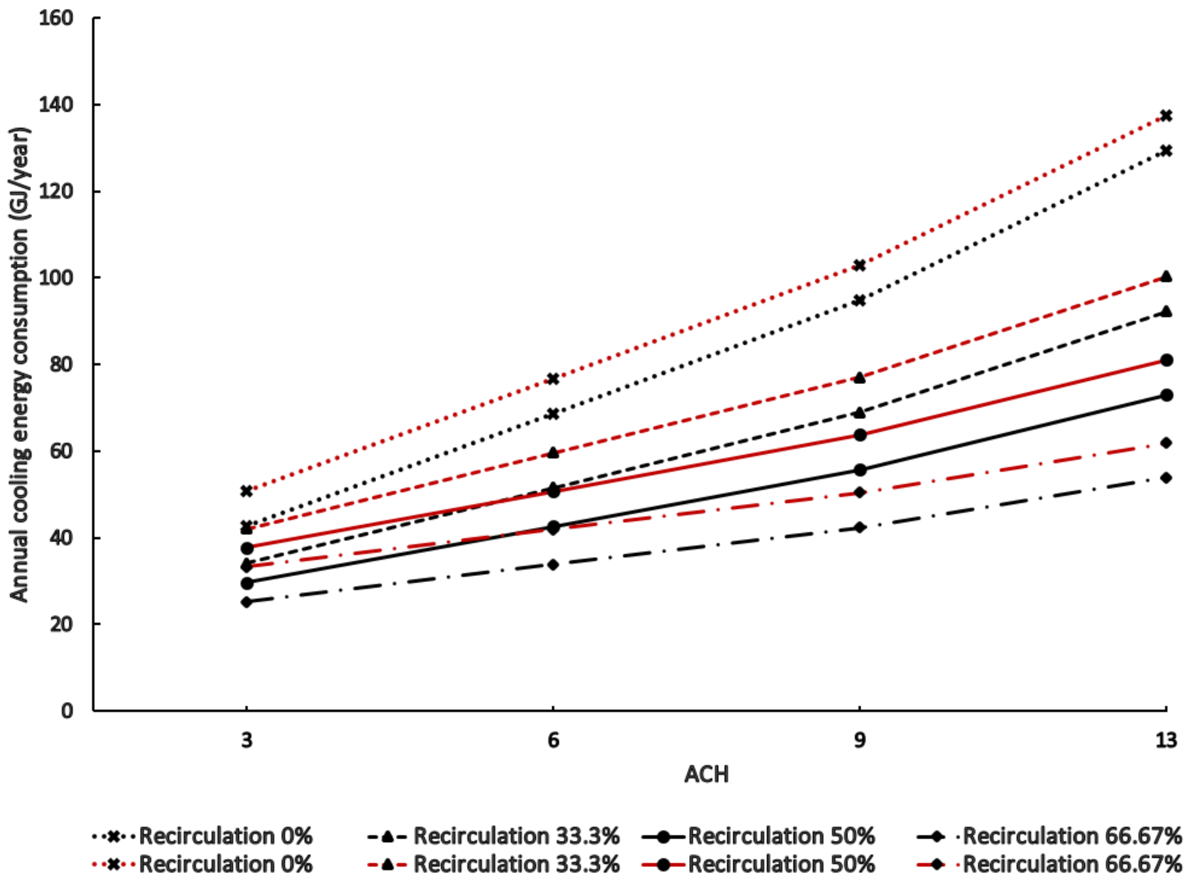

Figure 4.10 Annual cooling energy consumption vs Air change per hour (ACH) for different recirculation ratios. Color band depicts: use of minimum envelope heat gain condition, use of maximum envelope heat gain condition

4.5.3 Influence of lighting

Lighting is another significant contributor to hospital energy use. The variance in energy consumption for two lighting power densities provided for the inpatient scenario is depicted in Figure 4.11. According to the Electrical and Mechanical Services Department (EMSD) (EMSD, 2021) in Hong Kong, the lighting power density (LPD) specified for a patient room is 13 W/m^2, although the ANSI/ASHRAE/IES Standard 90.1 (2020) standard specifies a lower lighting power density of 7.3 W/m^2 for patient rooms. The diagram depicts various air change rates with a recirculation ratio of 50%. In section 4.5.2, it was deduced that the combination of the strategy that results in a decreased envelope heat gain and a recirculation ratio of 50% is an energy-efficient strategy for the ward. Adopting this method and reducing the lighting power density from 13 W/m^2 to 7.3 W/m^2 can result in energy savings of up to 9 percent at an air change rate of 3 h^{-1}, and roughly 5 percent at an air change rate of 9 h^{-1}. As a reduction in lighting power density can aid in reducing a space's internal heat buildup and, consequently, its cooling energy consumption, it is advised that hospitals utilize more energy-efficient lighting systems.

In addition, the effect of envelope heat gain conditions with selected recirculation ratio (50%) and lighting power density (7.3 W/m^2) on cooling energy consumption is compared. It is noted that the highest envelope heat gain condition with the chosen recirculation ratio and lighting power density compared to the minimum envelope heat gain condition reveals an increase in cooling energy consumption of 27.22 % and 14.4 % with an air change rate of 3 h^{-1} and 9 h^{-1} respectively. The combination of a lower envelope heat gain condition, a recirculation ratio of 50%, and a lighting power density of 7.3 W/m^2 would therefore be an energy-efficient strategy for the ward.

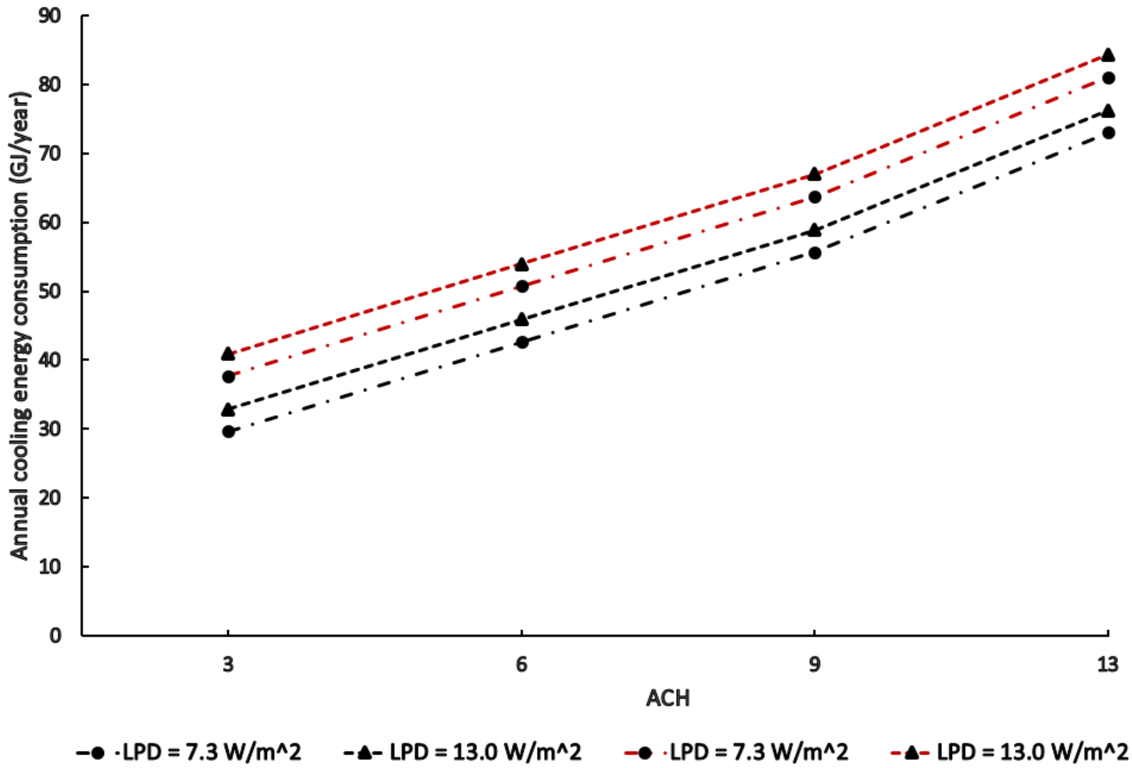

Figure 4.11 Annual cooling energy consumption vs Air change per hour (ACH) for different lighting power densities. Color band depicts: use of minimum envelope heat gain condition, use of maximum envelope heat gain condition.

4.5.4 Discussion

In the field of building energy simulation, hybrid simulation modelling is a sophisticated prediction methodology that, in comparison to other traditional methodologies, can estimate the amount of cooling energy consumption associated with a building in a shorter amount of time. Despite this, most of the hybrid simulation models that have been developed are limited to the simulation of a single type of building. A generalized hybrid simulation model that is based on Bayesian Regularization has been developed. This model would provide the user with the ability to estimate the energy consumption that relates to a variety of building types. Building engineers would be able to quickly identify optimal physical and operational characteristics that could minimize the envelope heat gain by integrating a genetic algorithm with a hybrid simulation model. This would eliminate the need for the engineers to manually search the design space in an exhaustive manner. In addition, a general inpatient ward was selected as an application example to highlight the tactics for lowering energy use. The wards encompass a significant portion of the hospital's floor space. Therefore, implementing energy-saving measures within the wards could potentially have a substantial impact on the facility's overall energy consumption and subsequent carbon emissions.

Building envelope is one of the primary components that can influence cooling energy consumption. An investigation was conducted, and the critical building envelope design parameter combination that either minimizes or maximizes the amount of heat gained by the envelope was found. It was found that a reduction of 69.4% in annual heat envelope heat gain can be achieved by adopting envelope design parameters (external window area of 20%, external window U-value = 3.2 W/m^2K, external wall U-value = 0.4 W/m^2K and shading coefficient S_c = 0.4). These parameters result in minimum envelope heat gain when compared to envelope design parameters (external window area of 80%, external window U-value = 6.9 W/m^2K, external wall U-value = 4.1 W/m^2K and shading coefficient S_c = 0.9) resulting in maximum envelope heat gain. Healthcare facilities typically maintain continuous operation of their ventilation and lighting systems throughout the year. Moreover, to control nosocomial infections, a higher amount of outdoor air is recommended. However, it is linked to a substantial level of energy consumption and cost. The results of this study suggest that adopting a combination of three factors—namely, (i) envelope design parameters that result in minimum envelope heat gain, (ii) recirculation ratio of 50%, and (iii) lowering lighting power density from 13 W/m^2 to 7.3 W/m^2—would prove to be an energy efficient strategy in an inpatient ward. The study demonstrated that a considerable quantity of energy can be conserved through the recirculation of air. It is imperative to prioritize air recirculation by investing in technologies that can effectively purify air. In addition, enhancing the energy efficiency of lighting systems can serve as a significant factor in reducing energy consumption within hospital settings. The present study suggests that stakeholders in the healthcare sector should prioritize the implementation of energy-efficient measures through the refurbishment of existing hospital facilities and the adoption of appropriate strategies in the development of new hospitals. The generalized hybrid simulation tool that is being proposed will be of assistance in the implementation of methods that would result in energy savings, which may, in turn, contribute to an effective reduction in carbon emissions linked with the construction sector.

4.6 Summary

The hybrid simulation model developed in Chapter 3 has a good generalisation capability, which is confirmed by the results of the goodness-of-fit test run for the envelope heat gain prediction for several different cases. In light of this development, it has been demonstrated that it is a powerful prediction tool that can be used to accurately predict the amount of cooling energy required by various kinds of buildings. In spite of the significant amount of computational work that was required for its development, the enormous benefits that the simulation model has to offer outweigh the costs associated with its development.

Tiny dwellings are thought to lessen environmental impact and make housing more accessible. In cities like Hong Kong, where there is a scarcity of buildable land, affordable housing, and no standards on minimum living space per person, many people are squeezed into small areas, resulting in discomfort and higher energy usage. The influence of apartment floor size, occupant per floor area, and indoor set-point temperature on annual cooling energy demand was analysed using a generalised hybrid simulation model. The area per occupant and indoor set-point temperatures are identified to be potential parameters that can be regulated within the tiny residential units to cut down the cooling energy demand.

The integration of an evolutionary algorithm with hybrid simulation model enables a user to quickly identify optimal combination of building related parameters that would reduce the cooling energy demand. Thus, eliminating the need for building engineers to manually search the design space exhaustively. In order to demonstrate the optimization procedure and its advantages, a general inpatient ward cubicle was chosen as an application case. The key drivers (envelope parameters, recirculation ratio, lighting power density) that could have a potential impact on lowering the cooling energy demand associated with the facility were analyzed and effective measures were advised. Moreover, in a general in-patient ward, infection control is significant if not less compared to energy demand. Thus, the strategies to mitigate the spread of infection in a general in-patient ward cubicle are explored in Chapter 5.

Chapter 5

Ventilation strategy to mitigate infection transmission in an inpatient ward

5.1 Introduction

Ventilation systems in buildings play an important part in preserving the quality of the air inside the building (IAQ). Its major purpose is to bring in cool air from the outdoors and remove the heat that is produced inside the building. However, at a hospital or other healthcare facility, the system should also contribute to the treatment and prevention of diseases for patients. Only in buildings that fall under the healthcare category does ventilation need to take infection control into consideration when formulating its functions (Yau et al., 2011). However, there is a lack of suitable guidelines in terms of ventilation design when it comes to patient environments such as wards, outpatient facilities, and other similar places (Beggs et al., 2008).

Hospitals would accommodate several patients with various disease severity. As patients, healthcare staff, and visitors use inpatient care facilities, their susceptibility to hospital acquired infections (HAIs) or nosocomial infections is substantial. The largest nosocomial outbreak of SARS in Hong Kong, China and the outbreak of MERS in South Korean hospitals caused significant morbidity and mortality. There are three primary modes of infection transmission. First, the impact of "sprayborne" droplets on the eyes, nose, or mouth of an infected person, which would otherwise descend to the ground nearby. The second mode of infection transmission is by touch: self-inoculation through the mucous membranes of the eyes, nose, and mouth after contacting a contaminated surface (a "fomite") or an infected person. Finally, "airborne transmission" refers to the spread of an infectious disease through breathing in an aerosol that has been floating in the air for many minutes or more. MERS coronavirus (MERS-CoV) is typically thought to be transmitted by close contact (Zumla et al., 2015), but airborne and fomite transmission are also considered to be feasible (Van Doremalen et al., 2013, Kim et al., 2016).

The severe respiratory bouts of sneezing and coughing can discharge large quantities of infectious viruses from an infected patient, which is crucial in spreading infectious respiratory infections in indoor settings, especially in hospital (Bourouiba et al., 2014). These ejected droplets could reach up to 8 meters and remain suspended in the air for many minutes due to the entrainment effect of sneeze-induced turbulence (Scharfman et al., 2016, Bourouiba, 2020). Hence, these exhalation actions from a patient admitted to a healthcare facility who is sick with an infectious disease such as COVID-19, or MERS-CoV can spread the disease. The fate of airborne infectious pathogens in indoor environment is controversial and a subject of extensive research. As per the traditional infection theory, bioaerosol particles with a diameter below 5 µm (e.g., droplet nuclei) remain airborne and are controlled by ventilation, while bigger particles (e.g., larger droplets from a sneeze, skin squama, etc.) deposit out of the air within a 2 m radius of the source. On the other hand, the reality is not quite so straightforward. Even if smaller particles stay in the air longer, there is still a chance that they will settle out onto surfaces, which creates a potential contact transmission risk (King et al., 2013).

Although indirect contact transmission pathway is not considered the most dominant mechanism for infection transmission by the majority of research, it does play a substantial role in the triggering the spread of respiratory infection (Atkinson and Wein, 2008, Reed, 1975, Mubareka et al., 2009). According to the findings of a study that Nicas and Jones (2009) conducted, approximately 31% of infection is spread when a person's hand comes into contact with the face membranes. Indirect contact transmission can also result in a longer period of exposure to the virus than the other mechanisms of transmission (Walther and Ewald, 2004). It is predicted that infectious pathogens in indoor air can live anywhere from a few seconds to hours, whereas pathogens that have deposited themselves on surfaces can live anywhere from a few hours to several weeks.

Ventilation influences particles that continue to float through the air, but it is unknown how much of an effect it has on droplet transmission or deposited particles, or on the subsequent exposure of vulnerable individuals to infectious pathogens through touch. So, it's important to evaluate, understand, and update ventilation design strategy to contain future virus epidemics.

Accurate airflow prediction is needed to estimate pathogen transport, dispersion, and deposition in mechanically ventilated spaces. With improvement in computing capacity, CFD has been increasingly used to simulate indoor environments. CFD numerical modelling techniques provide insights into airflow and bioaerosol distribution with high temporal as well as spatial resolution in an indoor environment. As there are few studies on design of ventilation systems for general inpatient wards with respect to air change rate and exhaust airflow rate, an investigation is done to evaluate the combined impacts of these two parameters on airflow and exposure risk distributions due to a droplet nuclei of size 0.167 µm (MERS-CoV) within an air-conditioned ward cubicle. A simple, cost-effective ventilation system design that can reduce infection transmission in a hospital ward is sort.

5.2 Ward design and ventilation scenarios

The inpatient facilities would vary by hospital type and patient need. Nonetheless, the most popular variants include the open ward, semi-private room, private room, isolation rooms, and intensive care unit. This study will focus on developing an effective ventilation strategy for the open ward design. In an open ward, many beds are arranged in a large space without partitions. This design is utilized frequently at Hong Kong's public hospitals and is intended to accommodate many patients cost-effectively (Hirst et al., 1964). Patients have access to shared restrooms and showers, and nurses are typically stationed nearby to administer treatment and monitor patients' status. Although open wards are less private than other inpatient facilities, they offer some benefits. They can provide patients with a sense of camaraderie and support by allowing them to interact with others in similar circumstances. Open wards also make it easier for nursing personnel to observe patients and address any difficulties that develop. There are, however, significant disadvantages to the open ward concept. Patients may be exposed to increased noise and disturbances from other patients and may have less privacy. In addition, there may be a more considerable risk of infection transmission in an open ward because patients are closer (Li et al., 2005).

A standard semi-enclosed general inpatient ward cubicle with six beds spaced one meter apart was utilized to conduct CFD simulations. The three-dimensional geometry of the cubicle with a length of 7 m, width of 6 m and height of 2.7 m is illustrated in Figure 5.1. The cubicle had mechanical ventilation (with a positive pressure towards the corridor), and it accommodated six patients who were lying supine. The supply air estimated based on the room volume and the air change rates (3 h^{-1}–13 h^{-1}), was brought into the cubicle by means of four diffusers that were positioned on the ceiling. The assumption was made that the room is supplied with 100% outdoor air. The supply air and the ward air that was expelled to the corridor were set equal for all the different air change rates in the base scenario, which is depicted in Figure 5.1 (a). Figure 5.1 (b) depicts the installation of six local exhaust grilles (grille size: 0.5 m x 0.2 m) for exhausting 10% and 50% of supply air (i.e., EA = 10% and EA = 50%). After extraction through local exhaust grilles, the remaining cubicle air was discharged into the corridor (Satheesan et al., 2020).

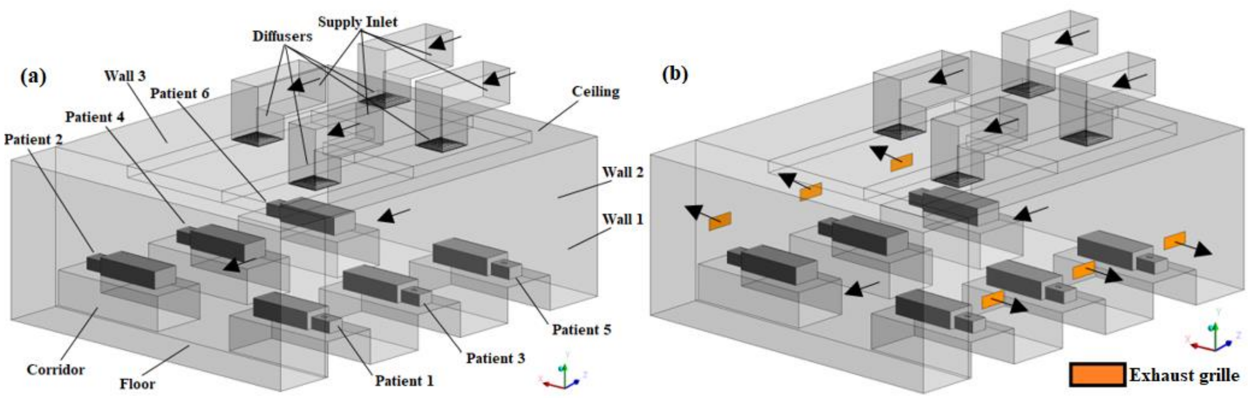

Figure 5.1 In-patient ward cubicle with patients: (a) without exhaust grilles; (b) with local exhaust grilles

5.3 Infection transmission within ward

In certain instances, a patient with an infectious disease could be nursed in an open ward cubicle before receiving a diagnosis, which could lead to an outbreak of the disease (Roy and Milton, 2004, Wong et al., 2019). Exhalation activities, such as sneezing of the source patient in the ward cubicle, would release several infectious pathogens into the ward air. Based on the bioaerosol transport, dispersion, and deposition mechanism, the possibilities for infection transmission in a general inpatient ward environment is classified into two categories in this study, namely, (i) by pathogens suspended in the air (airborne) and (ii) their subsequent deposition on to surfaces or patients (touch).

5.3.1 Airborne exposure to pathogens

The exposure of healthcare personnel, visitors, and patients to pathogens suspended in the air due to the exhalation (sneezing) of a source patient is investigated. The expelled pathogens will remain suspended in the air for a certain period, after which it most likely has three possible fates: inhalation by an individual, deposition on surfaces, and removal through the HVAC system. This section of the study considers the risk of exposure to ward users' due to pathogens suspended in the air, followed by its inhalation. Equation 5.1 accounts for an event where an individual gets exposed to infectious pathogens at their breathing height.

$$N_p(t) = \int_0^t n(t)dt \tag{5.1}$$

$N_p(t)$ is the total number of particles at time t, and $n(t)$ is the rate of change of particles with respect to time. The integral is taken over the interval between when the particle is expelled and when a particle resides in the breathing zone. In this study, the breathing zone is taken as a height that varies between 1.1 m to 1.7 m as depicted in Figure 5.2.

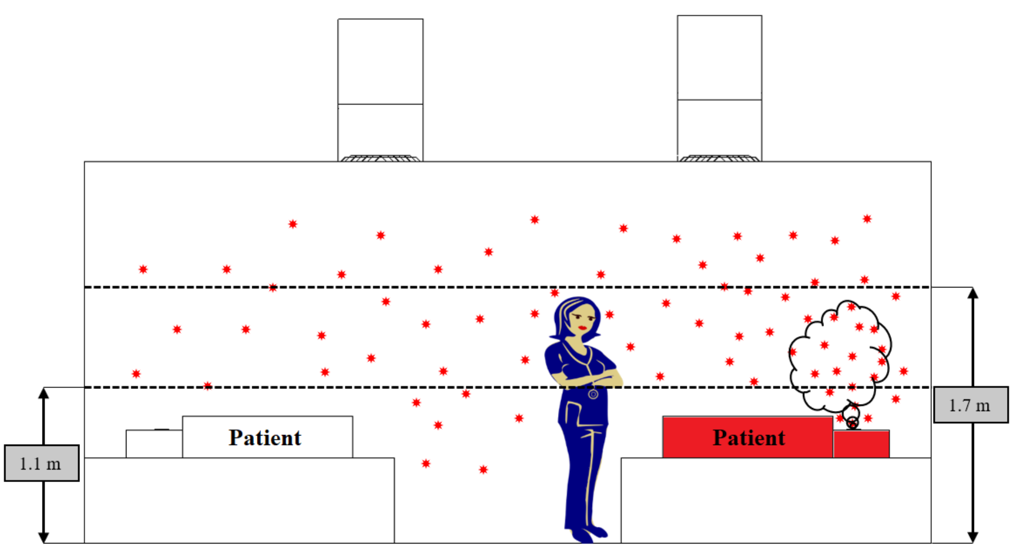

Figure 5.2 Breathing zone height and dispersion of infectious pathogens from an infected patient in an inpatient ward cubicle

The ward cubicle is segregated into several zones, as illustrated in Figure 5.3, to factor in the ward users' exposure to airborne pathogens due to exhalation activity of source patient (patient 5). This approach aims to estimate the spatial and temporal spread of the MERS-CoV droplet nuclei in the breathing zone of the ward users.

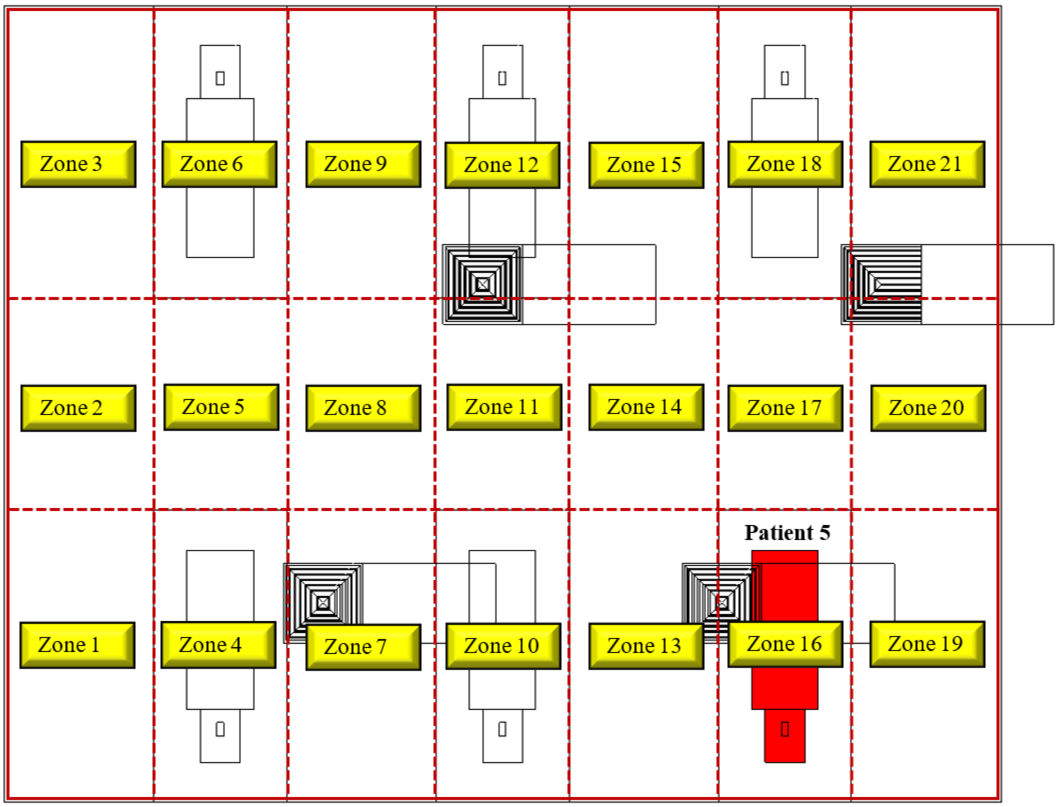

Figure 5.3 Breathing zones within the computational domain

5.3.2 Pathogen deposition within a ward cubicle

The deposition of particles on patients because of the exhalation of pathogens by other patients in the same ward can result in cross-infection. The intensity of cross-infection between patients is dependent on each patient's position and the overall airflow distribution pattern within the ward environment. Exposure to infection due to deposition of particles released through sneezing by other patients (Infectors) can be determined for patient *i* (Receptor Exposure):

$$E_i = \sum_{j=1}^{n} e_j; j \neq i \tag{5.2}$$

where E_i is the fractional exposure count for patient *i*, the fractional emission from patient *j* is denoted by e_j, and the total number of patients is denoted by *n*. Based on this expression, it is possible to estimate the location within the same ward cubicle that pose the highest and lowest risks of transmitting an infection to patients.

Hospital inpatient wards are advised to have relative humidity between 30 and 60 percent (ASHRAE, 2013a). It has been observed that MERS-CoV can survive for up to 72 hours on plastic or steel surfaces at 20 °C and 40% humidity (Oh et al., 2018). As a portion of exhaled particles will settle on surfaces such as the ceiling, floor, and walls in the ward, the investigation also accounted for infection by surface contamination. Based on the three deposition ratios expressed in Equation 5.3, namely wall deposition ratio r_w, ceiling deposition ratio r_c, and floor deposition ratio r_f, it is possible to estimate the infection transmission through surface contamination under all ventilation scenarios considered in this study.

$$r_w = \frac{\sum_{i=1}^{n} n_{w_i}}{n * n_s};\ r_c = \frac{\sum_{i=1}^{n} n_{c_i}}{n * n_s};\ r_f = \frac{\sum_{i=1}^{n} n_{f_i}}{n * n_s} \tag{5.3}$$

where n_s represents the number of particles evacuated by a patient by sneezing and n_w, n_c, and n_f represent the number of particles deposited on the walls, ceiling, and floor, respectively.

5.4 Numerical simulation

In recent years, numerical simulation conducted through CFD has become increasingly popular amongst building and ventilation designers. It has been specifically implemented in several studies to evaluate room airflow and contaminant dispersal with great success. CFD simulations, the primary instrument that is utilised in this investigation, provides an understanding of the probable airflow patterns and the behaviors of pollutants (droplet nuclei of MERS-CoV) in the simulated computational domain (hospital ward cubicle) under various ventilation strategies adopted. In this section, a brief overview of grid generation, airflow (continuous phase) and particle (discrete phase) modelling is detailed.

5.4.1 Airflow and grid modelling

A finite volume based CFD code (Ansys Fluent 13.0) was utilized to evaluate the airflow distribution and transport mechanisms of bioaerosols in the ward cubicle. The numerical simulation model has a continuous phase (air) and a discrete phase (droplet nuclei). In this investigation, the Eulerian framework was utilized for the formulation of the governing equations of continuity, momentum, and energy for the continuum phase, whereas the Lagrangian framework was utilized for the modelling of the discrete phase. The movement of ward users in the cubicle is a transient phenomenon that may cause disturbances to airflow and bioaerosol distribution. However, few studies indicate that its influence is temporary and considerably less significant than ventilation (Shih et al., 2007, Hang et al., 2014). Hence, this study has modelled the three-dimensional airflow as an incompressible steady-state turbulent flow, with no consideration for unsteady phenomena.

Although CFD possesses a diverse number of turbulence models, it is quite tough to single out one turbulence model as being superior to the others for every category of problems. Hence, the choice of turbulence model is a matter of striking a balance between competing considerations, including the physics of the flow being modelled, the standard method for making predictions about a given class of problems, the amount of computational power available, the accuracy required, and the amount of time required for the simulation (Gao and Niu, 2005). Reynolds-averaged Navier Stokes (RANS) simulations have been used in a great number of the studies that have been conducted on turbulent indoor airflow, although for some case studies, large eddy scale (LES) simulations have been utilized to accurately estimate flow field variables. However, LES has significantly greater grid needs in addition to longer computation times compared to RANS, making RANS the more popular method (Blocken, 2018). The Reynolds-averaged Navier Stokes (RANS) equation simplifies the simulation of turbulent flows considerably. The equations have variables for the flow field that are averaged across time, which would eliminate the turbulent fluctuations. However, this simplification results in the introduction of unknown Reynolds stress tensors into the equation, leading to closure difficulties. The closure to equations can be achieved by adopting the Eddy viscosity modeling, and the renormalization group (RNG) k-ε model is the most recommended eddy viscosity turbulence model to mimic the indoor airflow distribution. Thus, the RNG k-ε model was chosen to model air turbulence because it provides more accuracy, stability, and computing efficiency for low Reynolds number and near wall flows.

The diffuser inlets were defined as velocity-inlets, whilst the corridor and exhaust grilles were specified as outflow boundary conditions. In addition to treating outflow boundaries as having zero diffusion flux for all flow variables, Ansys Fluent implements a global mass balance correction. In addition, the outflow with flow rate weighting option gives the user the ability to have numerous outflow boundaries, each of which has a fractional flow rate (Ansys, 2010). To discretize the governing equations, a second-order upwind approach was used, and the SIMPLE algorithm was used for the pressure-velocity coupling in the continuum phase. It was estimated that a patient who was reclining would have a metabolic rate of 0.8 MET (ASHRAE, 2013b), and it was also assumed that convection would be responsible for the transmission of half of the heat (23.3 W/m^2) produced by each patient. A constant heat flux was imposed on the whole surface of the supine patients. Every other wall was presumed to be adiabatic, except for those that contained heat sources (the patients). The walls are specified with smooth non-slip conditions. The Boussinesq approximation was used to reduce modelling complexity resulting from density changes due to temperature gradients (Zeytounian, 2003).

The computational domain of the inpatient ward was partitioned into a several fluid zones. To construct hexahedral mesh for these distinct computational cell zones, ICEM-CFD 13.0 was used. The separate mesh files are combined into one utilizing the functionality of the tmerge filter. In tmerge, the necessary scaling factor, translation distance, and rotation information of the meshes must be given before the separate meshes can be combined into a single mesh file. The existence of mesh node locations that are not similar, as illustrated in Figure 5.4, along the boundaries of the individual cell zones of the computational domain results in the establishment of non-conformal interfaces between the individual cell zones. The transport of fluxes from one mesh to another is achieved by these interfaces that connect each cell zone (Ansys, 2010).

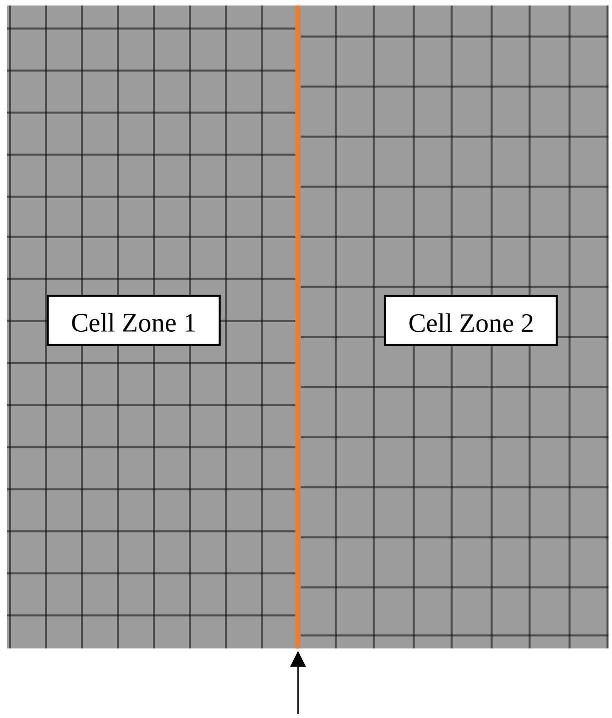

Figure 5.4 Non-identical mesh nodes along the boundary of two cell zones

A grid spacing of 1.2 is kept throughout the entirety of the domain, and the first cell height is always kept at a distance of 0.001 meters from the wall. The near-wall mesh was refined to a degree that allowed it to resolve the viscous sublayer (y+ less than 5), and the modelling of the near-wall region was carried out using the enhanced wall treatment method. For the grid convergence study, three grid systems were developed: 1002k (System 1), 3202k (System 2), and 5110k (System 3). Airflow simulations were carried out on each grid. The grid convergence index (GCI) concept was used to analyze the convergence of the three grid systems (Roache, 1998). The GCIs for the grid systems were determined using the root mean square of the relative error (e_{rms}) for the fluid flow mean velocities (u) detected at 100 sites along a vertical line in the center of the ward cubicle.

$$G\ C\ I(u) = F_s \frac{e_{rms}}{r^p - 1} \tag{5.4}$$

where the grid refinement factor *r* is defined as the ratio of the control volumes of fine and coarse grid systems in the aforementioned equation; *p* is the order of the discretization technique; F_s is the safety factor; and e_{rms} is obtained by:

$$e_{rms} = \sqrt{\frac{\Sigma_{m=1}^{100} \left|(u_{m,coarse} - u_{m,fine})/u_{m,fine}\right|^2}{100}} \tag{5.5}$$

$$r = \left(\frac{N_{fine}}{N_{coarse}}\right)^{1/3} \tag{5.6}$$

System 1 was used as a point of comparison, the GCIs for Systems 2 and 3 came out to be 3.11% and 3.40%, respectively. Because System 2 was sufficient for analyzing the flow characteristics of the fluid, it was chosen for further simulations after considering the amount of processing time as well as the correctness of the result.

5.4.2 Particle modelling

Individual particle trajectories were modelled using the Lagrangian framework, using the following modelling assumptions (Zhao et al., 2004, Tian et al., 2009):

- The transfer of heat and mass between air-particle as well as particle-particle were neglected.
- When a particle collides with a surface such as a wall, ceiling, or floor, it would not rebound.
- The deposition procedure did not account for particle coagulation.
- All particles were modelled as being spherical.

In a short time (0.1 second), the expelled droplets from exhalation actions such as sneezing will evaporate and reduce in size (Xie et al., 2007). Their dehydrated remnants, the droplet nuclei, could harbour infections (Wells, 1955). In this investigation, a small proportion (<10%) of the total virus-laden droplets from a strong sneeze were assumed. It has been demonstrated that virus particles will not cluster at such a low concentration. Further, droplet nuclei will be referred to as particles in this study for the sake of clarity. The Lagrangian particle tracking solves the following particle motion equation to calculate the discrete trajectories of individual particles in the fluid flow.

$$\frac{du_b}{dt} = \frac{18\mu}{\rho_b d_b^2}\frac{C_D Re}{24}(u_a - u_b) + \frac{g_a(\rho_b - \rho_a)}{\rho_b} + F_x \tag{5.7}$$

where u_a is the velocity of the fluid (ms^{-1}), u_b is the velocity of the particles (ms^{-1}), μ is the molecular viscosity of air (kgm^{-1}s^{-1}), ρ_a is the density of air (kgm^{-3}), ρ_b is the particle density (kgm^{-3}), and d_b is the particle diameter (m), Re is the Reynolds number of the particles, C_D is the coefficient of drag, g_a is the gravitational acceleration, and F_x represents the auxiliary forces acting on the particles. The Reynolds number of a particle is defined by,

$$Re = \frac{(u_a - u_b)d_b\rho_a}{\mu} \tag{5.8}$$

The coefficient of drag C_D for bioaerosol particles is described by,

$$C_D = \frac{K_D}{Re_b};\ Re_b < 1 \tag{5.9}$$

The constant of drag K_D for bioaerosol particles as defined by Equation 5.9 is given by,

$$K_D = \frac{d_b^2}{2} \tag{5.10}$$

In CFD simulations, the aforementioned equations were solved to determine the transport processes of bioaerosol particles in a Lagrangian scheme. The validity of Equations 5.9 and 5.10 was established for a range of particles with comparable bioaerosol diameters (d_b) ranging from 0.69 µm to 6.9 µm and further explored for particles with d_b as small as 0.054 µm (Wong et al., 2015).

In addition to the drag force, the basset force, magnus force, virtual mass force, Brownian force, and Saffman lift force can influence the velocity of particles. Despite the fact that the magnitudes of these forces are significantly affected by fluid flow conditions and particle properties, a few of these forces are tiny enough to be disregarded in some assessments (Zhao et al., 2004). Due to the particle size and non-isothermal flow circumstances in this investigation, Brownian, thermophoretic, and Saffman lift forces were accounted for determining the particle motion trajectories. Using stochastic tracking methods, the dispersion of particles caused by turbulence in the flow field can be tracked. This study utilized the discrete random walk (DRW) model, a prominent method that accounts for velocity fluctuations (Lai et al., 2012). Table 5.1 provides a summary of condition adopted for CFD simulations.

Table 5.1 CFD simulation parameters

Computational domain	7.5m(L) × 6m(W) × 2.7m(H), RNG k-ε turbulence model with enhanced wall treatment
Total supply airflow rate	0.1240kg·s^{-1} for ach=3, 0.2480kg·s^{-1} for ach=6, 0.3720kg·s^{-1} for ach=9, 0.5374kg·s^{-1} for ach=13, 285K (air temperature)
Inlet (0.6m×0.6m) airflow rate	0.031kg·s^{-1} for ach=3, 0.0620kg·s^{-1} for ach=6, 0.093kg·s^{-1} for ach=9, 0.1343kg·s^{-1} for ach=13, 285K (air temperature)
Diffuser (0.6m×0.6m)	Four supply diffusers, 4-way spread pattern, air supplied at an angle of 15° from the ceiling, adiabatic
Corridor (6m×2.7m)	Outflow with flow rate weighting, 295K (backflow temperature), adiabatic, escape boundary condition
Exhaust grille (0.5m×0.2m)	Outflow with flow rate weighting, 295K (backflow temperature), adiabatic, escape boundary condition, exhaust air=0%/10%/50% of total supply air
Walls, ceiling, floor and beds	No-slip wall boundary, adiabatic, trap boundary condition
Patient	Six patients, no-slip wall boundary, 23.3Wm^{-2} for each patient, trap boundary condition
Mouth of a patient (0.05m×0.05m)	Single-shot release with an upward velocity v_b=50ms^{-1} (Yu et al., 2017, Fontes et al., 2020), n_s=10,000 virus particles, bioaerosol density ρ_b=1,100kgm^{-3}
Species (aerodynamic diameters)	MERS-*CoV* (0.167±0.012μm)

To obtain the history of particles traversed through the breathing zones within the computational domain with respect to time, a region with prescribed coordinates is created in Ansys Fluent, and the discrete phase modelling (DPM) summary for the region is sorted for every second. After that, with the aid of a python programming code, the number of particles and residence time of each particle in each breathing zone is determined from the DPM summary for every simulation scenario considered in this study.

5.5 Model validation

A study conducted by Yu et al. (2017) was chosen for performing the model validation. Yu et al. (2017) estimated the influence of air change rates on the dispersion and deposition mechanism for bioaerosols, specifically, MER-CoV expelled by an infected patient in a mechanically ventilated inpatient ward cubicle. The particle exhausted ratio, as illustrated in Figure 5.5, is taken as a parameter to validate the CFD simulation. The exhausted ratio (r_e) is the amount of particle that is exhausted to corridor (n_e) divided by the total number of particles expelled by the infected patient (n_s) as shown in Equation 5.11.

$$r_e = \frac{n_e}{n_s} \tag{5.11}$$

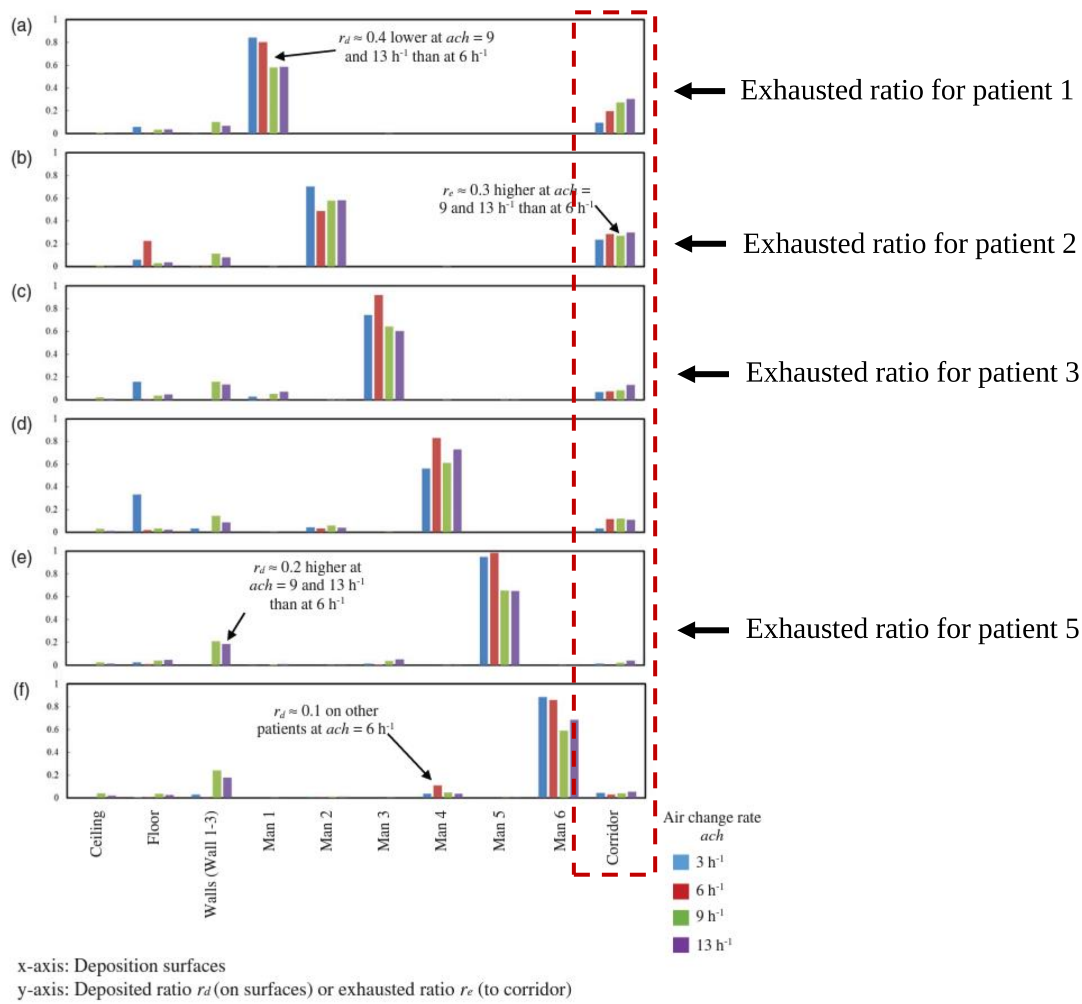

Figure 5.5 Deposited and exhausted ratios of MERS-CoV in an inpatient ward cubicle (Yu et al., 2017)

The exhausted ratio accounts for the possibilities of infection transmission from a ward cubicle to the corridor due to the spread of expelled particles from an infected patient to the corridor. According to Chen et al. (2011), these particles could also move to neighboring spaces connected to the corridor. The CFD simulation for validation was conducted for the base case scenario of the ward cubicle without any local exhaust grille. As shown in Figure 5.5, the exhausted ratio of four source patients, namely, patient 1, patient 2, patient 3 and patient 5 under an air change rate of 9 h^{-1} and 13 h^{-1} were taken for validation. As illustrated in the Figure 5.6, the exhausted ratio reported for different air change rates and different infected patients from this study matches well with simulation results of Yu et al. (2017). This reflects the accuracy and reliability of the CFD simulation of this study to conduct further exploration.

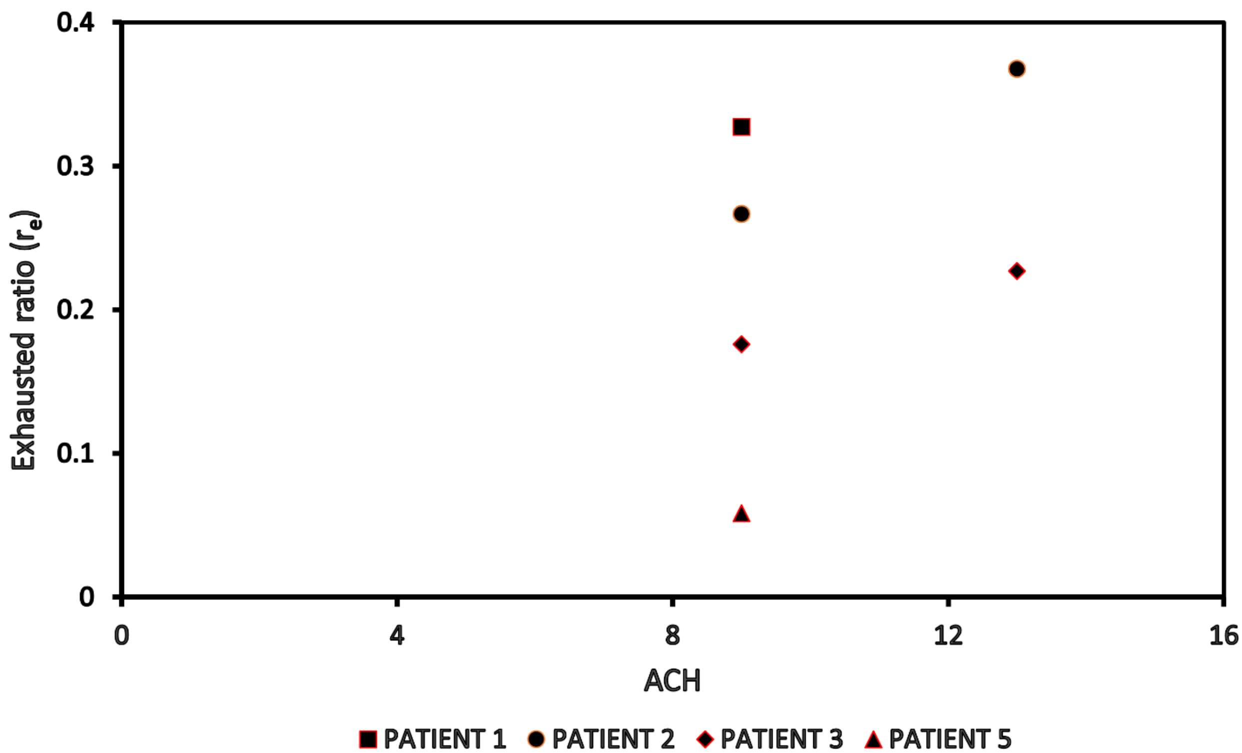

Figure 5.6 Exhausted ratio for an air change rate of 9 h^{-1} and 13 h^{-1}

5.6 Numerical simulation results

A brief discussion on the airflow patterns and particle distribution within the inpatient ward cubicle obtained by CFD simulations for various ventilation strategies are discussed in this section.

5.6.1 Airflow distribution and patterns

In a hospital ward, the overall airflow distribution pattern based on ventilation strategies can have a significant impact on the particle dispersion within the room. Figure 5.7 displays the air velocity distribution and velocity vector plot in a horizontal plane at y = 1.0 m for the base case, which is a standard ward cubicle without exhaust grilles. Air having a velocity of less than 0.05 ms^{-1} is observed near wall 2 in Figure 5.7 (a), and the overall airflow pattern in the cubicle is oriented towards the ward corridor in Figure 5.7 (b). These results parallel those given in a case study done by Yu et al. (2017). Several eddies can be noticed within the ward cubicle due to the presence of impediments such as patients and beds. Figures 5.8 and 5.9 depict the temperature distribution and velocity vector plot on a vertical plane at z = 1.625 m for air change rates of 6 h^{-1} and 9 h^{-1} with EA = 50%, respectively. As thermal manikins generate thermal plumes, the vertical airflow distribution reveals the effect of thermal plumes on the lateral airflow pattern. An upward airflow (towards the ward ceiling) returns to the floor level along the walls. When the cold supply air from the diffusers mixes with the upward airflow created by the thermal plumes, formation of recirculation zones is observed. In addition, the suction provided by the local exhaust grilles tends to change the airflow pattern around a patient, so assisting in the removal of airborne contaminants in the immediate proximity of the patient.

a)

b)

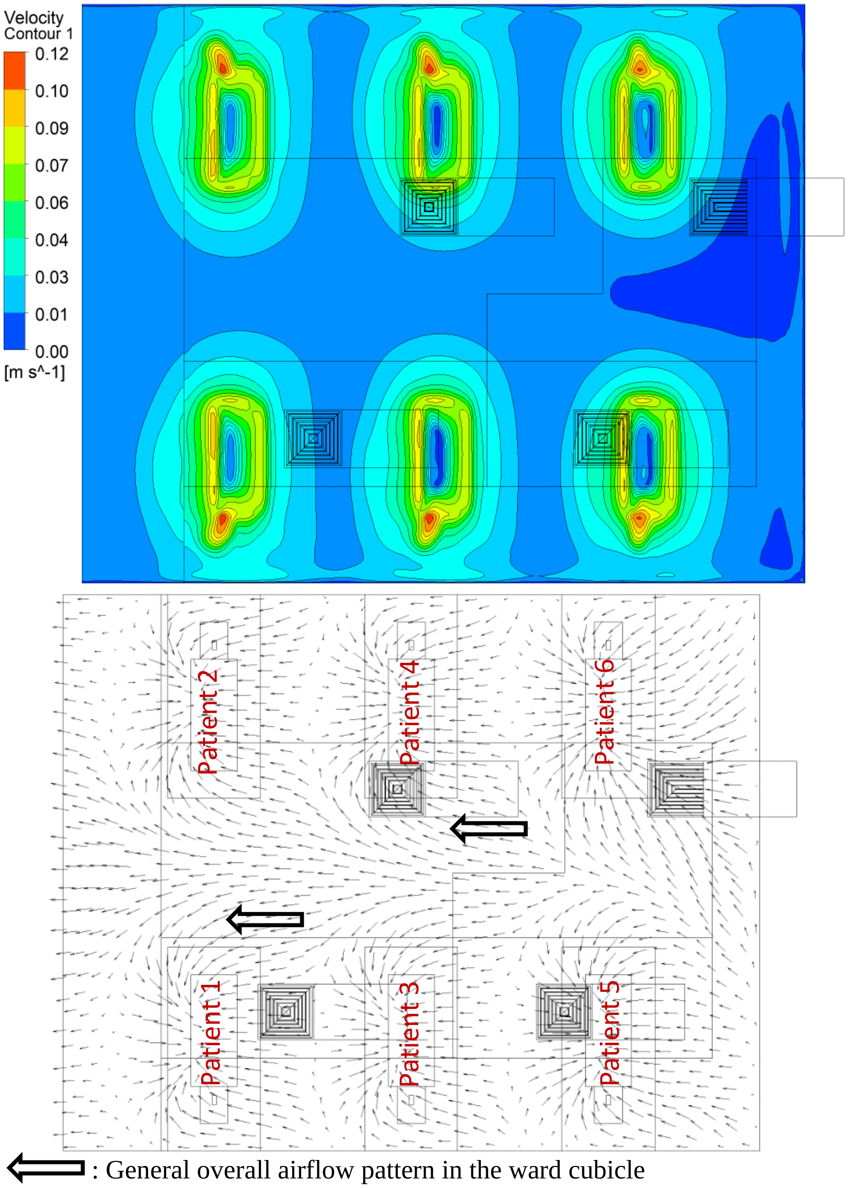

Figure 5.7 Simulation results of the ward cubicle with no exhaust grilles at 6ACH: (a) air velocity distribution; (b) velocity vector plot

a)

b)

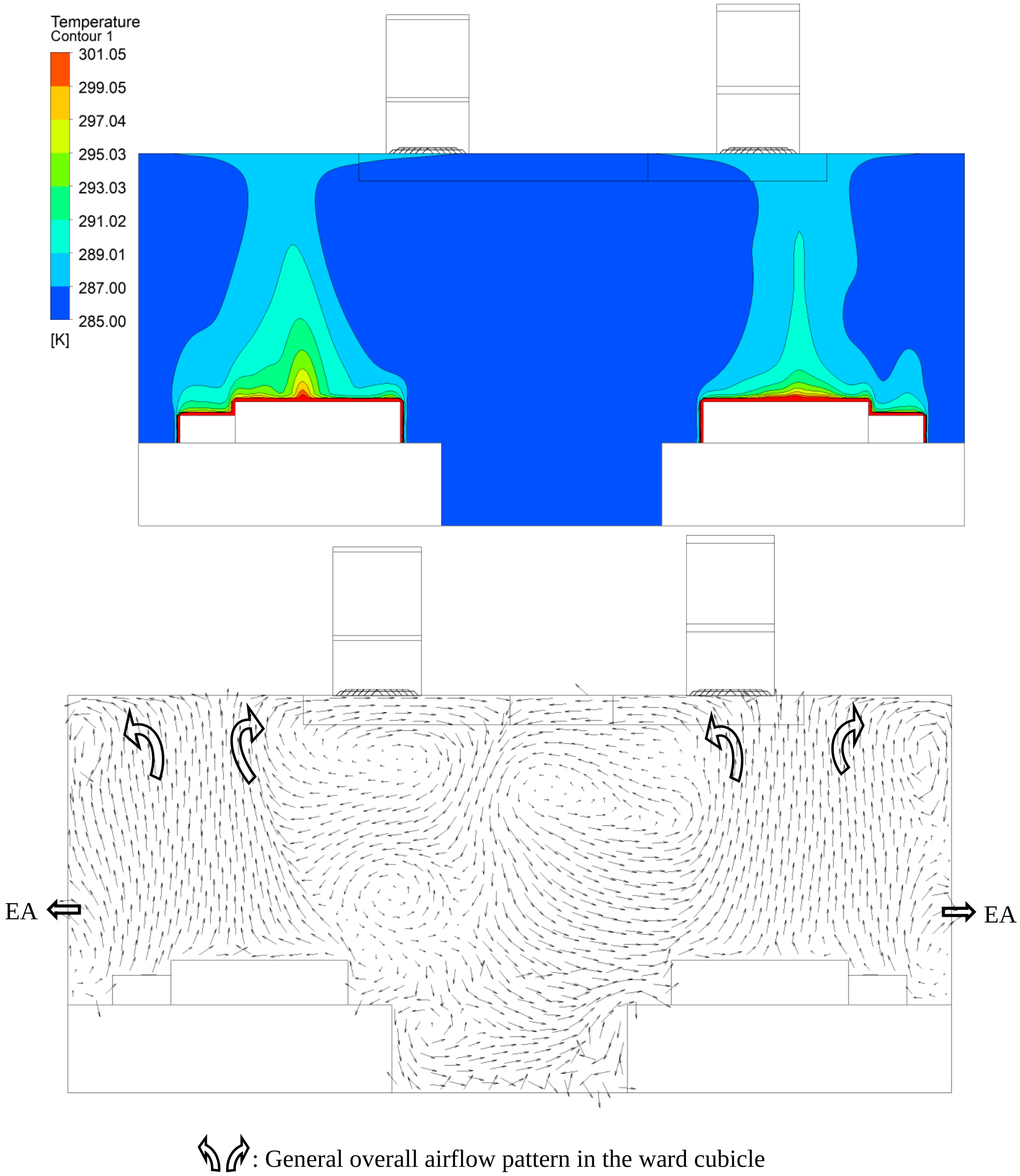

Figure 5.8 Simulation results of ward cubicle with exhaust grilles at 6ACH and exhaust air (EA)=50%: (a) temperature distribution; (b) velocity vector plot.

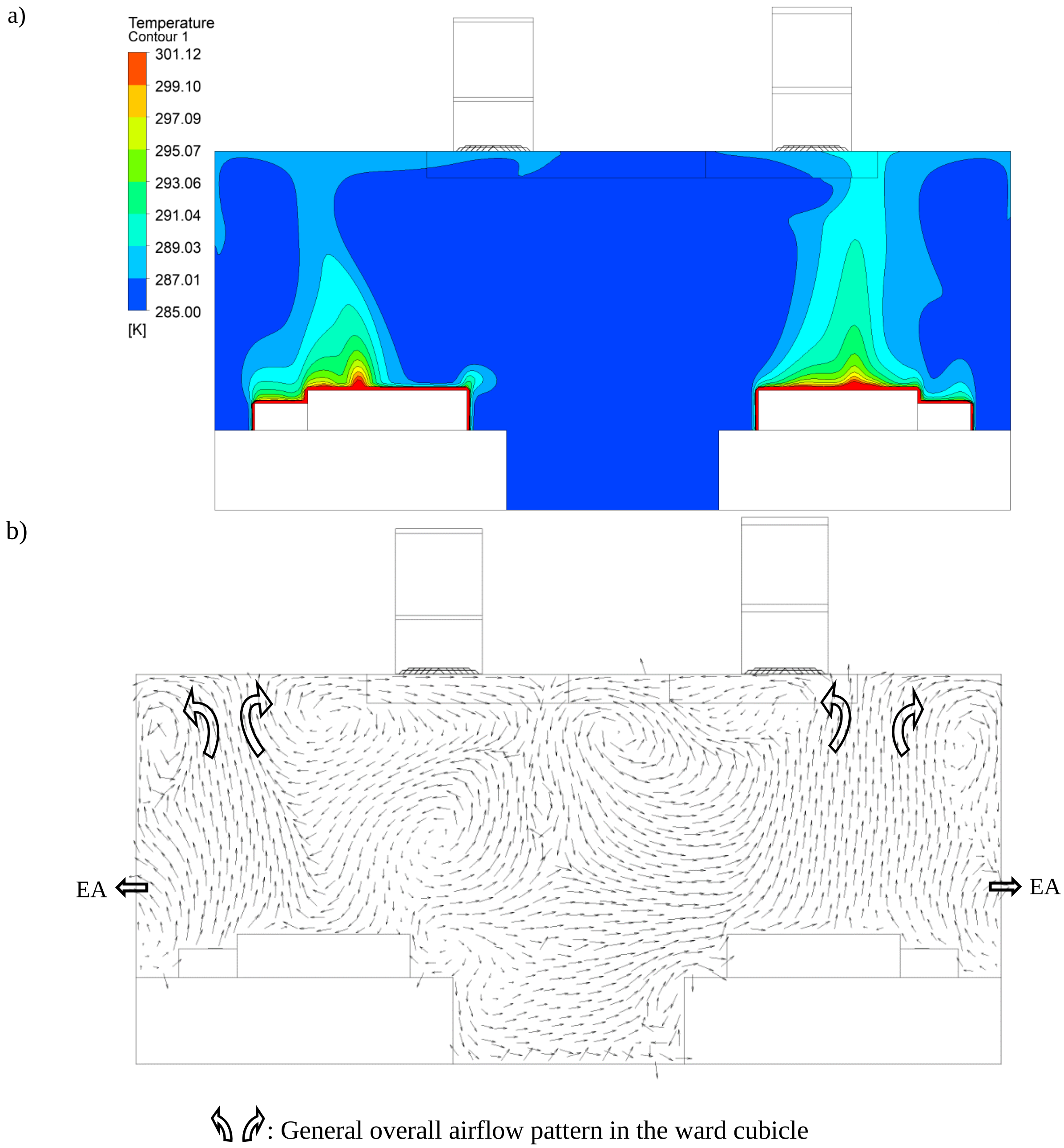

Figure 5.9 Simulation results of ward cubicle with exhaust grilles at 9ACH and exhaust air (EA)=50%: (a) temperature distribution; (b) velocity vector plot.

5.6.2 Particle distribution

This section is divided into two sub-sections to illustrate the possibilities of infection transmission through the pathogens dispersed in the ward air and their subsequent deposition on to surfaces/patients within the ward cubicle. In section 5.6.2.1, the exposure of ward users to airborne pathogens that are suspended in the air will be evaluated. The subsequent deposition of pathogens on to surfaces/patients creating the possibilities of infection transmission through touch will be investigated in section 5.6.2.2.

5.6.2.1 Spatial and temporal distribution of particles

The distribution of particles in different zones with regards to time is discussed. To improve the clarity of results and their associated insights, the results are presented by bringing the segregated zones in the ward under three main zones as shown in Table 5.2.

Table 5.2 Allocation of Zones

Patient Zones	Bedside Zones	Aisle zones
4,6,10,12,16,18	1,3,7,9,13,15,19,21	2,5,8,11,14,17,20
		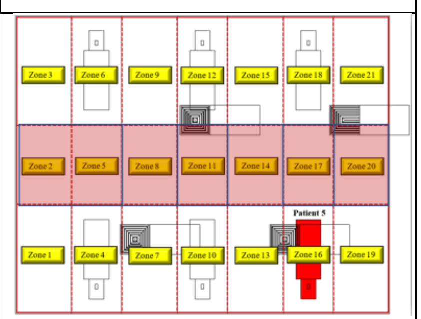

5.6.2.1.1 Patient Zones

At an air change rate of 3 h^{-1}, the maximum concentration of particles remaining suspended in air is observed primarily in the zone (zone 16) directly above the source patient, as indicated in Figure 5.10 (a). The particles reach this zone as soon as the source patient sneezes. Within 10 seconds, over half of all particles released during sneezing reach this region. After 10 seconds, there is a progressive decrease in the accumulation of particles in Zone 16. After 30 seconds, there is an increase in particle accumulation in the zone directly above the adjacent patient. This trend could arise from the movement of particles under the influence of airflow from Zone 16 to other locations within the ward. Over time, the patient zone adjacent to the source patient will likely be the most hazardous. The corridor-directed airflow distribution pattern plays a crucial role in the passage of particles from the contaminated source patient zone to the adjacent patient zone. The decrease in particle accumulation in zones 10 and 16 marks the beginning of the presence of particles across other patient zones. With the increased air change rate of 13 h^{-1}, the number of particles reaching the breathing zone directly above the source patient is drastically reduced, as indicated in Figure 5.10 (d). This could be attributed to the momentum of airflow guided by ceiling-mounted diffusers. This reduction in the number of particles would reduce the number of particles carried to different patient zones in the ward. This is significant compared to the results achieved with a lesser flow rate at 3 h^{-1}.

A significant reduction in particle concentration is evident with installing local exhaust grilles near the source patient, notably in Zone 16, as shown in Figures 5.10 (b) and (c). Installing the exhaust grille is beneficial, as seen by the decrease in suspended particles in the patient zones. After peaking at Zone 16, the number of particles declines within 30 seconds. Immediately after its decline, particle increase is seen in its adjacent zones. However, the most significant reduction in the number of particles remaining airborne is achieved with the increase in exhaust flow rate from 10% to 50% at a higher ACH (13 h^{-1}), as indicated in Figures 5.10 (e) and (f). Consequently, this particle decrease results in less particle migration to other zones. A local reduction in the number of particles reduces the availability of infectious pathogens to cause an infection.

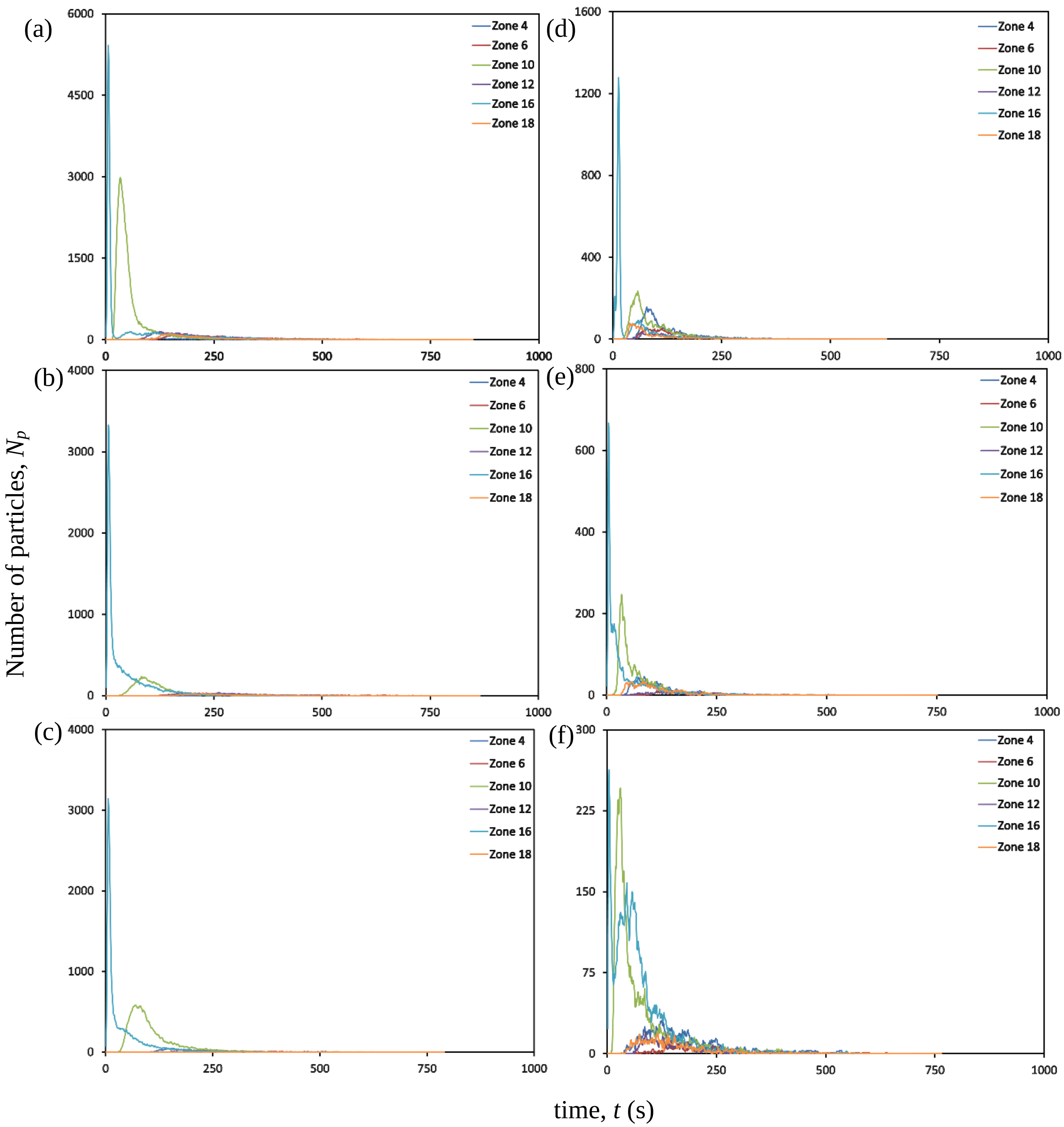

Figure 5.10 Particle distribution at patient zones at different air change and exhaust flow rates (a) ACH 3; (b) ACH 3 and exhaust flow rate 10%; (c) ACH 3 and exhaust flow rate 50%; (d) ACH 13; (e) ACH 13 and exhaust flow rate 10%; (f) ACH 13 and exhaust flow rate 50%.

5.6.2.1.2 Bedside Zones

As previously stated, the source patient's exhale triggers the discharge of infectious particles. The particles in the ward are transported and dispersed due to the airflow distribution established in the room. As indicated in Figure 5.11 (a), at an air change rate of 3 h^{-1}, particles in the bedside zone are first noticed in Zone 13, near the source patient. The particles reach this zone as soon as the source patient sneezes. Within 11 seconds, this zone occupies the highest number of particles; after that point, the number of particles staying suspended in Zone 13 decreases gradually. The accumulation of many particles in Zone 13 shortly after its emission can be linked to the airflow direction and the source patient's proximity. As particles in this zone decrease, particles migrate to other zones. Within 60 seconds after particle emission, particles are detected in zones 7, 15, and 21 that are located farther from the source patient. There is a gradual shift in the distribution of particles within the ward over time. Nonetheless, the particles reaching these zones are significantly lower than in the zone around the source patient. This is an important insight to consider in the spread of infection. The transfer of infectious pathogens via the air from their source to other sites may result in the transmission of infectious diseases to other ward users, including healthcare professionals, visitors, and patients.

The effectiveness of an exhaust grille positioned near the source patient is analysed. An increase in the number of particles is observed in the area immediately adjacent to the source patient, a situation analogous to the absence of a local exhaust grille. In Zone 13, the maximum accumulation of particles is observed 45 seconds following the emission of particles from the source patient. However, with a local exhaust grille and an exhaust flow rate of 10%, the number of particles suspended in air is dramatically reduced compared to the scenario without an exhaust grille, as indicated in Figure 5.11 (b). A reduction in Zone 13 signifies the beginning of the movement of particles to other zones within the ward. The accumulation of particles in Zones 9 and 15 is higher than in other zones after 100 seconds of the particle release. Although, after 500 seconds, the number of particles in most zones reduces to less than 10.

After the number of particles in the air peaks at 40 seconds, there is a progressive decrease in the accumulation of suspended particles. A gradual increase in particle accumulation is seen in Zone 7. Yet, when the particle accumulation in Zone 7 peaks at 117 seconds, the particles decrease gradually. Under an exhaust flow rate of 50%, the profile of particle build-up in Zone 13 is nearly identical to the case with an exhaust flow rate of 10%. However, at an exhaust flow rate of 50%, the transport of particles to other areas of the ward is severely constrained, as seen in Figure 5.11 (c).

One of the main advantages of adopting an air change rate of 13 h^{-1} is that there are fewer particles in the breathing zone than with an air change rate of 3 h^{-1}, as observed In Figure 5.11 (d). The number of particles accumulating in the breathing zone within seconds of discharge is cut in half compared to the scenario with an air change rate of 3 h^{-1}. After 300 seconds, the quantity of particles remaining in the bedside breathing zones is dramatically reduced. A modest particle increase is observed in Zones 7 and 19 shortly after a drop in suspended particles in Zone 13.

Including an exhaust grille reduces the presence of infectious particles remaining suspended in the bedside breathing zone. A decline in the accumulation of particles is noted for different bedside breathing zones within the ward, with an exhaust flow rate of 10% and 50%. After 200 seconds, fewer than 10 particles are observed to be suspended in the air, as indicated in Figures 5.11 (e) and (f). The maximum particle accumulation in the breathing zone is observed in Zone 13 after particle emission. This behaviour is identical in all the circumstances presented in this study, with the primary variable being the number of accessible particles that can promote airborne transmission. The most significant presence of particles in the breathing zones is observed without any local exhaust grille. Hence, the upgradation of the ward with the installation of a local exhaust grille would be a cost-effective solution. Within 200 seconds, an exhaust grille with an air change rate of 13 h^{-1} tends to make the breathing zones within the bedside less contaminated. This is exceptional compared to the other ventilation techniques considered in this study.

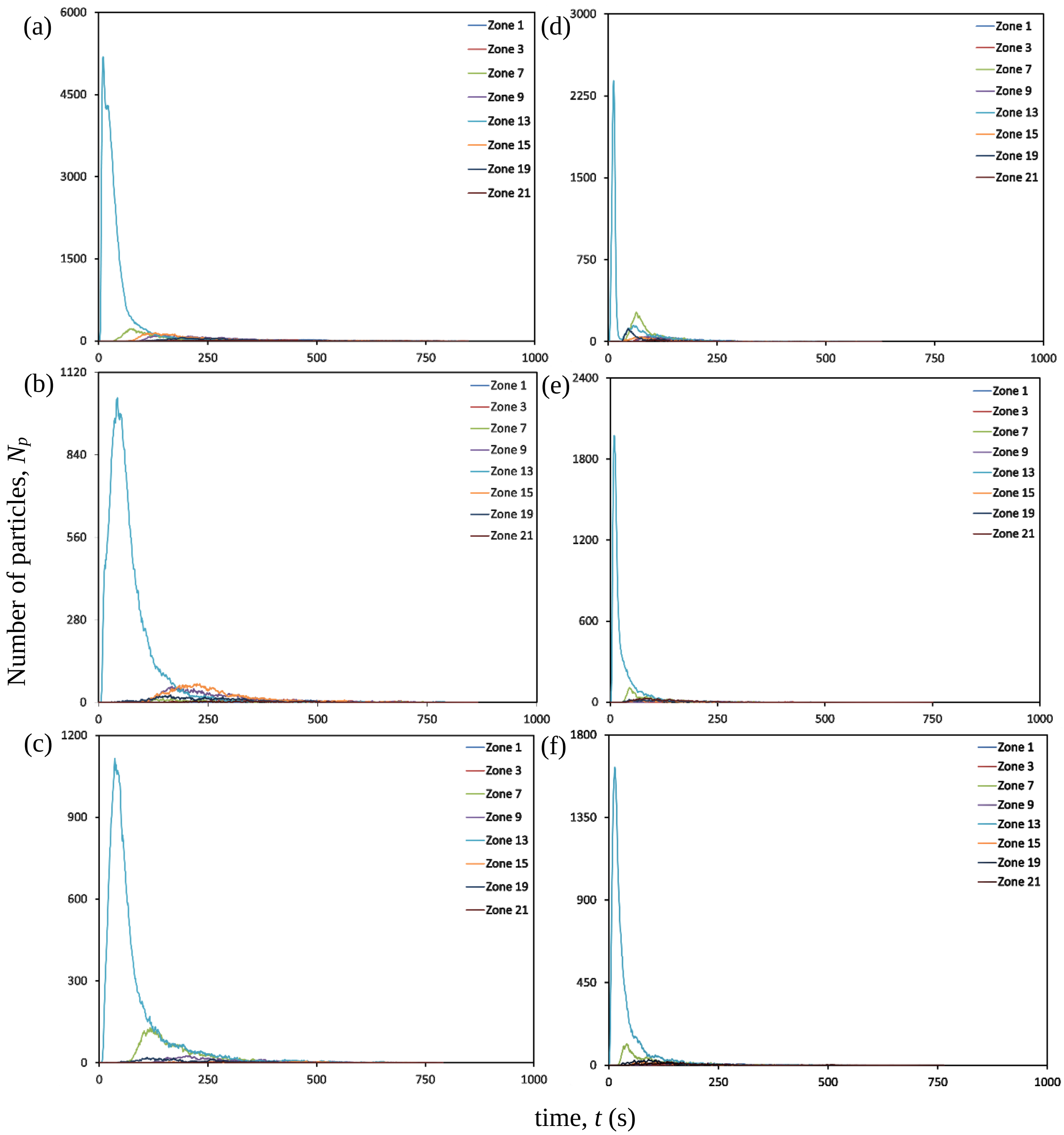

Figure 5.11 Particle distribution at bedside zones at different air change and exhaust flow rates (a) ACH 3; (b) ACH 3 and exhaust flow rate 10%; (c) ACH 3 and exhaust flow rate 50%; (d) ACH 13; (e) ACH 13 and exhaust flow rate 10%; (f) ACH 13 and exhaust flow rate 50%.

5.6.2.1.3 Aisle zones

At an air change rate of 3 h^{-1}, as indicated in Figure 5.12 (a), an increase in particle accumulation is experienced in Zone 11, followed by Zone 14 after 30 seconds of particle release. The highest accumulation is observed in Zone 11, which peaks at 80 seconds before gradually decreasing. The reduction in particle accumulation in these two zones marks the rise in particles across other zones. The proximity of Zones 11 and 14 to the source patient may be one of the primary causes of the increase in particle counts.

Analyses are conducted to determine the efficacy of a 10% exhaust flow rate on particle distribution. The concentration of particles is higher in Zones 11 and 14, as seen in the case with no local exhaust grille. However, a reduction in the number of particles remaining suspended in individual breathing zones is noticed with time, as shown in Figure 5.12 (b). With an increase in exhaust flow rate at an air change rate of 3 h^{-1}, the number of particles staying in the breathing zone decreases even further, as indicated in Figure 5.12 (c). With time, the presence of particles is discernible in all zones of the aisle. An increase in exhaust flow rate to 50% minimizes the particle build-up in the breathing zones of the aisle, and a considerable decrease is observed in Zone 14.

Under an air change rate of 13 h^{-1}, Zones 14 and 17 have the highest particle build-up within the aisle, as shown in Figure 5.12 (d). The maximum accumulation tends to occur within 20 seconds of particle emission from the source patient. However, after peaking, it reduces substantially within 50 seconds. The reduction in these zones marks the growth in other zones across the aisle, with zones 11 and 8 experiencing a considerable increase. Nonetheless, the build-up diminishes dramatically within 100 seconds in these zones. The aisle zones are clear of any infectious particles within 300 seconds after its discharge, as indicated in Figure 5.12 (d).

With the installation of a local exhaust grille, the accumulation of suspended particles in the aisle is significantly reduced. A notable decrease in particle accumulation is evident in zones 11, 14 and 17. Earlier, these zones accumulated particles in settings with no local exhaust grille. The presence of suspended particles reduces significantly with exhaust flow rates of 10% and 50%, as indicated in Figures 5.12 (e) and (f). Zone 14 appears to be the site with the most significant exposure to infectious particles in all scenarios represented under the air change rate of 3 and 13 per hour. The other zones are also exposed to particles expelled from Zone 16, although the number of particles is relatively low. Installing a local exhaust grille provides the benefit of dramatically reducing the availability of particles causing airborne disease transmission. In addition, it is essential to note that combining a high exhaust flow rate with a high ACH is preferable to a low ACH, as the former combination would decontaminate the space more quickly than the latter.

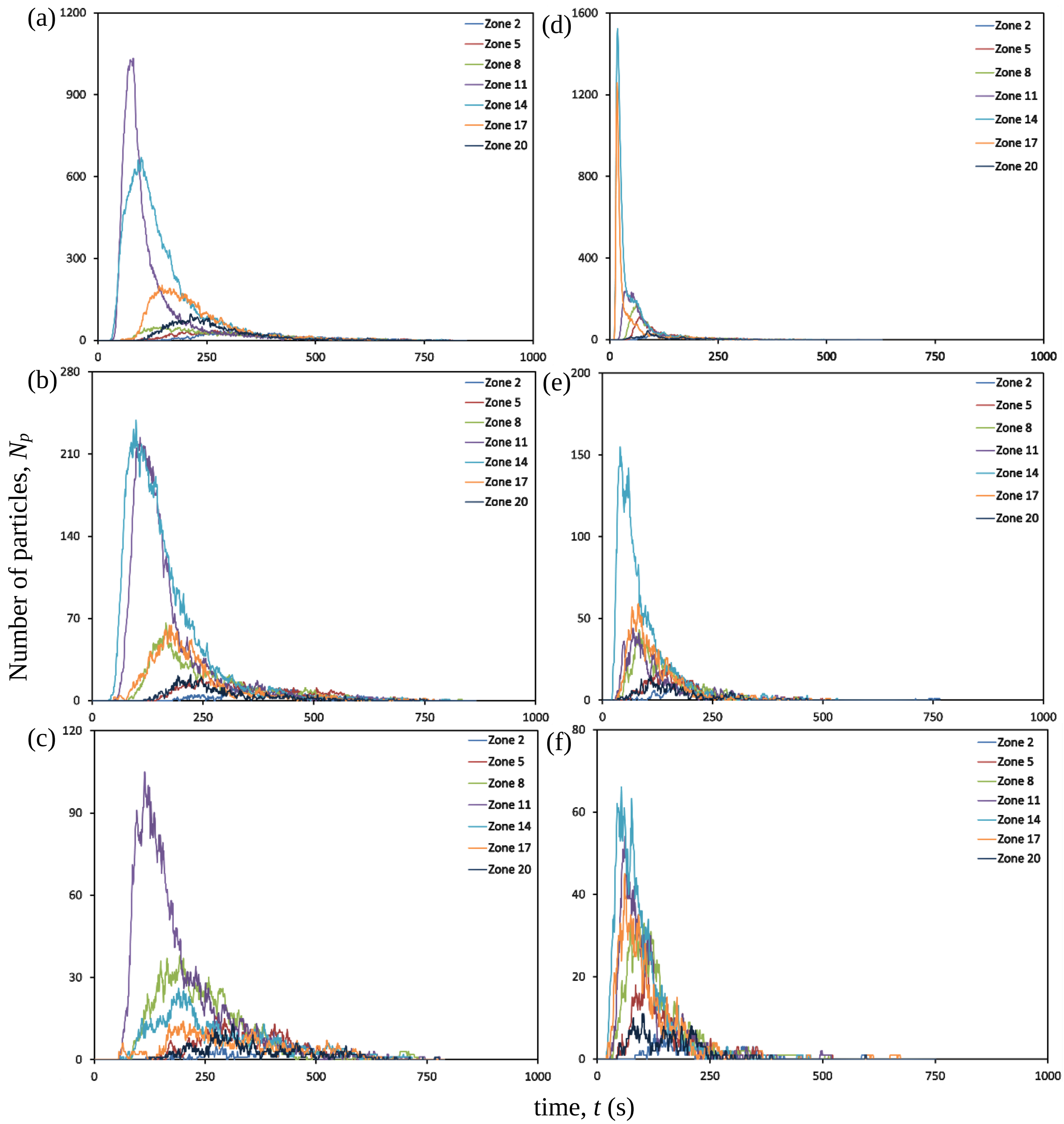

Figure 5.12 Particle distribution at aisle zones at different air change and exhaust flow rates (a) ACH 3; (b) ACH 3 and exhaust flow rate 10%; (c) ACH 3 and exhaust flow rate 50%; (d) ACH 13; (e) ACH 13 and exhaust flow rate 10%; (f) ACH 13 and exhaust flow rate 50%.

Figure 5.13 depicts a particle distribution plot to aid in the comprehension of the dispersion of particles throughout the ward. It represents particles' spatial and temporal distribution in various zones under the different air changes and exhaust flow rates addressed in this study. One minute after its release, it could be seen from the plot that the spread of particles is initially restricted to zones near the source patient. However, as time passes, the particles start to move away from its source towards other locations within the ward. The plot provides us an insight that under the effect of airflow, the particles could migrate several meters away from their point of origin, resulting in the transfer of infectious diseases within the ward. However, due to the effectiveness of the local exhaust grille, the number of particles available to flow across zones and induce infection transmission is significantly reduced. An increased ventilation rate complimented with an exhaust flow rate of 50% through a local exhaust grille is shown to provide a better performance in providing a localized control to restrict infection transmission. Our work has devised a cost-effective ventilation strategy that provides enhanced protection to ward users against airborne transmission of infectious pathogens without the need for massive revamp of the entire inpatient ward facility.

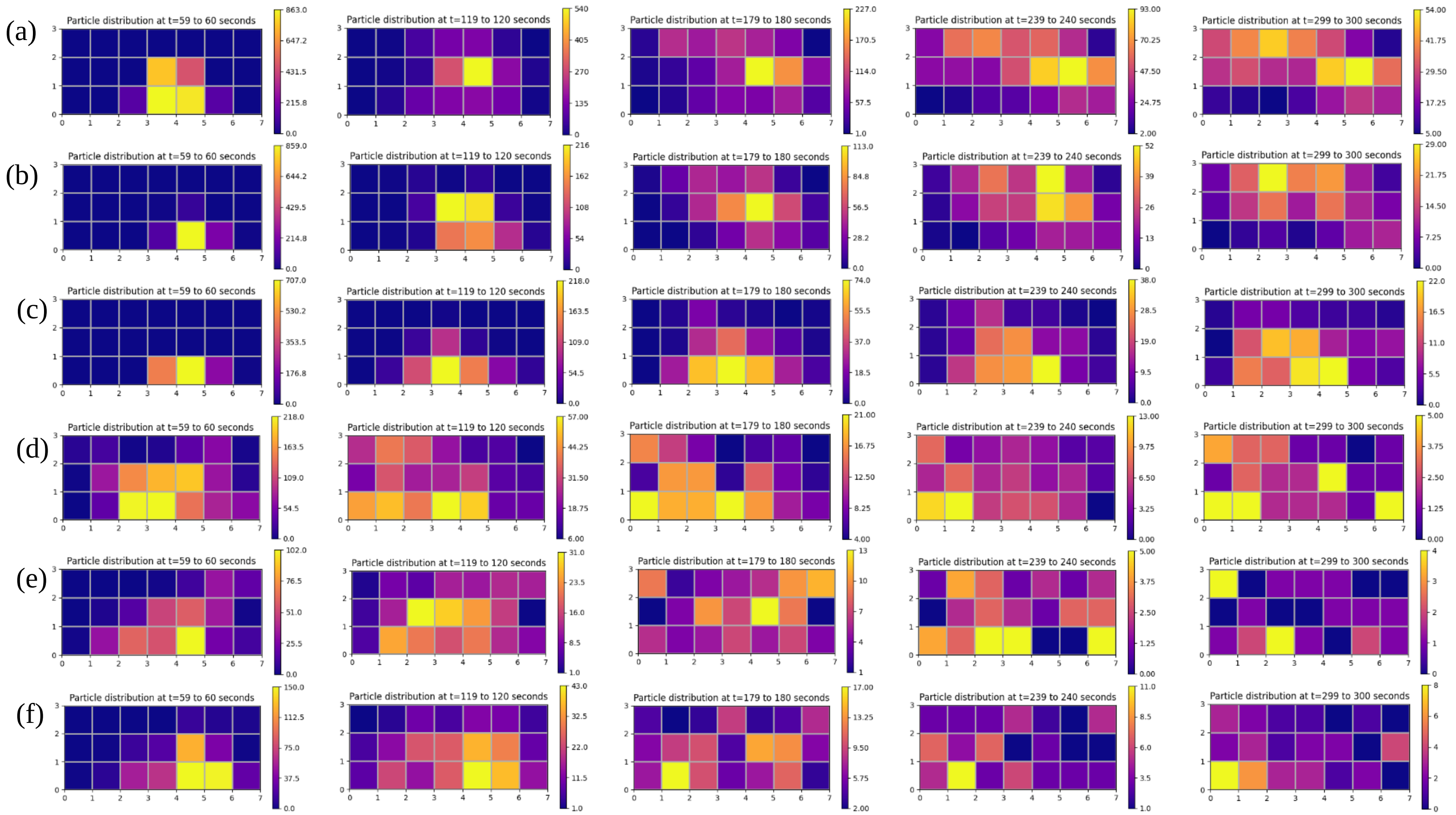

Figure 5.13 Spatial and temporal distribution of particles in different zones within the breathing height at different air change and exhaust flow rates (a) ACH 3 (b) ACH 3 and exhaust flow rate 10% (c) ACH 3 and exhaust flow rate 50% (d) ACH 13 (e) ACH 13 and exhaust flow rate 10% (f) ACH 13 and exhaust flow rate 50%

5.6.2.2 Pathogen deposition in a ward cubicle

In the base case scenario, nearly half of the virus particles exhaled by a patient land on the patient's body and bed. Figure 5.14 reveals that there were significant amounts of virus particles present on a variety of surfaces within the cubicle, including the walls, floor, and ceiling. A maximum r_c (≈ 0.26) can be seen at an air change rate of $3h^{-1}$ in Figure 5.14 (a), because of supine patients and their exhaled air velocity. As the air change rate increases, it is also possible to see in the figure that r_c will decrease. For example, r_c will reduce to 0.11 at 13 h^{-1} (a 57% decrease) and r_c will decrease to 0.17 at 6 h^{-1} (a 34% decrease). In fact, the air that is provided through the diffusers possesses a greater momentum as the air change rate increases, and as a result, it can direct the particles away from the ceiling and into other areas of the cubicle. In the base case, r_w and r_f were, respectively, more than 0.07 and 0.03 for all air change rates, as shown in Figures 5.14 (b) and (c).

As illustrated in Figure 5.15 (a), patients in beds located 1.625 meters away from the corridor (i.e., Patients 1 and 2) were the most susceptible to the spread of infection (with exposure risk (E) greater than 0.05), whereas patients in beds located 5.875 meters away (i.e., Patients 5 and 6) were the least susceptible (with E less than 0.025). Patients who were further away from the corridor experienced a marked decrease in their likelihood of contracting an infection as a result of an increase in air change rate. This is explicable by the general airflow patterns depicted in Figure 5.7. Patients 5 and 6 had a risk of exposure to infection that was on average about half of patients 1 and 2, across all the air change rates considered.

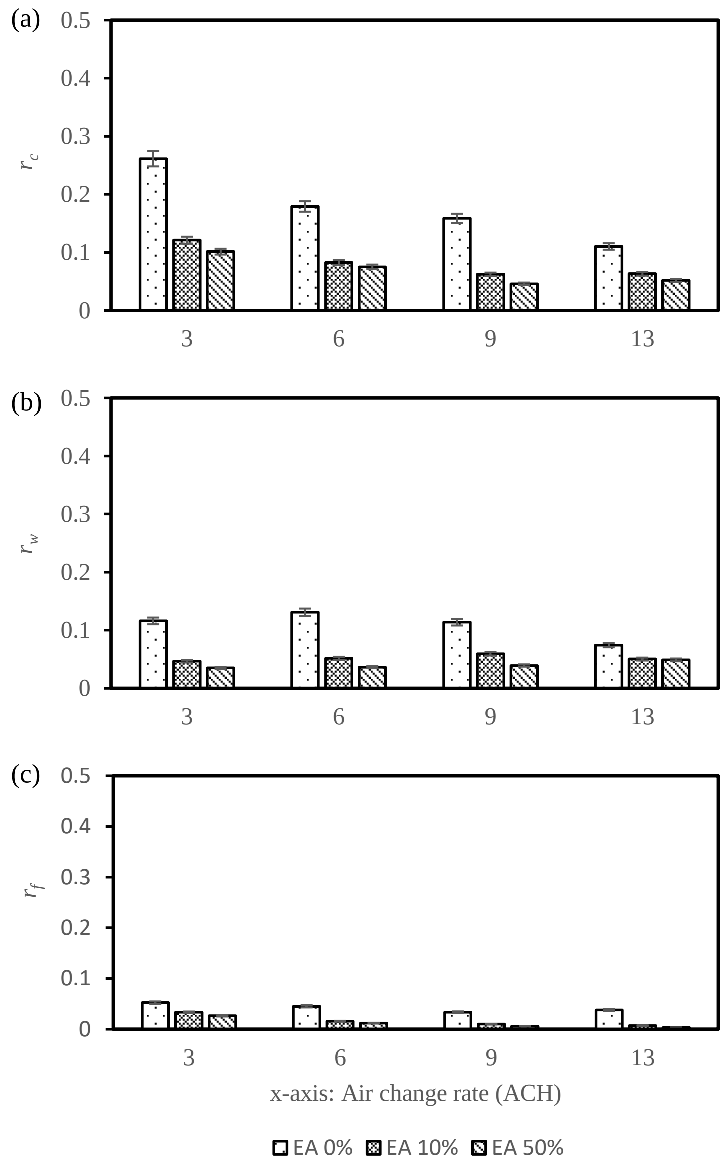

Figure 5.14 ACH vs deposition ratio on: (a) ceiling; (b) walls; (c) floor

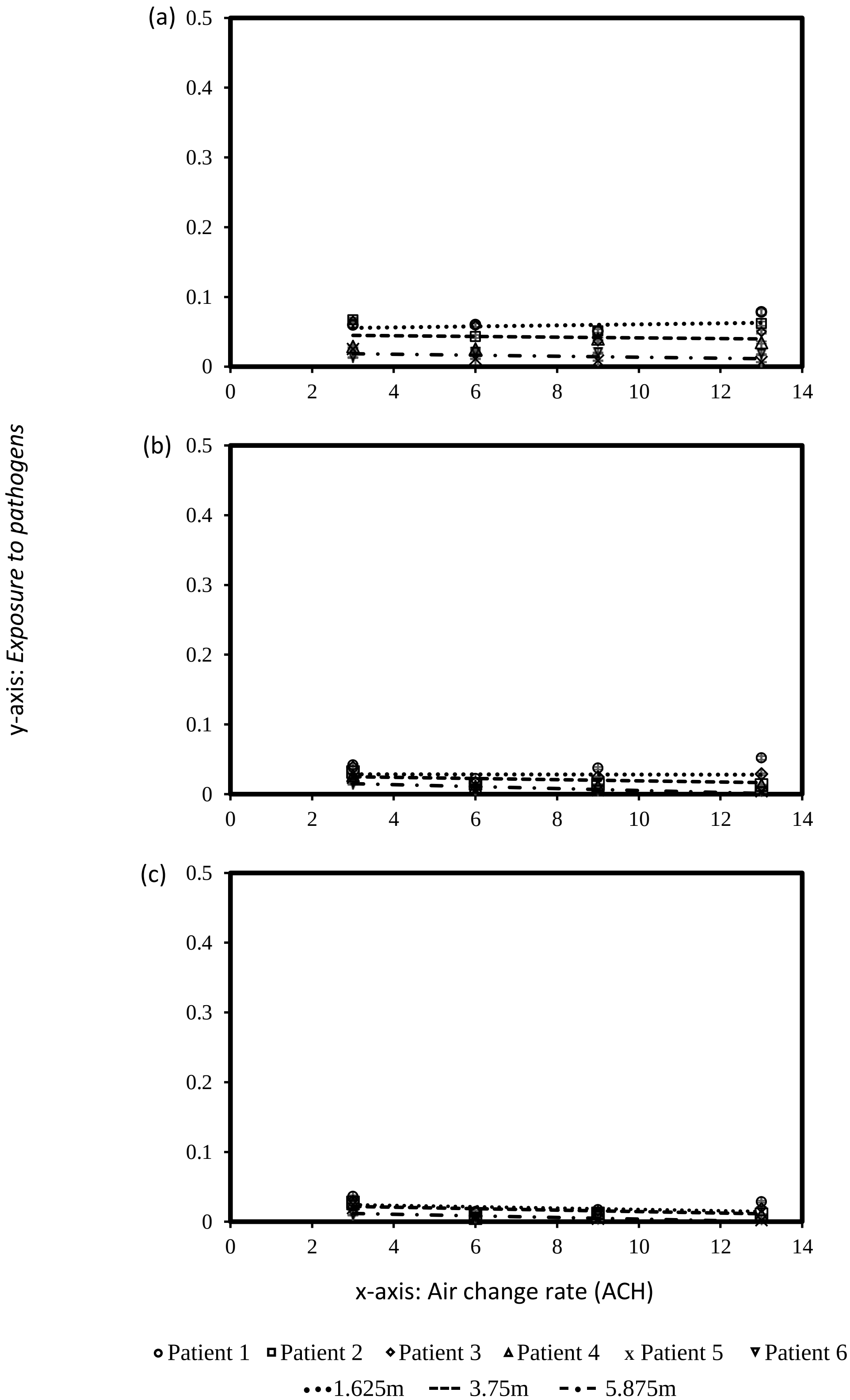

Figure 5.15 ACH vs exposure to pathogens: (a) EA=0%; (b) EA=10%;(c) EA=50%

Figures 5.8 and 5.9 show that the local exhaust grilles not only made it easier to remove a portion of the exhaled virus particles, but they also tended to increase the particle deposition in the body of the source patient, which led to a reduction in the amount of residual viral load that was present in the air. As shown in Figure 5.14 (a), the recorded values of r_c at 3 h^{-1} were around 0.12 and 0.10 for EA = 10% and EA = 50%, respectively. This represents a drop of 53% and 61% when compared to the base condition. In the same manner as the other cases presented in Figure 5.14 (a), r_c fell whenever the air change rate was raised. According to Figure. 5.14 (b) and 5.14 (c), the ratios of deposition on the wall and floor were greatly reduced when EA was set to 10% and 50% ($r_w < 0.05$ and $r_f < 0.03$).

However, it was found that all the scenarios resulted in the deposition of particles. Because the deposition is unpredictable by its very nature and frequently occurs regardless of the design of the ventilation system, this underscores the significance of maintaining regular and adequate ward cleanliness. Additionally, the randomness that is associated with particle deposition rates (r_w, r_c, and r_f) under various air change rate situations can be related to the asymmetric airflow distribution patterns that are present as well as the locations of the patients that are infected.

According to Figures 5.15 (b) and (c), the placement of exhaust grilles in close proximity to each patient can effectively mitigate particle migration from an infected patient to other areas within the ward. This measure also results in a noteworthy reduction in individual patient exposures, with a recorded value of E < 0.05. The findings indicate that the spatial positioning of a patient who has contracted an infection, the rate of exhaust airflow, and the frequency of air changes within the enclosed space all collaborate to impact the infection transmission mechanism.

5.6.3 Discussion

Within the confines of an air-conditioned general inpatient ward cubicle, the airborne route of infection transmission of MERS-CoV and the patterns of its subsequent deposition were analyzed. It was shown that both the air change and the exhaust airflow rates have substantial impacts, not only on the indoor airflow but also on the distribution of particles within a room that is mechanically ventilated. Furthermore, the location of a source patient within the ward cubicle is very important in evaluating the extent of the risk of infection to other ward users. The findings imply that the breathing zone directly above the source patient has the highest level of pathogen exposure, followed by the breathing zones at the bedside and adjacent patients close to the source patient. The dispersion of pathogens throughout the ward over time is also apparent. This provides us with an insight that under the effect of airflow, the particles could migrate several meters away from their point of origin, resulting in the transfer of infectious diseases within the ward. However, a key difference while adopting a lower ACH (3 h^{-1}) and a higher ACH (13 h^{-1}) in this study was that the latter had significantly lowered the number of pathogens available to cause infection transmission than the former. In addition, combining a higher air change rate (13 h^{-1}) with a high exhaust flow rate (50% of supply air) through a local exhaust grille dramatically reduced the number of available pathogens, further mitigating the risk of pathogen exposure for ward users. As a result, it is recommended that exhaust grilles be provided near a patient, preferably over each patient's bed. It is also recommended to have a high exhaust airflow rate to achieve infection prevention and control. Regardless of the ventilation configuration, each patient and surface inside the award cubicle needs to be cleaned and disinfected on a regular basis to eradicate any microbiological contamination. It is advised that UVGI lights be installed in the ward to further increase risk mitigation efforts. The results of this investigation can serve as a reference for developing more effective ventilation design solutions to reduce the likelihood of infections occurring in their facilities.

5.7 Optimization for design evaluation

With rapid advances in computing, CFD has become an indispensable tool for designing, analysing, and evaluating indoor environments' physical and operational configurations. CFD models can give a high-level spatial and temporal resolution of flow patterns, temperature, and pollutant dispersion within the computational domain of interest. In the prior section, a numerical study was carried out to lay out effective ventilation strategies to mitigate infection transmission in a general inpatient ward. Air change rate, location of exhaust grille, exhaust flow rate, and location of an infected patient is identified to have substantial impacts on the airflow and particle distribution within the facility. However, other factors, such as the type, size, and location of the air distribution device, space geometry, etc., could also be influential. The traditional trial and error approach to implementing strategies encompassing all these factors would undergo numerous revisions between the initial and final design. Each modification to the design would necessitate re-modelling, re-mesh, and re-execution of the numerical simulations. Thus, relying solely on sophisticated simulation tools, such as CFD, to systematically evaluate the designs may take many hours or days to attain a solution that may or may not meet the design objective. Thus, a coupled simulation strategy that integrates an evolutionary algorithm (genetic algorithm) with an evaluation mechanism (CFD) is developed.

5.8 Exposure to infection in a ward cubicle

Exposure to pathogens would increase the likelihood of an individual getting infected. There is a greater likelihood for an individual to be exposed in a healthcare facility such as an inpatient ward cubicle compared to other indoor environments. As previously noted, the distribution of pathogens within the facility may be influenced by various factors, including the location of an infected individual and their exhalation activity. By depositing pathogens on a patient who is susceptible to infection, an infected patient *i* contributes to the spread of infection inside the ward cubicle, and this contribution can be quantified as,

$$D_i = \sum_{j=1}^{n} d_j ; j \neq i \tag{5.12}$$

where D_i is the number of pathogens that have been deposited on other patients because of the exhalation activity of infected patient i, d_j is the particle that has been deposited to patient j, and n is the total number of patients in the ward cubicle. Contrary to section 5.3.1, in this investigation, only the number of pathogens deposited in patients is taken into consideration.

5.9 Coupling of CFD with genetic algorithm

Chapter 4 demonstrated the integration of genetic algorithm with an artificial neural network, in which the neural network was utilized as the fitness function. This chapter employs computational fluid dynamics (CFD) as a fitness function to determine the optimal parameter combinations that would effectively minimize the deposition of pathogens within the ward cubicle. Figures 5.16 and 5.17 show the GA process's components and overall outline adopted in this study.

In a general inpatient ward, the potential for infection can be linked to a variety of operational and physical aspects of the indoor environment. It's possible that several factors, such as the air change rate, the number, location, and size of air supply diffusers and exhaust grilles, the location of the infected patient, the type of exhalation activity, its direction, and its velocity, and other factors, could all play an important part in the transport, dispersion, and deposition of infectious pathogens. The initial population and parameters to be optimized through the GA process is formed from the insights gained from the numerical simulation results detailed in section 5.6.

In this investigation, the initial population consisted of 133 different chromosomes, each of which underwent a separate computational fluid dynamics (CFD) simulation. The CFD simulation would yield the deposition count in the ward cubicle, and Equation 5.12 in section 5.8 earmarks particle deposition count. In this single-objective optimisation, CFD simulations serve as the fitness function, and the count of deposited particles serves as the fitness score. A crossover rate of 0.5 and a mutation rate of 0.1 were utilised to conduct the GA process. In this investigation, the maximum number of generations is set as the stopping criteria for the GA process. Python was used as the programming language for the GA implementation, and the phases that make up the GA process are outlined as follows:

1. Using the input parameters, generate *n* random chromosomes to form the first population.
2. Determine the particle deposition count (fitness score) in the ward based on the CFD simulation (fitness function) for every chromosome in the population.

3. Based on the fitness score, chromosomes will be evaluated and selected.
4. The parents will undergo crossover and mutation.
5. Based on the crossover rate and mutation rate, new chromosomes will be created, resulting in the formation of a new population.
6. The fitness score of the new chromosomes will be determined using CFD simulation.
7. This concludes one iteration or generation of a genetic algorithm.
8. Repeat steps 3-6 until a predetermined stopping point is reached.

This investigation utilized the same numerical simulation procedure for airflow and particle modelling as adopted earlier in this thesis. Hence, more details regarding the same can be referred in section 5.4.

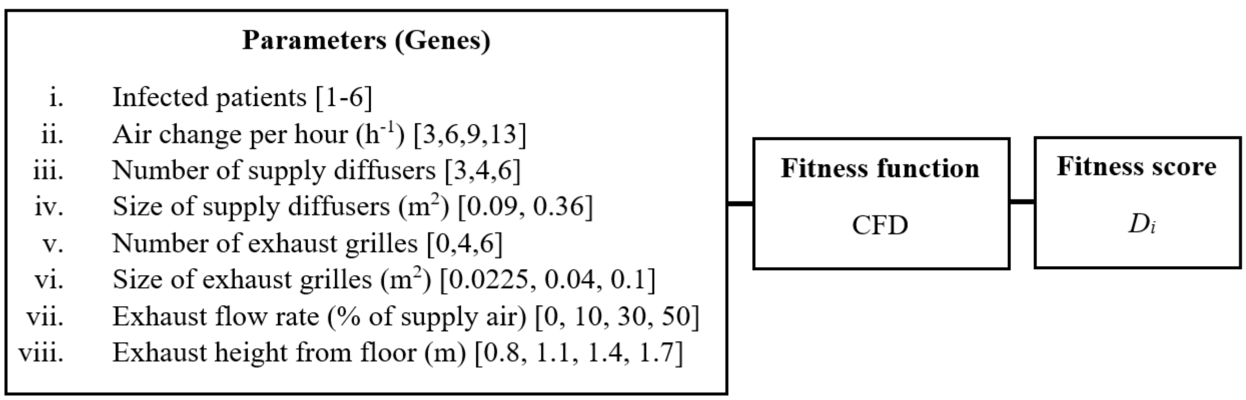

Figure 5.16 Components of the genetic algorithm process

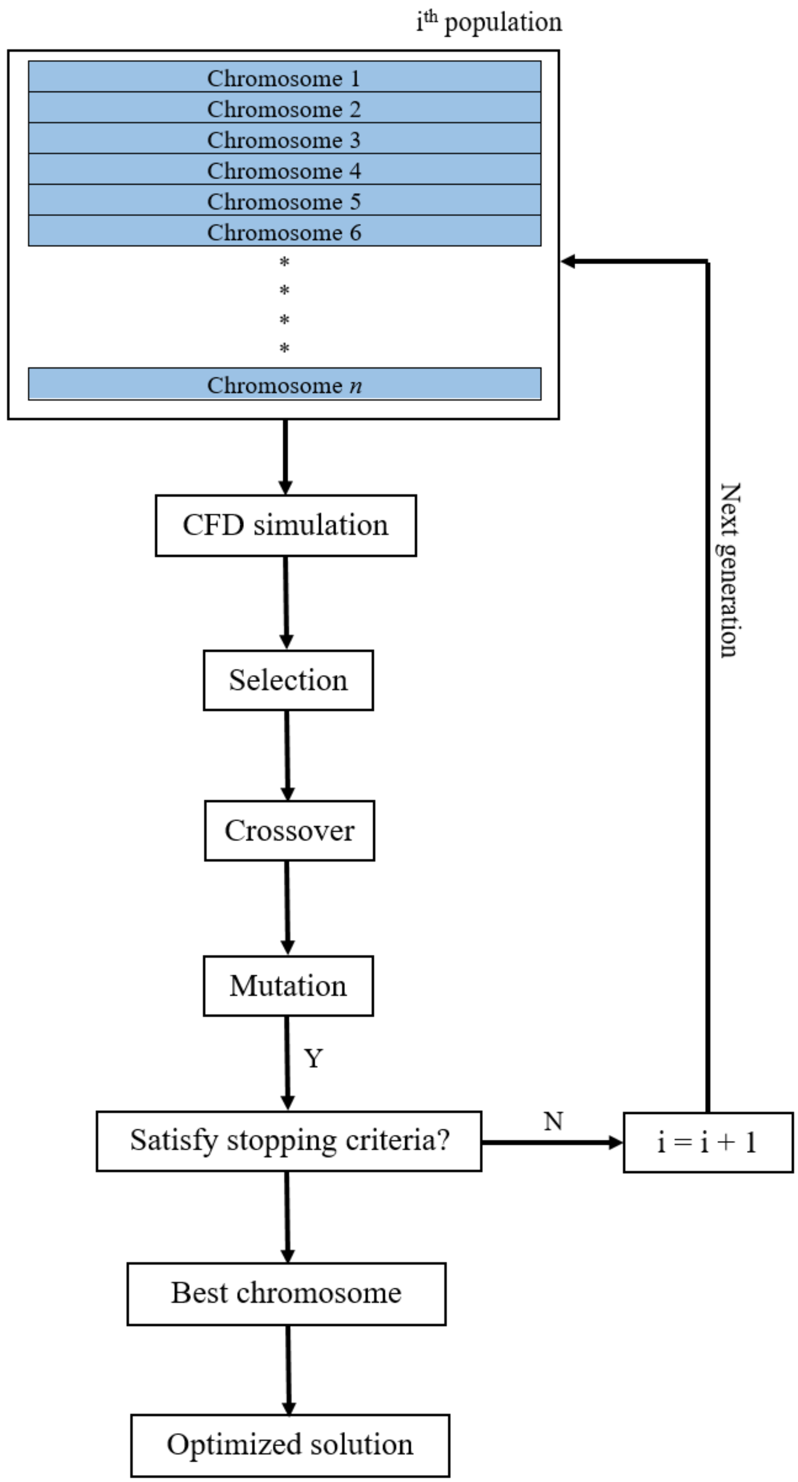

Figure 5.17 Flow chart of genetic algorithm process

5.10 Ward configurations and ventilation strategies

In this investigation, the existing ward configuration termed as base case in section 5.2 is used and its different variations with respect to design and operation is developed to form the initial population in the GA process. As can be seen in Figure 5.18 (a), the existing ward design, featured four supply diffusers measuring 0.6 m x 0.6 m each, each of which was situated on the ceiling of the ward. Positive pressure was maintained toward the corridor using mechanical ventilation in the six-bed ward cubicle. This investigation used four different air change rates: 3 h^{-1}, 6 h^{-1}, 9 h^{-1}, and 13 h^{-1}. Based on these air change rates; supply air was distributed throughout the cubicle using ceiling-mounted diffusers. For each air change rate condition, an exhaust flow of 10%, 30%, and 50% of the supply air was regulated through the exhaust grilles. Local exhaust grilles were put at different locations near the patient bed. To investigate how modifications to the design of ward cubicles affect the flow of air and the distribution of particles, the number, size, and location of supply diffusers and exhaust grilles were varied. A few configurations from the initial population are depicted in Figure 5.18 (a)–(f) and Figure 5.19 (a)–(b), respectively, to illustrate the existing ward, its modifications, and related terminologies.

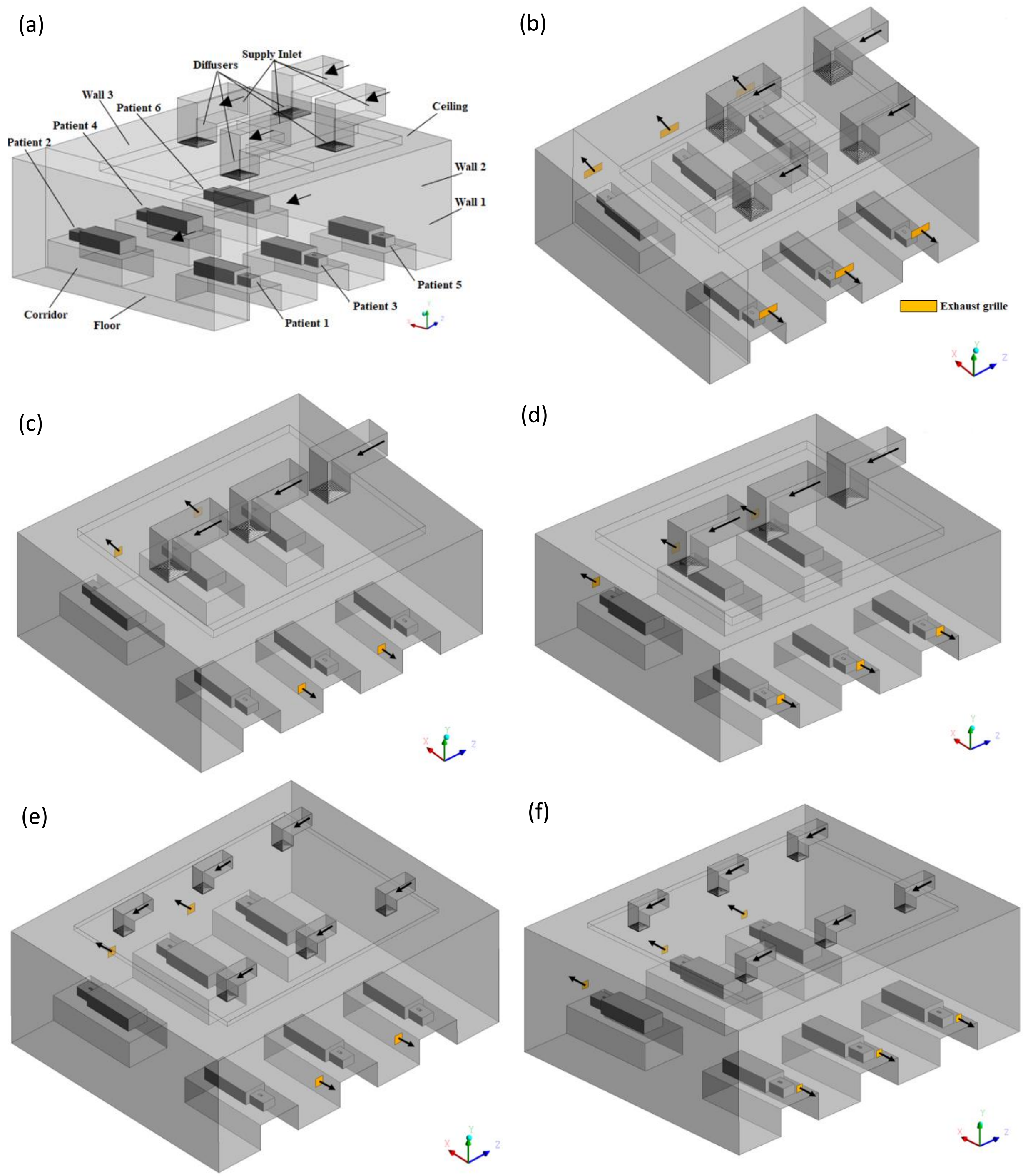

Figure 5.18 Inpatient ward cubicle designs with patients: (a) Existing cubicle with four supply diffusers and no local exhaust grilles (base case); (b) cubicle with four supply diffusers and six local exhaust grilles; (c) cubicle with three supply diffuser and four local exhaust grilles; (d) cubicle with three supply diffusers and six local exhaust grilles; (e) cubicle with six supply diffusers and four local exhaust grilles; (f) cubicle with six supply diffusers and six local exhaust grilles.

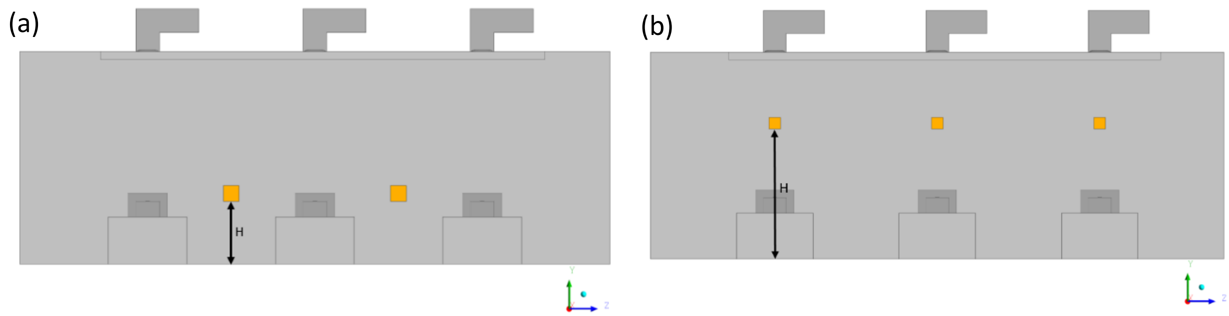

Figure 5.19 Height (H) of the exhaust grille from the floor

5.11 Numerical simulation results

This section provides a brief explanation of the airflow patterns and particle deposition within the inpatient ward cubicle as determined by CFD simulations coupled with GA.

5.11.1 Airflow distribution and patterns

A quantitative depiction of the distribution of velocity and temperature across the ward can be obtained using numerical simulations carried out using CFD. Both the patterns of airflow and the temperature distribution can play an important part in the mechanism by which infectious pathogens are transported, dispersed, and deposited. Figure 5.20 and 5.21 illustrates the velocity distribution and airflow pattern in the ward over the XZ plane at two distinct ACHs (9 h^{-1}, 13 h^{-1}). The location of this plane is at y = 1.35 m from the floor. It is clear from looking at Figure 5.20 (a) that the air velocity near patients 1 and 2 was much lower at 9 h^{-1} compared to the air velocity near the other patients who were being treated in the ward. In addition, as can be seen in Figure 5.20 (b), the predominant direction of airflow in the ward is toward the corridor. Therefore, as a result of these two circumstances, the patients positioned near the corridor will play a less significant part in the process of causing cross-infection among the other patients in the ward.

(a)

(b)

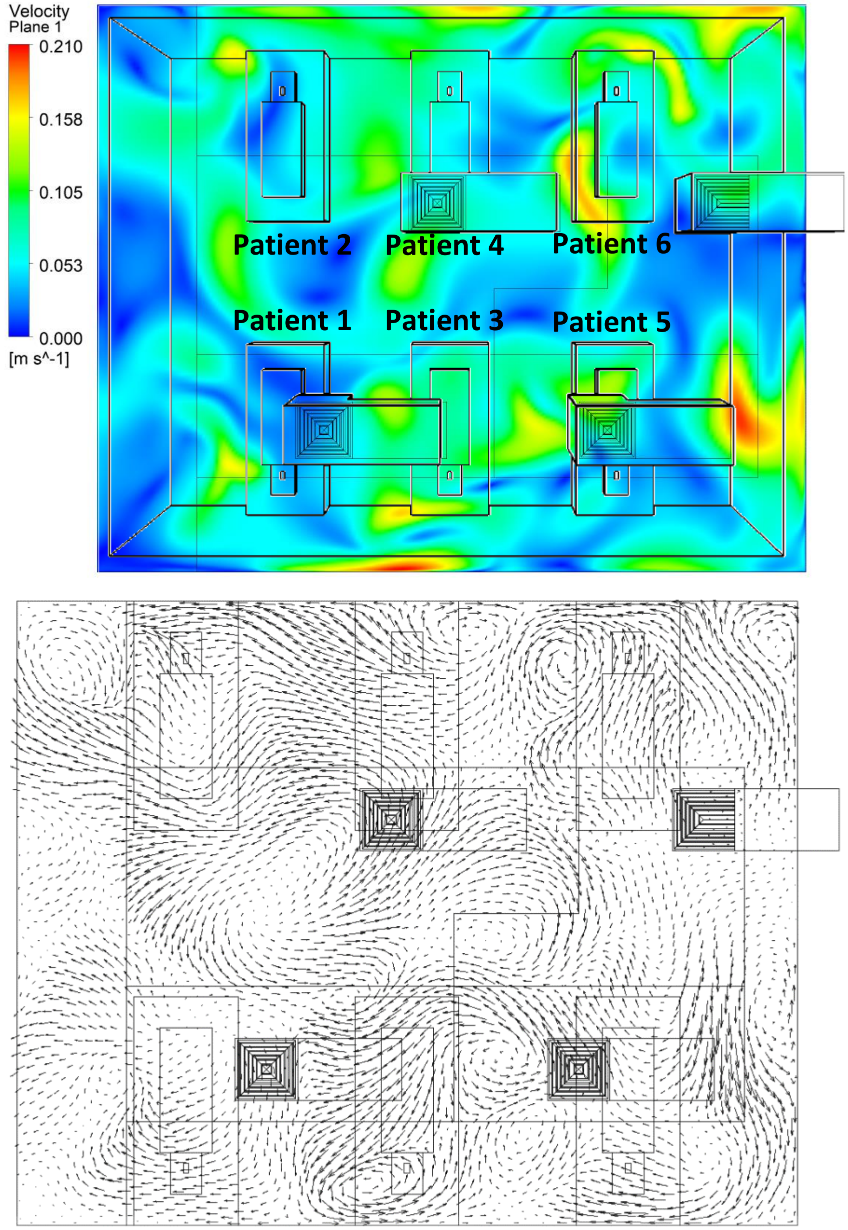

Figure 5.20 Airflow simulation results across a horizontal plane located at y = 1.35m at 9 ACH.

The existence of a blockage in the form of the patient and bed causes the production of multiple eddies. The recirculation zones have the potential to produce a dangerous environment because they have the capacity to hold infectious pathogens for an extended period, which in turn raises the likelihood of infection. As illustrated in Figures 5.21 (a) and (b), the observed improvement in the velocity distribution as well as the airflow pattern occurs in conjunction with an increase in ACH. Temperature distribution and airflow pattern on the XY plane placed at a distance of z = 1.6 m in the ward cubicle with a local exhaust grille installed on the bed sidewall are depicted in Figures 5.22 (a) and (b), respectively. Thermal plume is produced by thermal manikins, which have the potential to have a significant impact on the vertical airflow pattern within the ward cubicle. It is clear to observe in Figures 5.22 (a) and (b) that the cold supply air and the thermal plume are being mixed.

(a)

(b)

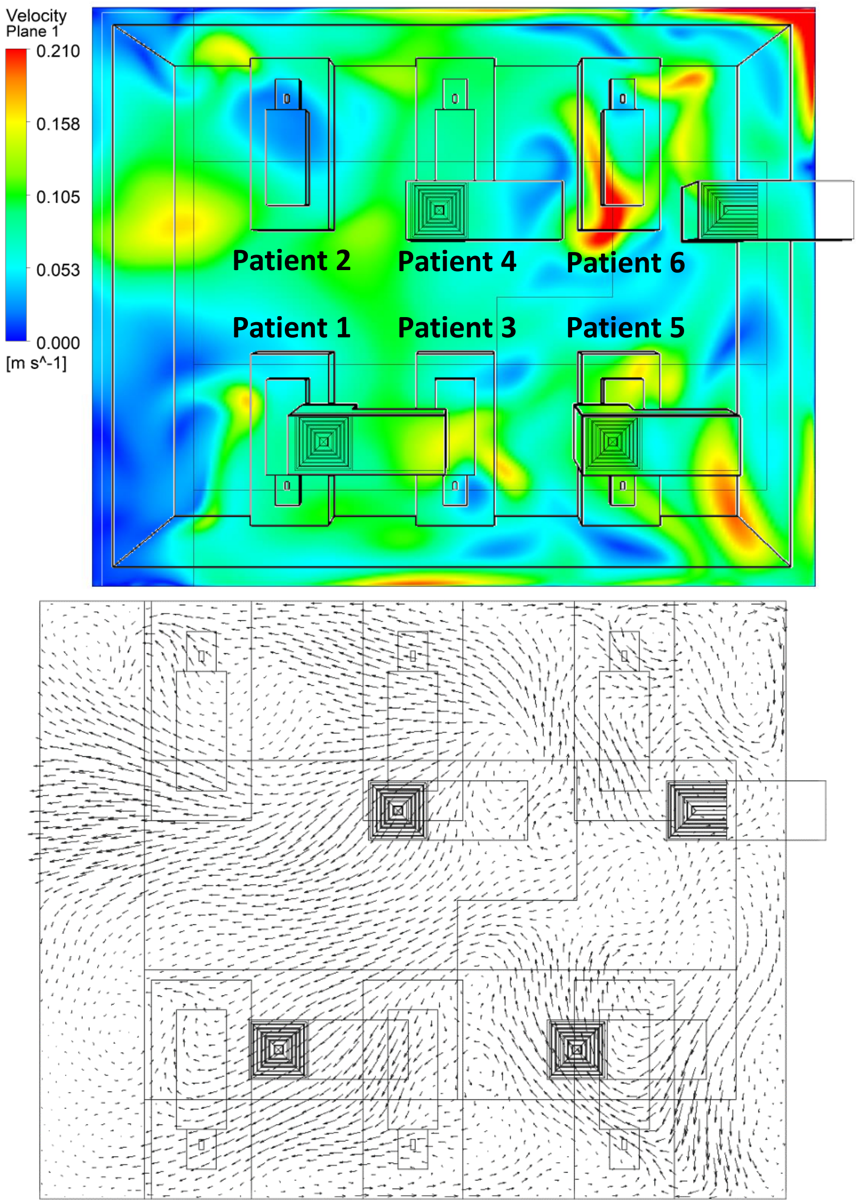

Figure 5.21 Airflow simulation results across a horizontal plane located at y = 1.35m at 13 ACH.

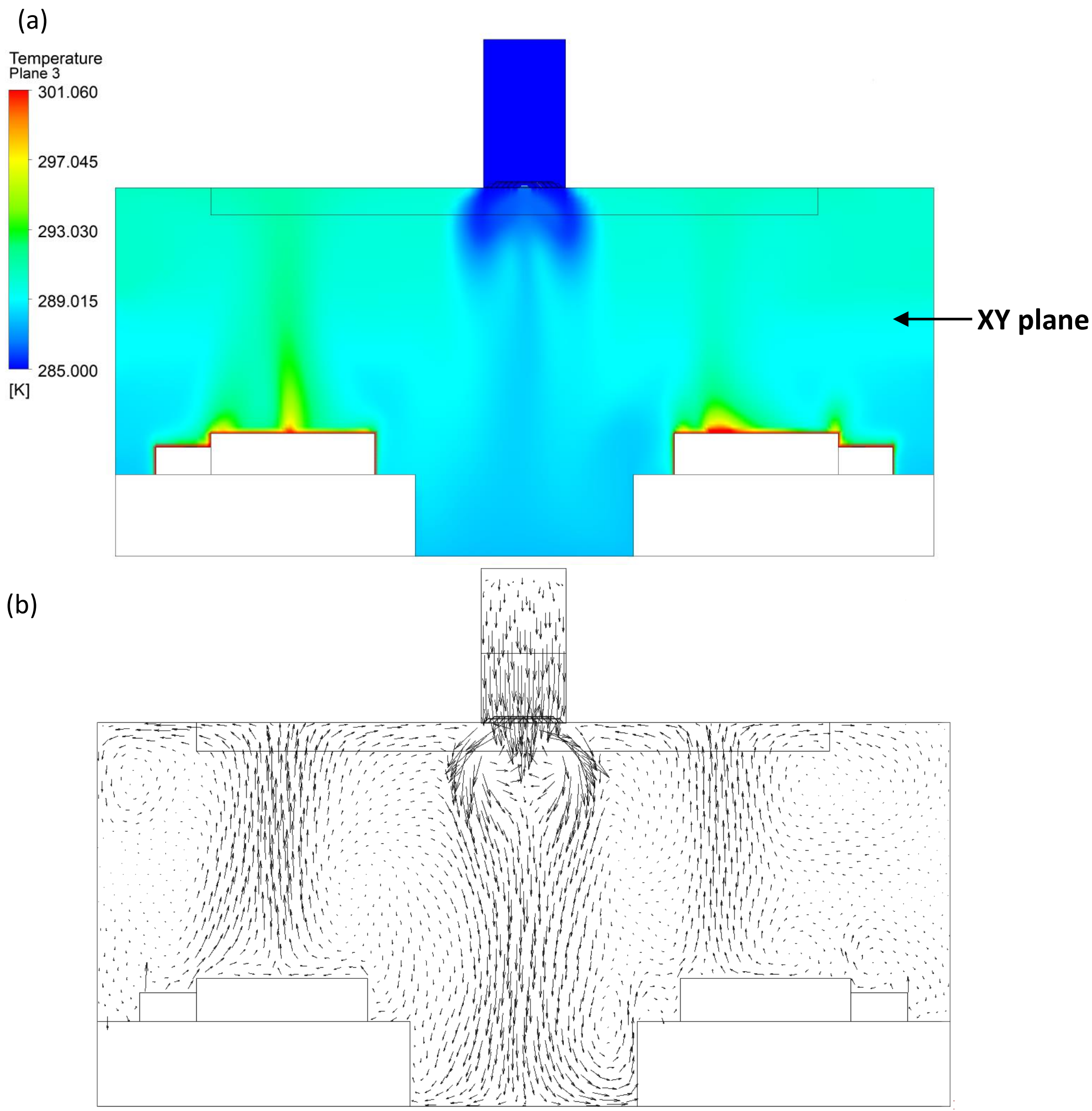

Figure 5.22 The plots of ward cubicle with three supply diffusers on the ceiling and four local exhaust grilles on the sidewall at 6 ACH and exhaust air = 30%: (a) temperature distribution (b) airflow pattern

5.11.2 Exposure risk for patients through cross-infection

Figure 5.23 is a plot depicting the progression of generations through the GA process, along with the fitness value for the optimal chromosome. Table 5.3 lists the best input parameter combinations that results in least deposition of pathogen after completing 10 generations. The fitness score (D_i) indicates the number of particles that were deposited on other patients because of an infected person exhaling in the ward cubicle.

It is clear from Table 5.3 that the patient 2 who is located closest to the corridor contribute the least to the spread of infection throughout the ward cubicle. It's possible that putting a new patient in a location close to the corridor for the first few days of their stay in the hospital would be the best way to prevent any infections from rapidly spreading throughout a ward cubicle. It is also clear from Table 5.3 that the design of the ventilation system would play a significant role in determining how effectively the ward can prevent the spread of infection from patient to patient.

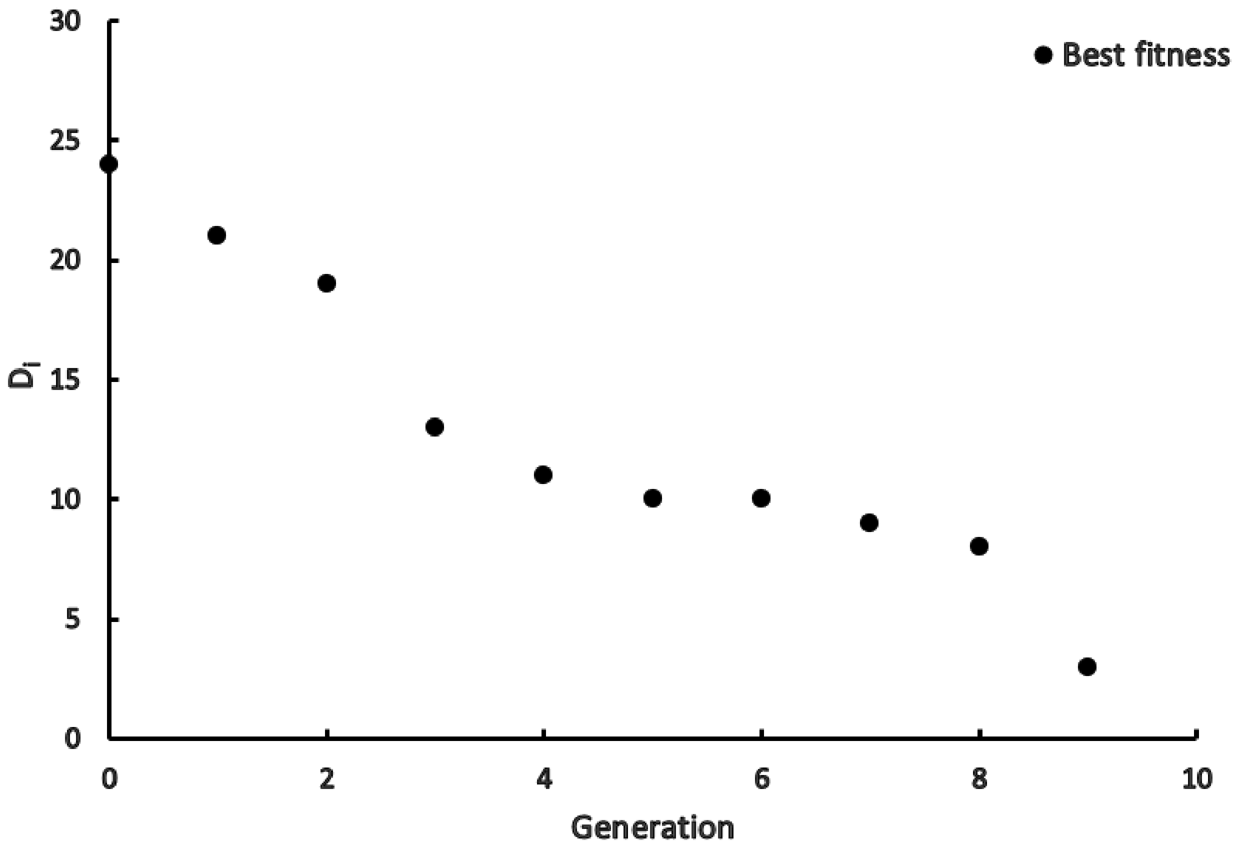

Figure 5.23 Evolution of generation in the GA process

In a ward cubicle that is kept at an air change rate of 6 h^{-1}, installing three supply diffusers of size 0.36 m^2 on the ceiling and exhaust flow (30% of supply air) through four exhaust grilles of size 0.04 m^2 that is located nearby patient beds has shown to be the optimal arrangement that results in the lowest possible risk of cross-infection. In addition, it is essential to emphasise that the installation of a local exhaust grille in close proximity to the patient could provide localised control to restrict the spread of infectious pathogens from an infected patient to other locations within the ward cubicle. In addition, regardless of the ventilation strategy that is utilised, it is of the utmost significance for medical personnel who are providing care to patients to adhere scrupulously to general recommendations concerning the prevention of infections. These recommendations include practising proper hand hygiene, protecting their eyes, and wearing face masks with high filtration efficiency.

Table 5.3 Input parameter combination with the lowest pathogen deposition

Parameters								
i	ii	iii	iv	v	vi	vii	viii	D_i
2	6	3	0.36	4	0.04	30	0.8	3

* Refer to Figure 5.16 for the denotation of roman numbers

5.12 Summary

Ventilation plays a significant role in maintaining indoor air quality and thermal comfort in indoor environments. Although, in a healthcare facility, it must additionally consider infection prevention in its control strategies. However, it is noted that there is a lack of proper guidelines for designing ventilation system for patient environment such as in-patient wards. Thus, a numerical study was conducted utilizing CFD to evaluate the influence of different ventilation strategies on the mitigation of infection transmission in a mechanically ventilated in-patient ward cubicle.

The conventional method of optimising ventilation strategy for an indoor environment requires exhaustive simulation of all possible combinations of design space parameters, followed by methodical evaluation of each scenario to propose the optimal solution. This strategy, on the other hand, would be extremely inefficient in terms of both time and cost. Hence, a coupled simulation approach by combining an evolutionary algorithm (Genetic algorithm) with an evaluation mechanism (Computational Fluid Dynamics) was developed to determine an optimal ventilation strategy to mitigate the spread of infection in an inpatient ward cubicle. This research aimed to improve patient safety by reducing the likelihood that an infection will be passed from one patient to the next. Compared to the conventional method, the proposed methodology would perform fewer CFD simulations while simultaneously evaluating a wider variety of design solutions in an iterative manner.

According to the findings of a design exploration conducted with GA-CFD, the combination of certain design parameters, such as the location of an infected patient; the air change rate; the flow rate through a local exhaust grille; the number, location, and size of supply diffusers and local exhaust grilles; and the flow rate through a local exhaust grille, can be crucial in reducing the likelihood of an infection spreading from one patient to another within a ward. In addition, the research highlights the necessity for healthcare workers to prudently practise and implement standard guidelines of infection control, such as practising proper hand hygiene, protecting their eyes, and always wearing a face mask that has a high filtration efficiency, regardless of the ventilation strategy that is being used.

Chapter 6

Conclusions

Energy conservation in buildings is a perennial topic compared to numerous research fields. The building sector is recognized as one of the significant contributors to global greenhouse gas (GHG) emissions. GHG is the leading cause of climate change, and climate change is driving an increase in heat waves and other extreme weather events. It is suggested that it could cause a dual effect: a decrease of 30% in global heating demand and an increase of 70% in global cooling demand. Thus, an effective way to cut down building cooling energy consumption and reduce the carbon footprint associated with buildings is to strategize a methodology that could aid in designing and developing sustainable buildings. One approach to do this is by developing a state-of-the-art simulation tool that could predict the cooling energy consumption of diverse types of buildings with sensitive changes in building characteristics in a minimal time. The literature review revealed a necessity for the creation of said models and significant advantages linked to their establishment. Moreover, the utilization of optimization algorithms is concentrated on improving the prediction performance of the simulation model. In contrast, there should be greater use of optimization methodology to identify critical parameter combinations that generate optimal solutions to minimize cooling energy demand without adhering to traditional methods' exhaustive and time-consuming approach.

The prediction tools currently available for forecasting building energy prediction can be classified into physical (white box), data-driven (black box) and hybrid methods. By solving thermal equilibrium and heat transfer equations, the physical method accurately forecasts thermal energy within a building. Despite its excellent accuracy, it is coupled with high processing costs and limited optimisation potential. In addition, dynamic building energy analysis necessitates high expertise. On the other hand, statistical analysis techniques such as support vector machines and artificial neural networks can respond rapidly to inputs and handle nonlinearities with ease. For training and development, these models, however, require extensive databases. Any deficiency or inaccuracy would significantly diminish its predictive ability. Additionally, the outcome of the forecast lacks physical interpretability. These drawbacks in physical and data-driven approaches can be overcome by implementing a hybrid method. The hybrid method combines the physics of the pure physical method and the statistics of the data-driven process. Not only does this method need less time to simulate than the physical simulation tool, but it also compensates for the issue that the purely statistical approach needs to provide a physical explanation of the relationship between the input and output data. Moreover, the hybrid method proves to be superior to its counterparts. This hybrid model's applicability is promising, and there is a current trend toward utilising this technique more frequently in modelling building energy use.

Thus, a hybrid simulation model for predicting the building energy demand is developed in this study. This concept demonstrates the potential of merging artificial intelligence techniques with a building energy simulation tool (EnergyPlus™) to anticipate buildings' annual cooling energy consumption. A building energy simulation tool, EnergyPlus (EP), simulates a series of hourly envelope heat gains based on the building's features. To construct the input/output database, the input parameters and their corresponding output values were retrieved from these simulated cases. This database is then utilised for training an artificial neural network (ANN). The envelope heat gain (by ANN), ventilation and internal heat gain (by physical expressions and literature results) are all added, considering the occupant AC operation schedule and system coefficient of performance to determine the total cooling energy requirement. This hybrid method will find crucial linkages between building physical attributes and operational measures to reduce cooling energy demand in a fraction of the time required by conventional energy estimation techniques. The significant reduction in the energy simulation process would reduce the project turnaround time and development cost.

The model's goodness of fit with energy plus simulations and peer literature data was evaluated to determine its validity. The validation examination revealed a satisfactory energy forecast performance, showing its applicability to be an efficient alternative to the conventional energy estimation methods used by building engineers. The hybrid simulation model can analyse the influence of building materials, construction solutions, and indoor–outdoor temperature fluctuations on cooling energy of a space. Thus, it would allow the user to conduct an energy audit by identifying areas that lead to energy wastage, thus aiding in early intervention and predictive maintenance. It has been determined that employing windows and external walls constructed from materials with low thermal conductivity can lower annual cooling energy usage by 8.19%. Bringing the windows-to-walls ratio down from 80% to 40% can save 18%. Additionally, changing the indoor set-point temperature from 24 °C to 26 °C can reduce annual cooling energy consumption by 13.65%. Taking global warming into perspective, when the external temperature rises by 1 °C, the yearly cooling energy demand for maintaining 24 °C and 25.5 °C indoor set-point temperatures increase by 4% and 2.5%, respectively. The observed changes in cooling energy consumption, as documented in this study, can be attributed to the fundamental principles of heat transfer. Thus, it can be deduced that the results predicted by the hybrid simulation model carry substantial physical significance. Thus, the hybrid simulation model that was developed can be considered to be physically plausible.

Developing these tools is a highly time-consuming and complex process. Thus, the development of single-building prediction models is often useless. Generating hybrid simulation models for a set of buildings would maximize its capacity, bringing huge benefits. Moreover, many case studies would justify the development expenses of hybrid simulation models. Hence, the generalization capability of the hybrid model was tested for parameters outside its training range. In this aspect, two diverse premises were chosen: (a) sub-divided units, which are residential spaces with specific building characteristics that fall below the lower limit of the training data range, and 2) healthcare facilities, which are non-residential spaces that have building parameters that fall beyond the upper limit of the training data range. The hybrid simulation model's goodness-of-fit test with energy plus simulations revealed that it could generalize well. Thus, additional research is conducted on the subdivided units using the generalized hybrid simulation model to analyze the different ways to lower the energy associated with this unit. The general perception is that tiny homes reduce environmental impact and increase housing accessibility. However, in high-density living environments like Hong Kong, where buildable land is scarce, unaffordable housing exists, and there are no minimum living space standards, many people live in cramped spaces such as SDUs, causing discomfort and higher energy use. A generalised hybrid simulation model analysed the influence of apartment floor size, occupant per floor area, and interior set-point temperature on annual cooling energy demand. It was identified that there is a urgent need to regulate the space per person in tiny residential units.

Exploration of design space via parametric analysis is arduous if performed using the traditional approach. In addition, the outcomes cannot be attributed to the optimal solution to the problem. Hence, this study's generalized hybrid simulation model is combined with an evolutionary algorithm to aid the user in iteratively evaluating the various design factors and their effect on cooling energy consumption. Combining a genetic algorithm (GA) with a hybrid simulation model would enable the user to quickly identify the optimal or sub-optimal solution for a given architectural setting from a pool of solutions. A general inpatient ward cubicle was selected as a case study to illustrate the optimization technique and its benefits. The primary drivers (envelope parameters, recirculation ratio, and lighting power density) that could impact the facility's cooling energy demand were analyzed. In this study, a genetic algorithm would improve the model parameters to achieve either the minimal or maximal envelope heat gain. This study suggests adopting a combination, namely (i) design parameters resulting in minimum envelope heat gain, (ii) higher recirculation ratio, and (iii) lowering lighting power density from 13 W/m^2 to 7.3 W/m^2, would be an energy-efficient strategy for a general inpatient ward. Furthermore, infection control is comparable to or greater than the energy requirement in a general inpatient ward unit. Thus, techniques to reduce the spread of infection within a general inpatient ward cubicle are investigated further.

Infections in healthcare facilities can cause substantial public health problems and cost obligations. It's unclear how these infections spread, and the best approach to treat them is debated. Understanding infection transmission modes is crucial, yet they are not well characterized or understood. Multiple transfer routes may also complicate the transmission of infection. Infection transmission through hidden infectious pathogen carriers in hospitals can create massive disease outbreaks in the community. Therefore, improving infection control in healthcare facilities is of the utmost importance.

The evaluation of the risk associated with exposure to infectious pathogens necessitates an understanding of the influence of ventilation strategies and the indoor environment. The ventilation rate within isolation and operations rooms is well established. However, the ventilation needs for other areas, such as wards and outpatient clinics, lack clarity. There exists a significant level of ambiguity regarding the determination of the optimal range of ventilation rates for the purpose of reducing the transmission of infections within hospital wards.

This study delved into several prediction techniques that are applicable in evaluating the airflow and dispersion of contaminants within an enclosed space. Despite their ease of use, inclusion of physical meaning, and minimal computational requirements, analytical methods have been found to be inadequate for addressing complex problems. The empirical models exhibit a comparable outcome that is associated with them. The experimental approach is useful. However, compared to numerical techniques, experimental approaches are costly and time-consuming. The predominant numerical methodologies employed for predicting airflow and contaminant distribution are the multizone, zonal, and computational fluid dynamics (CFD) approaches. CFD is acknowledged as the most effective and widely used numerical technique in comparison to the other two methods.

This study evaluated the impact of ventilation strategies on airflow distribution and the potential for infection transmission through droplet nuclei of size 0.167 µm (MERS-CoV) in an air-conditioned ward cubicle. The possibilities of infection transmission to ward users through pathogens that are dispersed into the ward air due to the exhalation activity of a source patient and their subsequent deposition are analyzed with CFD for different ventilation scenarios. The spatiotemporal dispersion of pathogens within the ward cubicle suggests that they are capable of traversing distances of several meters from their point of origin, facilitated by the influence of airflow, thereby contributing to the transmission of infectious diseases. One notable distinction observed in this study between the implementation of a lower air change rate of 3 h^{-1} and a higher air change rate of 13 h^{-1} was the significant reduction in the number of pathogens available for potential transmission of infection in the latter. Moreover, the combination of an increased air change rate of 13 h^{-1} and a substantial exhaust flow rate of 50% relative to the supply air via a localized exhaust grille resulted in a significant reduction in the number of available pathogens, thereby providing an additional layer of protection against potential pathogenic exposure for ward occupants. In addition, it is recommended to install exhaust grilles near a patient. The association between ventilation and the mechanism of infection transmission within the ward cubicle were apparent. The positioning of a source patient within the ward cubicle holds significant importance in assessing the magnitude of infection risk posed to other ward occupants. Thus, these results indicate that while devising infection control strategies, it is important to consider the design of the ventilation strategies as well as the location of vulnerable patients in relation to an infected individual. These factors have the potential to impact the effectiveness of infection control measures.

Several factors could influence airflow and pathogen distribution in an inpatient ward. The insights gained from numerical simulations conducted to evaluate the transport, dispersion, and deposition of MERS-CoV droplet nuclei formed the foundation for identifying crucial factors that were subsequently employed in an optimization investigation. The conventional approach of trial-and-error is required to devise efficient ventilation strategies that consider these factors, which would entail numerous modifications between the initial and final design. Computational fluid dynamics (CFD) offers highly precise and detailed flow parameters, but it is associated with significant computational time and cost. Thus, relying solely on sophisticated simulation methods, such as computational fluid dynamics (CFD), for the systematic evaluation of designs can result in a time-consuming process that may yield a solution that does not necessarily meet the design objective. The present study employed a coupled simulation technique that integrates an evolutionary algorithm, specifically a genetic algorithm, with an evaluation mechanism (CFD). The suggested approach aims to reduce the number of CFD simulations while simultaneously enabling the iterative assessment of a wider range of design alternatives. The objective of this study was to enhance patient safety by reducing the probability of infection transmission among patients. Thus, through the utilization of the GA-CFD approach, a design exploration was conducted to determine the optimal parameters for minimizing the spread of infection within a ward. The location of an infected patient; the air change rate; the flow rate through a local exhaust grille; the number, location, and size of supply diffusers and local exhaust grilles; and the flow rate through a local exhaust grille that would minimize the likelihood of an infection spreading from one patient to another within a ward was identified. This thesis proposes a ventilation system design that is both simple and cost-effective, with the aim of mitigating the risk of infection in hospital wards.

Perspective on future research direction:

This thesis gave insight into the domains of conventional energy simulation, computational fluid dynamics, artificial intelligence (AI) - particularly Artificial Neural Networks (ANNs) - and evolutionary algorithms, specifically Genetic Algorithm (GA). The study focused on the integration of these domains to develop targeted applications for energy consumption and infection mitigation. In this section, perspectives on potential directions for future research are discussed together with strategies for enhancing current work.

The generalized hybrid simulation model integrated with an optimization algorithm proved to be a powerful prediction tool for estimating the cooling energy consumption of buildings. The method proved significant in terms of simulation time, accuracy and flexibility compared to the conventional energy estimation methods. Nonetheless, there exists a potential for enhancement. The effect of interactions between buildings, such as shadowing from an adjacent building, on the cooling load has yet to be explored, but the maximum solar heat gain scenario has been examined in this work. In densely populated cooling-dominant places such as Hong Kong, it has been shown that shading reduces cooling energy demand further, which would be an extra benefit in terms of energy savings rather than a negative effect. Nevertheless, incorporating this component could increase the efficacy of the suggested model when applied to structures in various climatic zones. Future research about the development of the proposed technique of this study to include different scales of buildings in varied climatic conditions would increase the possibility of this approach to construct carbon-neutral structures. In addition, the incorporation of this research with a life cycle cost analysis would yield a comprehensive depiction of the ecological ramifications and cost benefits associated with low-energy facility design.

The utilization of CFD and an evolutionary algorithm in this thesis to evaluate the different ventilation strategies to mitigate infection transmission in an inpatient ward cubicle was more effective than the traditional approach. The effectiveness of optimal ventilation solution determined through GA-CFD application to mitigate airborne transmission needs to be addressed. Moreover, in this study, 100% outside air was assumed in every simulation. Therefore, it is necessary to consider the effectiveness of the suggested ventilation strategies while also taking air recirculation into account. Lastly, the impact of the movement of staff, patients and visitors should have been addressed. Nevertheless, this factor can cause disturbances in airflow and particle distribution. Few studies, however, indicate that its effect is temporary and considerably less significant than ventilation.

References

ABANDA, F. & BYERS, L. 2016. An investigation of the impact of building orientation on energy consumption in a domestic building using emerging BIM (Building Information Modelling). *Energy,* 97**,** 517-527.

AHMAD, A. S., HASSAN, M. Y., ABDULLAH, M. P., RAHMAN, H. A., HUSSIN, F., ABDULLAH, H. & SAIDUR, R. 2014. A review on applications of ANN and SVM for building electrical energy consumption forecasting. *Renewable and Sustainable Energy Reviews,* 33**,** 102-109.

AHMAD, M. W., MOURSHED, M. & REZGUI, Y. 2017. Trees vs Neurons: Comparison between random forest and ANN for high-resolution prediction of building energy consumption. *Energy and buildings,* 147**,** 77-89.

AHMAD, T., CHEN, H., GUO, Y. & WANG, J. 2018. A comprehensive overview on the data driven and large scale based approaches for forecasting of building energy demand: A review. *Energy and Buildings,* 165**,** 301-320.

AL-HOMOUD, M. S. 2001. Computer-aided building energy analysis techniques. *Building and Environment,* 36**,** 421-433.

AL-HOMOUD, M. S. 2005. A systematic approach for the thermal design optimization of building envelopes. *Journal of building physics,* 29**,** 95-119.

AL-HOMOUD, M. S. 1997. Optimum thermal design of office buildings. *International Journal of Energy Research,* 21**,** 941-957.

ALAIDROOS, A. & KRARTI, M. 2015. Optimal design of residential building envelope systems in the Kingdom of Saudi Arabia. *Energy and Buildings,* 86**,** 104-117.

ALBADRY, S., TARABIEH, K. & SEWILAM, H. 2017. Achieving net zero-energy buildings through retrofitting existing residential buildings using PV panels. *Energy Procedia,* 115**,** 195-204.

ALDAWOUD, A. 2013. Conventional fixed shading devices in comparison to an electrochromic glazing system in hot, dry climate. *Energy and Buildings,* 59**,** 104-110.

ALEMU, A. Y., ENDALAMAW, A. & BAYIH, W. A. 2020. The burden of healthcare-associated infection in Ethiopia: a systematic review and meta-analysis. *Tropical medicine and health,* 48**,** 1-11.

ALLERY, C., BÉGHEIN, C. & HAMDOUNI, A. 2005. Applying proper orthogonal decomposition to the computation of particle dispersion in a two-dimensional ventilated cavity. *Communications in Nonlinear Science and Numerical Simulation,* 10**,** 907-920.

ÁLVAREZ, S., CABEZA, L. F., RUIZ-PARDO, A., CASTELL, A. & TENORIO, J. A. 2013. Building integration of PCM for natural cooling of buildings. *Applied Energy,* 109**,** 514-522.

AMASYALI, K. & EL-GOHARY, N. 2022. Hybrid approach for energy consumption prediction: Coupling data-driven and physical approaches. *Energy and Buildings,* 259**,** 111758.

AMASYALI, K. & EL-GOHARY, N. M. 2018. A review of data-driven building energy consumption prediction studies. *Renewable and Sustainable Energy Reviews,* 81**,** 1192-1205.

AMIRI, S. S., MOTTAHEDI, M. & ASADI, S. 2015. Using multiple regression analysis to develop energy consumption indicators for commercial buildings in the US. *Energy and Buildings,* 109**,** 209-216.

ANDER, G. D. 2014. Windows and Glazing. *Whole Building Design Guide.*

ANNA SIKORA & FARAH ZAHRA. 2022. *Nosocomial Infections* [Online]. StatPearls. Available: https://www.ncbi.nlm.nih.gov/books/NBK559312/ [Accessed].

ANSI/ASHRAE STANDARD 169 2013. Climatic data for building design standards. ANSI/ASHRAE.

ANSI/ASHRAE/IES STANDARD 90.1 2020. Energy Standard for Buildings Except Low-Rise Residential Buildings. Atlanta, GA: American Society of Heating, Refrigerating and Air–Conditioning Engineers.

ANSYS 2010. Ansys Fluent 13.0 Documentation. Lebanon, NH, USA: Ansys Inc.

APTE, J. & ARASTEH, D. 2006. Window-Related Energy Consumption in the US Residential andCommercial Building Stock. Lawrence Berkeley National Lab.(LBNL), Berkeley, CA (United States).

ARJMANDI, H., AMINI, R. & FALLAHPOUR, M. 2022. Minimizing the respiratory pathogen transmission: Numerical study and multi-objective optimization of ventilation systems in a classroom. *Thermal Science and Engineering Progress,* 28**,** 101052.

ASADI, S., AMIRI, S. S. & MOTTAHEDI, M. 2014. On the development of multi-linear regression analysis to assess energy consumption in the early stages of building design. *Energy and Buildings*, 85**,** 246-255.

ASCIONE, F., BIANCO, N., DE MASI, R. F. & VANOLI, G. P. 2013. Rehabilitation of the building envelope of hospitals: Achievable energy savings and microclimatic control on varying the HVAC systems in Mediterranean climates. *Energy and Buildings,* 60**,** 125-138.

ASHRAE 2013a. Ventilation for Health Care Facilities. Atlanta, GA, USA: American Society of Heating, Refrigerating and Air-Conditioning Engineers.

ASHRAE 2013b. ASHRAE Fundamentals SI Handbook. Atlanta, GA, USA: American Society of Heating, Refrigerating and Air-Conditioning Engineers.

ASHRAE STANDARD 55 2020. Thermal Environmental Condition for Human Occupancy. Atlanta, GA: American Society of Heating, Refrigerating and Air–Conditioning Engineers.

ASHRAE STANDARD 90-75 1975. Energy Conservation in New Building Design. Atlanta, GA: American Society of Heating, Refrigeration and Air Conditioning Engineers.

ASHRAE STANDARD 90.1 2010. Energy Standard for Buildings Except Low-Rise Residential Buildings. Atlanta, GA, USA: American Society of Heating, Refrigerating and Air–Conditioning Engineers.

ASHRAE STANDARD 90.1 2013. Energy Standard for Building Except Low–Rise Residential Buildings. Atlanta, GA, USA: American Society of Heating, Refrigerating and Air–Conditioning Engineers.

ATKINSON, J., Y. CHARTIER, C.L. PESSOA-SILVA, P. JENSEN, Y. LI, AND W.-H. SETO 2009. Natural ventilation for infection control in health-care settings. WHO.

ATKINSON, M. P. & WEIN, L. M. 2008. Quantifying the routes of transmission for pandemic influenza. *Bulletin of mathematical biology*, 70**,** 820-867.

AXLEY, J. 2007. Multizone airflow modeling in buildings: History and theory. *HVAC&R Research,* 13**,** 907-928.

AYATA, T., ARCAKLıOĞLU, E. & YıLDıZ, O. 2007. Application of ANN to explore the potential use of natural ventilation in buildings in Turkey. *Applied Thermal Engineering,* 27**,** 12-20.

AYDINALP-KOKSAL, M. & UGURSAL, V. I. 2008. Comparison of neural network, conditional demand analysis, and engineering approaches for modeling end-use energy consumption in the residential sector. *Applied energy,* 85**,** 271-296.

AYDINALP, M., UGURSAL, V. I. & FUNG, A. S. 2002. Modeling of the appliance, lighting, and space-cooling energy consumptions in the residential sector using neural networks. *Applied energy,* 71**,** 87-110.

BAMBROOK, S., SPROUL, A. B. & JACOB, D. 2011. Design optimisation for a low energy home in Sydney. *Energy and Buildings,* 43**,** 1702-1711.

BANSAL, N. K., HAUSER, G. & MINKE, G. 1994. *Passive building design: a handbook of natural climatic control*, Elsevier science BV Amsterdam, The Netherlands.

BEGGS, C. B., KERR, K. G., NOAKES, C. J., HATHWAY, E. A. & SLEIGH, P. A. 2008. The ventilation of multiple-bed hospital wards: review and analysis. *American journal of infection control,* 36**,** 250-259.

BICHIOU, Y. & KRARTI, M. 2011. Optimization of envelope and HVAC systems selection for residential buildings. *Energy and Buildings,* 43**,** 3373-3382.

BISWAS, M. R., ROBINSON, M. D. & FUMO, N. 2016. Prediction of residential building energy consumption: A neural network approach. *Energy,* 117**,** 84-92.

BLOCKEN, B. 2018. LES over RANS in building simulation for outdoor and indoor applications: A foregone conclusion? *Building Simulation,* 11**,** 821-870.

BOJIĆ, M. & YIK, F. 2007. Application of advanced glazing to high-rise residential buildings in Hong Kong. *Building and Environment,* 42**,** 820-828.

BOJIC, M., YIK, F., WAN, K. & BURNETT, J. 2002. Influence of envelope and partition characteristics on the space cooling of high-rise residential buildings in Hong Kong. *Building and Environment,* 37**,** 347-355.

BOLASHIKOV, Z. D., MELIKOV, A. K., KIERAT, W., POPIOŁEK, Z. & BRAND, M. 2012. Exposure of health care workers and occupants to coughed airborne pathogens in a double-bed hospital patient room with overhead mixing ventilation. *Hvac&R Research,* 18**,** 602-615.

BOODI, A., BEDDIAR, K., AMIRAT, Y. & BENBOUZID, M. 2022. Building Thermal-Network Models: A Comparative Analysis, Recommendations, and Perspectives. *Energies,* 15**,** 1328.

BOSER, B. E., GUYON, I. M. & VAPNIK, V. N. A training algorithm for optimal margin classifiers. Proceedings of the fifth annual workshop on Computational learning theory, 1992. 144-152.

BOUCHLAGHEM, N. & LETHERMAN, K. 1990. Numerical optimization applied to the thermal design of buildings. *Building and environment,* 25**,** 117-124.

BOUROUIBA, L., DEHANDSCHOEWERCKER, E., & BUSH, J. W. 2014. Violent expiratory events: on coughing and sneezing. *Journal of Fluid Mechanics*, 745, 537-563.

BOUROUIBA, L. 2020. Turbulent gas clouds and respiratory pathogen emissions: Potential implications for reducing transmission of COVID-19. *Jama*, 323(18), 1837-1838.

BRACKNEY, L., PARKER, A., MACUMBER, D. & BENNE, K. 2018. *Building energy modeling with OpenStudio*, Springer.

BRØGGER, M., BACHER, P. & WITTCHEN, K. B. 2019. A hybrid modelling method for improving estimates of the average energy-saving potential of a building stock. *Energy and Buildings,* 199**,** 287-296.

BRUN, A., WURTZ, E., HOLLMULLER, P. & QUENARD, D. 2013. Summer comfort in a low-inertia building with a new free-cooling system. *Applied energy,* 112**,** 338-349.

BUONOMANO, A., CALISE, F., FERRUZZI, G. & PALOMBO, A. 2014. Dynamic energy performance analysis: Case study for energy efficiency retrofits of hospital buildings. *Energy*, 78**,** 555-572.

BÜYÜKALACA, O., BULUT, H. & YıLMAZ, T. 2001. Analysis of variable-base heating and cooling degree-days for Turkey. *Applied Energy,* 69**,** 269-283.

CAO, G., AWBI, H., YAO, R., FAN, Y., SIRÉN, K., KOSONEN, R. & ZHANG, J. J. 2014. A review of the performance of different ventilation and airflow distribution systems in buildings. *Building and environment,* 73**,** 171-186.

CDC. *Lesson 1: Introduction to epidemiology-section 8* [Online]. Centers for Disease Control and Prevention. Available: https://www.cdc.gov/csels/dsepd/ss1978/lesson1/section8.html#:~:text=The%20triad%20consists%20of%20an,a%20source%20to%20that%20host. [Accessed].

CDC 2007. Guideline for isolation precautions: preventing transmission of infectious agents in healthcare settings. Centers for Disease Control and Prevention.

CENSTATD 2020. Hong Kong Population Projections 2020–2069. Census and Statistics Department Hong Kong: Hong Kong, China.

CHADDOCK, J. B. 1983. Ventilation and exhaust requirements for hospitals. ASHRAE Research Project. Final Report.

CHAE, Y. T., HORESH, R., HWANG, Y. & LEE, Y. M. 2016. Artificial neural network model for forecasting sub-hourly electricity usage in commercial buildings. *Energy and Buildings,* 111**,** 184-194.

CHAN, K. & CHOW, W. K. 1998. Energy impact of commercial-building envelopes in the sub-tropical climate. *Applied Energy,* 60**,** 21-39.

CHEN, C., ZHAO, B., YANG, X. & LI, Y. 2011. Role of two-way airflow owing to temperature difference in severe acute respiratory syndrome transmission: revisiting the largest nosocomial severe acute respiratory syndrome outbreak in Hong Kong. *Journal of the Royal Society Interface,* 8**,** 699-710.

CHEN, Q. 2009. Ventilation performance prediction for buildings: A method overview and recent applications. *Building and environment,* 44**,** 848-858.

CHEN, Q., ZHAI, Z., YOU, X. & ZHANG, T. 2017. *Inverse design methods for the built environment*, Routledge.

CHEUNG, C. K., FULLER, R. J. & LUTHER, M. B. 2005. Energy-efficient envelope design for high-rise apartments. *Energy and buildings,* 37**,** 37-48.

CHO, Y., AWBI, H. B. & KARIMIPANAH, T. 2008. Theoretical and experimental investigation of wall confluent jets ventilation and comparison with wall displacement ventilation. *Building and Environment,* 43**,** 1091-1100.

CHOU, J.-S. & BUI, D.-K. 2014. Modeling heating and cooling loads by artificial intelligence for energy-efficient building design. *Energy and Buildings,* 82**,** 437-446.

CHUA, K. & CHOU, S. 2010. Energy performance of residential buildings in Singapore. *Energy,* 35**,** 667-678.

CHUNG, W., HUI, Y. & LAM, Y. M. 2006. Benchmarking the energy efficiency of commercial buildings. *Applied energy,* 83**,** 1-14.

CIULLA, G. & D'AMICO, A. 2019. Building energy performance forecasting: A multiple linear regression approach. *Applied Energy,* 253**,** 113500.

CLARKE, J. A. 2007. *Energy simulation in building design*, Routledge.

COLEY, D. A. & SCHUKAT, S. 2002. Low-energy design: combining computer-based optimisation and human judgement. *Building and Environment,* 37**,** 1241-1247.

CORNICK, S. & KUMARAN, M. 2008. A comparison of empirical indoor relative humidity models with measured data. *Journal of Building Physics,* 31**,** 243-268.

CRAWLEY, D. B., HAND, J. W., KUMMERT, M. & GRIFFITH, B. T. 2008. Contrasting the capabilities of building energy performance simulation programs. *Building and environment,* 43**,** 661-673.

CRAWLEY, D. B., LAWRIE, L. K., WINKELMANN, F. C., BUHL, W. F., HUANG, Y. J., PEDERSEN, C. O., STRAND, R. K., LIESEN, R. J., FISHER, D. E. & WITTE, M. J. 2001. EnergyPlus: creating a new-generation building energy simulation program. *Energy and buildings,* 33**,** 319-331.

CRISTIANINI, N. & SHAWE-TAYLOR, J. 2000. *An introduction to support vector machines and other kernel-based learning methods*, Cambridge university press.

DE ROSA, M., BIANCO, V., SCARPA, F. & TAGLIAFICO, L. A. 2014. Heating and cooling building energy demand evaluation; a simplified model and a modified degree days approach. *Applied energy,* 128**,** 217-229.

DELGARM, N., SAJADI, B., KOWSARY, F. & DELGARM, S. 2016. Multi-objective optimization of the building energy performance: A simulation-based approach by means of particle swarm optimization (PSO). *Applied energy,* 170**,** 293-303.

DEMUTH, H. B., BEALE, M.H. 2010. Matlab Neural Network Toolbox: User's Guide. Portola Valley, CA, USA: Mathworks.

DOAN, C. D. & LIONG, S.-Y. Generalization for multilayer neural network bayesian regularization or early stopping. Proceedings of Asia Pacific association of hydrology and water resources 2nd conference, 2004. 5-8.

DOE. 2021a. *Building energy software tools directory* [Online]. Department of Energy. Available: https://www.buildingenergysoftwaretools.com/ [Accessed].

DOE. 2021b. *Energy efficiency and Renewable Energy Office, Building Technology Program* [Online]. United States: Department of Energy. Available: https://energyplus.net/downloads [Accessed].

DONG, B., CAO, C. & LEE, S. E. 2005. Applying support vector machines to predict building energy consumption in tropical region. *Energy and Buildings,* 37**,** 545-553.

EB 2017. Hong Kong's Climate Action Plan 2030+. Hong Kong, China: Environment Bureau of the HKSAR Government and Steering Committee on Climate.

EKONOMOU, L. 2010. Greek long-term energy consumption prediction using artificial neural networks. *Energy,* 35**,** 512-517.

ELHADIDI, B. & KHALIFA, H. E. 2005. Application of Proper Orthogonal Decomposition to Indoor Airflows. *Ashrae Transactions,* 111.

EMSD 2020. Hong Kong Energy End-use Data 2020. Hong Kong, China: Hong Kong Special Administrative Region.

EMSD 2021. Code of practice for energy efficiency of building services installation. Hong Kong, China: Electrical and Mechanical Services Department.

ENGLISH, T. R. 2016. A Brief History Of Health-Care Ventilation. *ASHRAE Journal,* 58**,** 52-60.

EVENS, A., GARASCIA, M. & ISAACSON, M. 2017. Utilities and health: Energy efficiency as a common link. *The Electricity Journal,* 30**,** 10-14.

EVINS, R. 2013. A review of computational optimisation methods applied to sustainable building design. *Renewable and sustainable energy reviews,* 22**,** 230-245.

FARZANA, S., LIU, M., BALDWIN, A. & HOSSAIN, M. U. 2014. Multi-model prediction and simulation of residential building energy in urban areas of Chongqing, South West China. *Energy and Buildings,* 81**,** 161-169.

FENG, Y. 2004. Thermal design standards for energy efficiency of residential buildings in hot summer/cold winter zones. *Energy and buildings,* 36**,** 1309-1312.

FERRARA, M., FILIPPI, M., SIROMBO, E. & CRAVINO, V. A simulation-based optimization method for the integrative design of the building envelope. Energy Procedia, 2015. 2608-2613.

FESANGHARY, M., ASADI, S. & GEEM, Z. W. 2012. Design of low-emission and energy-efficient residential buildings using a multi-objective optimization algorithm. *Building and environment,* 49**,** 245-250.

FITZGERALD, S. D. & WOODS, A. W. 2008. The influence of stacks on flow patterns and stratification associated with natural ventilation. *Building and Environment,* 43**,** 1719-1733.

FLEMING, K., LONG, N. & SWINDLER, A. 2012. Building Component Library: an online repository to facilitate building energy model creation. National Renewable Energy Lab.(NREL), Golden, CO (United States).

FONTES, D., REYES, J., AHMED, K., & KINZEL, M. 2020. A study of fluid dynamics and human physiology factors driving droplet dispersion from a human sneeze. *Physics of Fluids*, *32*(11), 111904.

FORESEE, F. D. & HAGAN, M. T. Gauss-Newton approximation to Bayesian learning. Proceedings of international conference on neural networks (ICNN'97), 1997. IEEE, 1930-1935.

FOUCQUIER, A., ROBERT, S., SUARD, F., STÉPHAN, L. & JAY, A. 2013. State of the art in building modelling and energy performances prediction: A review. *Renewable and Sustainable Energy Reviews,* 23**,** 272-288.

FUKS, N. A. 1989. *The mechanics of aerosols,* Dover Publications.

FUMO, N. 2014. A review on the basics of building energy estimation. *Renewable and sustainable energy reviews,* 31**,** 53-60.

FUMO, N., MAGO, P. J. & CHAMRA, L. M. 2009. Energy and economic evaluation of cooling, heating, and power systems based on primary energy. *Applied Thermal Engineering,* 29**,** 2665-2671.

GAGNE, J. & ANDERSEN, M. 2012. A generative facade design method based on daylighting performance goals. *Journal of Building Performance Simulation,* 5**,** 141-154.

GALTON, F. 1886. Regression towards mediocrity in hereditary stature. *The Journal of the Anthropological Institute of Great Britain and Ireland,* 15**,** 246-263.

GAO, N. & NIU, J. 2005. CFD study of the thermal environment around a human body: a review. *Indoor and built environment,* 14**,** 5-16.

GASSAR, A. A. A. & CHA, S. H. 2020. Energy prediction techniques for large-scale buildings towards a sustainable built environment: A review. *Energy and Buildings,* 224**,** 110238.

GHISI, E. & TINKER, J. A. 2005. An ideal window area concept for energy efficient integration of daylight and artificial light in buildings. *Building and environment,* 40**,** 51-61.

GU, J., WANG, J., QI, C., MIN, C. & SUNDÉN, B. 2018. Medium-term heat load prediction for an existing residential building based on a wireless on-off control system. *Energy,* 152**,** 709-718.

GUYOT, D., GIRAUD, F., SIMON, F., CORGIER, D., MARVILLET, C. & TREMEAC, B. 2019. Overview of the use of artificial neural networks for energy-related applications in the building sector. *International Journal of Energy Research*, 43**,** 6680-6720.

HAGAN, M. T. & MENHAJ, M. B. 1994. Training feedforward networks with the Marquardt algorithm. *IEEE transactions on Neural Networks,* 5**,** 989-993.

HALE, E., MACUMBER, D., WEAVER, E. & SHEKHAR, D. 2012. Flexible Framework for Building Energy Analysis. National Renewable Energy Lab.(NREL), Golden, CO (United States).

HANG, J., LI, Y., & JIN, R. 2014. The influence of human walking on the flow and airborne transmission in a six-bed isolation room: Tracer gas simulation. *Building and Environment*, 77, 119-134.

HATHWAY, E., NOAKES, C., SLEIGH, P. & FLETCHER, L. 2011. CFD simulation of airborne pathogen transport due to human activities. *Building and Environment,* 46**,** 2500-2511.

HAYDEN, C. S., EARNEST, G. S. & JENSEN, P. A. 2007. Development of an empirical model to aid in designing airborne infection isolation rooms. *Journal of occupational and environmental hygiene,* 4**,** 198-207.

HIRST, J. S., WONG, E., SPENCE, ROBINSON, EASTON, ROBERTSON, CUSDIN, PRESTON, SMITH, & FOOK LEE AND COMPANY. 1964. The Queen Elizabeth Hospital, Hong Kong. *Official Architecture and Planning*, 27(5), 537–542.

HOES, P., HENSEN, J. L., LOOMANS, M. G., DE VRIES, B. & BOURGEOIS, D. 2009. User behavior in whole building simulation. *Energy and buildings,* 41**,** 295-302.

HOLLAND, J. H. 1975. *Adaptation in natural and artificial systems: An introductory analysis with applications to biology, control, and artificial intelligence,* Ann Arbor, University of Michigan Press.

HOLST, J. N. Using whole building simulation models and optimizing procedures to optimize building envelope design with respect to energy consumption and indoor environment. Eigth International Conference, 2003.

HONG KONG HOUSING AUTHORITY 2013. Housing in Figures 2009–2013. Hong Kong, China: The Government of Hong Kong Special Administrative Region.

HONG KONG HOUSING AUTHORITY 2021. Standard Block Typical Floor Plans. Hong Kong, China: The Government of Hong Kong Special Administrative Region.

HOU, Z. & LIAN, Z. An application of support vector machines in cooling load prediction. 2009 International Workshop on Intelligent Systems and Applications, 2009. IEEE, 1-4.

HU, B., FREIHAUT, J., BAHNFLETH, W., AUMPANSUB, P. & THRAN, B. 2007. Modeling particle dispersion under human activity disturbance in a multizone indoor environment. *Journal of architectural engineering,* 13**,** 187-193.

HUANG, Y., NIU, J.-L. & CHUNG, T.-M. 2014. Comprehensive analysis on thermal and daylighting performance of glazing and shading designs on office building envelope in cooling-dominant climates. *Applied energy,* 134**,** 215-228.

HUI, S. C. Overall thermal transfer value (OTTV): how to improve its control in Hong Kong. Proc. of the One-day Symposium on Building, Energy and Environment, 1997. 12-1.

HUMMELGAARD, J., JUHL, P., SÆBJÖRNSSON, K., CLAUSEN, G., TOFTUM, J. & LANGKILDE, G. 2007. Indoor air quality and occupant satisfaction in five mechanically and four naturally ventilated open-plan office buildings. *Building and Environment,* 42**,** 4051-4058.

HYGH, J. S., DECAROLIS, J. F., HILL, D. B. & RANJITHAN, S. R. 2012. Multivariate regression as an energy assessment tool in early building design. *Building and environment,* 57**,** 165-175.

IEA. 2022a. *Building Envelopes* [Online]. Paris, France: International Energy Agency. Available: https://www.iea.org/reports/building-envelopes [Accessed].

IEA. 2022b. *Space Cooling* [Online]. Paris, France: International Energy Agency. Available: https://www.iea.org/reports/space-cooling [Accessed].

IEA. 2023. *Electricity Market Report 2023* [Online]. Paris, France: International Energy Agency. Available: https://www.iea.org/reports/electricity-market-report-2023 [Accessed].

ISAAC, M. & VAN VUUREN, D. P. 2009. Modeling global residential sector energy demand for heating and air conditioning in the context of climate change. *Energy policy,* 37**,** 507-521.

ISO-10077-1 2009. Thermal performance of windows, doors, and shutters: Calculation of thermal transmittance, Part 1. Cor. 1.: International Organization for Standardization.

JIANG, S., HUANG, L., CHEN, X., WANG, J., WU, W., YIN, S., CHEN, W., ZHAN, J., YAN, L. & MA, L. 2003. Ventilation of wards and nosocomial outbreak of severe acute respiratory syndrome among healthcare workers. *Chinese Medical Journal,* 116**,** 1293-1297.

KAO, P. & YANG, R.-J. 2006. Virus diffusion in isolation rooms. *Journal of Hospital infection,* 62**,** 338-345.

KARTHIKEYAN, C. & SAMUEL, A. A. 2008. CO2-dispersion studies in an operation theatre under transient conditions. *Energy and Buildings,* 40**,** 231-239.

KATO, S. & LEE, J. H. Optimization of hybrid air-conditioning system with natural ventilation by GA and CFD. 25th AIVC conference, ventilation and retrofitting, 2004.

KAYRI, M. 2016. Predictive abilities of bayesian regularization and Levenberg–Marquardt algorithms in artificial neural networks: a comparative empirical study on social data. *Mathematical and Computational Applications,* 21**,** 20.

KEMPTON, W., FEUERMANN, D. & MCGARITY, A. E. 1992. "I always turn it on super": user decisions about when and how to operate room air conditioners. *Energy and Buildings,* 18**,** 177-191.

KESHTKARBANAEEMOGHADAM, A., DEHGHANBANADAKI, A. & KABOLI, M. H. 2018. Estimation and optimization of heating energy demand of a mountain shelter by soft computing techniques. *Sustainable cities and society,* 41**,** 728-748.

KHAN, H. A., BAIG, F. K. & MEHBOOB, R. 2017. Nosocomial infections: Epidemiology, prevention, control and surveillance. *Asian Pacific Journal of Tropical Biomedicine,* 7**,** 478-482.

KHOUKHI, M., YOSHINO, H. & LIU, J. 2007. The effect of the wind speed velocity on the stack pressure in medium-rise buildings in cold region of China. *Building and Environment,* 42**,** 1081-1088.

KIM, D. D. & SUH, H. S. 2021. Heating and cooling energy consumption prediction model for high-rise apartment buildings considering design parameters. *Energy for Sustainable Development,* 61**,** 1-14.

KIM, S.-H., CHANG, S. Y., SUNG, M., PARK, J. H., BIN KIM, H., LEE, H., CHOI, J.-P., CHOI, W. S. & MIN, J.-Y. 2016. Extensive viable Middle East respiratory syndrome (MERS) coronavirus contamination in air and surrounding environment in MERS isolation wards. *Reviews of Infectious Diseases,* 63**,** 363-369.

KING, M.-F., NOAKES, C., SLEIGH, P. & CAMARGO-VALERO, M. 2013. Bioaerosol deposition in single and two-bed hospital rooms: A numerical and experimental study. *Building and environment,* 59**,** 436-447.

KING, M. F., NOAKES, C. J. & SLEIGH, P. A. 2015. Modeling environmental contamination in hospital single-and four-bed rooms. *Indoor Air,* 25**,** 694-707.

KISHORE, R. A., BIANCHI, M. V., BOOTEN, C., VIDAL, J. & JACKSON, R. 2020. Modulating thermal load through lightweight residential building walls using thermal energy storage and controlled precooling strategy. *Applied Thermal Engineering,* 180**,** 115870.

KOSAR, D. 2006. Dehumidification system enhancements. *ASHRAE journal,* 48**,** 48.

KRAMER, A., SCHWEBKE, I. & KAMPF, G. 2006. How long do nosocomial pathogens persist on inanimate surfaces? A systematic review. *BMC infectious diseases,* 6**,** 1-8.

KUMAR, R., AGGARWAL, R. & SHARMA, J. 2013. Energy analysis of a building using artificial neural network: A review. *Energy and Buildings,* 65**,** 352-358.

KWOK, S. S., YUEN, R. K. & LEE, E. W. 2011. An intelligent approach to assessing the effect of building occupancy on building cooling load prediction. *Building and Environment,* 46**,** 1681-1690.

LAFRANCE, G. & PERRON, D. 1994. Evolution of residential electricity demand by end-use in Quebec 1979-1989: a conditional demand analysis. *Energy Studies Review,* 6.

LAI, A., WONG, L. T., MUI, K. W., CHAN, W. & YU, H. 2012. An experimental study of bioaerosol (1–10 μm) deposition in a ventilated chamber. *Building and environment,* 56**,** 118-126.

LAI, A. C. & CHEN, F. 2006. Modeling particle deposition and distribution in a chamber with a two-equation Reynolds-averaged Navier–Stokes model. *Journal of aerosol science,* 37**,** 1770-1780.

LAM, J. C. 2000. Residential sector air conditioning loads and electricity use in Hong Kong. *Energy Conversion and Management,* 41**,** 1757-1768.

LAM, J. C. & LI, D. H. 2000. Household energy use and comfort cooling in Hong Kong. *International Journal for Housing Science and Its Applications,* 24**,** 195-203.

LAM, J. C., TSANG, C., LI, D. H. & CHEUNG, S. 2005. Residential building envelope heat gain and cooling energy requirements. *Energy,* 30**,** 933-951.

LAM, J. C., WAN, K. K., WONG, S. & LAM, T. N. 2010. Principal component analysis and long-term building energy simulation correlation. *Energy Conversion and Management,* 51**,** 135-139.

LARSEN, T. S. & HEISELBERG, P. 2008. Single-sided natural ventilation driven by wind pressure and temperature difference. *Energy and buildings,* 40**,** 1031-1040.

LASTINGER, L. M., ALVAREZ, C. R., KOFMAN, A., KONNOR, R. Y., KUHAR, D. T., NKWATA, A., PATEL, P. R., PATTABIRAMAN, V., XU, S. Y. & DUDECK, M. A. 2022. Continued Increases in HAI Incidence During the Second Year of the COVID-19 Pandemic. *Infection Control & Hospital Epidemiology***,** 1-19.

LCS 2016. Housing ISSH09/16-17. Hong Kong, China: Legislative Council Secretariat.

LCS 2018. Subdivided units in Hong Kong. ISSH32/17-18. Hong Kong, China: Legislative Council Secretariat.

LEI, H., LI, Y., XIAO, S., YANG, X., LIN, C., NORRIS, S. L., WEI, D., HU, Z. & JI, S. 2017. Logistic growth of a surface contamination network and its role in disease spread. *Scientific reports,* 7**,** 1-10.

LESKOVAR, V. Ž. & PREMROV, M. 2011. An approach in architectural design of energy-efficient timber buildings with a focus on the optimal glazing size in the south-oriented façade. *Energy and Buildings,* 43**,** 3410-3418.

LI, A., XIAO, F., FAN, C. & HU, M. 2021. Development of an ANN-based building energy model for information-poor buildings using transfer learning. *Building Simulation,* 14**,** 89-101.

LI, Q., MENG, Q., CAI, J., YOSHINO, H. & MOCHIDA, A. 2009. Applying support vector machine to predict hourly cooling load in the building. *Applied Energy,* 86**,** 2249-2256.

LI, X. & WEN, J. 2014. Review of building energy modeling for control and operation. *Renewable and Sustainable Energy Reviews,* 37**,** 517-537.

LI, Y. 2021. Basic routes of transmission of respiratory pathogens—a new proposal for transmission categorization based on respiratory spray, inhalation, and touch. *Indoor Air,* 31**,** 3.

LI, Y., HUANG, X., YU, I., WONG, T. & QIAN, H. 2005. Role of air distribution in SARS transmission during the largest nosocomial outbreak in Hong Kong. *Indoor air,* 15**,** 83-95.

LI, Y., LEUNG, G. M., TANG, J., YANG, X., CHAO, C., LIN, J. Z., LU, J., NIELSEN, P. V., NIU, J. & QIAN, H. 2007a. Role of ventilation in airborne transmission of infectious agents in the built environment-a multidisciplinary systematic review. *Indoor air,* 17**,** 2-18.

LI, Z., HAN, Y. & XU, P. 2014. Methods for benchmarking building energy consumption against its past or intended performance: An overview. *Applied Energy,* 124**,** 325-334.

LI, Z., JIANG, Y. & WEI, Q. 2007b. Survey on energy consumption of air conditioning in summer in a residential building in Beijing. *J. Heat. Vent. Air Cond,* 37**,** 46-51.

LIN, Z. & DENG, S. 2003. The outdoor air ventilation rate in high-rise residences employing room air conditioners. *Building and Environment,* 38**,** 1389-1399.

LIONS, J. L. 1971. optimal control of systems governed by partial differential equations problemes aux limites. *Springer*.

LIU, S. & NOVOSELAC, A. 2014. Lagrangian particle modeling in the indoor environment: A comparison of RANS and LES turbulence methods (RP-1512). *HVAC&R Research,* 20**,** 480-495.

LIU, W. & CHEN, Q. 2015. Optimal air distribution design in enclosed spaces using an adjoint method. *Inverse Problems in Science and Engineering,* 23**,** 760-779.

LIU, W., JIN, M., CHEN, C. & CHEN, Q. 2016. Optimization of air supply location, size, and parameters in enclosed environments using a computational fluid dynamics-based adjoint method. *Journal of Building Performance Simulation,* 9**,** 149-161.

LIU, W., ZHANG, T., XUE, Y., ZHAI, Z. J., WANG, J., WEI, Y. & CHEN, Q. 2015. State-of-the-art methods for inverse design of an enclosed environment. *Building and Environment,* 91**,** 91-100.

LIU, Z., WU, D., LIU, Y., HAN, Z., LUN, L., GAO, J., JIN, G. & CAO, G. 2019. Accuracy analyses and model comparison of machine learning adopted in building energy consumption prediction. *Energy Exploration & Exploitation,* 37**,** 1426-1451.

LONG, N., BALL, B., GOLDWASSER, D., PARKER, A., ELLING, J., DAVIS, O. & KRUCHTEN, D. 2013. Leveraging OpenStudio's application programming interfaces. National Renewable Energy Lab.(NREL), Golden, CO (United States).

LOOMANS, M. & LEMAIRE, T. Particle concentration calculations using CFD. Proceedings Roomvent, 2002. 393-396.

LOOMANS, M., VAN HOUDT, W., LEMAIRE, A. & HENSEN, J. 2008. Performance assessment of an operating theatre design using CFD simulation and tracer gas measurements. *Indoor and Built Environment,* 17**,** 299-312.

LU, C., LI, S. & LU, Z. 2021. Building energy prediction using artificial neural networks: A literature survey. *Energy and Buildings***,** 111718.

LUMLEY, J. L. 1967. The structure of inhomogeneous turbulent flows. *Atmospheric turbulence and radio wave propagation***,** 166-178.

LUO, X., OYEDELE, L. O., AJAYI, A. O., AKINADE, O. O., OWOLABI, H. A. & AHMED, A. 2020. Feature extraction and genetic algorithm enhanced adaptive deep neural network for energy consumption prediction in buildings. *Renewable and Sustainable Energy Reviews,* 131**,** 109980.

MAATOUK, K. 2007. A simplified procedure to investigate airflow patterns inside tall buildings using COMIS. *Architectural Science Review,* 50**,** 365-369.

MAGILL, S. S., O'LEARY, E., JANELLE, S. J., THOMPSON, D. L., DUMYATI, G., NADLE, J., WILSON, L. E., KAINER, M. A., LYNFIELD, R. & GREISSMAN, S. 2018. Changes in prevalence of health care–associated infections in US hospitals. *New England Journal of Medicine,* 379**,** 1732-1744.

MAHAPATRA, S. & SOOD, A. K. 2012. Bayesian regularization-based Levenberg–Marquardt neural model combined with BFOA for improving surface finish of FDM processed part. *The International Journal of Advanced Manufacturing Technology,* 60**,** 1223-1235.

MAHDAVI, A., MOHAMMADI, A., KABIR, E. & LAMBEVA, L. 2008. Occupants' operation of lighting and shading systems in office buildings. *Journal of building performance simulation,* 1**,** 57-65.

MALKAWI, A. M., SRINIVASAN, R. S., YI, Y. K. & CHOUDHARY, R. 2003. Performance-based design evolution: The use of genetic algorithms and CFD. *Eighth International IBPSA. Eindhoven, Netherlands***,** 793-798.

MALKAWI, A. M., SRINIVASAN, R. S., YUN, K. Y. & CHOUDHARY, R. 2005. Decision support and design evolution: integrating genetic algorithms, CFD and visualization. *Automation in construction,* 14**,** 33-44.

MANZAN, M. 2014. Genetic optimization of external fixed shading devices. *Energy and Buildings,* 72**,** 431-440.

MASTRUCCI, A., BAUME, O., STAZI, F. & LEOPOLD, U. 2014. Estimating energy savings for the residential building stock of an entire city: A GIS-based statistical downscaling approach applied to Rotterdam. *Energy and Buildings,* 75**,** 358-367.

MATLAB 2022. Natick, Massachusetts, USA: The Mathworks Inc.

MAZUMDAR, S. & CHEN, Q. 2009. A one-dimensional analytical model for airborne contaminant transport in airliner cabins. *Indoor air,* 19**,** 3.

MEGRI, A. C. & HAGHIGHAT, F. 2007. Zonal modeling for simulating indoor environment of buildings: Review, recent developments, and applications. *Hvac&R Research,* 13**,** 887-905.

MELILLO, J. M., TERESE (T.C.) RICHMOND, AND GARY W. YOHE 2014. Chapter 9.:Human Health. Climate Change Impacts in the United States: The Third National Climate Assessment. U.S. Global Change Research Program.

MEMARZADEH, F. & XU, W. 2012. Role of air changes per hour (ACH) in possible transmission of airborne infections. *Building Simulation,* 5**,** 15-28.

MENA, R., RODRÍGUEZ, F., CASTILLA, M. & ARAHAL, M. R. 2014. A prediction model based on neural networks for the energy consumption of a bioclimatic building. *Energy and Buildings,* 82**,** 142-155.

MÉNDEZ, C., SAN JOSÉ, J., VILLAFRUELA, J. & CASTRO, F. 2008. Optimization of a hospital room by means of CFD for more efficient ventilation. *Energy and Buildings,* 40**,** 849-854.

MENZIES, D., FANNING, A., YUAN, L., FITZGERALD, J. M. & TB*, C. C. G. I. N. T. O. 2000. Hospital ventilation and risk for tuberculous infection in Canadian health care workers. *Annals of Internal Medicine,* 133**,** 779-789.

MIHALAKAKOU, G., SANTAMOURIS, M. & TSANGRASSOULIS, A. 2002. On the energy consumption in residential buildings. *Energy and buildings,* 34**,** 727-736.

MINGFANG, T. 2002. Solar control for buildings. *Building and Environment,* 37**,** 659-664.

MOAZZAMI, M., KHODABAKHSHIAN, A. & HOOSHMAND, R. 2013. A new hybrid day-ahead peak load forecasting method for Iran's National Grid. *Applied Energy,* 101**,** 489-501.

MORAWSKA, L., TANG, J. W., BAHNFLETH, W., BLUYSSEN, P. M., BOERSTRA, A., BUONANNO, G., CAO, J., DANCER, S., FLOTO, A. & FRANCHIMON, F. 2020. How can airborne transmission of COVID-19 indoors be minimised? *Environment international,* 142**,** 105832.

MORGENSTERN, P., LI, M., RASLAN, R., RUYSSEVELT, P. & WRIGHT, A. 2016. Benchmarking acute hospitals: Composite electricity targets based on departmental consumption intensities? *Energy and buildings,* 118**,** 277-290.

MORSING, S., STRØM, J., ZHANG, G. & KAI, P. 2008. Scale model experiments to determine the effects of internal airflow and floor design on gaseous emissions from animal houses. *Biosystems Engineering,* 99**,** 99-104.

MOUSAVI, M. S., ASHRAFI, K., MOTLAGH, M. S. P., NIKSOKHAN, M. H. & VOSOUGHIFAR, H. 2018. Design of a correlated validated CFD and genetic algorithm model for optimized sensors placement for indoor air quality monitoring. *Heat and Mass Transfer,* 54**,** 509-521.

MUBAREKA, S., LOWEN, A. C., STEEL, J., COATES, A. L., GARCÍA-SASTRE, A. & PALESE, P. 2009. Transmission of influenza virus via aerosols and fomites in the guinea pig model. *The Journal of infectious diseases,* 199**,** 858-865.

MUI, K. W., SATHEESAN, M. K. & WONG, L. T. 2022. Building cooling energy consumption prediction with a hybrid simulation Approach: Generalization beyond the training range. *Energy and Buildings,* 276**,** 112502.

MUI, K. W. & WONG, L. T. 2007a. Cooling load calculations in subtropical climate. *Building and Environment,* 42**,** 2498-2504.

MUI, K. W. & WONG, L. T. 2007b. Neutral temperature in subtropical climates—a field survey in air-conditioned offices. *Building and Environment,* 42**,** 699-706.

MUI, K. W., WONG, L. T., SATHEESAN, M. K. & BALACHANDRAN, A. 2021. A Hybrid Simulation Model to Predict the Cooling Energy Consumption for Residential Housing in Hong Kong. *Energies,* 14**,** 4850.

NETO, A. H. & FIORELLI, F. A. S. 2008. Comparison between detailed model simulation and artificial neural network for forecasting building energy consumption. *Energy and buildings,* 40**,** 2169-2176.

NGUYEN, A.-T., REITER, S. & RIGO, P. 2014. A review on simulation-based optimization methods applied to building performance analysis. *Applied energy,* 113**,** 1043-1058.

NICAS, M. & JONES, R. M. 2009. Relative contributions of four exposure pathways to influenza infection risk. *Risk Analysis: An International Journal,* 29**,** 1292-1303.

NIELSEN, P. V. 2009. CFD in ventilation design: a new REHVA guide book.

NIGHTINGALE, F. 1883. *Notes on Hospitals*, Harvard College Press.

NIU, D., WANG, H. & CAI, C. Application of Neural Network-based Combining Forecasting Model Optimized by Ant Colony In Power Load Forecasting. 2010 Asia-Pacific Power and Energy Engineering Conference, 2010. IEEE, 1-4.

OH, M.-D., PARK, W. B., PARK, S.-W., CHOE, P. G., BANG, J. H., SONG, K.-H., KIM, E. S., KIM, H. B. & KIM, N. J. 2018. Middle East respiratory syndrome: what we learned from the 2015 outbreak in the Republic of Korea. *The Korean journal of internal medicine,* 33**,** 233.

OLMEDO, I., NIELSEN, P. V., RUIZ DE ADANA, M., JENSEN, R. L. & GRZELECKI, P. 2012. Distribution of exhaled contaminants and personal exposure in a room using three different air distribution strategies. *Indoor air,* 22**,** 64-76.

OLOFSSON, T. & ANDERSSON, S. 2001. Long-term energy demand predictions based on short-term measured data. *Energy and Buildings,* 33**,** 85-91.

OURGHI, R., AL-ANZI, A. & KRARTI, M. 2007. A simplified analysis method to predict the impact of shape on annual energy use for office buildings. *Energy conversion and management,* 48**,** 300-305.

PACHECO, R., ORDÓÑEZ, J. & MARTÍNEZ, G. 2012. Energy efficient design of building: A review. *Renewable and Sustainable Energy Reviews,* 16**,** 3559-3573.

PAN, D., CHAN, M., DENG, S. & LIN, Z. 2012. The effects of external wall insulation thickness on annual cooling and heating energy uses under different climates. *Applied Energy,* 97**,** 313-318.

PANTELIC, J. & THAM, K. W. 2013. Adequacy of air change rate as the sole indicator of an air distribution system's effectiveness to mitigate airborne infectious disease transmission caused by a cough release in the room with overhead mixing ventilation: a case study. *HVAC&R Research,* 19**,** 947-961.

PAPANTONIOU, S., KOLOKOTSA, D. & KALAITZAKIS, K. 2015. Building optimization and control algorithms implemented in existing BEMS using a web based energy management and control system. *Energy and Buildings,* 98**,** 45-55.

PARTI, M. & PARTI, C. 1980. The total and appliance-specific conditional demand for electricity in the household sector. *The Bell journal of economics***,** 309-321.

PAUDEL, S., ELMTIRI, M., KLING, W. L., LE CORRE, O. & LACARRIÈRE, B. 2014. Pseudo dynamic transitional modeling of building heating energy demand using artificial neural network. *Energy and Buildings,* 70**,** 81-93.

PEDERSEN, L. 2007. Use of different methodologies for thermal load and energy estimations in buildings including meteorological and sociological input parameters. *Renewable and Sustainable Energy Reviews,* 11**,** 998-1007.

PEREIRA, C. D. & GHISI, E. 2011. The influence of the envelope on the thermal performance of ventilated and occupied houses. *Energy and buildings,* 43**,** 3391-3399.

PERSILY, A., EMMERICH, S., TRECHSEL, H. & BOMBERG, M. 2009. Effects of air infiltration and ventilation, moisture control in buildings. *The key factor in mold prevention. West Conshohocken, PA: ASTM International***,** 110-110.

QIAN, H., LI, Y., NIELSEN, P. V., HYLDGAARD, C.-E., WONG, T. W. & CHWANG, A. 2006. Dispersion of exhaled droplet nuclei in a two-bed hospital ward with three different ventilation systems. *Indoor air,* 16**,** 111-128.

QIAN, H., LI, Y., NIELSEN, P. V. & HYLDGAARD, C. E. 2008. Dispersion of exhalation pollutants in a two-bed hospital ward with a downward ventilation system. *Building and Environment,* 43**,** 344-354.

QIAN, H. & ZHENG, X. 2018. Ventilation control for airborne transmission of human exhaled bio-aerosols in buildings. *Journal of thoracic disease,* 10**,** S2295.

QIN, H. & PAN, W. 2020. Energy use of subtropical high-rise public residential buildings and impacts of energy saving measures. *Journal of Cleaner Production,* 254**,** 120041.

QIN, R., YAN, D., ZHOU, X. & JIANG, Y. 2012. Research on a dynamic simulation method of atrium thermal environment based on neural network. *Building and environment,* 50**,** 214-220.

RADHI, H. 2009. Evaluating the potential impact of global warming on the UAE residential buildings–A contribution to reduce the CO2 emissions. *Building and environment,* 44**,** 2451-2462.

RADWAN, A. F., HANAFY, A. A., ELHELW, M. & EL-SAYED, A. E.-H. A. 2016. Retrofitting of existing buildings to achieve better energy-efficiency in commercial building case study: Hospital in Egypt. *Alexandria engineering journal,* 55**,** 3061-3071.

REED, S. E. 1975. An investigation of the possible transmission of rhinovirus colds through indirect contact. *Epidemiology & Infection,* 75**,** 249-258.

REILLY, S., SELKOWITZ, S. & WINKELMANN, F. 1992. Optical properties database for high performance glazings. Berkley, CA.: Lawrence Berkeley Laboratory.

REN, J., WANG, Y., LIU, Q. & LIU, Y. 2021. Numerical study of three ventilation strategies in a prefabricated COVID-19 inpatient ward. *Building and Environment,* 188**,** 107467.

REN, X., YAN, D. & WANG, C. 2014. Air-conditioning usage conditional probability model for residential buildings. *Building and Environment,* 81**,** 172-182.

REYNOLDS, J., HIPPOLYTE, J.-L. & REZGUI, Y. A smart heating set point scheduler using an artificial neural network and genetic algorithm. 2017 International Conference on Engineering, Technology and Innovation (ICE/ITMC), 2017. IEEE, 704-710.

RICHARDSON, I., THOMSON, M. & INFIELD, D. 2008. A high-resolution domestic building occupancy model for energy demand simulations. *Energy and buildings*, *40*(8), pp.1560-1566.

ROACHE, P. J. 1998. Verification of codes and calculations. *AIAA journal,* 36**,** 696-702.

ROBINSON, C., DILKINA, B., HUBBS, J., ZHANG, W., GUHATHAKURTA, S., BROWN, M. A. & PENDYALA, R. M. 2017. Machine learning approaches for estimating commercial building energy consumption. *Applied energy,* 208**,** 889-904.

RODRÍGUEZ-SORIA, B., DOMÍNGUEZ-HERNÁNDEZ, J., PÉREZ-BELLA, J. M. & DEL COZ-DÍAZ, J. J. 2014. Review of international regulations governing the thermal insulation requirements of residential buildings and the harmonization of envelope energy loss. *Renewable and Sustainable Energy Reviews,* 34**,** 78-90.

ROUAULT, F., BRUNEAU, D., SEBASTIAN, P. & LOPEZ, J. 2013. Numerical modelling of tube bundle thermal energy storage for free-cooling of buildings. *Applied energy,* 111**,** 1099-1106.

ROY, C. J., & MILTON, D. K. 2004. Airborne transmission of communicable infection-the elusive pathway. *The New England Journal Of Medicine*, 350:1710-1712.

RUGGIERO, S., TARIELLO, F. & VANOLI, G. P. 2022. Evaluation of Comfort Models Considering the Peculiarities of Hospitalization: Bedding, Clothing and Reduced Activity of Patients. *Buildings,* 12**,** 343.

RUNGE, J. & ZMEUREANU, R. 2019. Forecasting energy use in buildings using artificial neural networks: A review. *Energies,* 12**,** 3254.

SADEGHIFAM, A. N., ZAHRAEE, S. M., MEYNAGH, M. M. & KIANI, I. 2015. Combined use of design of experiment and dynamic building simulation in assessment of energy efficiency in tropical residential buildings. *Energy and Buildings,* 86**,** 525-533.

SADINENI, S. B., MADALA, S. & BOEHM, R. F. 2011. Passive building energy savings: A review of building envelope components. *Renewable and sustainable energy reviews,* 15**,** 3617-3631.

SAHU, M., BHATTACHARJEE, B. & KAUSHIK, S. 2012. Thermal design of air-conditioned building for tropical climate using admittance method and genetic algorithm. *Energy and Buildings,* 53**,** 1-6.

SANG, X., PAN, W. & KUMARASWAMY, M. 2014. Informing energy-efficient building envelope design decisions for Hong Kong. *Energy Procedia,* 62**,** 123-131.

SATHEESAN, M. K., MUI, K. W. & WONG, L. T. A numerical study of ventilation strategies for infection risk mitigation in general inpatient wards. Building simulation, 2020. Springer, 887-896.

SCHARFMAN, B. E., TECHET, A. H., BUSH, J. W. M., & BOUROUIBA, L. (2016). Visualization of sneeze ejecta: steps of fluid fragmentation leading to respiratory droplets. *Experiments in Fluids*, 57, 1-9.

SCHWEIKER, M. & SHUKUYA, M. 2009. Comparison of theoretical and statistical models of air-conditioning-unit usage behaviour in a residential setting under Japanese climatic conditions. *Building and Environment,* 44**,** 2137-2149.

SEMPEY, A., INARD, C., GHIAUS, C. & ALLERY, C. 2009. Fast simulation of temperature distribution in air conditioned rooms by using proper orthogonal decomposition. *Building and Environment,* 44**,** 280-289.

SHAJAHAN, A., CULP, C. H. & WILLIAMSON, B. 2019. Effects of indoor environmental parameters related to building heating, ventilation, and air conditioning systems on patients' medical outcomes: A review of scientific research on hospital buildings. *Indoor Air,* 29**,** 161-176.

SHANGDONG, Y. & XIANG, L. A new ANN optimized by improved PSO algorithm combined with chaos and its application in short-term load forecasting. 2006 International Conference on Computational Intelligence and Security, 2006. IEEE, 945-948.

SHAO, M., WANG, X., BU, Z., CHEN, X. & WANG, Y. 2020. Prediction of energy consumption in hotel buildings via support vector machines. *Sustainable Cities and Society,* 57**,** 102128.

SHIH, Y. C., CHIU, C. C., & WANG, O. 2007. Dynamic airflow simulation within an isolation room. *Building and environment*, 42(9), 3194-3209.

SHIMODA, Y., ASAHI, T., TANIGUCHI, A. & MIZUNO, M. 2007. Evaluation of city-scale impact of residential energy conservation measures using the detailed end-use simulation model. *Energy,* 32**,** 1617-1633.

SHIU, E. Y., LEUNG, N. H. & COWLING, B. J. 2019. Controversy around airborne versus droplet transmission of respiratory viruses: implication for infection prevention. *Current opinion in infectious diseases,* 32**,** 372-379.

SOHN, M. D., APTE, M. G., SEXTRO, R. G. & LAI, A. C. 2007. Predicting size-resolved particle behavior in multizone buildings. *Atmospheric Environment,* 41**,** 1473-1482.

SONG, F., ZHAO, B., YANG, X., JIANG, Y., GOPAL, V., DOBBS, G. & SAHM, M. 2008. A new approach on zonal modeling of indoor environment with mechanical ventilation. *Building and Environment,* 43**,** 278-286.

SPANDAGOS, C. & NG, T. L. 2017. Equivalent full-load hours for assessing climate change impact on building cooling and heating energy consumption in large Asian cities. *Applied energy,* 189**,** 352-368.

SULIMAN, A. & OMARO, B. S. 2018. Applying Bayesian regularization for acceleration of Levenberg-Marquardt based neural network training. *IJIMAI,* 5**,** 68-72.

SWAN, L. G., UGURSAL, V. I. & BEAUSOLEIL-MORRISON, I. 2013. Hybrid residential end-use energy and greenhouse gas emissions model–development and verification for Canada. *Journal of Building Performance Simulation,* 6**,** 1-23.

TELLIER, R., LI, Y., COWLING, B. J. & TANG, J. W. 2019. Recognition of aerosol transmission of infectious agents: a commentary. *BMC infectious diseases,* 19**,** 1-9.

THAM, K. W. & WILLEM, H. C. 2010. Room air temperature affects occupants' physiology, perceptions and mental alertness. *Building and Environment,* 45**,** 40-44.

TIAN, L., LIN, Z., WANG, Q. & LIU, J. 2009. Numerical investigation of indoor aerosol particle dispersion under stratum ventilation and under displacement ventilation. *Indoor and Built Environment,* 18**,** 360-375.

TORRECILLA, J., OTERO, L. & SANZ, P. 2007. Optimization of an artificial neural network for thermal/pressure food processing: Evaluation of training algorithms. *Computers and Electronics in Agriculture,* 56**,** 101-110.

TOUTOU, A., FIKRY, M. & MOHAMED, W. 2018. The parametric based optimization framework daylighting and energy performance in residential buildings in hot arid zone. *Alexandria engineering journal,* 57**,** 3595-3608.

TRČKA, M. & HENSEN, J. L. 2010. Overview of HVAC system simulation. *Automation in Construction,* 19**,** 93-99.

TSO, G. K. & YAU, K. K. 2003. A study of domestic energy usage patterns in Hong Kong. *Energy,* 28**,** 1671-1682.

TUHUS-DUBROW, D. & KRARTI, M. 2009. Comparative analysis of optimization approaches to design building envelope for residential buildings. *ASHRAE Transactions,* 115**,** 554-563.

TUHUS-DUBROW, D. & KRARTI, M. 2010. Genetic-algorithm based approach to optimize building envelope design for residential buildings. *Building and environment,* 45**,** 1574-1581.

TURHAN, C., KAZANASMAZ, T., UYGUN, I. E., EKMEN, K. E. & AKKURT, G. G. 2014. Comparative study of a building energy performance software (KEP-IYTE-ESS) and ANN-based building heat load estimation. *Energy and Buildings,* 85**,** 115-125.

UNITED NATIONS 2018a. 68% of the world population projected to live in urban areas by 2050, says UN. Department of Economic and Social Affairs.

UNITED NATIONS 2018b. World Population Prospects: 2018 Revision. New York, NY, USA: Department of Economic and Social Affairs.

VALOVCIN, S., HERING, A., POLLY, B. & HEANEY, M. 2014. A statistical approach for post-processing residential building energy simulation output. *Energy and buildings,* 85**,** 165-179.

VAN DOREMALEN, N., BUSHMAKER, T. & MUNSTER, V. 2013. Stability of Middle East respiratory syndrome coronavirus (MERS-CoV) under different environmental conditions. *Eurosurveillance,* 18**,** 20590.

VINCENT, J.-L., BIHARI, D. J., SUTER, P. M., BRUINING, H. A., WHITE, J., NICOLAS-CHANOIN, M.-H., WOLFF, M., SPENCER, R. C. & HEMMER, M. 1995. The prevalence of nosocomial infection in intensive care units in Europe: results of the European Prevalence of Infection in Intensive Care (EPIC) Study. *Jama,* 274**,** 639-644.

WALTHER, B. A. & EWALD, P. W. 2004. Pathogen survival in the external environment and the evolution of virulence. *Biological Reviews,* 79**,** 849-869.

WAN, K. & YIK, F. H. 2004. Representative building design and internal load patterns for modelling energy use in residential buildings in Hong Kong. *Applied energy,* 77**,** 69-85.

WAN, M. P., CHAO, C. Y. H., NG, Y., SZE TO, G. N. & YU, W. 2007. Dispersion of expiratory droplets in a general hospital ward with ceiling mixing type mechanical ventilation system. *Aerosol Science and Technology,* 41**,** 244-258.

WANG, J.-X., CAO, X. & CHEN, Y.-P. 2021. An air distribution optimization of hospital wards for minimizing cross-infection. *Journal of cleaner production,* 279**,** 123431.

WANG, J., ZHANG, T., ZHOU, H. & WANG, S. 2018. Inverse design of aircraft cabin environment using computational fluid dynamics-based proper orthogonal decomposition method. *Indoor and Built Environment,* 27**,** 1379-1391.

WANG, L. L. & CHEN, Q. 2008. Evaluation of some assumptions used in multizone airflow network models. *Building and Environment,* 43**,** 1671-1677.

WELLS, W. F. 1955. Airborne Contagion and Air Hygiene. An Ecological Study of Droplet Infections. Cambridge, USA: Harvard University Press.

WESTPHAL, F. S. & LAMBERTS, R. Building simulation calibration using sensitivity analysis. Ninth International IBPSA Conference, 2005. 1331-1338.

WILCOX, B., GUMERLOCK, A., BARNABY, C., MITCHELL, R. & HUIZENGA, C. The effects of thermal mass exterior walls on heating and cooling loads in commercial buildings. Proceedings of the ASHRAE/DOE/BTECC Conference on Thermal Performance of the Exterior Envelopes of Buildings, 1985. 2-5.

WILCOX, S. & MARION, W. 2008. Users manual for tmy3 data sets (revised). National Renewable Energy Lab.(NREL), Golden, CO (United States).

WILSON, J. & LIU, J. 1994. Backward tracking to find the source of pollution. *Water Manage. Risk Remed,* 1**,** 181-199.

WONG, L. T. 2018. Tiny affordable housing in Hong Kong. *Indoor and Built Environment,* 27**,** 1159-1161.

WONG, L. T. & MUI, K. W. 2006. An occupant load survey for residential buildings in Hong Kong. *International Journal for Housing Science and its applications,* 30**,** 195-204.

WONG, L. T., MUI, K. W. & SHI, K. 2008. Energy impact of indoor environmental policy for air-conditioned offices of Hong Kong. *Energy Policy,* 36**,** 714-721.

WONG, L. T., YU, H., MUI, K. W. & CHAN, W. 2015. Drag constants for common indoor bioaerosols. *Indoor and Built Environment,* 24**,** 401-413.

WONG, S.C.Y., KWONG, R.S., WU, T.C., CHAN, J.W.M., CHU, M.Y., LEE, S.Y., WONG, H.Y. & LUNG, D.C. 2020. Risk of nosocomial transmission of coronavirus disease 2019: an experience in a general ward setting in Hong Kong. *Journal of Hospital Infection*, 105(2), pp.119-127.

WU, J., LIAN, Z., ZHENG, Z. & ZHANG, H. 2020. A method to evaluate building energy consumption based on energy use index of different functional sectors. *Sustainable Cities and Society,* 53**,** 101893.

XIAO, S., LI, Y., SUNG, M., WEI, J. & YANG, Z. 2018. A study of the probable transmission routes of MERS-CoV during the first hospital outbreak in the Republic of Korea. *Indoor air,* 28**,** 51-63.

XIE, X., LI, Y., CHWANG, A., HO, P. & SETO, W. 2007. How far droplets can move in indoor environments--revisiting the Wells evaporation-falling curve. *Indoor air,* 17**,** 211-225.

YAN, D., O'BRIEN, W., HONG, T., FENG, X., GUNAY, H. B., TAHMASEBI, F. & MAHDAVI, A. 2015. Occupant behavior modeling for building performance simulation: Current state and future challenges. *Energy and buildings,* 107**,** 264-278.

YAN, K., WANG, X., DU, Y., JIN, N., HUANG, H. & ZHOU, H. 2018. Multi-step short-term power consumption forecasting with a hybrid deep learning strategy. *Energies,* 11**,** 3089.

YANG, L., LAM, J. C. & TSANG, C. L. 2008. Energy performance of building envelopes in different climate zones in China. *Applied energy,* 85**,** 800-817.

YAU, Y. & HASBI, S. 2013. A review of climate change impacts on commercial buildings and their technical services in the tropics. *Renewable and Sustainable Energy Reviews,* 18**,** 430-441.

YAU, Y. H., CHANDRASEGARAN, D. & BADARUDIN, A. 2011. The ventilation of multiple-bed hospital wards in the tropics: a review. *Building and Environment,* 46**,** 1125-1132.

YEZIORO, A., DONG, B. & LEITE, F. 2008. An applied artificial intelligence approach towards assessing building performance simulation tools. *Energy and Buildings,* 40**,** 612-620.

YI, Y. K. & MALKAWI, A. M. 2011. Integrating neural network models with computational fluid dynamics (CFD) for site-specific wind condition. *Building Simulation,* 4**,** 245-254.

YIN, Y., XU, W., GUPTA, J. K., GUITY, A., MARMION, P., MANNING, A., GULICK, B., ZHANG, X. & CHEN, Q. 2009. Experimental study on displacement and mixing ventilation systems for a patient ward. *HVAC&R Research,* 15**,** 1175-1191.

YOKOYAMA, R., WAKUI, T. & SATAKE, R. 2009. Prediction of energy demands using neural network with model identification by global optimization. *Energy Conversion and Management,* 50**,** 319-327.

YOSHINO, H., MURAKAMI, S., AKABAYASHI, S., KURABUCHI, T., KATO, S., TANABE, S. & ADACHI, M. Survey on minimum ventilation rate of residential buildings in fifteen countries. Proceedings of the 25th AIVC Conference-Ventilation and retrofitting, Prague, 2004. 227-238.

YU, H., LIAO, C.-M., LIANG, H.-M. & CHIANG, K.-C. 2007. Scale model study of airflow performance in a ceiling slot-ventilated enclosure: Non-isothermal condition. *Building and environment,* 42**,** 1142-1150.

YU, H., MUI, K. W., WONG, L. T. & CHU, H. 2017. Ventilation of general hospital wards for mitigating infection risks of three kinds of viruses including Middle East respiratory syndrome coronavirus. *Indoor and Built Environment,* 26**,** 514-527.

YU, J., CHANG, W.-S. & DONG, Y. 2022. Building Energy Prediction Models and Related Uncertainties: A Review. *Buildings,* 12**,** 1284.

ZEYTOUNIAN, R. K. 2003. Joseph Boussinesq and his approximation: a contemporary view. *Comptes Rendus Mecanique,* 331**,** 575-586.

ZHAI, Z. J., ZHANG, Z., ZHANG, W. & CHEN, Q. Y. 2007. Evaluation of various turbulence models in predicting airflow and turbulence in enclosed environments by CFD: Part 1—Summary of prevalent turbulence models. *Hvac&R Research,* 13**,** 853-870.

ZHANG, C., LI, J., ZHAO, Y., LI, T., CHEN, Q. & ZHANG, X. 2020a. A hybrid deep learning-based method for short-term building energy load prediction combined with an interpretation process. *Energy and Buildings,* 225**,** 110301.

ZHANG, N., CHEN, W., CHAN, P. T., YEN, H. L., TANG, J. W. T. & LI, Y. 2020b. Close contact behavior in indoor environment and transmission of respiratory infection. *Indoor air,* 30**,** 645-661.

ZHANG, T.-H. & YOU, X.-Y. 2014. Applying neural networks to solve the inverse problem of indoor environment. *Indoor and Built Environment,* 23**,** 1187-1195.

ZHANG, T. & CHEN, Q. 2007a. Identification of contaminant sources in enclosed environments by inverse CFD modeling. *Indoor air,* 17**,** 167-177.

ZHANG, T. & CHEN, Q. 2007b. Identification of contaminant sources in enclosed spaces by a single sensor. *Indoor air,* 17**,** 439-449.

ZHANG, T., LIU, Y., RAO, Y., LI, X. & ZHAO, Q. 2020c. Optimal design of building environment with hybrid genetic algorithm, artificial neural network, multivariate regression analysis and fuzzy logic controller. *Building and Environment,* 175**,** 106810.

ZHANG, T. T., YIN, S. & WANG, S. 2013. An inverse method based on CFD to quantify the temporal release rate of a continuously released pollutant source. *Atmospheric environment,* 77**,** 62-77.

ZHANG, Z. & CHEN, Q. 2007c. Comparison of the Eulerian and Lagrangian methods for predicting particle transport in enclosed spaces. *Atmospheric environment,* 41**,** 5236-5248.

ZHANG, Z., CHEN, X., MAZUMDAR, S., ZHANG, T. & CHEN, Q. 2009. Experimental and numerical investigation of airflow and contaminant transport in an airliner cabin mockup. *Building and Environment,* 44**,** 85-94.

ZHANG, Z., ZHANG, W., ZHAI, Z. J. & CHEN, Q. Y. 2007. Evaluation of various turbulence models in predicting airflow and turbulence in enclosed environments by CFD: Part 2—Comparison with experimental data from literature. *Hvac&R Research,* 13**,** 871-886.

ZHAO, B., ZHANG, Y., LI, X., YANG, X. & HUANG, D. 2004. Comparison of indoor aerosol particle concentration and deposition in different ventilated rooms by numerical method. *Building and Environment,* 39**,** 1-8.

ZHAO, H.-X. & MAGOULÈS, F. 2012. A review on the prediction of building energy consumption. *Renewable and Sustainable Energy Reviews,* 16**,** 3586-3592.

ZHOU, D., ZHAO, C.-Y. & TIAN, Y. 2012. Review on thermal energy storage with phase change materials (PCMs) in building applications. *Applied energy,* 92**,** 593-605.

ZNOUDA, E., GHRAB-MORCOS, N. & HADJ-ALOUANE, A. 2007. Optimization of Mediterranean building design using genetic algorithms. *Energy and buildings,* 39**,** 148-153.

ZUMLA, A., HUI, D. S. & PERLMAN, S. 2015. Middle East respiratory syndrome. *The Lancet,* 386**,** 995-1007.